University of Alberta

Evaluating the Role of the Neurocentral Junction in Adolescent Idiopathic Scoliosis

by

©

Talib Rajwani

A thesis submitted to the Faculty of Graduate Studies and Research in partial fulfillment
of the requirements for the degree of Doctor of Philosophy
in

Medical Sciences - Radiology and Diagnostic Imaging

Edmonton, Alberta

Fall 2004

Library and
Archives Canada

Published Heritage
Branch

395 Wellington Street
Ottawa ON K1A 0N4
Canada

Bibliothèque et
Archives Canada

Direction du
Patrimoine de l'édition

395, rue Wellington
Ottawa ON K1A 0N4
Canada

Your file Votre référence
ISBN: 0-612-96008-0
Our file Notre référence
ISBN: 0-612-96008-0

The author has granted a non-exclusive license allowing the Library and Archives Canada to reproduce, loan, distribute or sell copies of this thesis in microform, paper or electronic formats.

The author retains ownership of the copyright in this thesis. Neither the thesis nor substantial extracts from it may be printed or otherwise reproduced without the author's permission.

L'auteur a accordé une licence non exclusive permettant à la Bibliothèque et Archives Canada de reproduire, prêter, distribuer ou vendre des copies de cette thèse sous la forme de microfiche/film, de reproduction sur papier ou sur format électronique.

L'auteur conserve la propriété du droit d'auteur qui protège cette thèse. Ni la thèse ni des extraits substantiels de celle-ci ne doivent être imprimés ou aturement reproduits sans son autorisation.

In compliance with the Canadian Privacy Act some supporting forms may have been removed from this thesis.

While these forms may be included in the document page count, their removal does not represent any loss of content from the thesis.

Conformément à la loi canadienne sur la protection de la vie privée, quelques formulaires secondaires ont été enlevés de cette thèse.

Bien que ces formulaires aient inclus dans la pagination, il n'y aura aucun contenu manquant.

Canada

DEDICATION

This work is dedicated to my parents and sister, who have been the pillars of support throughout my undergraduate and graduate education.

ACKNOWLEDGEMENTS

I wish to express my sincere gratitude:

To my supervisors, supervisory committee members and committee chair; Dr. Ravi Bhargava, Dr. Tapio Videman, Dr. Keith Bagnall, Dr. Marc Moreau, Dr. Robert Lambert and Dr. Larry Filipow for their continuous support and guidance, both professional and personal, throughout my graduate program. Under the mentorship of these individuals, my research experience has been more challenging and more rewarding than I ever imagined.

To Prof. James Raso, Mr. Doug Hill, Dr. James Mahood and the staff at the Northern Alberta Scoliosis Research Center for their active participation in my studies and fostering in me a lasting enthusiasm for scoliosis research.

To Dr. Hubert Labelle, Dr. Carl-Eric Aubin and Anne-Marie Huynh for welcoming me into the Biomechanical Modeling Lab at Saint Justine Hospital, fostering meaningful collaboration and broadening my research experience.

To Jessie Kautz, Eric Huang and Donovan Nunweiler for their technical assistance and invaluable suggestions.

To the University of Alberta Department of Radiology and Diagnostic Imaging, University of Alberta Faculty of Graduate Studies, University of Alberta Faculty of Medicine and the Alberta Heritage Foundation for Medical Research for funding my graduate studies and allowing me to devote full attention to my thesis.

TABLE OF CONTENTS

CHAPTER PAGE

1. Introduction and statement of the problem 1

2. Critical review of the literature 8

The necessity for a new approach 8

Overview of adolescent idiopathic scoliosis 9

Morphology of vertebrae from AIS patients 18

Vertebral growth 24

The neurocentral junction 29

Fluorochrome-based techniques of evaluating bone growth 38

Biomechanical analysis of scoliosis 40

3. MRI characteristics of the image of the normal neurocentral junction 59

4. Evaluating the use of MRI as a technique for visualizing the neurocentral junction 75

5. Asymmetric neurocentral junction development in adolescent idiopathic scoliosis patients 94

6. Pedicle asymmetry in normal subjects and adolescent idiopathic scoliosis patients 111

7. Vertebral canal growth in a rat model 134

8. Asymmetric neurocentral junction growth as a potential cause of scoliosis in a porcine model 169

9. Computerized biomechanical simulation of pedicle asymmetry as a potential cause of adolescent idiopathic scoliosis 202

10. General conclusions and discussion 230

LIST OF TABLES

TABLE		PAGE
2-1	Vertebral deformities in scoliosis	21
2-2	Animal models of asymmetric NCJ growth as a potential cause of scoliosis	35
3-1	Distribution of NCJs by stage	62
4-1	Comparison of gross anatomic visualization of the vertebra, visual examination of unstained sections and microscopic visualization of stained sections as a means of evaluating the open or closed status of the NCJ	79
4-2	Comparison of gross anatomic visualization of the intact vertebrae with microscopic visualization of the stained transverse NCJs	80
5-1	Staging system for NCJ development	99
5-2	Comparison of right and left NCJ development in AIS patients	100
6-1	Normal and AIS patient information	113
6-2	Summary of statistical analysis	119
6-3	Indices for vertebrae from AIS patients exhibiting disparate NCJ development	121
7-1	Age of rats on arrival, fluorochrome injection and euthanization for each group	138
7-2	Statistical analysis for NCJ, vertebral canal and neural arch parameters	146
7-3	Average area, perimeter, AP diameter and lateral diameter of the vertebral canal at different ages	156
8-1	Average weight and length for the porcine specimens from the time of surgery to 18 weeks post-operatively	177
9-1	Results from simulations involving asymmetry of pedicle geometry	213
9-2	Results from simulations involving asymmetry of pedicle geometry in combination with scenarios tested by Villemure et al. (2004)	214
9-3	Results from simulations involving asymmetry of pedicle growth	215

rates in combination with scenarios tested by Villemure et al. (2004)

9-4 Configurations from simulations involving constant and graded pedicle asymmetry from T6-T10 at 1, 12 and 24 months of simulation 218

9-5 Configurations from simulations involving 3 mm displacement of T8 anteriorly, 3 mm displacement of T8 to the right and rotation of T8 by 5° all with symmetric pedicle growth 219

LIST OF FIGURES

FIGURE		PAGE
3-1	The position of the NCJ in transverse and sagittal views	60
3-2	Sagittal MRI of the thoracolumbar NCJs in a two year old and a 12 year old patient	66
3-3	Age of closure of the NCJ at different vertebral levels	70
4-1	Examination of the NCJ by gross visualization of the lateral surface of the vertebral body and microscopic examination of a transverse section through the vertebra	81
4-2	Sagittal and transverse sections through the vertebra from a six-month-old porcine specimen	82
4-3	MRI and digital photomicrographs of the NCJ from six-month-old and 13-month-old porcine specimens	83
4-4	MRI-histologic correlation of a partially closed NCJ	86
5-1	Typical transverse and sagittal MRIs of open NCJs	97
5-2	Typical transverse and sagittal MRIs of the partially closed NCJ	101
5-3	Asymmetric NCJ development in the T8 vertebra of a 15 year old female patient	104
5-4	Asymmetric NCJ development in consecutive vertebrae from a 14 year old male patient	105
6-1	Definitions for pedicle and lamina measurements	115
6-2	Definitions for NCJ angle measurements	116
6-3	Vertebrae from normal and AIS patients showing asymmetry of the pedicles and laminae	123
7-1	The image of the T8 vertebra from a one-week-old Sprague-Dawley rat superimposed on the image of the T8 vertebra from a ten-week-old Sprague-Dawley rat	135
7-2	Definitions for NCJ length, width and area measurements	142
7-3	Definitions for vertebral canal area, perimeter and diameter measurements	143

7-4 Definitions for pedicle and lamina measurements 145
7-5 Complete montage image of the T8 vertebra from a Group 8 rat showing the deposition of tetracycline and alizarin 148
7-6 Fluorochrome deposition in the vertebral trabeculae of a Group 3 rat 151
7-7 Visualization of the posterior synchondrosis in a Group 1 rat showing bipolar fluorochrome deposition 152
7-8 Visualization of the NCJ in Group 2 and Group 3 rats showing bipolar fluorochrome deposition 153
7-9 Area, perimeter and diameters of the vertebral canal in rats of ages one to eleven weeks 157
8-1 Depiction of Nicoladoni's original asymmetric growth hypothesis 170
8-2 Anatomic specimen from a two-month-old pig showing the angle of screw insertion relative to the vertebral midline 174
8-3 Schematic diagram of the vertebra showing the points used to measure vertebral rotation using Stokes method 179
8-4 Definitions for pedicle and lamina measurements from CT images of the porcine vertebrae 181
8-5 Serial AP composite radiographs obtained from Pig 1 183
8-6 Serial AP composite radiographs obtained from Pig 2 184
8-7 Serial AP composite radiographs obtained from Pig 3 185
8-8 Serial AP composite radiographs obtained from Pig 4 186
8-9 Three sets of composite radiographs obtained from Pig 3 at 11 weeks to test the accuracy of acquiring and piecing together individual radiographs 187
8-10 Rotation of the thoracolumbar vertebrae in Pig 3 at 9, 11 and 13 weeks post-operatively 188
8-11 CT images at the mid-pedicle level of the T8, T9 and T10 vertebrae from Pig 2 190
8-12 CT images acquired at the level of screw insertion and 5 mm above and below the level of screw insertion in T9 from Pig 2 191

8-13	Visual explanation of the role of periosteal mechanisms in changing pedicle length	194
8-14	Visual explanation of the relationship between increased laminar thickness and an increase in the measured pedicle length based on measurement definitions	196
9-1	Depiction of Nicoladoni's original asymmetric growth hypothesis	203
9-2	PA and lateral radiographs from the female subject used for the reference spinal configuration	206
9-3	Steps involved in producing a finite element model from calibrated radiographs	207
9-4	Schematic representation of the finite element model used in this thesis	208

CHAPTER 1

INTRODUCTION AND STATEMENT OF THE PROBLEM

In 1966, Roaf commented that idiopathic scoliosis was an unsolved deformity with obscure causes and limited treatment options. Unfortunately, despite extensive research, this suggestion still holds true today. While scoliosis has been better characterized, the limited advances made in understanding its etiology have hampered the development of new methods of diagnosis and therapy. As a cure for scoliosis is not apparent in the near or even distant future, it seems that a fundamental change in approach might be quite appropriate.

The term scoliosis refers to a spinal deformity that is characterized by an abnormal lateral curvature of the spine often accompanied by rotation of the vertebrae. Although there are several different forms of scoliosis, 80% of cases are still classified as idiopathic since they present without a known cause (Lovell and Winter, 2001). The most common type of idiopathic scoliosis appears during adolescence, resulting in the description of adolescent idiopathic scoliosis (AIS). Although numerous different etiologies have been suggested for AIS including genetic, structural, metabolic, endocrine, neural and chemical factors, none of these factors have been shown to be all encompassing and studies within each field have often generated contradictory findings (Rinsky and Gamble, 1988; Robin, 1990; Lonstein, 1994, Miller, 2001). As a result, there has been little advancement in the understanding of the etiology of AIS and its treatment has remained focused on symptoms rather than cause.

The lack of progress in understanding the etiology of AIS suggests perhaps that it is time to reconsider the manner in which AIS research is approached at a fundamental level. The traditional paradigm of attributing a specific abnormal condition to one main cause may not apply to AIS. In fact, circumstantial evidence strongly suggests that AIS has multiple different causes and yet this is often ignored. When scoliosis was first identified many years ago, all cases were idiopathic or of unknown cause. Some common factors were identified (cerebral palsy, Friedrich's ataxia, neurofibromatosis) as known causes and these cases were culled out from the idiopathic pool so that the percentage of cases that could be considered idiopathic decreased. Unfortunately, approximately 80% of scoliosis cases still remain of idiopathic origin (Lovell and Winter, 2001). However, it seems unlikely that these 80% of scoliosis cases could have a single cause, particularly when there are a large number of causes for the 20% of scoliosis cases not considered idiopathic. Furthermore, there is extensive variation in the way that the idiopathic cases present, with curves that vary in parameters such as size, site, side, type, progressive properties and age of presentation, all of which perhaps suggests more than one underlying cause. To complicate this idea further, each cause may in fact have several interacting components where just a few of the components may be sufficient for the development of scoliosis. Based on all of this evidence, a growing number of researchers would suggest that AIS does not have a single cause and is actually the final common pathway of several completely separate disorders (Lonstein, 1994). Although this idea is becoming more accepted, this does not appear to have been considered in many past experiments where experimental design has been based on scoliosis having a single cause. Often, a potential cause has been identified and a group of AIS patients examined to explore this hypothesis. Yet, if AIS has multiple causes, then any random sample of AIS patients would likely include patients with completely different and separate causes, making it impossible to isolate and identify any one particular etiology. Instead of using the traditional approaches to scoliosis research, much more progress might be made if attention was focused on a particular potential cause and a complete model was developed based on this cause. The potential symptoms of patients with this single underlying cause could be identified using animal models, computer simulations and clinical observation. A group of patients with the same cause of scoliosis could then be assembled and a particular etiology of AIS could be assessed and determined. This thesis has attempted to take this approach.

In addition to the realization that AIS may be due to multiple causes, there is also evidence that different mechanisms may be involved in initial curve development compared to further curve progression when the normal biomechanics of the spine have been altered (Lonstein, 1994). As an extension, this would imply that a scoliotic curve might continue to progress even if the initial factors responsible for curve development were no longer present or identifiable. Therefore, obtaining measurements from patients who already have well-established scoliosis may not reflect the initial cause of the deformity. This is an important point for consideration and this aspect has also not been fully realized in many past studies. For example, in investigating the theory that scoliosis might be the result of decreased melatonin levels, several authors (Bagnall et al., 1996; Hilibrand et al., 1996; Fagan et al., 1998; Brodner, 2000) have compared urine or serum melatonin levels between normal patients and patients with severe scoliosis and have found no significant differences. However, since these patients had well-established scoliosis, it is entirely possible that they were selected too late in the course of scoliosis for the initial melatonin deficiency to still be present. Considering that AIS likely has multiple causes it is also possible that even if low melatonin levels were a cause of scoliosis, none of the randomly selected patients in these studies represented this particular cause.

The study of AIS etiology is further complicated by the fact that it is impossible to separate cause and effect in the development of spinal curves. Patients typically present to a family physician or a scoliosis clinic after their vertebral deformities are well-established. This is primarily because patients, or more commonly their parents and friends, are usually alerted to the presence of scoliosis on the basis of external cosmetic deformities such as asymmetrical shoulder heights, rib prominence or waist asymmetry. Unfortunately, the extent of this cosmetic deformity is much less than the extent of the vertebral deformity, which is obscured by the location of the vertebral column deep inside the thorax and abdomen. As a result, there is often a very narrow window of time between the initial presentation of patients to the scoliosis clinic and the development of secondary biomechanical changes in the vertebrae as a result of a well-established scoliosis. In a patient with well-established scoliosis, it becomes almost impossible to determine unambiguously if a given condition, especially a vertebral change, is a cause or an effect of scoliosis. Faced with this limitation, the development of a complete theory of scoliosis requires supplementation of clinical studies with animal and computer models, which enable evaluation of the early stages of curve development and the determination of cause and effect relationships.

Among the numerous theories of scoliosis, it has long been thought that scoliosis could be the result of abnormal vertebral growth since vertebrae from scoliosis patients are deformed. It seems logical to say that growth into this shape would produce scoliosis, but the confounding issue is that the accompanying scoliosis might further enhance the degree of abnormal vertebral growth. Numerous authors have proposed that scoliosis is due to the asymmetric growth of bilateral elements, most notably the neurocentral junctions (NCJs) (Nicoladoni, 1909; Knutsson, 1966; Roaf, 1966; Yamazaki et al., 1998). The NCJ is situated between the neural arch and the centrum and represents the hyaline cartilage that remains from the embryonic model after the ossification centers for the centrum and neural arch have appeared. As a growth plate, this site is thought to contribute to the growth of both the vertebral body and the neural arch and is certainly in a position to do so (Vital, 1989).

The NCJ has been implicated as a potential cause of scoliosis for nearly a century with Nicoladoni (1909) hypothesizing that asymmetrical growth of the NCJ could create a torsional force that would result in vertebral rotation and scoliosis. However, the idea that abnormal NCJ closure could account for the development of scoliosis in adolescents was dismissed by the results of autopsy studies which showed that the NCJ closed long before the adolescent period (Ottander, 1963; Knutsson, 1966; Roaf, 1966; Schmorl and Junghanns, 1971; Beguiristain et al., 1980; Taylor, 1983; Mineiro in Vital, 1989; Williams et al., 1989; Maat et al., 1996). Recently, the asymmetrical closure hypothesis has been resurrected by magnetic resonance imaging (MRI) studies that have suggested that the NCJ does not close, at least in some vertebrae, until 11-16 years of age (Yamazaki, 1998). If the results of these MRI studies are correct, then abnormal NCJ development might well prove to be a mechanism for the development of AIS at least in some cases. This knowledge would have repercussions on the development of new methods of diagnosis and treatment of AIS. For example, MRI might be used to identify cases where one NCJ has remained open after the contralateral NCJ has closed and a corrective epiphyseodesis might prevent the onset of scoliosis, 'reverse' an existing case of scoliosis or prevent a scoliotic curve from increasing.

The specific aim of this thesis is to examine the asymmetric NCJ growth model of scoliosis. This will require understanding of the appearance, growth and development of the NCJ, as well as exploration of the potential role of the NCJ in AIS using clinical studies, animal models and biomechanical simulations.

From a more global perspective, this thesis is also being used as a vehicle to explore general principles of bone growth, to foster critical evaluation of the manner in which scoliosis is studied, to develop a general approach that can be applied to all studies of scoliosis etiology and to offer insight into the way that scoliosis research should be conducted in the future.

REFERENCES

Beguiristain JL, De Salis J, Oriaifo A, Canadell J. Experimental scoliosis by epiphyseodesis in pigs. Int Ortho 1980;3:317-21.

Knutsson F. Vertebral genesis of idiopathic scoliosis in children. Acta Radiol 1966;4:395-402.

Lonstein JE. Adolescent idiopathic scoliosis. Lancet 1994;344:1407-1412.

Lovell W, Winter B. Pediatric orthopaedics. Lippincott, Williams and Wilkins. Philadelphia, 2001.

Maat GJ, Matricali B, Van Meerten EL. Postnatal development and structure of the neurocentral junction. Spine 1996;21:661-66.

Miller NH. Adolescent idiopathic scoliosis: etiology. In : Weinstein SL (ed.). The pediatric spine : principles and practice, 2nd ed. Lippincott Williams and Wilkins. Philadelphia, 2001: 347-354.

Nicoladoni C. Anatomie und mechanismus der skoliose. Urban and Schwarzernburg. Munchen, 1909.

Ottander HG. Experimental progressive scoliosis in a pig. Acta Orthop Scand 1963;33:91-7.

Rinsky L, Gamble J. Adolescent idiopathic scoliosis. Western J Medicine 1988;148:182-191.

Roaf R. The basic anatomy of scoliosis. J Bone Joint Surg (Br) 1966;48-B:786-92.

Robin GC. The aetiology of idiopathic scoliosis. Freund Publishing House. Boca Raton, 1990.

Schmorl G, Junghanns H, Besemann EF (ed.). The human spine in health and disease. Grune and Stratton. New York and London, 1971.

Somerville EW. Rotational lordosis: the development of the single curve. J Bone Joint Surg (Br) 1952;34-B:421-428.

Taylor JR. Scoliosis and growth : patterns of asymmetry in normal vertebral growth. Acta Orthop Scand 1983;54:596-602.

Vital JM, Beguiristain JL, Algara C, Villas C, Lavignolle B, Grenier N, Sénégas J. The neurocentral vertebral cartilage: anatomy, physiology and physiopathology. Surg Radiol Anat 1989;11:323-28.

Williams PL (ed.), Warwick, Dyson et al. Gray's Anatomy, 37th ed. Churchill Livingstone. Edinburgh and New York, 1989.

Yamazaki A, Mason DE, Caro PA. Age of closure of the neurocentral cartilage in the thoracic spine. J Ped Ortho 1998;18:168-72.

CHAPTER 2

CRITICAL REVIEW OF THE LITERATURE

The goal of this review is to synthesize and reflect critically on scoliosis research to date while highlighting areas worthy of further consideration. A simple and exhaustive description of scoliosis research to date has been avoided since this has already been comprehensively presented elsewhere (see Robin, 1990).

THE NECESSITY FOR A NEW APPROACH

In his book 'DNA: The Secret of Life' James Watson (2003) reflected on the work of Charles Davenport (1911) who attempted to use pedigree analysis to determine the mode of inheritance of complicated traits such as intelligence and musical ability. Watson (2003) concluded that the work was 'useless' because it was based on false assumptions and failed to consider fundamental principles. A review of the literature relating to scoliosis is full of contradictory results. This is possibly due to the poor design of many experiments which have examined groups of patients with AIS without considering the underlying principle of whether or not AIS has a single cause. As was explained in the first chapter, if AIS has more than a single cause then experiments in which patients with AIS have been assigned to a single group are fundamentally unsound in design. Consequently, after reviewing current scoliosis literature which is full of studies in which a single cause of scoliosis has been an underlying principle in experimental design, the reader is led to question whether this literature is 'worthless' in the same vein as Watson (2003) evaluated the work of Davenport (1911).

Ironically, while being very critical of the literature and the experimental design of many studies, this same literature may actually contain several, very valuable clues into the problem of scoliosis. For example, the diversity and abundance of contradictory results relating to AIS could be explained if it was assumed that AIS develops from a variety of separate causes which manifest with different symptoms, natural history and progressive properties. The implication is that specific theories of AIS would need to be limited to subgroups of patients and attempts to explain all cases of AIS with an all-encompassing theory would not be possible. For future progress to be made, perhaps large changes are required in the approach to experimental design and the way that past literature is reviewed. For example, experiments would need to be carefully designed with the knowledge that AIS is the common endpoint of multiple causes. In the clinic, identification of the specific underlying cause for a particular AIS patient would be absolutely imperative because it would direct treatment therapy that was cause-based rather than symptom-based. Finally, past research needs to be carefully evaluated with this approach in mind to determine what conclusions could be gleaned from previous experiments because they almost certainly contain important information but which unfortunately is buried under poor experimental design.

In recent years, it has been shown that there is an association between low levels of folic acid in the maternal diet and neural tube defects (e.g. spina bifida). The government-regulated addition of folic acid to the maternal diet has led to a drastic reduction of such defects. This represents a huge achievement for spina bifida researchers in their search for a method to eradicate this abnormality. A comparison to the current state and direction of AIS research suggests that a similar cure for AIS does not appear probable even within the next fifty years with our current approaches and suggests that it may be time for a radical change.

OVERVIEW OF ADOLESCENT IDIOPATHIC SCOLIOSIS

Another example of the fundamental problems associated with scoliosis research is demonstrated simply by considering the traditional definition of scoliosis. According to the Scoliosis Research Society (Lovell and Winter, 2001), scoliosis has been defined simply as a lateral curvature of the spine greater than 10 degrees Cobb presumably as viewed on a two-dimensional radiograph. Although this definition has served well and has been driven by treatment considerations, it seems inadequate and too simplistic to be of any real use in understanding the overall deformity. Scoliosis is clearly a three-dimensional deformity (Lovell and Winter, 2001) and yet the current definition of scoliosis is based on two dimensions which limits considerably the conception and understanding of this condition. This might be best expressed as 'Measure in 2-D, think in 2-D'. Scoliosis needs to be regarded as a three-dimensional deformity and so we need to measure in 3-D. The development of classification systems that rely on more than one viewing plane such as the recent Lenke system (Lenke et al., 2001) appears to have much potential, although the reliability of such systems remains to be determined (Lenke et al., 2001; Ogon et al., 2002; Richards et al., 2003). In addition to this problem, numerous authors also disagree as to whether vertebral rotation should be included in the definition of scoliosis (Keim, 1979; Miller et al., 2001). The presence of vertebral rotation does not appear to be conclusively established (Robin, 1990) even though all images of AIS clearly show the spinous process in the concavity (Keim, 1979) and it is considered to be a staple condition for any model. Among the authors who argue for the presence of both vertebral rotation and lateral curvature in the definition of scoliosis, it has not been determined whether the rotation or the curvature is primary. Although this question might theoretically be investigated by looking for cases of scoliosis in which patients present with a curve but no vertebral rotation (or alternatively vertebral rotation without a curve), this approach is nearly impossible in practice. AIS patients without a scoliotic curve do not present to the scoliosis clinic, and conversely, by the time that patients present clinically, vertebral deformities are well-developed and curves are usually accompanied by vertebral rotation. To complicate further the problems surrounding the definition of scoliosis, some authors argue that all cases of scoliosis present with a hypokyphosis in the thoracic region which is fundamental to the development of the scoliosis (Somerville, 1952; Dickson, 1988), while other authors have found that hypokyphosis appears only in a subgroup of AIS patients (Lovell and Winter, 2001; Villemure et al., 2001). Those authors who argue for hypokyphosis (Somerville, 1952; Dickson, 1988) maintain that this hypokyphosis creates an unstable mechanical environment which causes scoliosis. However this theory appears to be based largely on anecdotal clinical evidence or extremely limited animal work and requires further verification with systematic studies and animal models.

With many authors disputing the very definition of scoliosis, other uncertainties relating to scoliosis are almost unavoidable since authors potentially include different entities and aspects in their discussions of scoliosis. Although a clear and precise definition of scoliosis would help to clarify the problem, perhaps the very nature of scoliosis is so varied that such a definition would be impossible to formulate in an all-encompassing manner.

Characteristics of adolescent idiopathic scoliosis

A review of the research into AIS reveals that many studies on this topic are contradictory and confusing, with few definitive facts having been formulated about scoliosis (Robin, 1990). Interestingly, all of these definitive facts would likely be observed within just minutes of attending a scoliosis clinic! According to Asher (in Burwell et al., 2000), four main facts are currently known about AIS:

- **Predilection for females** – Although the incidence of AIS is almost equal in males and females (Lovell and Winter, 2001), 70% of severe and progressive cases of AIS occur in females (Keim, 1979).
- **Dependence on growth** – There is a clear and positive association between periods of accelerated growth, such as puberty, and scoliotic curve progression and development (Burwell, 1971; Weinstein, 1986; Lonstein, 1994). In fact, it has been suggested that the increased susceptibility in females to AIS is due to the shorter and more rapid adolescent growth spurt as compared with males (Lowe et al., 2000). The dependence of scoliosis on growth raises the interesting question of whether there are some children with all the necessary components to develop scoliosis but who do not develop scoliosis because they are not growing.
- **Familial pattern of inheritance** – Formalized population studies (MacEwen, 1969; Riseborough and Wynne-Davies, 1973; Miller, 2001) show that 11% of the first-degree relatives of the index patient are affected with scoliosis (Riseborough and Wynne-Davies, 1973). Unfortunately, the mode of inheritance of AIS remains unknown with different studies suggesting that it may be autosomal dominant, X-linked or multifactorial (Cziezel et al., 1978; Bell and Teebi, 1995; Miller et al., 1998; Miller, 2001). This confusion likely reflects that different causes of AIS are inherited in a different manner.
- **Variable presentation** – There is extensive variation in the way that AIS cases present, with curves varying in parameters such as size, site, side, type, progressive properties and age of presentation.

Examining these basic facts, it is striking how little information about AIS is currently known. Despite the wealth of recorded experiments, very little is understood about AIS and, other than these basic facts it seems that for every group of patients in which positive results are found to support a particular association, there is a comparable group which shows negative results (Bagnall et al., 2004).

Diagnosis

Scoliosis is often suspected on the basis of screening examinations for back asymmetry and the method normally used to confirm the diagnosis is radiographic visualization of a Cobb angle of at least 10 degrees (Miller, 2001). Although this definition is used clinically, it is important to note that Cobb angle measurements have a high degree of intraobserver and interobserver variation, with a 95% confidence interval for radiographic determination ranging from 2.8 degrees to 10 degrees (Shea et al., 1998). In addition, it has been found that in cases of moderate to severe scoliosis, there is a significant difference in Cobb angle when the same patient is measured at different times in the day (Beauchamp et al., 1993), with the effect of gravity presumably accounting for a five degree increase from morning to evening measurements. As a result of these variations in Cobb angle, diagnosis of early cases of scoliosis on the basis of Cobb angle alone is extremely difficult. In practice, Cobb angle measurements serve as a means to confirm a diagnosis of scoliosis that is evident on visual examination of back asymmetry and as a method of monitoring scoliosis progression, rather than as a purely diagnostic tool.

Currently, scoliosis is primarily evaluated and assessed by measuring the Cobb angle using two-dimensional radiographs that are acquired each time the patient visits the scoliosis clinic. This approach to assessment provides a limited understanding of AIS since scoliosis is a continuous process and cannot be evaluated properly with static images. For this reason, the technique of 'morphing' has been applied to patient radiographs to create a continuous visualization of curve development, with the usefulness and accuracy of this method depending on the number of radiograph images available (Bagnall et al., 1998). Unfortunately, the time consuming nature of the morphing technique has prevented its widespread clinical use but the basic concept should be explored further. It is also necessary to consider that radiographs acquired and depicted in two dimensions cannot fully describe the three-dimensional deformity of a scoliotic spine and so the use of three-dimensional imaging techniques also needs to be explored further. An interesting concept of determining and visualizing the plane of maximal deformity in three dimensions is captured in the "plan d'élection" introduced by Stagnara (see Stokes, 1994). It is currently in use at a few major centers and may provide a more useful method of assessment of AIS and a more valid indicator of treatment outcomes than simple measurement of Cobb angle from plane radiographs.

Treatment

As there is so little understanding of aetiology, most research and presentations at scientific meetings are predominantly concerned with treatment methods. Yet at the most basic level, there are many popular misconceptions about the necessity and reasons for AIS treatment. In the majority of cases, treatment of AIS is not required to prevent mortality due to this condition but is instead primarily aimed at reducing the cosmetic deformity of scoliosis. This cosmetic deformity is very significant as it occurs at a fragile time of personality development which affects patient compliance (Bagnall et al., 2004) and has potential long-term effects on quality of life if left untreated. It has been found that women with untreated AIS are less likely to marry and that individuals with untreated AIS have an increased incidence of back pain (Fowles et al., 1978; Weinstein, 1989). Of course, with extreme cases of AIS, there is also the danger of cardiopulmonary compromise as the rotation of the vertebrae and adjoining ribs can impinge on the heart and lungs (Keim, 1979; Lonstein, 1994). However, the number of these extreme cases is small in relation to the number of total cases of AIS. Future work is still being completed on the long-term effects of untreated scoliosis and it is anticipated that a greater understanding of this area would potentially determine the merits of treatment in different cases.

The current approaches used in scoliosis management include non-operative and operative forms of treatment. Of the different non-operative methods explored (Lonstein et al., 1994), only bracing has been shown to be effective at preventing further curve development during periods of growth although bracing has still not been accepted in some countries. It is important to stress that the goal of bracing is not to correct a curve, but rather to prevent a curve from progressing (Lovell and Winter, 2001). Although it is known that vertebral deformities in animal models can be reversed or altered with the application of forces (Mente et al., 1997), little work appears to have been done to establish if and how vertebral morphology in AIS changes with the use of bracing. Although it seems logical that the site and magnitude of the force applied by a brace would need to be altered continuously as a scoliotic curve showed some degree of correction, this is not commonly done in practice and further research in this area may be warranted. If a scoliotic curve continues to progress after bracing or if the patient's curve reaches 45-50° with significant trunk asymmetry, then spinal fusion and the implantation of rods in the spine is indicated (Lonstein, 1994; Lovell and Winter, 2001). This stabilization is based on fixation of the spine in a balanced position in the coronal and sagittal projections while fusing the minimum number of vertebrae so that the greatest number of mobile segments possible can be maintained.

The absence of an indicator which separates future progressive curves from non-progressive curves is a major concern in scoliosis. Currently, the two main factors used to predict potential curve progression are patient maturity and the severity of the curvature. In general, larger curves in a younger child have a greater chance of progression (Lonstein, 1994). For example, the chance of progression for a curve over 20 degrees has been estimated at 68% for an immature adolescent, with this probability decreasing to 22% for a smaller curve of less than 20 degrees (Bunnell, 1986; Nachemson, 1993). Although these general factors have value in predicting the probability of curve progression, the discovery of specific factors such as genetic markers or specific vertebral morphologies that could be used to identify progressive and non-progressive curves in individual cases would be a major advance. However, for these specific factors to be useful they would also have to be supplemented with greater knowledge of how to manipulate spinal curves so that existing or new treatment modalities could be applied earlier or in a more aggressive manner to subgroups of AIS patients with a greater risk of progression.

Etiology

Over the past century, much research has been completed concerning the etiology of AIS and yet the cause (or causes) of this disorder remains elusive. Different studies have focused on genetic factors, connective tissue abnormalities, metabolic factors, biochemical factors, abnormalities of the central nervous system, hormonal variations, biomechanical factors and differing growth patterns (for a comprehensive review, see Robin, 1990; Lowe et al., 2000; Miller, 2001, Ahn et al., 2002). Unfortunately, these studies have failed to establish conclusively any one of the above as the causative agent of AIS (Rinsky and Gamble, 1988; Robin, 1990; Lonstein, 1994, Miller, 2001) and it is debatable whether such a single factor even exists.

The greatest problem with studies of AIS etiology is that it is impossible to separate cause and effect in the development of spinal curves since patients present after vertebral deformities are well-established. As a result, there is often no window of time between the initial presentation of patients to the scoliosis clinic and the development of secondary biomechanical changes in the vertebrae as a result of the scoliosis. In a patient with well-established scoliosis, it becomes almost impossible to determine unambiguously if a given condition, especially a vertebral change, is a cause or an effect of scoliosis.

Much of the confusion surrounding AIS also relates to the diverse range of opinions about the etiology of scoliosis even at the most fundamental levels. For example, some authors have acknowledged that two mechanisms may be involved in the development of scoliotic curvatures with one being responsible for initial development and another accounting for curve progression once the normal biomechanics of the spine have been altered (Lonstein, 1994). As an extension, this would imply that a scoliotic curve might continue to progress even if the initial factors responsible for curve development were no longer present or identifiable. Therefore, obtaining measurements from patients who already have well-established scoliosis would not reflect the initial cause of the deformity. By the time that a patient has scoliosis, the window of time when the factor responsible for scoliosis was present may have been missed.

The similarity of patients with AIS is also sufficiently specific for some authors to suggest that it is a single entity, while conversely there is also enough diversity for others to believe that AIS is the final common pathway of a number of different causes, with each cause potentially requiring or interacting with other factors (Lonstein, 1994). With most research suggesting that AIS may have several, completely separate underlying causes (Robin, 1990; Coillard and Rivard, 1996; Bagnall et al., 2004), there is a need to reconsider the way that etiologic studies are designed. If AIS has multiple causes, then any random sample of AIS patients would likely include patients with completely different and separate causes, making it impossible to identify and study any one particular etiology. In fact, it is likely that any measured value noted in a few patients with the same cause of scoliosis would be obscured by the average results from the total group of AIS patients. A better approach might entail the development of a plausible theory of AIS development and the testing of this theory in an animal model to determine if there are specific clinical markers that would be exhibited in a group of AIS patients with the same cause for their scoliosis (Bagnall et al., 2004). If specific markers could be identified (e.g. asymmetric NCJ development with the more open NCJ on the concavity as seen on MRI), then a group of patients with this presentation could be assembled to provide a more suitable pool to explore a particular cause of AIS.

Although it is generally assumed that different causes of scoliosis present in a different manner and that a single cause of scoliosis presents similarly, it is important to further investigate this assumption. In fact, an in-house study of 40 pinealectomized chickens with scoliosis (Soochan et al., in press) demonstrated that curves varied extensively in terms of direction (15 right, 18 left, 7 double), Cobb angle (11-68 degrees), number of vertebrae involved (3-11), apical location (T5-L5) and extent of wedging. These results strongly suggest that the etiology and the pathogenesis of specific curves must be considered separately. This work does not disprove the idea that specific clinical markers are associated with scoliosis due to the same cause, but it does suggest that these specific clinical markers are not parameters such as the direction, extent and location of the scoliotic curvature. Further work is required to determine which parameters and vertebral changes are consistent and inconsistent between cases of scoliosis due to different causes. Hopefully, this will aid in determining how patients with different causes of scoliosis can be accurately separated.

Animal Models of Scoliosis

The study of AIS etiology has also been hampered by the difficulties in creating a suitable and representative animal model. Reviewing the work completed to date, it seems that scoliosis has been easy to produce with the use of numerous interventions (see Robin, 1990 for a comprehensive review). Yet, many of these methods, such as the resection of the ends of the ribs (Sevastik, 2000), are obviously not the same means by which AIS results in human subjects. Furthermore, few of the models created have resulted in curves that bear any resemblance to those seen in AIS patients. With relatively few bipedal animals to choose from, most test animals have been quadrupeds and have not possessed the unique bipedal stance that affects spinal biomechanics and curvatures in the human (Wever et al., 1999). One exception to these studies involves the pinealectomized chicken model (Thillard, 1959; Machida et al. 1993, 1994, 1995, Bagnall et al., 2004) in which the scoliosis created has shown many of the characteristics seen in patients with AIS, although there are obvious difficulties extending this work to the human because of the large differences in human and avian phylogeny. The recent use of bipedal rats may also have merit (Machida et al., 1999), although this model is still in the early stages. Despite all of the above difficulties inherent in finding an appropriate model, scoliosis research requires the use of animal models. The study of an appropriate animal model would allow scoliotic curves to be observed from their initial stages, in contrast to studies of human patients where the curves present well after any evidence of cosmetic deformity. By observing curves in their earlier stages, it would become possible to develop early diagnostic methods and it would enable the separation of the primary and secondary effects of the scoliotic curvature. The use of an animal model may also allow the development of more appropriate treatment methods that are based on etiology rather than symptoms (Bagnall et al., 2004). Finally, a reliable animal model would also allow the development of methods by which the spine can be manipulated regardless of the cause of scoliosis, especially if the underlying cause is no longer present and the problem is simply biomechanical.

Requirements for an acceptable solution for AIS

In consideration of the characteristics and presentation of AIS, any solution to the problem of AIS must address the following questions:

-Why do females tend to present with curves that are more severe and progressive?

-Why is the development and progression of AIS associated with the growth spurt of puberty?

-Why is there a clear familial pattern to the presence of AIS?

-Why do some curves regress, others get worse and some stay the same?

-Why are most thoracic curves directed to the right side?

-Why are the primary and the secondary curves always adjacent to one another and never separated by a region of unaffected vertebrae?

-How does the given cause explain the vertebral rotation, lateral curvature and atypical morphology of the vertebrae seen in AIS?

-What factors are responsible for the initial production of the scoliotic curve and which factors are responsible for progression of the scoliotic curve? At what stage or stages is AIS still reversible?

MORPHOLOGY OF VERTEBRAE FROM AIS PATIENTS

Knowledge of vertebral morphology and its abnormal development in AIS patients is essential in evaluating theories of AIS etiology, understanding the biomechanical forces involved in scoliosis and refining treatment strategies such as brace management and surgical correction. Unfortunately, in AIS it is extremely difficult to assess whether the abnormal vertebral morphology is a reflection of initial, underlying asymmetric development of the vertebrae, asymmetric force distribution secondary to the scoliosis or a combination of both. Some authors have considered asymmetric vertebral growth to be a primary cause of scoliosis (see Lonstein, 1994; Ahn et al., 2002). Among this school of thought, AIS has often being attributed to asymmetric NCJ development (Nicoladoni, 1909; Knutsson, 1963; Roaf, 1963; Michelsson, 1965; Vital et al., 1989; Yamazaki et al., 1998). Other authors have suggested that AIS is due to the increased growth of the anterior portion of the vertebra or decreased growth of the posterior segment (Somerville, 1952; Dickson, 1988; Guo et al., 2003). A recognized complication for both schools of thought is well expressed in Roaf's "vicious circle" model (1960, 1963) which suggests that the asymmetric vertebral morphology resulting from scoliosis alters the force distribution in the scoliotic spine and causes asymmetric loading, which then results in further progression of the initial vertebral asymmetry as an effect of the deforming force.

In contrast, other authors believe that any vertebral asymmetry is strictly a secondary change (Dale-Stewart, 1952; Roaf, 1960; Fidler et al., 1976; Spencer and Eccles, 1976; Burwell and Dangerfield, 1977; Sahlstrand et al., 1978, 1979; Khosla et al., 1980; Sahlstrand, 1980; Sahlstrand and Lidstrom, 1980; Ford et al., 1984; Geissel et al., 1991; Goldberg et al., 1995; Wever et al., 1999; Ahn et al., 2002). This conclusion is usually based on observations and measurements that show progression of vertebral and rib deformities well after the initial scoliotic curvature. However, it is important to recognize that this would not rule out the important possibility that asymmetric growth is both a primary cause and a secondary result of AIS.

Although there have been many studies involving vertebral measurements, the irregular shape of the vertebra has led to a variety of definitions for what are supposedly the same parameters. For example, the length of the pedicle has been extremely difficult to define as its contacts with the body and the lamina are not immediately obvious. Second to this initial problem is that as the vertebra becomes deformed, landmarks often move making unreliable many measurements that were reliable for normal vertebrae. Acknowledging these difficulties, further investigation of vertebral asymmetry in AIS will still require the creation of measurement definitions that apply to both normal and deformed vertebrae so that vertebrae from AIS patients can be accurately compared with normal vertebrae. Furthermore, investigation of vertebral asymmetry will benefit from studies with suitable animal models for scoliosis, in which primary and secondary changes in vertebrae can be more accurately monitored and new methods of treatment can be attempted. Although it has been shown that vertebral wedge deformities in a rat model can be corrected by reversing the side and the direction of the load used to create such deformities (Mente et al., 1997, 1999), it remains unclear whether techniques such as bracing can alter the abnormal morphology of the vertebrae in AIS or even have the potential to do so (Mente et al., 1999). In fact, it has been found in numerous animal models and clinical studies that the deformation of the intervertebral disc caused by long-term asymmetrical loading is semipermanent (Wynarsky and Schultz, 1991) or perhaps even irreversible (Taylor et al., 1981; Bibby et al., 2002). To date, it also remains unknown whether this asymmetric growth is localized in the vertebral column or is a more generalized somatic phenomenon, as suggested by studies that have found shortening of the upper limb on the concave side of the curvature (Burwell and Dangerfield, 1977).

Vertebral Deformities in Scoliosis

In general, studies on vertebral morphology in scoliosis have generated conflicting results (Table 2-1), which are partially due to the varying methods used to measure vertebral morphology in scoliosis patients. In most cases, studies have used different definitions for vertebral measurements and therefore comparisons of the same parameters between studies are difficult. For example, starting and end points are difficult to define for the measurement of pedicle length in the transverse plane and therefore different landmarks have often been used, with some studies measuring length parallel to the vertebral midline and others measuring along the pedicle axis. In most cases, intraobserver and interobserver variation have not been measured or even mentioned in these studies which makes comparison between studies difficult. To complicate the issue further, different studies have used different methods to gather data including measurement from anatomic or histologic specimens (Nicoladoni in Knutsson, 1966; Enneking and Harrington, 1969; Taylor, 1983, Vital et al., 1989), plain radiographs (Xiong et al., 1994; O'Brien et al., 2000), CT images (Vital et al., 1989; Smith et al., 1991; Xiong et al., 1995; Wever et al., 1999; Liljenqvist et al., 2000; O'Brien et al., 2000), MRIs (Liljenqvist et al., 2002) and three-dimensional digitizing protocols (Parent et al., 2002). Unfortunately, all of these in-vivo imaging techniques do not appear to be equally effective. For example, the assessment of vertebral morphology using conventional plane radiographs has been difficult due to the overlapping of landmarks. Although computed tomography (CT) has also been used, the gantry cannot be aligned to compensate for curves in the coronal plane and as a result some vertebrae are always transected obliquely, which affects measurement accuracy. Currently, magnetic resonance imaging (MRI) is being promoted as the most accurate means of characterizing pedicle morphology since the plane of acquisition can be predetermined and altered in all three dimensions on an individual basis to obtain precise images. MRI also has the

Table 2-1. Vertebral deformities in scoliosis

Plane	Deformity	Comment
Sagittal	**Hypokyphosis** - The primary deformity in the sagittal plane is thought to be the hypokyphosis in the region of the apical vertebra for thoracic curves (Somerville, 1952; Roaf, 1960; Smith et al., 1991).	Some authors have found that hypokyphosis only appears in a subgroup of AIS patients (Lovell and Winter, 2001; Villemure et al., 2001). To date, the theory that hypokyphosis is an essential aspect of scoliosis appears to be based largely on anecdotal clinical evidence or extremely limited animal work and requires further exploration.
Coronal	**Wedging** - Anatomic and radiologic studies have shown that the vertebrae display wedging with decreased vertebral height and disc thickness on the side of the concavity, with this wedging decreasing in magnitude further away from the curve apex (Roaf, 1960; Enneking and Harrington, 1969; Keim, 1979; Dickson et al., 1984; Smith et al., 1987; Perdriolle et al., 1993; Xiong et al., 1995, Parent et al., 2002).	Although these vertebrae exhibit decreased height on one side of the vertebra in relation to the other side, it remains unclear how the heights of the deformed vertebra compare to those of a normal vertebra.
Transverse	**Vertebral body rotation** - In idiopathic scoliosis, authors consistently agree that the direction of rotation for the apical and adjacent vertebral bodies is towards the convexity of the scoliotic curve (see Keim, 1979).	In thoracic scoliosis, the accompanying rotation of the ribs results in a posterior bulge of the ribs on the convexity of the curve and the appearance of the characteristic "rib hump."
Transverse	**Spinous process deviation** - Due to the vertebral rotation, the base of the spinous process also rotates towards the concavity (see Smith et al., 1991). However, while some authors have found that the tip of the spinous process points into the concavity and thus remains in line with the rest of the vertebra (Knutsson, 1966; Enneking and Harrington, 1969; Keim, 1979; Porter, 2000; Liljenqvist et al., 2000), others have found that the tip of the spinous process bends towards the convexity (Knutsson, 1966; Wever et al., 1999).	Bending of the spinous process has been attributed to the tethering effect of the muscles and ligaments in the posterior spine (Wever et al., 1999).
Transverse	**Pedicle thickness** - Studies have consistently shown that in the apical region of a scoliotic curve the pedicle on the convex side is thicker in the transverse plane while the pedicle on the concave side is thinner (Roaf, 1960; Smith et al., 1991; Wever et al., 1999; Liljenqvist et al., 2000, 2002; Parent et al., 2002). To date, it has not been established whether changes in pedicle thickness are present at all stages of AIS. In fact, Vital et al. (1989) found no difference in pedicle thickness during the early stages of AIS, which may suggest that changes in pedicle thickness are a result of the altered biomechanical forces in AIS.	The changes in pedicle thickness have been attributed to the changed axis of rotation for the deformed vertebra, which is thought to result in a compressive force on the pedicle on the convex side and a resulting increase in appositional bone growth (Smith et al., 1991), as suggested by Wolff's law.
Transverse	**Pedicle length** - Studies of pedicle length have generated widely	The variation in findings may reflect the variety of definitions and

	conflicting results. Although Liljenqvist et al. (2002) found no differences in pedicle length in the apical region where it is generally accepted that the extent of deformity is greatest, several authors have reported pedicle length asymmetry in AIS. Some authors have found that the longer pedicle is consistently located in the apical and adjacent vertebrae on the concave side of the scoliotic curve (Nicoladoni, 1909; Knutsson, 1963; Taylor, 1983; Vital et al., 1989), whereas Roaf (1960) found that the longer pedicle is on the convex side. Artistic representations of vertebrae from scoliosis patients are unclear and in one case, the same artist has depicted exact opposite representations (Keim, 1972 and 1979).	techniques used for measurement (Vital et al., 1989; Smith et al., 1991; Xiong et al., 1995; Wever et al., 1999; Liljenqvist et al., 2000, 2002; O'Brien et al., 2000; Parent et al., 2002). In these studies, pedicle length has been compared between the two sides of vertebrae from AIS patients and it remains unknown how pedicle lengths in AIS compare to pedicle lengths in normal patients.
Transverse	**Lamina width** – Relatively few studies have examined changes in the lamina (Coillard and Rivard, 1996). Roaf (1960) has found that the laminae are larger in all dimensions (presumably length and width) on the convex side of the curve although he does not describe his measurement definitions or techniques. Other authors have agreed the laminae are thicker on the convex side in relation to the concave side but make no mention of lamina length (Enneking and Harrington, 1969; White and Panjabi, 1990).	In considering that the pedicle and the lamina are adjacent anatomic regions, it would be interesting to determine if growth in length at one site (such as the pedicle) resulted in an increased or a decreased growth at the adjacent site (such as the lamina) as this type of correlation does not appear to have been performed. Performing this correlation would help determine whether the pedicle and lamina length developed in concert to maintain a constant neural arch length protecting the spinal cord.
Transverse	**Vertebral canal deviation** - In examining the vertebral canal in cadavers whose scoliosis had long been established, it has been found (Smith et al., 1991; Porter, 2000) that although the vertebral bodies in AIS rotate towards the convexity, the vertebral canal retains its midline orientation. As a result, the long axis of the canal rotates towards the concavity and the spinal cord comes to lie against the concave pedicle.	Unfortunately, further work is needed to characterize the vertebral canal and to verify these findings since neither Porter (2000) nor Smith et al. (1991) systematically measured the position of the vertebral canal and both instead relied on visual observation or deduction. To add to the confusion surrounding the position and morphology of the vertebral canal, Netter in Keim (1972, 1979) has produced two artistic representations clearly showing that the vertebral canal is narrower on one side of the scoliotic curve. However the side depicted as narrower has changed from the convexity to the concavity between the two illustrations.

additional benefit of being radiation-free, which facilitates routine clinical use in the visualization of patients in the early stages of AIS although it is often expensive and unavailable.

In addition to problems with the method of measurement, vertebral morphology studies have encountered problems with the patient pools used. Most studies have been conducted on patients with severe AIS (Xiong et al., 1995; Liljenqvist 2000) or even outside the adolescent age group (Smith et al., 1991; Wever et al., 1999; Parent et al., 2002). Unfortunately, the selection of advanced cases of AIS has the potential to affect significantly the vertebral morphology noted (Vital et al., 1989) and leads to further difficulty differentiating primary and secondary changes in morphology. It might be better to examine patients in the early stages of AIS when asymmetries are developing directly in conjunction with spinal curves. Furthermore, in those cases in which measurements have been acquired from unknown cadaveric specimens whose scoliosis has been long established, the idiopathic nature of this scoliosis cannot necessarily be verified. With these types of skeletal specimens, any conclusions about etiology must be approached with extreme caution, since the deformities are fixed in time and it is difficult to determine if they are a primary cause or a secondary result of AIS.

Future directions

To advance further the knowledge of vertebral morphology in AIS, a new approach will be needed. The ideal approach will require the creation of reliable definitions for the measurement of vertebral parameters. These definitions will need to apply to both normal and deformed vertebrae and must be applied in conjunction with an in-vivo imaging technique. Patients would need to be selected early in the course of scoliosis development to minimize secondary changes in vertebrae and therefore provide the most value for the evaluation of AIS etiology and the development of new techniques of diagnosis. Finally, in recognizing that AIS is due to numerous different causes, it would be useful to determine if the morphology of vertebrae from AIS patients was consistent or if subgroups of vertebrae could be identified, each potentially representing a different cause.

VERTEBRAL GROWTH

A basic understanding of vertebral growth is a necessary prerequisite for the investigation of vertebral pathology, yet to date, the process of vertebral growth has remained largely a mystery, especially with regards to the contribution of different growth plates and the mechanism of growth after closure of these plates. It is difficult to explain how a vertebra that was initially small enough to fit completely inside the vertebral canal of an adult has the potential to grow and remodel to attain the full adult dimensions especially with the early elimination of cartilaginous junctions. Vertebral growth is further complicated by the fact that in evolutionary terms a vertebra is a composite of several bones, each of which has possibly retained its own identity in relation to growth and development but also has the potential to affect neighboring elements (Roaf, 1960). Of the different components, the vertebral body is thought to have the greatest influence on the other components and in the production of anomalies (Roaf, 1960) and yet is itself a composite bone.

Chondrification and ossification

In the sixth week of embryonic development, the mesenchymal model of the vertebra chondrifies to form the cartilaginous vertebra. Six chondrification centers appear : two centers that come to unify in the centrum, two centers in each half of the neural arch and two centers at the junction of the neural arch and the centrum. It is suspected by some authors (Bagnall et al., 2004) that the six chondrification centers may correspond to the separate bones that make up the composite vertebra, although this is difficult to prove. After these chondrification centers expand and the cartilaginous axial skeleton forms, the next developmental stage is primary ossification. Three primary centers of ossification appear in each vertebra (except for C1, C2 and the sacral vertebrae), one in the centrum and one in each half of the neural arch extending just beyond the pedicle. Three plates of hyaline cartilage are thought to remain as these ossification centers expand towards one another: the two neurocentral junctions (NCJs) between the centrum and the neural arch, and the posterior synchondrosis between the two halves of the spinous process (PS) (for a diagram of vertebral growth plates and ossification centers refer to Moore, 1999), although Chandraraj and Briggs (1991) claim to have found three growth cartilages for each half of the neural arch. The PS has been observed to close between three months (Lord et al., 1995) and six years of age (Moore et al., 1999) based on anatomic and radiologic visualization. Similarly, the age of NCJ closure remains highly variable and controversial with some studies of anatomical specimens suggesting that the NCJ closes well before the age of 10 (Ottander, 1963; Knutsson, 1966; Roaf, 1966; Taylor, 1983; Williams et al., 1989; Maat et al., 1996) whereas recent MRI studies have found that closure occurs between 11-16 years (Yamazaki et al., 1998). For both the PS and the NCJ, the age of closure may depend on the region of the vertebral column (Vital et al., 1989), although the specific sequence of closure ages in the different regions has not been clarified. This is highly significant since it would suggest that vertebral growth patterns may be different depending on the level of the vertebral column. Both the NCJ and the PS have been shown to be bipolar (Tondury and Theiler, 1990; Ganey and Ogden, 2001), which suggests that asymmetric growth on either surface of the growth plate (for either the PS or the NCJ), along one portion of the growth plate (for either the PS or the NCJ) or on one side of the vertebra (in the case of the NCJ) might lead to the development of abnormal vertebral morphology. Determining the normal pattern of growth and development of these growth plates would be valuable for predicting the time period during which any abnormal vertebral morphology would manifest. In addition to the PS and the NCJ, the expansion of the enlarging primary ossification center in the centrum also creates the superior and inferior physeal growth plates (Bick and Copel, 1950; François and Dhem, 1974; Doskocil et al., 1993; Ganey and Ogden, 2001), which are characterized by an area of rapidly maturing cartilage that melds imperceptibly into the cartilage of the chondroepiphysis (Ganey and Ogden, 2001). These growth plates are unipolar (Doskocil et al., 1993) and have been found to close between 16 to 22 years of age (Ganey and Ogden, 2001).

In addition to the primary ossification centers, five secondary ossification centers develop in each vertebra during puberty: one at the tip of the spinous process, one at the tip of each transverse process and two annular apophyses, on the superior and inferior edges of the centrum. These apophyses should not be confused with the epiphyses of long bones, since the apophyses do not make any significant contribution to growth

(Ganey and Ogden, 2001). Interestingly, mammals other than the human have a complete plate-like epiphysis (Ganey and Ogden, 2001) instead of an apophysis. Since a true epiphysis would protect the underlying physis from shear forces, the presence of an apophysis in humans may make the superior and inferior physeal growth plates more susceptible to abnormal biomechanical forces.

Three dimensional growth of the vertebra

As a three-dimensional structure, a vertebra grows in all directions simultaneously, although growth in each dimension probably occurs in a different manner, at a different time in development and likely at a different rate. In fact, every growth plate in the vertebra undulates in three dimensions and therefore must have vector components of growth in each dimension. To simplify the description of vertebral growth, growth in each dimension will be considered separately although no dimensions of vertebral growth can be considered independent.

Longitudinal growth

The growth of vertebrae in height is due to the superior and inferior end plate physes (Bick and Copel, 1950; François and Dhem, 1974; Doskocil et al., 1993; Ganey and Ogden, 2001), with no interstitial growth occurring in the vertebral body (Haas, 1939). In this sense, the growth of the vertebral body in height has often been viewed using the model of a long bone with the vertebral body representing the diaphysis, although cell column formation in the physeal growth plates is not as organized as in a long bone physis (Lord et al., 1995). However, the long bone model is not entirely appropriate since the growth of the vertebral body in height also shows elements of round bone growth such as the absence of a primary bone collar and the lack of a true epiphysis. In considering the appearance of the physeal growth plates, there is likely some degree of regional variation based on Roaf's finding (1960) that the cephalic vertebrae grow at a slower rate than the caudal vertebrae. Considering that the two growth plates in a typical long bone such as the femur grow at different rates, there is every reason to assume that the superior and inferior end plate physes do not make equivalent contributions to growth. In fact, Moser (in Knutsson, 1961) used radiation to injure the physeal growth plates in a pig and found that growth in height was only due to growth at the superior end plate physis. Unfortunately, Moser's study (in Knutsson, 1961) did not include controls nor quantify the extent of damage done by radiation. In contrast to Moser, Knutsson (1961) suggested that both physes contribute equally to growth. His conclusion was based on the fact that the equator of Hanson, a translucent venous sinus visualized radiographically, remained equidistant from both physes throughout development. This conclusion is not definitive, since any landmark could move by longitudinal growth through the continuous process of bone remodeling. To date, the relative growth rate of the superior and inferior physeal growth plates remains to be elucidated and would be a valuable prerequisite to any surgical intervention in these areas. The growth rates could potentially be explored using fluorochrome markers and histomorphometric measurements from sagittal or coronal vertebral sections, although it would be difficult to conduct a longitudinal study of a single vertebra over a significant length of time.

Although most explanations of growth in vertebral height focus on the vertebral body, it is also necessary to consider the growth of the posterior elements which contribute to the height of the vertebral body. Ganey and Ogden (2001) suggested that the laminar and pedicular regions grew in height by means of growth plates at the NCJ and the PS, although this has not been supported with empirical evidence. If this were true and growth was restricted to cartilage growth plates, it would mean that growth in height of the posterior elements would be completed well before the growth in height of the anterior elements since the NCJ and the PS close well before the superior and inferior physeal growth plates, which are thought to close between 16 to 22 years of age (Ganey and Ogden, 2001). As a result, this would mean that a significant kyphosis would be present in normal development until the anterior elements grew to the same extent as the posterior elements. Although this may be the case according to Bernhardt and Bridwell (1989), who found that the thoracic kyphosis increases progressively until the end of adolescence, the link between kyphosis and scoliosis has not been sufficiently explored.

Growth in the coronal and sagittal plane

The growth in width of the vertebral body has been accounted for by two different mechanisms (Ganey and Ogden, 2001). Firstly, the processes of perichondrial and periosteal apposition have been found to account for an increase in vertebral body width, although these processes are only thought to be significant during the first few years of development. Secondly, all of the growth plates of the vertebrae have been found to enlarge interstitially by cell division and matrix expansion within the physis. Although both of these mechanisms are feasible, the current concept of growth in width of the vertebra appears overly simplistic. The extent of periosteal growth in later development has not been adequately assessed. In fact, studies on rat vertebrae (Hammond et al., 1974) have suggested that bone growth of the vertebral body occurs exclusively on the periosteal surface in early development, but occurs on both the endosteal and periosteal surfaces in later development. Furthermore, the traditional paradigm of bone growth suggests that periosteal growth does not change the size of a bone significantly, although this mechanism is involved in gradual changes in bone shape. Yet, the tremendous potential of the vertebra to grow in width and the continued growth of the vertebra in width after adolescence strongly suggest that the role of periosteal mechanisms in vertebral growth may need to be reevaluated.

Vertebral canal growth

The existing model of vertebral canal growth also requires further exploration. The current paradigm suggests that vertebral canal growth is primarily dependent on growth of the neural arch, since the position of the posterior surface of the vertebral body is determined early in development with the absence of subsequent periosteal deposition at this site (Erdheim in Knutsson and Wiberg, 1958; Lord et al., 1995). Accordingly, the progressive expansion of the vertebral canal in children is facilitated by the presence of three cartilaginous junctions within each vertebra. The initial growth in width of the vertebral canal is thought to be due to the PS, with continued growth dependent on the NCJs. Once the PS and the NCJs have closed, this model would suggest that the vertebral canal has attained its adult diameter. Some authors have stated that subsequent changes in the shape of the vertebral canal are possible by the process of periosteal deposition and resorption, but are thought to be quite minimal (Ganey and Ogden, 2001). To date, most knowledge of vertebral canal growth has been assessed primarily from measurement of canal diameter rather than direct measurement of bone deposition.

Studies on the anteroposterior diameter of the vertebral canal have produced conflicting findings, with Tulsi (1971) suggesting that the adult sagittal diameter is attained by four years, Knutsson (1961) finding that the final diameter is reached by age 10 and Larsen (1982) finding that the sagittal diameter still increases slightly between age four and adulthood. Studies on the transverse diameter are also controversial, with Tulsi (1971) and Larsen (1982) suggesting that approximately 85% of the transverse diameter is achieved by age four and Knutsson finding that the transverse diameter is completely attained by age 10 (1961). The conflicting results from studies on the diameters of the vertebral canal may be due to the canal changing shape with age and strongly suggest that studies of vertebral canal development cannot be exclusively based on measurement of diameter but should also include measurement of other markers, such as area. Regardless of these conflicting results, further knowledge of canal development will be useful if it can be shown that growth in different dimensions is under the control of different growth plates or different mechanisms. This could mean that a particular pattern of abnormal vertebral canal development, such as spinal stenosis could be traced to a specific growth plate or mechanism, depending on the phase of development.

Future directions

To date, much research has been done on the topic of vertebral growth. The challenge lies in integrating this research, explaining bone growth at the macroscopic level on the basis of bone tissue growth at the microscopic level and relating growth of the individual components to growth of the entire vertebra. Most importantly, vertebral growth needs to be explored outside the paradigm of traditional single bone growth, which is not appropriate for the three dimensional growth of a composite bone such as a vertebra.

THE NEUROCENTRAL JUNCTION

In their study on the basic morphology and radiology of the thoracic spine, Lord et al. (1995) concluded that the postnatal development of vertebrae has received virtually no attention in the orthopedic, anatomic and radiologic literature. This lack of basic information has limited the ability to understand the relationship between normal and abnormal patterns of vertebral growth. This generalization is exemplified by the investigation of the neurocentral junction (NCJ) which Maat et al. (1996) suggested has lost the attention of embryologists and anatomists. In fact, most knowledge about the NCJ has been acquired indirectly during the evaluation of the potential role of the NCJ in AIS. For this reason, understanding of this growth plate remains incomplete.

Role of the NCJ in growth

Each vertebra has two NCJs which are cartilaginous growth plates, situated one on each side, between the centrum and the neural arch. From an embryonic standpoint, the NCJ is the remnant of the hyaline cartilage model of the vertebra and could be identified as the ossification centers of the centrum and neural arch advanced towards each other (Sadler, 1995). Although the terms 'vertebral body' and 'centrum' are commonly used to refer to the same region, this is a mistake. The site of the NCJ marks the posterior limit of the 'centrum' and so the 'vertebral body' includes the 'centrum' as well as the contributions of the anterior portions of the neural arch. This is an important distinction because abnormal development of the posterior elements of a vertebra may affect the vertebral body as far as the site of the NCJ. Interestingly, this contribution of the posterior elements to the vertebral body varies considerably, with the cervical NCJs being the most sagitally oriented and thus making a significant contribution to the growth of the lateral portion of the vertebral body. In contrast, the thoracic and the lumbar NCJs are less sagitally oriented and therefore perhaps make less of a contribution to the growth of the lateral portion of the vertebral body (Ganey and Ogden, 2001).

As a growth plate, the NCJ does not conform to the traditional model of an epiphysis as seen in a long bone since it is bipolar with distinct growth columns on both surfaces (Vital et al., 1989, Töndury and Theiler, 1990; Maat et al., 1996; Yamazaki et al., 1998). In this respect, in examining NCJ growth it would be valuable to compare quantitatively the rate of growth on both surfaces, since these two surfaces do not necessarily grow at the same rate. In fact, the finding that the angle of the NCJ relative to the anterior border of the vertebral canal changes with age in any single vertebra (Taylor, 1983; Vital et al., 1989) would suggest that these surfaces might be growing at different rates. The further suggestion by Vital et al. (1989) that the medial aspect of the NCJ stays in a relatively constant position throughout development, while the lateral aspect moves further posteriorly would suggest that growth rates along parts of a given surface of the NCJ might vary.

Since the NCJ extends throughout most of the height of the vertebral body and from the most medial to lateral aspects, it could be inferred that the NCJ may contribute to anterior and posterior vertebral growth in all three dimensions, at least to some extent. To date, most attention has simply focused on the contributions of the NCJ to vertebral growth in the transverse plane. Most authors would contend that the NCJ contributes to the growth of the vertebral body and the neural arch in the transverse plane (Vital et al., 1989; Töndury and Theiler, 1990; Maat et al., 1996; Yamazaki et al., 1998) and this seems quite reasonable given its site, orientation and morphology. However, the precise contribution of the NCJ to this growth remains unknown and only Vital et al. (1989) have quantitatively estimated the contribution of the NCJ, suggesting that it is responsible for one third of the overall growth of both the vertebral body and the neural arch. Unfortunately, the methods used to derive this conclusion were not documented. In the transverse plane, the NCJ is also thought to play the principal role in determining the dimensions of the vertebral canal (Knutsson, 1966; Ganey and Ogden, 2001). As an application of this idea, Knutsson (1966) proposed that the age at which the adult diameter of the vertebral canal is attained could be used to derive the age of closure of the NCJ although this is based on the assumption that the NCJ cartilage does not lie dormant before becoming absent, which may not be true. The contributions of the NCJ to vertebral canal growth have been supported by the work of Canadell et al. (in Vital, 1989) who placed screws along both pedicles to restrict NCJ growth and found that the vertebral canal was significantly narrower with shorter pedicles. Interestingly, the same study found no decrease in height of the posterior portion of the vertebral body following screw placement. The results of this study appear to conflict with the speculation that the NCJ must contribute to growth in height of the posterior third of the vertebral body (Vital et al., 1989; Ganey and Ogden, 2001), but this may be due to the fact that screws were placed perpendicular to the direction of growth that was being measured and therefore may not have affected NCJ growth in this alternative plane. The mechanism of action for the screws used in this study was not specified and it remained unclear as to what extent screw placement resulted in the destruction of NCJ cartilage, particularly on the peripheral aspect of the growth plate or whether these screws functioned by providing tension across the growth plate. In addition to the growth contributions already discussed, Ganey and Ogden (2001) proposed that the NCJ also grows diametrically by the mechanism of interstitial growth and the addition of cells from the periphery of the vertebral body, although the source of these cells was not specified.

In summary, most knowledge to date regarding the role of the NCJ in growth has not yet been substantiated by suitable experimentation and remains largely qualitative and speculative. Greater knowledge of the growth patterns of the NCJ may allow further insight into the clinical presentation of patients with abnormal or asymmetrical NCJ development. Furthermore, knowledge of the role of the NCJ in growth may help to answer the question of how the vertebra continues to grow after NCJ closure. The traditional paradigm of bone growth suggests that a bone stops growing in size after cartilaginous junctions have closed, yet the vertebral body continues to grow in the transverse plane (Knutsson, 1961) well after the latest age suggested by any author for NCJ closure.

Age of NCJ closure

In addition to the controversy surrounding the role of the NCJ in growth, there are also many conflicting opinions about such simple matters as the age at which the NCJ closes. Typically, the term 'open' is used to refer to the period when cartilage is present at the NCJ site and implies the potential for growth (although this may not be true), while the term 'closed' is used to refer to the absence of cartilage and the termination of growth at this site. Although most authors would agree with these definitions, the methods used to determine the presence or absence of cartilage have included different techniques such as gross anatomic examination, visualization of stained and unstained sections, and imaging. Consequently, these terms have different meanings depending on the technique being used. Most anatomic studies have suggested that the NCJ closes between the ages of five and 10 years (Ottander, 1963; Knutsson, 1966; Roaf, 1966; Taylor, 1983; Williams et al., 1989; Maat et al., 1996). A few anatomic studies have found that very small remnants of NCJ cartilage may persist into the adolescent period but have implied that growth had ceased well before this age (Schmorl and Junghanns, 1971; Beguiristain et al., 1980; Mineiro in Vital, 1989). In contrast, imaging studies based on CT visualization have suggested that the NCJ remains open until at least adolescence (Vital et al., 1989; Maat et al., 1996). Furthermore, Yamazaki et al. (1998) who performed the only MRI study done to date have found that the NCJ closed between ages 11-16 years. The work of Yamazaki et al. (1998) was based on the assumption that the disappearance of an NCJ image correlated with the closure of this growth plate, although this concept remains to be verified.

The large discrepancy in the age of NCJ closure as determined by anatomic and imaging studies is significant (10 years) and difficult to reconcile. This discrepancy may be due to the decreased sensitivity of anatomic methods in identifying regions of NCJ cartilage. Conversely, this discrepancy could also result if imaging techniques identified an artifact that was not NCJ cartilage such as the presence of woven bone or bony bridges at the NCJ site that had yet to be resorbed. In addition, the range of closure ages of the NCJ, even when using the same method of assessment, may be due to the fact that the NCJs in different regions close at different times. Alternatively, the conflicting data regarding NCJ closure age may result from confusing a decrease in the rate of growth at the NCJ site with true closure (Vital et al., 1989).

The potential role of the NCJ in AIS

The debate over the age of NCJ closure has actually evolved in the context of assessing the potential role of the NCJ in AIS. In 1909, Nicoladoni was the first to suggest that asymmetrical NCJ growth could lead to vertebral rotation and the development of an abnormal spinal curve. After conducting autopsy studies of four children with infantile scoliosis he found that asymmetrical NCJ development was consistently seen at the apex of the primary curve with the NCJ on the concave side being open to a much greater degree than the NCJ on the convex side. As a consequence of this disparate growth, Nicoladoni found that the concave pedicle was longer (1909) and this finding has been noted in analysis of vertebrae from animals with scoliosis (Michelsson, 1965; Karraharju, 1967), analysis of human vertebral specimens (Taylor, 1983; Vital et al. 1989) and tetracycline marker studies (Karraharju, 1967). In contrast, authors such as

Roaf (1966) have found that the more advanced NCJ is consistently located on the convex side at the apex of the primary curve although no quantitative analysis was performed. An example that illustrates the confusion surrounding the issue of the relationship between disparate NCJ growth and the sides of the scoliotic curve is shown in two different editions of a well-known orthopedic reference (Netter in Keim, 1972 and 1979) where the deformity has been reversed in the same picture. One approach that may be useful for resolving this discrepancy would simply be to measure the pedicle lengths on both the convex and concave sides of the scoliotic curve in patients with adolescent idiopathic scoliosis. To date, this does not appear to have been done.

Animal models of asymmetric NCJ growth

The idea that asymmetrical growth of the NCJ as proposed initially by Nicoladoni (1909) could lead to scoliosis has been applied with limited success using experimental animal models (Ottander, 1963; Beguiristain et al., 1980; Coillard et al., 1999). Unfortunately, the different studies have produced conflicting results (see Table 2-2) and each study has had some major limitations. After using a dental drill to destroy the right NCJ of the L2 vertebrae, Ottander (1963) claimed to have created a slight scoliosis with convexity to the right. Yet, the extent of lateral curvature noted radiographically was almost negligible and the Cobb angle appeared to be far less than 10 degrees. Ottander's results begged the question of whether intervention with a single NCJ was sufficient to cause scoliosis or if surgical intervention would be required on numerous NCJs. To answer this question, Beguiristain et al. (1980) inserted pedicle screws through four or five mid-thoracic NCJs in a porcine specimen. This intervention was found to produce a structural scoliosis, convex on the side of the operation where NCJ growth was presumably restricted. The findings of Beguiristain et al. (1980) appeared to support the idea that asymmetric NCJ growth could lead to scoliosis, however the lack of control or sham groups made it difficult to infer if the scoliosis created was the result of NCJ perturbation or inadvertent muscular, ligamentous or periosteal interference during the surgical approach. Attempting to overcome this limitation, Coillard et al. (1999) decided to replicate Beguiristain's work (1980) and include control, sham and experimental groups. Interestingly, this group chose to use a mini-pig model, which was considered

Table 2-2. Animal models of asymmetric NCJ growth as a potential cause of scoliosis

Author	Method	Result/Conclusions	Comments
Ottander (1963)	Used a rotating dental drill to destroy the NCJ at L2 in a one- month old pig. Pig was sacrificed at 4 months.	Slight scoliosis. Suggested that L1-L4 showed some degree of pathologic change. Thought that this scoliosis corresponded to infantile scoliosis.	**Extent of Lateral Curvature** : Slight. **Rotation** : Suggested that the vertebral bodies of L1-L4 had rotated, but this was difficult to assess from the photographs presented. **Orientation of the Scoliosis** : Operated NCJ was on the convexity. **Vertebral Morphology** : Neural arches short and irregular on injured side. No wedging or compensatory curve noted.
Beguiristain et al. (1980)	In eight two-month old pigs, cancellous screws were placed in five successive mid-thoracic vertebrae. Pigs sacrificed four– 12 months post-operatively.	Scoliosis was apparent, with the degree of scoliosis depending on the evolution time (E.g. 20 degrees at four months, 80 degrees at 12 months).	**Extent of Lateral Curvature** : Ranging from 10-80 degrees. **Rotation** : Rotation clearly seen. **Orientation of the Scoliosis** : Operated NCJ was on the convexity. **Vertebral Morphology** : Shorter pedicle on convexity, spinous process rotated towards the concavity, neural arch on concavity thinner. No compensatory curves. Vertebral bodies wedged with reduced height on concavity, but no appreciable alteration in epiphyseal growth plate thickness.
Coillard et al. (1999)	Used eight one-month old mini-pigs, with 4 treated pigs, 2 control pigs and 2 sham pigs. For the treated group, screws were placed through the NCJ from T5-T9. In the control group, the NCJ was perforated by a drill but no screw was placed. In the sham group, the vertebral muscles were dissected on one side and there was no perturbation of the NCJ. Serial radiographs were acquired at 1,6 and 12 months post-operatively. Animals were sacrificed at 12 and 13 months post-operatively.	Suggested that scoliosis was noted in all of the groups initially, but the scoliosis regressed to zero degrees in the control and sham groups. There does not appear to be a significant extent of scoliosis in the experimental group, as Cobb angles are consistently less than 10 degrees and initially are even less than the control group.	**Extent of Lateral Curvature :** Initially 5-22 degrees at one month, decreasing to a maximum of 10 degrees at six months and only a slight curvature (10 degrees or less) at 12 months in treated group. **Rotation** : Rotation clearly seen. **Orientation of the Scoliosis** : Operated NCJ was on the convexity. **Vertebral Morphology** : Operated pedicle was shorter, spinous process bent towards the convexity. Vertebrae above the primary curve showed compensatory changes, with the opposite patterns of morphology. Vertebrae below the curve were morphologically normal. All thoracic curves showed wedging and the presence of a compensatory curve above (in 2-4 vertebrae).

biologically similar to the human (Swindle et al., 1988) and apparently chosen for the convenience of housing and raising a smaller animal. Coillard et al. (1999) contended that follow-up of all mini-pigs to one year post-operatively showed that scoliosis was initially present in all groups, but only remained present in the experimental group. However, this statement did not appear to be correct as none of the mini-pigs in the experimental group had Cobb angles of greater than 10 degrees at six or 12 months of age. Aside from the lateral curvature, other changes in the mini-pig vertebrae such as a shorter pedicle on the side of the convexity, spinous process rotation and vertebral wedging agreed with the vertebral morphology seen in AIS. Unfortunately, direct comparisons with Beguiristain's work were made difficult since Coillard et al. (1999) later suggested that the mini-pig might not be a good model for scoliosis, since its growth velocity is slow and progressive, whereas animals that are predisposed to scoliosis generally show periods of rapid growth in length. Nonetheless, Coillard's study (1999) raised the question of whether intervention with the NCJ was sufficient for the production of a permanent three-dimensional spinal deformity or whether these changes only produced temporary deformities.

These three animal studies on the potential role of the NCJ in AIS highlight several common problems (Ottander, 1963; Beguiristain et al., 1980; Coillard et al., 1999) inherent in experimental scoliosis models. Firstly, in many studies, the creation of any vertebral changes or any degree of lateral curvature has been interpreted to represent a positive result. Although this may be due to the inherent bias for only positive results to be published in scientific journals, it is necessary to recognize that not all lateral curvatures can be considered to represent the type of curvature seen in AIS. Instead of using the creation of a curvature as an endpoint, the focus in animal studies must be on the extent to which a lateral curvature is similar to curves seen in AIS. Secondly, there has been a great deal of difficulty replicating the results of different animal studies both in general and in investigations of vertebral asymmetry as a cause of AIS. Although the discrepancy between the work of Beguiristain et al. (1980) and Coillard (1999) may be due to the choice of an animal model, the careful description of experimental procedures and the use of control groups to eliminate confounding variables may help increase the reproducibility of experimental results.

Despite these problems with animal studies, the continued use of animal models is absolutely essential in understanding AIS. As discussed earlier, animal models overcome many of the fundamental limitations involved in clinical studies of AIS patients and permit evaluation of the early stages of curve development as well as determination of cause and effect relationships. Unlike clinical studies in which it is difficult to determine if patients manifest with the same cause for their scoliosis, animal models usually allow unambiguous determination of the potential cause for scoliosis since it a result of the experimental intervention. For this reason, animal models must always be integrated into complete theories of AIS development.

Further Work Required on the Asymmetric NCJ Growth Model of AIS

Upon review of the clinical and animal studies of asymmetric NCJ growth, it is apparent that the asymmetric growth model of AIS is highly controversial. Most clinical studies on the past have refuted this model on the basis that the NCJ closes well before adolescence, as this would eliminate the possibility of disparate growth at this site in the adolescent period. Even if the NCJ can be shown to remain open until the adolescent period, this model requires further development to understand the precise mechanism by which asymmetrical NCJ development causes vertebral rotation and lateral curvature. Furthermore, the possibility that asymmetric NCJ development is an effect, rather than a cause of scoliosis, must be explored. Growth plates and vertebral morphology throughout the body are secondarily affected by a variety of conditions including trauma, metabolic abnormalities, dietary deficiencies and altered biomechanical forces. There is no reason to suspect that the NCJ would not also be susceptible to these states. In developing and understanding the asymmetric NCJ growth model, further work with animal models may help to determine if NCJ changes are a primary cause or a secondary result of scoliosis. If animal models produce scoliosis, careful analysis of the scoliosis created may aid in predicting the presentation of potentially affected patients. If a model can be created and authenticated, it would be exciting to determine if surgical epiphyseodesis of the NCJ on a given side of the scoliotic curve could be used to treat or reverse curve development due to asymmetric NCJ growth or other causes of AIS.

FLUOROCHROME BASED TECHNIQUES OF EVALUATING BONE GROWTH

Fluorochromes are substances that bind to calcium without affecting bone deposition and they can therefore be used as direct markers to determine the site and rate of bone growth (Milch et al., 1957; Frost, 1969; Sun et al., 1992). On exposure to high intensity light the fluorescent species in a sample are excited and emit light of a longer wavelength, which can be easily differentiated from the background image even in those cases where the background shows some degree of autofluorescence. Accordingly, the serial administration of two or more fluorochromes with a specific time interval between injections will provide sequential information about bone deposition and can be used to determine unambiguously both the direction and amount of bone growth.

Two of the most commonly used fluorochromes are tetracycline hydrochloride and alizarin red S. Tetracycline is commonly used to study bone formation and remodeling but the exact mechanism behind this phenomenon remains controversial with some authors suggesting that tetracycline binds to calcium orthophosphate (Hilton, 1962; Wallman and Hilton, 1962) while others have found that tetracycline binds to the surface of microcrystals of apatite (Urist and Ibsen, 1963). In contrast, there appears to be no dispute with alizarin red S which forms an alizarin red S-calcium complex by the process of chelation and binds to calcium hydroxyapatite (Cleall et al., 1964). While in the circulation, both compounds are deposited at the calcification front when new osteoid is being actively mineralized and will therefore indicate sites of new bone formation.

Fluorochrome Protocol

The successful study of bone growth using fluorochromes in rats has been common (Landry et al., 1964; Baylink et al., 1970; Hammer et al., 1973; Hammond and Storey, 1974; Deeb and Herrmann, 1974; Baron et al., 1984; Sontag et al., 1986; Sun et al., 1992; Ito et al., 1993; Lepola et al., 1996; Kidder et al., 1997; Mente et al., 1999), although there are minor variations in dosages (Harris et al., 1968; Sun et al., 1992), dosing intervals (Hammond and Storey, 1974; Baron et al., 1984; Sontag et al., 1986; Ito et al., 1993; Kidder et al. 1997) and sectioning procedures between studies (Cleall et al., 1964, Hansson, 1967). Upon visualization of sections, a variety of histomorphometric indices can be calculated (see Kidder et al., 1997). Calculations of parameters such as bone formation rates, bone resorption rates and mineral apposition rates are based on measurement of the distance between two sequentially administered fluorochromes divided by the time between their administration.

The use of fluorochromes in the rat model

Although the rat has become a widely accepted model for human bone conditions (Frost and Jee, 1992), it is important to note several differences in bone growth between the rat and the human. Most importantly, rats exhibit very little or no haversian remodeling in compact bone (Frost, 1976; Baron et al., 1984; Frost and Jee, 1992) although remodeling can be seen in trabecular bone (Baron et al., 1984; Erben, 1996). In fluorochrome studies, this enables the processes of bone modeling and growth to be clearly visualized in cortical bone since any evidence of bone deposition cannot be due to remodeling. Although it is sometimes thought that rat skeletons continue to grow in length throughout life this is not true as in older rats it has been shown that longitudinal bone growth becomes trivial or stops (Frost and Jee, 1992). As an example, by the age of 8 months longitudinal growth of vertebrae is barely detectable in the rat and by the age of eighteen months, the linear growth of long bones such as the tibia has stopped due to the complete closure of tibial growth plates (Frost and Jee, 1992).

Although numerous fluorochrome studies have been completed on bone growth, they have mainly been concerned with long bones and few studies have attempted to characterize patterns of vertebral growth which is more complex. In one study on the rabbit, Smith et al. (1991) found that fluorochrome deposition was consistently noted on the outer surface of the layer of compact bone surrounding the vertebral canal and on the periosteal surface of the vertebral body. On the basis of this observation, it was concluded that the vertebra grew in the transverse plane by expansion in all directions. This finding conflicted with results from Hammond and Storey (1974), who found that bone formation occurred exclusively on the periosteal surface and bone resorption occurred exclusively on the endosteal surface in the vertebrae of young rats although it remained unclear how a layer of compact bone could be maintained on the endosteal surface of the canal in this model. In the most conclusive fluorochrome study done on the rat vertebra to date, Sontag (1994) found that the lumbar vertebrae of Wistar rats grew in length and width from birth up to the age of 200 days, although the bone formation rate decreased sharply over this time period from 8000%/year at birth to 115%/year at 9 months of age. Unfortunately, patterns of vertebral growth were not evaluated since the focus of the study was on comparison of morphometric changes in the rat femur and the vertebrae at different ages and vertebrae were only sectioned in the sagittal plane.

In summary, the use of fluorochrome markers is a commonly used technique for the assessment of bone deposition and growth. Although there are minor variations in the protocol used and bone growth in the rat differs slightly from human bone growth, the rat appears to be an acceptable model for the assessment of vertebral growth using fluorochromes.

BIOMECHANICAL ANALYSIS OF SCOLIOSIS

In recent years, the advent of numerical modeling of the spine using the finite element method has provided a new technique to improve understanding of scoliosis biomechanics and to predict the potential effect of altering numerous parameters. In finite element models of the spine, the vertebral column is divided into a number of meshes each of which are composed of a number of finite elements connected with associated nodes. There are numerous different types of finite elements with different geometric forms such as truss elements (linear), triangular elements (linear), quadrilateral elements (linear) and tetrahedral elements (quadratic). The type of elements chosen to represent a structure depend on the type of problem being investigated. In general, choosing a larger number of elements and nodes to model a particular structure will make the solution more accurate but will also increase the computational time and memory required. After element selection, every node in the model is associated with the unknowns to be solved which are typically the displacements and rotations in three dimensions. After model geometry has been defined the material properties for each particular element are specified, which represent the typical stress and strain laws applied to each element. Boundary conditions are established for each element and serve as limits on values such as displacements, forces, temperatures and rotations at specific sites in the model. For example, in many finite element models of the vertebral column, the displacement of the L5 vertebra is fixed to represent the tethering effect of the pelvis. Once the boundary conditions are set, the model equations for each element can be solved and the outputs are the predictions of the simulation and the mechanical effects (e.g. displacement, force) on the trunk (Aubin in Burwell et al., 2000).

To date, finite element modeling has been applied in numerous studies to simulate the effects of bracing and surgical treatment of scoliosis. For example, numerous authors have developed models to assess brace treatment and simulate brace mechanisms on scoliosis patients (Andriacchi et al., 1976; De Georgi et al., 1990; Wynarsky and Schultz, 1991; Aubin et al., 1993; Gignac et al., 1998; Gignac et al., 2000). These models have produced new ideas about the application of forces and loads on the thorax for maximal curve correction. However, with some exceptions (Wynarsky and Schultz, 1991; Gignac et al., 2000), most of the studies have not included clinical verification by comparing predicted correction with actual patient correction. Surgical treatment of scoliosis using numerous instrumentation systems (Stokes and Laible, 1990; Aubin et al., 1995; Poulin et al., 1998) has also been modeled. Modeling of most surgical techniques has shown good agreement with measured effects of surgery in the coronal plane (Aubin in Burwell et al., 2000) however results in the sagittal and transverse plane have shown much less agreement and depend heavily on boundary conditions and assigned mechanical properties.

Over time, current finite element models have become more refined and now represent a greater number of structures in addition to the vertebral column. Finite element models such as the initial model developed by Stokes and Laible (1990) have been refined to include the anterior and posterior portions of the T1 to L5 vertebrae, the articular facets, the intervertebral discs, the spinal ligaments, the rib cage and the pelvis. Yet, the addition of muscles and motor control to these types of models has proved quite difficult (Feldman et al., 1986; Loeb et al., 1990; Cholewicki et al., 1995; Nussbaum et al., 1997; Stokes and Gardner-Morse, 1991). The major challenge is to find a way to represent the large number of strategies available for the central nervous system to recruit muscles and to predict complicated strategies such as the co-contraction of antagonistic muscles.

Recent work has also attempted to incorporate growth and growth modulation into the model of Aubin et al. (1995). The incorporation of growth has been successful and the model created (Villemure et al., 2002) may have the potential to predict if a given growth deformity or displacement will produce scoliosis over a period of time. This type of model is based on an iterative process. An initial change in the spine, such as a displacement, shape asymmetry, or external force is used as an input into the cycle. At each iteration, a small increment of baseline growth is applied, the geometry of the vertebra is updated and the stresses are reset to zero. Upon application of the external loads (such as the altered gravitational forces induced by a geometric shift), the new stresses and effects of growth modulation (based on the Heuter-Volkmann principle) are calculated and used to update the local geometry of the vertebrae. This process can be carried out for a number of steps, which often represent discrete units of time. As a sample application of this type of model, Villemure et al. (2002) predicted that a displacement of two mm to the right at the T8 vertebra (in a child between 10-15 years of age) would result in a scoliosis of approximately 34 degrees after two years had elapsed. Similar to clinical observations, the vertebral wedging angle was found to increase with curve progression and vertebral rotation of the thoracic apex increased to 10 degrees. However, the prediction of this model still requires clinical verification and is based on several simplifications. In the Villemure et al. (2002) model, longitudinal growth was only included for the anterior portions of the vertebrae on the assumption that posterior portions of the vertebra had completed their longitudinal growth before the end of the first decade (Vital et al., 1989). Growth of the intervertebral discs was not included, as in-house studies had shown mean disc growth to be negligible (Villemure et al., 2002). Furthermore, growth of the vertebrae in the transverse plane was not modeled as this was thought to have a negligible effect on changes in vertebral dimensions and growth modulation. Despite these limitations, this model appeared to reproduce many of the clinical aspects of spinal and vertebral deformity seen in scoliosis. With further refinement and clinical verification, this type of model appears to have great value for potentially understanding the mechanisms involved in curve progression and development.

Biomechanical modeling of the vertebral column has several advantages over clinical studies since it allows a greater number of variables to be altered, allows the determination of cause and effect relationships and could potentially have predictive value in determining the shape of the spine in relation to growth or treatment applications. Yet, it is also important to understand the limitations of this particular approach. The primary disadvantage of the finite element method remains that the value of the models created depends on the data used to create these models. To date, most models have been verified by a combination of literature review and experimental verification with cadaveric specimens. Literature reviews have often been used to establish parameters such as growth rates of different aspects of the vertebral column (Villemure et al., 2002), yet unfortunately many of the values reported in the literature are not based on large sample sizes and lack independent verification by other authors. Although some mechanical properties such as the lateral bending of the spine have been determined from clinical specimens (Beausejour et al., 1999), most mechanical parameters are taken from experimental studies made on cadaveric specimens which represent non-scoliotic individuals (see Aubin in Burwell et al., 2000). This has limited the ability of models to make predictions based on the mechanical properties of scoliotic vertebrae. For example, the center of mass used for vertebrae in conventional finite element models is based on the center of mass from vertebrae from non-scoliotic individuals. Unfortunately, in models that aim at producing scoliosis, these values are not accurate once vertebral deformities arise and result in a change in the center of mass. Furthermore, due to the way that current mechanical properties have been acquired, material properties and other model data are not specific to individual patients which may also potentially affect simulation results. It is clear that much work remains to be done on model validation and for this reason it is important the finite element models not be applied beyond the scope of their validity (Aubin in Burwell et al., 2000). Despite the limitations inherent in the creation and application of biomechanical models, these models have enormous potential value particularly when used in combination with clinical and animal studies. Future progress in scoliosis biomechanics will likely depend on understanding the advantages and disadvantages of finite element models of the spine and acquiring the numerous parameters necessary to successfully define and validate these models.

REFERENCES

Ahn UM, Ahn NU, Nallamshetty L, Buchowski JM, Rose PS, Miller NH, Kostuik JP, Sponseller PD. The etiology of adolescent idiopathic scoliosis. Am J Orthop 2002;31:387-395.

Andriacchi TP, Schultz AB, Belytschko RB, DeWald RL. Milwaukee brace correction of idiopathic scoliosis: a biomechanical and a retrospective study. J Bone Joint Surg (Am) 1976;58-A:806-815.

Asher MA. Foreword. In : Burwell et al. (eds.). Etiology of adolescent idiopathic scoliosis. Hanley and Belfus. Philadelphia, 2000: Xiv-xv.

Aubin CE, Dansereau J, Labelle H. Biomechanical simulation of the Boston brace effect on a model of the scoliotic spine and thorax. Ann Chir 1993;47:881-887.

Aubin CE, Descrimes JL, Dansereau J, Skalli W, Lavaste F, Labelle H. Geometrical modeling of the spine and the thorax for the biomechanical analysis of scoliotic deformities using the finite element method. Ann Chir 1995;49:749-761.

Aubin CE. Finite element analysis for the biomechanical study of scoliosis. In : Burwell et al. (eds.). Etiology of adolescent idiopathic scoliosis. Hanley and Belfus. Philadelphia, 2000: 489-504.

Bagnall KM, Thomas B, Moreau M, Raso VJ, Mahood J, Hill D, Zhao J, Kautz J. A new tool by which to visualize adolescent idiopathic scoliosis as a continuous process. In : IAF Stokes (ed.). Research into Spinal Deformities 2. IOS Press. Oxford, 1998: 65-68.

Bagnall KM, Rajwani T, Kautz J, Moreau M, Raso VJ, Mahood J, Daniel A, Demianczuk C, Wilson J, Wang X. The role of melatonin in the development of scoliosis. In :

SR Pandi-Perumal (ed.). Melatonin: Biological Basis of its Function in Health and Disease. Eurekah. 2004.

Baron R, Tross R, Vignery A. Evidence of sequential remodeling in rat trabecular bone : morphology, dynamic histomorphometry, and changes during skeletal maturation. Anat Rec 1984;208:137-145.

Baylink D, Stauffer M, Wergedal J, Rich C. Formation, mineralization and resorption of bone in Vitamin D-deficient rats. J Clin Invest 1970;49:1122-1134.

Beguiristain JL, De Salis J, Oriaifo A, Canadell J. Experimental scoliosis by epiphyseodesis in pigs. Int Ortho 1980;3:317-21.

Bell M, Teebi AS. Autosomal dominant idiopathic scoliosis? Am J Med Genet 1995;55:112.

Bernhardt M, Bridwell KH. Segmental analysis of the sagittal plane alignment of the normal thoracic and lumbar spines and thoracolumbar junction. Spine 1989;14:717-21.

Bibby SR, Fairbank JC, Urban MR, Urban JP. Cell viability in scoliotic discs in relation to disc deformity and nutrient levels. Spine 2002;27:2220-8.

Bick EM, Copel JW. Longitudinal growth of the human vertebra; a contribution to human osteogeny. J Bone Joint Surg Am 1950;32:803-14.

Bunnell WP. The natural history of idiopathic scoliosis before skeletal maturity. Spine 1986;11:773-6.

Burwell RG, Dangerfield PH. Anthropometry and scoliosis. In: Zorab PA (ed.). Scoliosis and Growth 5th Symposium. Academic Press. London, 1977:123-64.

Bylund P, Aaro S, Gottfries B, Jansson E. Is lateral electric surface stimulation an effective treatment for scoliosis? J Pediatr Orthop 1987;7:298-300.

Chandraraj S, Briggs CA. Multiple growth cartilages in the neural arch. Anat Rec 1991;230:114-20.

Cleall JF, Perkins RE, Gilda JE. Bone marking agents for the longitudinal study of growth in animals. Arch Oral Biol 1964;115:627-46.

Coillard C, Rhalmi S, Rivard CH. Experimental scoliosis in the minipig: study of vertebral deformations. Ann Chir 1999;53:773-80.

Dale-Stewart T. Flattening of centra in Pueblo and Eskimo adult vertebral bodies. Amer J Phys Anthrop 1952;10:17.

Davenport CB. Heredity in relation to eugenics. Henry Holt. New York, 1911.

De Giorgi G, Gentile A, Mantriota G, Gafario G. Analisi, con programma agli elementi finiti, delle spine correttive sviluppate dai corsetti nella scoliosis lombare. Riv Int Technica Orthopedica Internacional. 1990.

Deeb S, Herrmann H. Tetracycline-labeling as a method for detecting the bone demineralization of parathormone-treated rats. Acta Histochem 1974;50:35-42.

Dickson RA, Lawton JO, Archer IA, Butt WP. The pathogenesis of idiopathic scoliosis: Biplanar spinal asymmetry. J Bone Joint Surg (Br) 1984;66-B:8-15.

Dickson RA. The aetiology of spinal deformities. Lancet 1988;1(8595):1151-5.

Doskocil M, Valouch P, Pazderka V. On vertebral body growth. Funct Dev Morphol 1993;3:149-55.

Enneking WF, Harrington P. Pathological changes in scoliosis. J Bone Joint Surg (Am) 1969;51-A:165-84.

Fidler MW, Jowett RL. Muscle imbalance in the aetiology of scoliosis. J Bone Joint Surg (Br) 1976;58-B:200-1.

Ford DM, Bagnall KM, McFadden KD, Greenhill BJ, Raso VJ. Paraspinal muscle imbalance in adolescent idiopathic scoliosis. Spine 1984;9:373-6.

Fowles JV, Drummond DS, L'Ecuyer S, Roy L, Kassab MT. Untreated scoliosis in the adult. Clin Orthop 1978;134:212-7.

Francois RJ, Dhem A. Microradiographic study of the normal human vertebral body. Acta Anat (Basel) 1974;89:251-65.

Frost HM. Some concepts crucial to the effective study of bone turnover and bone balance in human skeletal disease and in experimental models of skeletal physiology and pathophysiology. In : ZFG Jaworski (ed.). Bone Morphometry. Ottawa University Press. Ottawa, 1976: 219-223.

Frost HM, Jee WSS. On the rat model of human osteopenias and osteoporoses. Bone Miner 18:227-236;1992.

Ganey TM, Ogden JA. Development and maturation of the axial skeleton. In : Weinstein SL (ed.). The pediatric spine : principles and practice, 2nd ed. Lippincott Williams and Wilkins. Philadelphia, 2001: 3-54.

Gignac D, Aubin CE, Dansereau J. Biomechanical study of new orthotic approaches for 3D orthotic correction of scoliosis. Ann Chir 1998;52:795-800.

Gignac D, Aubin CE, Dansereau J, Labelle H. Optimization method for 3D bracing correction of scoliosis using a finite element model. Eur Spine J 2000;9:185-90.

Goldberg CJ, Dowling FE, Forgarty EE, Moore DP. Adolescent idiopathic scoliosis as developmental instability. Genetica 1995;96:247-55.

Grealou L, Aubin CE, Labelle H. Rib cage surgery for the treatment of scoliosis: a biomechanical study of correction mechanisms. J Orthop Res 2002;20:1121-8.

Guo X, Chau WW, Chan YL, Cheng JC. Relative anterior spinal overgrowth in adolescent idiopathic scoliosis: Results of disproportionate endochondral-membranous bone growth. J Bone Joint Surg Br 2003;85:1026-31.

Hammer WS, Soni NN, Fraleigh CM. Quantitative study of bone activity in the diabetic rat mandible: triple fluorochrome study. Oral Surg 1973;35:718-729.

Hammond RH, Storey E. Measurement of growth and resorption of bone in the seventh caudal vertebra of the rat. Calc Tiss Res 1974;15:11-20.

Hansson LI. Daily growth in length of diaphysis measured by oxytetracycline in rabbit normally and after medullary plugging. Acta Orthop Scand 1967;Suppl 101.

Harris WH, Lavorgna J, Hamblen DL, Haywood EA. The inhibition of ossification *in vivo*. Clin Orthop Rel Res 1968;61:52-60.

Hilton HE. Skeletal pigmentation due to tetracycline. J Clin Path 1962;15:112-115.

Ito H, Ke HZ, Jee WSS, Sakou T. Anabolic responses of an adult cancellous bone site to prostaglandin E_2 in the rat. Bone Min 1993;21:219-236.

Keim HA. Scoliosis. Clin Symp 1972;24:3-32.

Keim HA. Scoliosis. Clin Symp 1979;31:2-34.

Khosla S, Tredwell SJ, Day B, Shinn SL, Ovalle WK Jr. An ultrastructural study of multifidus muscle in progressive idiopathic scoliosis: Changes resulting from a sarcolemmal defect at the myotendinous junction. J Neurol Sci 1980;46:13-31.

Kidder LS, Schmidt IU, Evans GL, Turner RT. Effects of growth hormone and low dose estrogen on bone growth and turnover in long bones of hypophysectomized rats. Calc Tiss Int 1997;61:327-335.

Knutsson B, Wiberg G. On surgically treated herniated intervertebral discs. Acta Orthop Scand 1958;28:108-23.

Knutsson F. Growth and differentiation of the postnatal vertebra. Acta Radiol 1961;55:401-408.

Knutsson F. A contribution to the discussion of the biological cause of idiopathic scoliosis. Acta Orthop Scand 1963;33:98-104.

Knutsson F. Vertebral genesis of idiopathic scoliosis in children. Acta Radiol 1966;4:395-402.

Landry LM, Fleisch DH. The influence of immobilization on bone formation as evaluated by osseous incorporation of tetracyclines. J Bone Joint Surg (Br) 1964;46-B:764-771.

Larsen JL. The lumbar spinal canal in children: Development of the lumbar spinal canal in relation to the development of the lumbar vertebral bodies. Eur J Radiol 1982;2:66-71.

Lenke LG, Betz RR, Haher TR, Lapp MA, Merola AA, Harms J, Shufflebarger HL. Multisurgeon assessment of surgical decision-making in adolescent idiopathic scoliosis: curve classification, operative approach, and fusion levels. Spine 2001;26:2347-53.

Lepola VT, Hannuniemi R, Kippo K, Laurén L, Jalovaara P, Väänänen HK. Long-term effects of clodronate on growing rat bone. Bone 1996;18:191-196.

Liljenqvist UR, Link TM, Halm HF. Morphometric analysis of thoracic and lumbar vertebrae in idiopathic scoliosis. Spine 2000;25:1247-1253.

Liljenqvist UR, Allkemper T, Hackenberg L, Link TM, Steinbeck J, Halm HFH. Analysis of vertebral morphology in idiopathic scoliosis with use of magnetic resonance imaging and multiplanar reconstruction. J Bone Joint Surg (Am) 2002;84-A:359-368.

Lonstein JE. Adolescent idiopathic scoliosis. Lancet 1994;344:1407-1412.

Lord MJ, Ogden JA, Ganey TM. Postnatal development of the thoracic spine. Spine 1995;20:1692-1698.

Lovell W, Winter B. Pediatric orthopaedics. Lippincott, Williams and Wilkins. Philadelphia, 2001.

Lowe TG, Edgar M, Margulies JY, Miller NH, Raso VJ, Reinker KA, Rivard CH. Etiology of idiopathic scoliosis: current trends in research. J Bone Joint Surg (Am) 2000;82-A:1157-68.

Maat GJ, Matricali B, Van Meerten EL. Postnatal development and structure of the neurocentral junction. Spine 1996;21:661-66.

Machida M, Dubousset J, Imamura Y, Iwaya T, Yamada T, Kimura J, Toriyama S. Pathogenesis of idiopathic scoliosis: SEPs in chicken with experimentally induced scoliosis and in patients with idiopathic scoliosis. J Pediatr Orthop 1994;14:329-335.

Machida M, Murai I, Miyashita Y, Dubousset J, Yamada T, Kimura J. Pathogenesis of idiopathic scoliosis: Experimental study in rats. Spine 1999;24:1985-9.

Mente PL, Aronsson DD, Stokes IAF, Iatridis JC. Mechanical modulation of growth for the correction of vertebral wedge deformities. J Ped Ortho 1999;17:518-24.

Michelsson JE. The development of spinal deformity in experimental scoliosis. Acta Orthop Scand 1965;36(Suppl 81):9-91.

Milch RA, Rall DP, Tobie JE. Bone localization of the tetracyclines. J Natl Cancer Inst 1957;19:87-93.

Miller NH. Adolescent idiopathic scoliosis: etiology. In : Weinstein SL (ed.). The pediatric spine : principles and practice, 2nd ed. Lippincott Williams and Wilkins. Philadelphia, 2001: 347-354.

Moore KL, Dalley AF. Clinically oriented anatomy, 4th ed. Lippincott Williams and Wilkins. Baltimore, 1999.

Nachemson AL. Evaluation of results in lumbar spine surgery. Acta Orthop Scand Suppl 1993;251:130-3.

Nicoladoni C. Anatomie und mechanismus der skoliose. Urban and Schwarzernburg. Munchen, 1909.

O'Brien MF, Lenke LG, Mardjetko S, Lowe TG, Kong Y, Eck K, Smith D. Pedicle morphology in thoracic adolescent idiopathic scoliosis. Spine 2000;25:2285-93.

Ogon M, Giesinger K, Behensky H, Wimmer C, Nogler M, Bach CM, Krismer M. Interobserver and intraobserver reliability of Lenke's new scoliosis classification system. Spine 2002;27:858-62.

Ottander HG. Experimental progressive scoliosis in a pig. Acta Orthop Scand 1963;33:91-7.

Parent S, Labelle H, Skalli W, Latimer B, de Guise J. Morphometric analysis of anatomic scoliotic specimens. Spine 2002;27:2305-11.

Perdriolle R, Becchetti S, Vidal J, Lopez P. Mechanical process and growth cartilages: Essential factors in the progression of scoliosis. Spine 1993;18:343-9.

Porter RW. Idiopathic scoliosis: the relation between the vertebral canal and the vertebral bodies. Spine 2000;25:1360-6.

Poulin F, Aubin CE, Stokes IAF. Biomechanical modeling of scoliotic spine instrumentation using flexible mechanisms: feasibility study. Ann Chir 1998;52:761-767.

Roaf R. Vertebral growth and its mechanical control. J Bone Joint Surg (Br) 1960;42-B:40-59.

Roaf R. The treatment of progressive scoliosis by unilateral growth arrest. J Bone Joint Surg (Br) 1963;45-B:637-51.

Roaf R. The basic anatomy of scoliosis. J Bone Joint Surg (Br) 1966;48-B:786-92.

Robin GC. The aetiology of idiopathic scoliosis. Freund Publishing House. Boca Raton, 1990.

Richards BS, Sucato DJ, Konigsberg DE, Ouellet JA. Comparison of reliability between the Lenke and King classification systems for adolescent idiopathic scoliosis using radiographs that were not premeasured. Spine 2003;28:1148-56.

Rinsky L, Gamble J. Adolescent idiopathic scoliosis. Western J Medicine 1988;148:182-191.

Roaf R. The basic anatomy of scoliosis. J Bone Joint Surg (Br) 1966;48-B:786-92.

Robin GC. The aetiology of idiopathic scoliosis. Freund Publishing House. Boca Raton, 1990.

Sadler TW. Langman's medical embryology, 7th ed. Williams and Wilkins. Philadelphia, 1995.

Sahlstrand T, Ortengren R, Nachemson A. Postural equilibrium in adolescent idiopathic scoliosis. Acta Orthop Scand 1978;49:354-65.

Sahlstrand T, Petruson B. A study of labyrinthine function in patients with adolescent idiopathic scoliosis. I. An electro-nystagmographic study. Acta Orthop Scand 1979;50:759-69.

Sahlstrand T. An analysis of lateral predominance in adolescent idiopathic scoliosis with special reference to convexity of the curve. Spine 1980;5:512-8.

Sahlstrand T, Lidstrom J. Equilibrium factors as predictors of the prognosis in adolescent idiopathic scoliosis. Clin Orthop 1980;152:232-6.

Schmorl G, Junghanns H, Besemann EF (ed.). The human spine in health and disease. Grune and Stratton. New York and London, 1971.

Shea KG, Stevens PM, Nelson M, Smith JT, Masters KS, Yandow S. A comparison of manual versus computer-assisted radiographic measurement: Intraobserver measurement variability for Cobb angles. Spine 1998;23:551-5.

Smith RM, Dickson RA. Experimental structural scoliosis. J Bone Joint Surg (Br) 1987;69:576-81.

Smith RM, Pool RD, Butt WP, Dickson RA. The transverse plane deformity of structural scoliosis. Spine 1991;16:1126-9.

Somerville EW. Rotational lordosis; the development of a single curve. J Bone Joint Surg (Br) 1952;34-B:421-7.

Sontag W. Quantitative measurement of periosteal and cortical-endosteal bone formation and resorption in the midshaft of female rat femur. Bone 1986;7:55-62.

Sontag W. Age-dependent morphometric change in the lumbar vertebrae of male and female rats : comparison with the femur. Bone 1994;15:593-601.

Spencer GS, Eccles MJ. Spinal muscle in scoliosis: The proportion and size of type 1 and type 2 skeletal muscle fibres measured using a computer-controlled microscope. J Neurol Sci 1976;30:143-154.

Stokes IAF. Scoliosis research society working group on 3-d terminology of spinal deformity: Three-dimensional terminology of spinal deformity. Spine 1994;19:236-48.

Stokes IA, Gardner-Morse M. Analysis of the interaction between vertebral lateral deviation and axial rotation in scoliosis. J Biomech 1991;24:753-759.

Stokes IAF, Laible JP. Three-dimensional osseo-ligamentous model of the thorax representing initiation of scoliosis by asymmetric growth. J Biomech 1990;23:589-595.

Sun TC, Mori S, Roper J, Brown C, Hooser T, Burr DB. Do different fluorochrome labels give equivalent histomorphometric information? Bone 1992;13:443-446.

Taylor TK, Ghosh P, Bushell GR. The contribution of the intervertebral disk to the scoliotic deformity. Clin Orthop 1981;156:79-90.

Taylor JR. Scoliosis and growth : patterns of asymmetry in normal vertebral growth. Acta Orthop Scand 1983;54:596-602.

Thillard MJ. Vertebral column deformities following epiphysectomy in the chick. C R Hebd Seances Acad Sci 1959;248:1238-40.

Töndury G, Theiler K. Entwicklungsgeschichte und fehlbildungen der wirbelsäule, 2nd edn. Hippokrates Verlag. Stuttgart, 1990.

Tulsi RS. Growth of the human vertebral column: An osteological study. Acta Anat 1971;79:570-80.

Urist MR, Ibsen KH. Chemical reactivity of mineralized tissue with oxytetracycline. Arch Path 1963;76:484-496.

Villemure I, Aubin CE, Grimard G, Dansereau J, Labelle H. Progression of vertebral and spinal three-dimensional deformities in adolescent idiopathic scoliosis: a longitudinal study. Spine 2001;26:2244-50.

Villemure I, Aubin CE, Dansereau J, Labelle H. Simulation of progressive deformities in adolescent idiopathic scoliosis using a biomechanical model integrating vertebral growth modulation. J Biomech Eng 2002;124:784-790.

Vital JM, Beguiristain JL, Algara C, Villas C, Lavignolle B, Grenier N, Sénégas J. The neurocentral vertebral cartilage: anatomy, physiology and physiopathology. Surg Radiol Anat 1989;11:323-28.

Wallman IS, Hilton HB. Teeth pigmented by tetracycline. Lancet 1962;1:827-828.

Watson JD. DNA: The secret of life. Random House. New York, 2003.

Weinstein SL. Idiopathic scoliosis: natural history. Spine 1986;11:780-3.

Weinstein SL. Idiopathic scoliosis in adolescence: Incidence and progression of untreated scoliosis. Orthopade 1989;18:74-86.

Wever DJ, Veldhuizen AG, Klein JB, Webb PJ, Nijenbanning G, Cool JC, v Horn JR. A biomechanical analysis of the vertebral and rib deformities in structural scoliosis. Eur Spine J 1999;8:252-60.

White AA, Panjabi MM. Clinical biomechanics of the spine, 2nd ed. Lippincott. Philadelphia, 1990.

Williams PL (ed.), Warwick, Dyson et al. Gray's Anatomy, 37th ed. Churchill Livingstone. Edinburgh and New York, 1989.

Wynarsky GT, Schultz AB. Optimization of skeletal configuration: studies of scoliosis correction biomechanics. J Biomech 1991;24:721-732.

Xiong B, Sevastik JA, Hedlund R, Sevastik B. Radiographic changes at the coronal plane in early scoliosis. Spine 1994;19:159-64.

Xiong B, Sevastik B, Sevastik J. Horizontal plane morphometry of normal and scoliotic vertebrae : A methodological study. Eur Spine J 1995;4:6-10.

Yamazaki A, Mason DE, Caro PA. Age of closure of the neurocentral cartilage in the thoracic spine. J Ped Ortho 1998;8:168-172.

CHAPTER 3

MRI CHARACTERISTICS OF THE IMAGE OF THE NORMAL NEUROCENTRAL JUNCTION*

INTRODUCTION

The neurocentral junction (NCJ) is a cartilaginous growth plate located between the neural arch and the centrum of the vertebrae. Unlike the epiphysial plate of a long bone, this growth plate is bipolar and therefore contributes to the growth of both the vertebral body and the posterior arch (Vital et al., 1989; Töndury and Theiler, 1990; Maat et al., 1996; Yamazaki et al., 1998) (Figure 3-1). Since the early 1900s, it has been hypothesized that disparate growth at this site could lead to vertebral deformation and ultimately, the development of abnormal spinal curves (Michelsson, 1965; Knutsson, 1966; Roaf, 1966; Vital et al., 1989; Yamazaki et al., 1998). In elucidating the potential role of the NCJ in adolescent idiopathic scoliosis (AIS), previous studies have concentrated primarily on the age of closure. Numerous methods have been used to determine this age including gross anatomic or histologic visualization (Ottander, 1963; Knutsson, 1966; Roaf, 1966; Schmorl et al., 1971; Taylor, 1983; Vital et al., 1989), radiography (Lord et al., 1995; Maat et al., 1996), CT (Vital et al., 1989; Maat et al., 1996) and MRI (Yamazaki et al., 1998). These studies have produced conflicting results and therefore the potential role of the NCJ in AIS has not been conclusively confirmed. Anatomic and radiographic studies have shown that the NCJ closes well before adolescence, whereas more recent MRI studies of the NCJ have concluded that the NCJ does not close until 11-16 years of age (Yamazaki et al., 1998). If the results of these MRI studies prove to be reliable and valid, then abnormal development of the NCJ might well prove to be a mechanism by which AIS can develop. Before the development of the NCJ in AIS patients can be assessed for abnormalities, it is essential that the normal characteristics of these images be determined. The aim of this study was to use MRI techniques to characterize the stages that precede the disappearance of the NCJ image, which will aid in interpreting both the normal and abnormal development of this growth

---

** A version of this chapter has been published.*

Rajwani T, Bhargava R, Moreau M, Mahood J, Raso VJ, Jiang H, Bagnall KM. MRI characteristics of the neurocentral synchondrosis. Pediatric Radiology 2002;32:811-816.

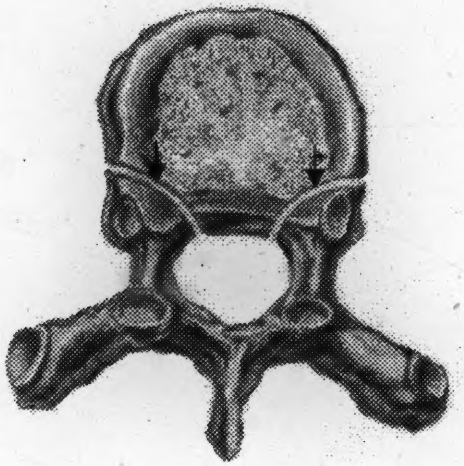

Figure 3-1a. Drawing indicating the position of the NCJ (indicated by arrows) in transverse view.

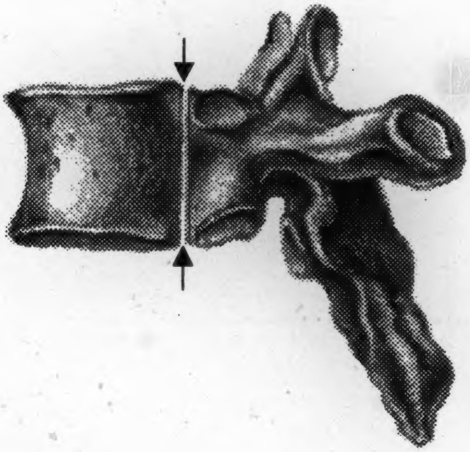

Figure 3-1b. Drawing indicating the position of the NCJ (indicated by arrows) in sagittal view.

plate.

MATERIALS AND METHODS

Four hundred and five NCJs from 11 normal pediatric patients (6 males, 5 females) who underwent MRI, were examined retrospectively with the full permission of the institutional review board. The age range of these patients was 2 months to 15 years, with a mean age of 7 years, 11 months.

Stringent criteria were established to select normal patients, while also recognizing that each of these patients had clinical indications for MRI. All patients included in this study displayed no abnormal findings on MRI examination. Patients with any clinical history of conditions that may have affected vertebral growth or NCJ development were excluded (e.g. neoplastic growths, vertebral abnormalities, muscular abnormalities, scoliosis, neurological conditions, vertebral surgeries). Although 98 potential patients were identified for the study, only 11 patients were found to meet all of the necessary criteria. Since these patients exhibited no pathology, only a single MRI examination was performed making a serial MRI not possible.

The clinical symptoms of the study population included sudden onset of back or neck pain (n=3), suspected spinal lesions (n=2), toe-walking (n=1), suspected osteomyelitis (n=1), suspected spinal cord tethering (n=1), premature birth (n=1), developmental delay (n=1) and sciatica (n=1). In each case, the MRI examination revealed no abnormality, as determined by a pediatric radiologist.

MR imaging was performed using a 1.5 T imager (Siemens, Germany) and T_2 Turbo Spin Echo (TSE) transverse and sagittal views were acquired (TR = 3100, TE = 120, matrix = 230 X 512, slice thickness = 3.0 mm). In some patients, T_1 transverse and sagittal views were also acquired for comparison (TR = 425, TE = 12.0, matrix = 144 x 256, slice thickness = 3.0 mm). For each patient, eleven sections were acquired through the vertebral column in the sagittal plane and three to four sections were acquired per vertebra in the transverse plane.

MR images from each patient were examined randomly, with all patient identifying information removed. The NCJ was defined and its appearance was recorded both

Table 3-1. Distribution of NCJs by stage

	Pictorial Representation	MRI Visualization – medial	MRI Visualization – lateral	Number of NCJs	Percentage of NCJs (%)
Stage 1	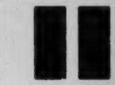	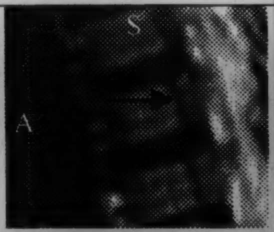	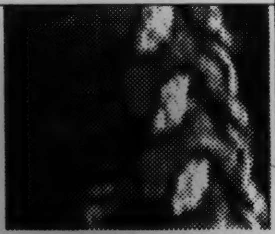	143	43.5
Stage 2	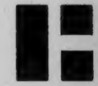	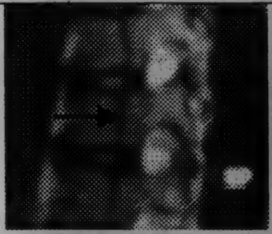	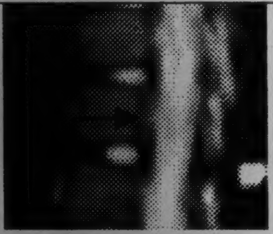	44	13.4
Stage 3a	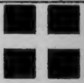	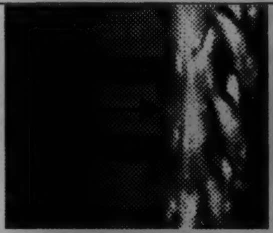	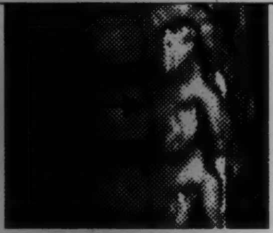	26	7.9
Stage 3b	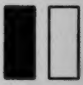	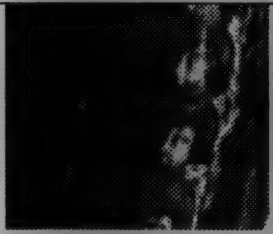	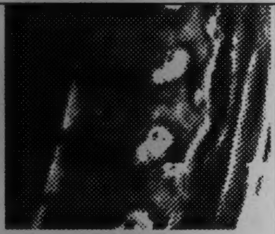	12	3.7
Stage 4	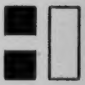	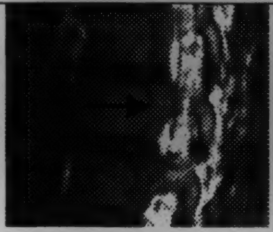	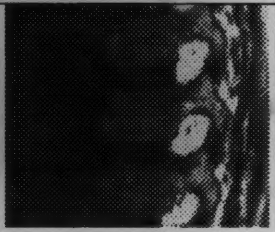	6	1.8

	Pictorial Representation	MRI Visualization – medial	MRI Visualization – lateral	Number of NCJs	Percentage of NCJs (%)
Stage 5	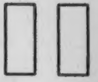	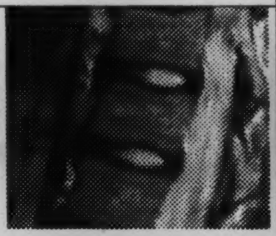	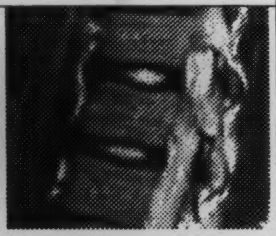	98	29.8
Total				329	100.1

Table 3-1. In the pictorial representation, the medial view is represented on the left. The black areas correspond to the presence of the NCJ as a low intensity line, whereas the areas of no black correspond to the absence of the NCJ. Therefore, stages 1-3 represent stages where the low intensity line is greater than 50% present, whereas stages 4 and 5 represent stages where the low intensity line is greater than 50% absent. The stages are arranged in developmental sequence, with each NCJ passing through either of stage 3a or stage 3b. Only 329/405 NCJs were classified by stage, since there was only one view of the remaining NCJs. In cases where there were 3 views of the NCJ (33/329), the two most prominent views were used to classify the NCJ by stage. The data in the table fulfils the chi squared test, using $\alpha \leq 0.05$.

digitally and as a schematic drawing. The complete NCJ was usually seen on sagittal view as a composite of 2 images and these composite pairs of images were categorized. In this way, the total number of sagittal images was reduced to just 5 categories (Table 3-1). Conclusions reached by viewing individual images of the NCJ were confirmed by three-dimensional reconstruction, using the 3D Voxblast© software application.
The five categories of NCJ appearance were placed in sequential order to represent developmental stages. The intraobserver reliability of the staging system was approximately 95%. This value was determined by having the same observer reclassify all of the NCJs a second time, while being blinded to the stages originally assigned. From in-house testing with a second observer, the interobserver reliability was approximately 90%.

The latest age at which the NCJ of a particular vertebra was classified as greater than 50% present (Stage 3) and the earliest age at which the NCJ was classified as less than 50% present (Stage 4) were noted. The arithmetic mean of these two ages was taken to represent the midpoint of the window of time when the image of the NCJ started to become absent. In cases where no stage 3 or stage 4 NCJs were seen at a particular vertebral level, the NCJ that most closely resembled stage 3 or stage 4 was used in the calculation. This measurement was more valuable than simply determining when the image of the NCJ was no longer present, since the latter encompasses an extremely large window of time and would be much less useful as a marker of vertebral development. The window of time when the NCJ started to become absent was used to determine the difference in NCJ development between different regions of the vertebral column. Since the choice of which stages to use to determine the age of NCJ closure was subjective, the same method as described was also applied with the arithmetic mean of the ages for Stage 2 and Stage 3 being used to determine the age of NCJ closure. The use of Stage 2 and Stage 3 in place of Stage 3 and Stage 4 generated the same pattern of closure ages, with specific vertebrae showing a maximal two year difference in closure ages depending on the specific approach used.

RESULTS

On the T_2 weighted views, the NCJ appeared as a low intensity black line between the neural arch and the centrum. The NCJ image appeared as a concave line posteriorly directed in the transverse plane and as a vertical line in the sagittal plane. In younger patients, the line was particularly easy to identify in sagittal sections since the low intensity black line appeared to be continuous with that in the adjacent vertebrae (Figure 3-2). In sagittal views of older patients, the line was thinner and was no longer continuous across large sections of the vertebral column, but was still easily discerned among several adjacent vertebrae by its position and intensity (Figure 3-2).

The T_2 weighted views provided better visualization of the NCJ than the T1 images. Sagittal imaging was preferred since more vertebrae could be assessed in a given acquisition time. Furthermore, the sagittal sections prevented artifacts within the intervertebral disc from being averaged into the image of the NCJ because a clear space could be visualized between each disc and the vertebra on both sides (Figure 3-2). The T2 transverse images and three-dimensional reconstructions were primarily used in cases of uncertainty.

In the sagittal plane, there were usually two images of the NCJ on either side of the midline (296/405), although there was sometimes a single view (76/405) or 3 views (33/405). In the cases where three views of the NCJ were seen, only two views were dominant with the third view showing only a portion of the NCJ. In successive sagittal views, the image of the NCJ usually appeared further anteriorly as the sagittal sections became more lateral in position. This is due to the fact that the NCJ is an oblique plate of curved cartilage, with the lateral edge being more anterior in position (Figure 3-1). The T_2 transverse views clearly showed that the lateral border of the image of the NCJ became absent before the medial border. Furthermore, the image of an individual NCJ remained the same in consecutive axial images, suggesting that this sequence of lateral to medial closure occurred throughout the complete height of the vertebra. After examining the T_2 sagittal views, it was noted that each individual image of the NCJ in the sagittal plane became fragmented with development, with some variation present in this fragmentation. There were 141 sagittal views of the NCJ where a difference was noted between the superior and inferior portions of the image of the NCJ. In 86.5% of cases

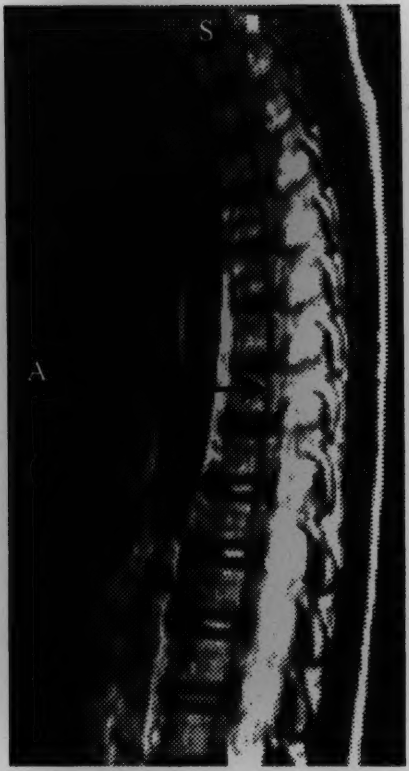

Figure 3-2a. NCJs (indicated by arrow) in the thoracic and upper lumbar region of a 2 year old female appear as thick low intensity black lines that are continuous throughout the vertebrae.

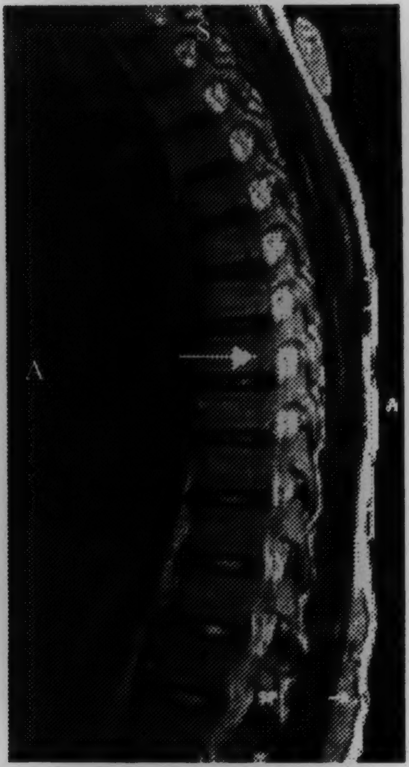

Figure 3-2b. Fewer NCJs (indicated by arrow) are visible in the thoracic and upper lumbar region of a 12 year old male. The low intensity line also becomes thinner and lighter in color. Furthermore, the NCJ images are not continuous throughout the vertebral column, but are only visible in 2 or 3 consecutive vertebrae.

(122/141 NCJs), the sagittal image of the NCJ showed that the NCJ first became less visible in the middle section between the clearly defined superior and inferior areas (Table 3-1, Image 3a). In 8.5% of cases (12/141 NCJs), the inferior portion of the image was the first to become absent whereas in 5.0% of cases (7/141 NCJs), the superior portion of the image became absent first.

The different fragmentation patterns permitted the identification of three distinct variations of an individual image of the NCJ. Since there were generally 2 views of the NCJ on either side of the midline, these three variations occurred in different combinations, resulting in five possible views for any particular NCJ with two possible variations at stage 3 (Table 3-1). These five sets of views were ordered in terms of the most likely course of development, using the concepts that the image of the NCJ becomes absent from lateral to medial and from the middle towards the superior and inferior borders. Using this model, the image of the NCJ became absent in five distinct stages (Table 3-1). Stages 1-3 represented NCJs in which more than 50% of the low intensity line was present, whereas stages 4-5 represented NCJs in which more than 50% of the low intensity line was absent in at least one of the views.

Using these developmental stages, a difference between the right and left NCJ images was seen in 34/143 pairs (23.8%) of NCJs. In each of these 130 cases, there were at least 2 adequate views of NCJ development on either side of the midline where the right and left sides were both clearly visualized. Among these 34 pairs of images, there were 17 cases where the right-sided image was more advanced in terms of the developmental stage and 17 cases where the left-sided image was more advanced. Although this difference in development was noted, it usually involved one developmental stage, except for seven cases where a difference of two developmental stages was noted.

Although the development of the NCJ was characterized into stages, it is important to note that the NCJ becomes absent as part of a continuous process, rather than as a series of discrete steps. The age at which the NCJ first becomes absent was calculated by defining the age at which the image switched from being more than 50% present to less than 50% present, or the age of transition (arithmetic mean) between Stage 3 and Stage 4.

The image of the NCJ became absent in a sequence along the vertebral column although this was not very precise in terms of vertebral level (Figure 3-3). The low intensity line first became absent in the lower cervical region at the age of 6, and then became absent in both cranial and caudal directions. At the thoracic 1 and thoracic 2 levels, the image of the NCJ became absent around the age of 10. Absence of the NCJ images was next noted in the lumbar region at age 12, with the NCJ images becoming absent progressively later in the cranial direction. By age 13, the image of the NCJ had become absent in the entire lumbar spine. By age 14, the NCJ image was not visible at the T9-T12 vertebrae. The image of the NCJ was present for the longest time period in the midthoracic region (T4-T8), where the image remained until the age of 15.

DISCUSSION

The NCJ can be visualized in both T_1 and T_2 weighted images. However, the T_2 weighted sagittal and transverse images were preferred since they provided more clarity and better resolution. This is in contrast to Yamazaki et al. (1998) who preferred the T_1 transverse view of the NCJ for reasons that are unclear. With the advent of MRI technology, the NCJ can be clearly imaged *in situ* and its development determined. From this determination, comparisons can be made between NCJ development at different vertebral levels as well as in abnormal conditions such as AIS. As a potential diagnostic tool, MRI has the advantage of being radiation free and non-invasive.

This study represents the first characterization of the developmental stages of the MR image of the NCJ. However, it is important to realize that the five stages identified are not equal in duration. The results have shown that there is only a small window of time during which the image of the NCJ changes from a very clear, intense dark line to becoming completely absent. This change follows a similar pattern in different vertebrae but occurs at different times of development. The majority of NCJs in this study were classified in the first or the last stage and a larger sample size would be required to better determine the precise duration of each stage. When examining the distribution of NCJs according to stage, it is interesting to note that the number of NCJs in each successive stage decreases from stage 2 to stage 4. This may suggest that the rate of development of the NCJ is not constant, but rather increases with time. Furthermore, it is also noted that

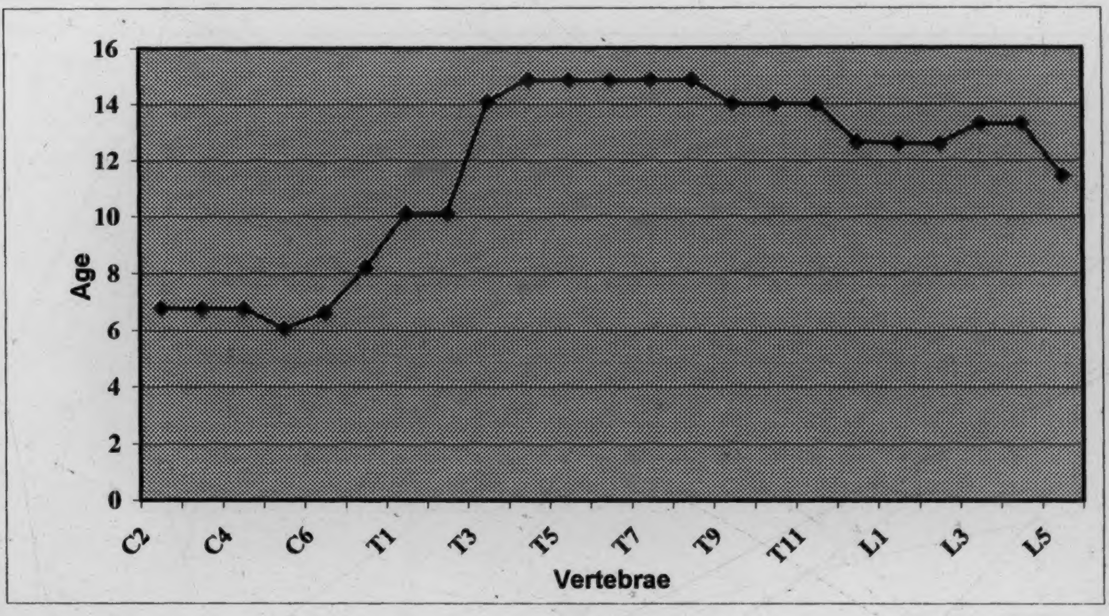

Figure 3-3. Age of closure of the NCJ at different vertebral levels.

only 26.7% of NCJs of a given vertebra correspond to stages 2-4, whereas 73.3% of NCJs are found to be either completely present (Stage 1) or completely absent (Stage 5). The window of time when the NCJ can be found partially present or absent is significantly narrower than the duration of time that the NCJ is seen to be present or absent, which suggests that the developmental stages 2-4 may have use as milestones to mark vertebral development.

In terms of regional patterns, the NCJ shows a sequence of development along the vertebral column, with absence of the NCJ images occurring first in the cervical spine, next in the lumbar spine and last in the thoracic spine. The NCJs in the midthoracic region remain present the longest, until the age of 15 (Figure 3-3). Interestingly, this pattern of NCJ development parallels the sequence of ossification of the neural arch centers in the fetus. Instead of occurring in a cephalocaudal sequence, as once thought, a group of neural arch centers first appears in the lower cervical/upper thoracic region and another appears at the same time in the lower thoracic/upper lumbar region. The remaining centers then appear in a sequential pattern both in a caudal and a cranial direction (Bagnall et al., 1977).

In both this study and that of Yamazaki et al. (1998), it was assumed that the image of the NCJ correlated with an open growth cartilage and the absence of this image correlated with a closed one. The validity of this assumption remains to be proved especially when autopsy studies have shown that the NCJ closes long before the adolescent period, while this study and other imaging studies have suggested that the NCJ is still open at this time. To examine this idea, we subsequently correlated histological images of the NCJ with corresponding MR images (Chapter 4).

In this study, stage was correlated with chronological age. However, since the sequence of closure is related to bone development, perhaps it would be more appropriate to correlate the staging with skeletal age. Furthermore, the well-defined difference in bone development between males and females would suggest that there may be slight differences in the age at which the image of the NCJ becomes absent, at any particular vertebral level (Sinclair, 1985). In this study, the difficulty of acquiring normal patients prevented the gender comparison from being made. A larger population would also allow for the degree of asymmetry in right and left sided development of the NCJ to be better examined. For example, based on the fact that most adolescents exhibit a slight right scoliosis (Taylor, 1983; Sevastik et al., 1995), it might be predicted that the right NCJ would show earlier closure. This concept would be of particular interest because of Taylor's additional finding that the left pedicle in a thoracic vertebra is normally longer than the right pedicle after the age of 7 (Taylor, 1983).

The finding that the image of the NCJ becomes absent last in the midthoracic region is interesting in the context of AIS, since it implies that the NCJ in the midthoracic region likely has the longest time to develop and thus the greatest probability of potentially asymmetrical growth. This would correlate well with the high incidence of apical scoliotic vertebrae in this region in AIS patients (Sevastik et al., 1995; Yamazaki et al., 1998).

The characteristics of the image of the NCJ are an important landmark by which to compare vertebral development at different times and between different individuals, regardless of the significance of this image. The narrow window of time in which the image of the NCJ is seen partially present or partially absent (Stages 2-4) lends itself to use for the characterization of stages of vertebral development. Furthermore, an understanding of the pattern of development of the NCJ is absolutely essential in predicting the behavior of this growth plate in normal and abnormal circumstances.

REFERENCES

Bagnall KM, Harris PF, Jones PRM. A radiographic study of the human fetal spine : 2. The sequence of development of ossification centres in the vertebral column. J Anat 1977;124:791-802.

Beguiristain JL, De Salis J, Oriaifo A, Canadell J. Experimental scoliosis by epiphysiodesis in pigs. Int Ortho 1980;3:317-21.

Knutsson F. Vertebral genesis of idiopathic scoliosis in children. Acta Radiol 1966;4: 395-402.

Lord MJ, Ogden JA, Ganey TM. Postnatal development of the thoracic spine. Spine 1995;20:1692-1698.

Maat GJ, Matricali B, Van Meerten EL. Postnatal development and structure of the neurocentral junction. Spine 1996;21:661-66.

Michelsson JE. The development of spinal deformity in experimental scoliosis. Acta Orthop Scand 1965;36(Suppl 81):9-91.

Ottander HG. Experimental progressive scoliosis in a pig. Acta Orthop Scand 1963;33:91-7.

Roaf R. The basic anatomy of scoliosis. J Bone Joint Surg (Br) 1966;48-B:786-92.

Schmorl G, Junghanns H, Besemann EF (ed.). The human spine in health and disease. Grune and Stratton. New York and London, 1971.

Sevastik B, Xiong B, Sevastik J, Hedlund R, Suliman I. Vertebral rotation and pedicle length asymmetry in the normal adult spine. Eur Spine J 1995;4:95-97.

Sinclair D. Human growth after birth, 4th edn. Oxford University Press. New York, 1985.

Taylor JR. Scoliosis and growth : patterns of asymmetry in normal vertebral growth. Acta Orthop Scand 1983;54:596-602.

Töndury G, Theiler K. Entwicklungsgeschichte und fehlbildungen der wirbelsäule, 2nd edn. Hippokrates Verlag. Stuttgart, 1990.

Vital JM, Beguiristain JL, Algara C, Villas C, Lavignolle B, Grenier N, Sénégas J. The neurocentral vertebral cartilage: anatomy, physiology and physiopathology. Surg Radiol Anat 1989;11:323-28.

Yamazaki A, Mason DE, Caro PA. Age of closure of the neurocentral cartilage in the thoracic spine. J Ped Ortho 1998;8:168-172.

CHAPTER 4

EVALUATING THE USE OF MRI AS A TECHNIQUE FOR VISUALIZING THE NEUROCENTRAL JUNCTION*

INTRODUCTION

The neurocentral junction (NCJ) is a growth plate situated between the neural arch and the centrum of a vertebra. The NCJ is considered important in the growth of both the vertebral body and the posterior arch, although its precise contribution to vertebral development is still unclear (Vital et al., 1989; Töndury and Theiler, 1990; Maat et al., 1996; Yamazaki et al., 1998). In describing NCJ development, the term 'open' is used to refer to the presence of cartilage at this site and the term 'closed' is used to describe its absence. In progressing from open to closed, the NCJ undergoes the process of 'closure' which begins with the completion of the first bridge of bone between both sides of the growth plate (Haines, 1975) and ends when there is a complete absence of cartilage. Historically the process of closure in a typical growth plate is thought to be quite rapid, which has led to difficulty acquiring histological specimens that show the progression of this process (Haines, 1975).

Since the early 1900s, it has been hypothesized that unilateral closure or asymmetrical growth of the NCJ could lead to vertebral rotation, altered biomechanics in the vertebral column and the subsequent development of an abnormal spinal curve (Nicoladoni, 1909; Knutsson, 1966). In assessing the potential role of the NCJ in adolescent idiopathic scoliosis (AIS), some debate has centered on the age of its closure. An important aspect of the debate is that for asymmetrical NCJ growth to account for AIS, it must be shown that at least one NCJ is open during adolescence when the curve is developing. To date, studies on the age of NCJ closure have yielded conflicting results. Anatomic studies (Ottander, 1963; Roaf, 1966; Schmorl et al., 1971; Taylor, 1983; Vital et al., 1989; Yamazaki et al., 1998) and many medical textbooks (Williams et al., 1989) have refuted the role of the NCJ in AIS by suggesting that it closes well before age 10,

---

**A version of this chapter has been accepted for publication.*
Rajwani T, Bagnall KM, Lambert R, Huang EM, Secretan C, Moreau M, Mahood J, Raso VJ, Bhargava R. Evaluating the use of MRI as a technique for visualizing the neurocentral junction. Spine.

which in many cases has prevented further development of the asymmetric growth model of AIS. In contrast, a more recent MRI study by Yamazaki et. al. (1998) has suggested that closure does not occur until 11-16 years, resurrecting the asymmetric growth model. However, Yamazaki's study (1998) was based on the assumption that a line seen on MRI at the NCJ site represented an open growth plate whereas the absence of this line corresponded with growth plate closure. This assumption is yet to be proven and forms the basis of this paper.

The aim of this study was to investigate the discrepancy between the ages of NCJ closure as suggested by anatomic and imaging studies. In addition, MR images of the NCJ were precisely correlated with porcine histological sections to determine the composition of the NCJ image as seen by MRI.

MATERIALS AND METHODS

All of the thoracic vertebrae (14 in each specimen) and lumbar vertebrae (five in each specimen) were harvested from a six-month-old pig and two thirteen-month-old pigs. In total, 114 porcine NCJs in various stages of development (38 open, 64 closing, 12 closed as verified by histologic examination) were examined by gross visualization of the intact vertebrae, MRI and microscopic visualization.

MR images were acquired from each specimen with a 1.5 T system (Siemens, Erlanger, Germany) using a variety of available sequences. Visual observation by an experienced radiologist (R.B.) determined that the T2 Dual Echo Steady State (DESS) sequence produced the best result. Consequently, the T2 DESS sequence (TR = 20, TE = 6, slice thickness = 1.0 mm) was used to acquire sagittal and transverse images throughout the entire porcine spine. In using the above sequence, parameters were defined so that cartilage appeared white (hyperintense) whereas woven and trabecular bone appeared gray (hypointense). These images were supplemented with another complete set of images acquired using the T2 Turbo Spin Echo (TSE) sequence (TR = 3900, TE = 98, slice thickness = 3.0 mm), which represented the routine clinical protocol for most scoliosis patients requiring an MRI at this center. Using the T2 TSE sequence the appearance of the NCJ was reversed when compared to the T2 DESS images, with cartilage appearing black and woven bone and trabecular bone appearing grey. For both sequences, "scout images" were included which displayed the exact sites at which the MR slices had been acquired based on the inbuilt three-dimensional coordinate system of the MR magnet.

After image acquisition, the vertebral column was further dissected into individual vertebrae (19 vertebrae per specimen). These vertebrae were grossly examined for any evidence of open NCJs (T.R., E.M.H.). The tip of a fine #30 needle was also used as a probe to examine for any external difference in bone density that might indicate the NCJ site.

Using the "scout images", each vertebra was sectioned at the precise position that the MR images were acquired. Digital photographs of both surfaces of each section were taken and included an external ruler for magnification purposes. The vertebrae were sectioned serially using a bone cutter and a diamond wafering blade with a thickness of 300 μm (Buehler, Lake Bluff, Illinois). Using this procedure, each anatomic section was 700 μm in thickness, with a 300 μm gap between sections. Ninety-five percent of the vertebrae (n=54) in this study were sectioned in the transverse plane, with the remaining 5% of vertebrae (n=3) sectioned in the sagittal plane. For all vertebrae sectioned in the transverse plane, sections were obtained through the entire longitudinal height of the NCJ and for all vertebrae sectioned in the sagittal plane, sections were obtained through the entire anteroposterior width of the NCJ.

Digital photographs were also taken of the MR images with an external ruler also included in the image. By measuring the distance between several bony landmarks on the MR image and the corresponding anatomic sections, a conversion factor was generated to convert the photograph of the section to the same size as the MR image. Since these sections were taken at exactly the same site as the MR images were acquired ('in-position correlations'), the photograph of the section could be overlayed on the photograph of the MR image to permit accurate correlation (T.R., E.M.H.). The overlaying was made easier by using the layer function in Adobe Photoshop 6.0 (Adobe Systems Inc., Kennesaw, Georgia, United States) which allowed easy alteration of the opacity of the photograph of the MR image or the anatomic section using a sliding scale. In addition to correlating sections taken at the same site as the MR images were acquired, correlations were also performed for adjacent serial sections of the NCJ that were approximately 1 mm to 3 mm away from the position at which a particular MR slice was acquired ('out-of-position correlations') to confirm the accuracy of the overlaying procedure. The accuracy and precision of these correlations was assessed visually. To prevent observer bias, the observer performing a correlation was always blinded as to whether the MR image was an 'in-position correlation' or an 'out-of-position correlation.'

To determine further the composition of the NCJ image, the gross anatomic sections were visualized using a light microscope by four independent observers (T.R., K.M.B., E.M.H., C.S.). The serial sections were first viewed unstained but were then stained with routine 0.1% toluidine blue to allow better visualization of the NCJ cartilage. Digital photographs of the histological sections were taken at both the 100X and 250X magnifications using a digital camera and these images were correlated with the corresponding MR images using the same technique as described above for the unstained sections. This technique allowed a more detailed investigation of the composition of the NCJ image.

RESULTS

The results of gross visualization of the intact vertebrae, visual examination of unstained sections of the NCJ and microscopic visualization of the stained NCJs are summarized in Table 4-1 and Table 4-2.

Analysis of the various MRI sequences available showed that both the TSE and the DESS sequences could be used to observe the NCJ. When the two sequences were compared, the thickness and orientation of the lines on both sequences were exactly the same. However, the correlations were primarily performed with the DESS images since this sequence provided greater visualization due to increased contrast. In comparing the transverse and sagittal MR images, the transverse images provided clearer visualization of the NCJ particularly during later development.

The validation of the correlation procedure showed that the quality of the out-of-position correlations was poor. In all cases, these correlations were significantly inferior to the in-position correlations when both were compared.

Table 4-1. Comparison of gross anatomic visualization of the vertebra, visual examination of unstained sections and microscopic visualization of stained sections as a means of evaluating the open or closed status of the NCJ.

Technique	Summary
Gross visualization of the intact vertebrae	On gross visualization of the intact vertebrae the NCJ was not seen even after removal of all muscular and ligamentous attachments. The NCJ could not be visualized from either the superior or inferior surfaces of the vertebrae since the porcine specimens exhibited epiphysial growth plates on these surfaces, which obscured the underlying NCJ site. On gross examination of the lateral surface, the NCJ could not usually be identified even in cases where it was known to be open from other experiments. The only exceptions arose in three vertebrae from the six-month-old specimen in which the NCJ was faintly seen from the lateral aspect after as much of the periosteum as possible was removed. In these cases, the NCJ appeared as a continuous line indicated by a very subtle change in color (Figure 4-1a). The technique of using the tip of the #30 needle as a probe to identify the NCJ also proved to be ineffective even in these three vertebrae. Similarly, in the case where a vertebra from the six-month-old specimen had been hemisected in the transverse plane to identify the NCJ, and all periosteum had been removed, the external site of the NCJ could not be identified using the #30 needle.
Visual examination of unstained sections of the NCJ	Visual examination of the unstained sections allowed clear determination of the presence or absence of the NCJ site although this site could not be identified as open or closed without microscopic visualization. Where the NCJ site was clearly visible it was seen as an undulating line between the vertebral centrum and the neural arch, which did not extend laterally through the periosteum (Figure 4-1b, Figure 4-2). Interestingly, in the sagittal sections, the NCJ site was clearly and smoothly continuous with the superior and the inferior physeal growth plates which reflected the original cartilaginous vertebral model prior to ossification (Figure 4-2).
Microscopic visualization of the stained transverse NCJs	Microscopic visualization of the stained transverse NCJs confirmed the open or closed status of the growth plate. The NCJ appeared as an undulating line of irregular thickness at all levels. Under light microscopy it was evident that the NCJ cartilage was bipolar with growth columns seen on both surfaces of the growth plate. In all specimens, a region of woven bone was found between the growth plate and the trabecular bone of the vertebra (Figure 4-3a). A general comparison of the NCJs from the six-month-old and thirteen-month-old specimens revealed that the thickness of the cartilage and the degree of organization of the growth columns had decreased significantly in the corresponding vertebrae of the older pigs (Figure 4-3b).

Table 4-2. Comparison of gross anatomic visualization of the intact vertebrae with microscopic visualization of the stained transverse NCJs.

	Number of completely open NCJs on histologic visualization	**Number of completely closed NCJs on histologic visualization**
Number of NCJs seen to be present on gross visualization of the intact vertebrae (and therefore assumed to be open)	6 (True positives)	0 (False positives)
Number of NCJs not visualized on gross visualization of the intact vertebrae (and therefore assumed to be closed)	96 (False negatives)	12 (True negatives)

Table 4-2. On the basis of these findings, gross visualization of the intact vertebrae as a technique of determining the open or closed status of the NCJ has a sensitivity of 5.9% and a specificity of 100%. The low sensitivity reflects the fact that many of the NCJs that were in fact open, as verified by histologic visualization, were assumed to be closed on gross anatomic visualization. The high specificity reflects the fact that no NCJs were falsely identified as being open on the basis of gross anatomic visualization. A similar table comparing the results of MRI and histologic visualization of the NCJ was not created. This is because MRI visualization and histologic visualization of the NCJ agreed exactly in terms of characterizing the NCJs as open or closed and only differed in evaluating the extent of closure.

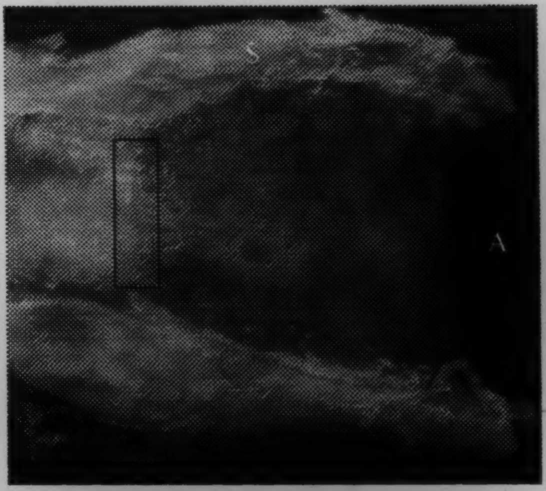

Figure 4-1a. Gross visualization of the lateral surface of the T5 vertebral body in a six-month porcine specimen showing a subtle interface (within the black rectangle) that corresponded to the NCJ site. Only in a very few cases could the site of the NCJ be recognized by gross visualization, even with removal of the periosteum.

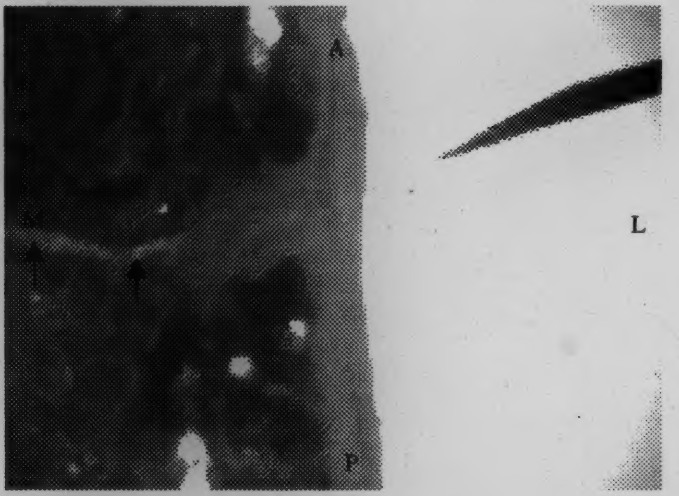

Figure 4-1b. Photograph of the T6 vertebral body from a six-month-old porcine specimen showing that the NCJ does not extend through the periosteum. The cartilage within this junction (indicated by arrows) was quite thin as seen by the comparison to the diameter of the #30 needle on the right and therefore could not be identified by using the needle as a probe.

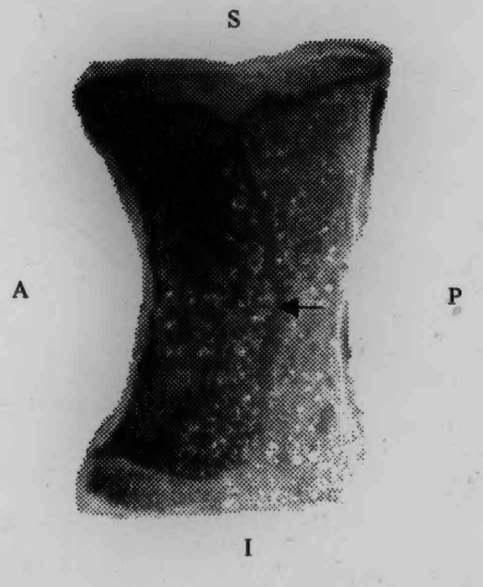

Figure 4-2a. Sagittal section through the L3 vertebra from a six-month-old porcine specimen (NCJ indicated by arrow). Note the NCJ is continuous with the superior and inferior epiphyseal growth plates.

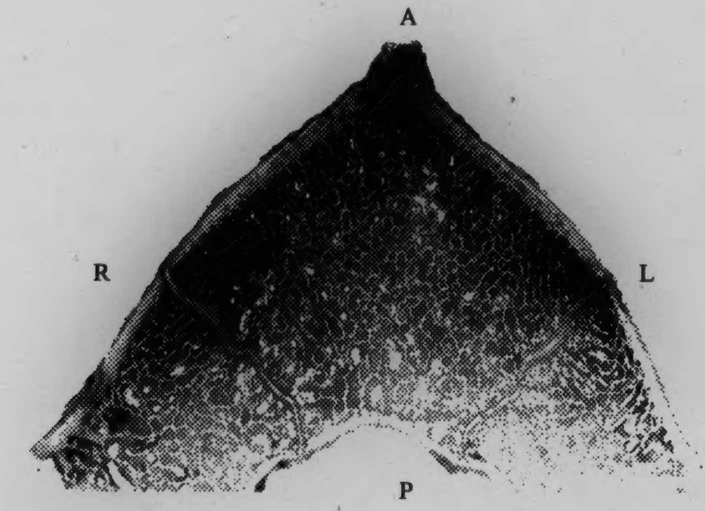

Figure 4-2b. Transverse section through the L2 vertebra from same specimen.

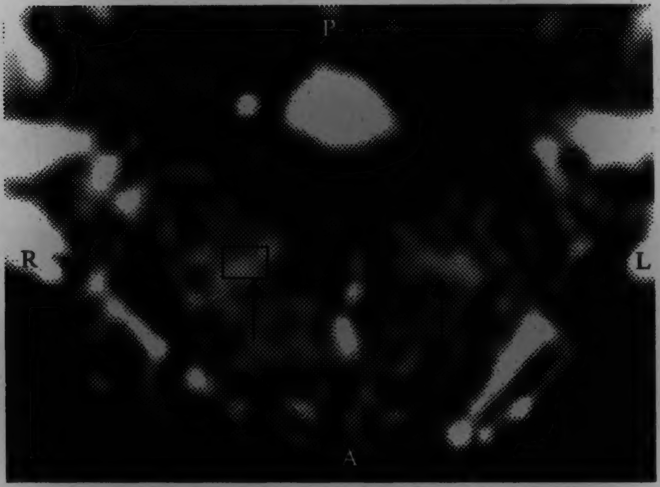

Figure 4-3a. T2 DESS image of T6 from a six-month-old pig. The NCJs appear as two T2 hyperintense white lines (indicated by arrows). The histology of the region within the black rectangle is shown in Figure 4-3b.

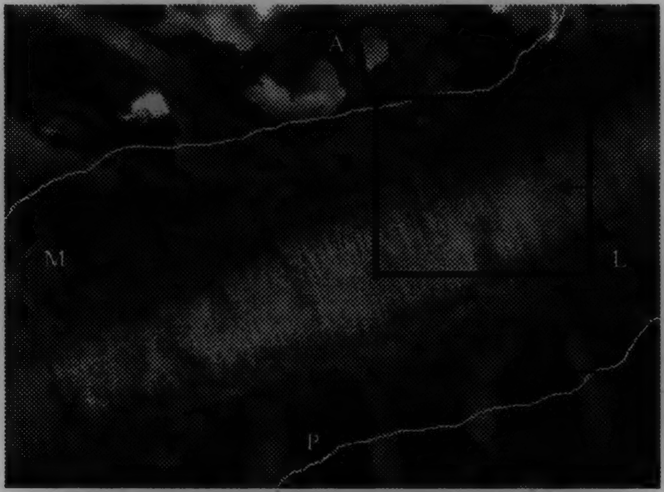

Figure 4-3b. Digital photomicrograph of the NCJ from a six-month old pig stained with toluidine blue (250X magnification) demonstrating the bipolar nature of the growth columns. The area between the thin white lines represented the boundaries of the image of the NCJ, which encompassed portions of the NCJ cartilage (gray arrow), the woven bone (black arrow) on either side of the cartilage and the trabecular bone (diamond-tipped arrow) of the vertebra. The black rectangle on the diagram represents the approximate size of an MR pixel in relation to the growth plate.

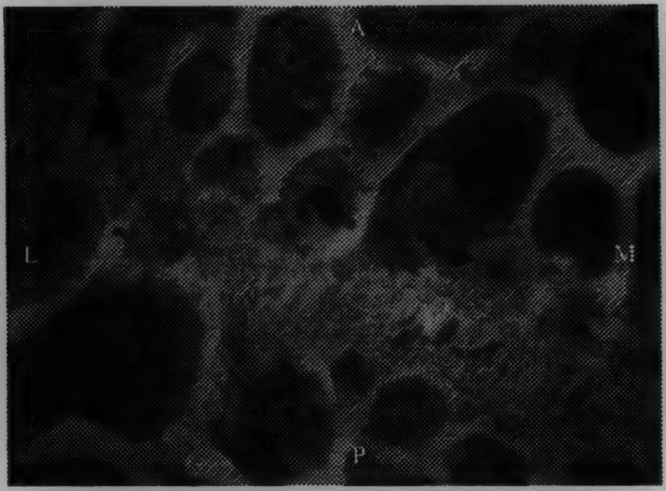

Figure 4-3c. Digital photomicrograph of a typical NCJ (300X magnification) from the lumbar region of a 13-month-old pig. Note the decrease in organization of the NCJ cartilage seen in comparison to Figure 4-3b.

In the six-month-old porcine specimen, it was evident that the NCJ image seen on MRI incorporated the NCJ cartilage (Figure 4-3). However, it was immediately apparent that the MR image of the NCJ was two to three times thicker than the hyaline cartilage and effectively included the newly deposited woven and trabecular bone present on both sides of the growth plate (Figure 4-3a). Upon histologic visualization of the 38 NCJs from the six-month-old porcine specimen, it was clear that all of the NCJs were completely open, with cartilage present from the lateral to the medial aspect at the NCJ site.

In 64 of the 76 NCJs examined in the 13-month-old specimens, histologic visualization confirmed that cartilage was still present on the lateral aspect of the growth plate. However this cartilage did not show the same degree of organization as the cartilage present in the six-month-old specimen (Figure 4-3b). In contrast, the cartilage on the medial aspect of the NCJ in the 13-month-old pigs was very disorganized and interspersed between regions of woven bone. Although histologic visualization revealed that a continuous line of cartilage could not be seen in the transverse plane in these specimens, the DESS and the TSE images showed continuous lines in the transverse plane across the whole of the NCJ site (Figure 4-4). Similar to the six-month specimen, the thickness of these lines was two to three times thicker than the hyaline cartilage in regions where the growth plate could be seen.

In 12 of the 76 NCJs from the 13-month-old specimens, the NCJ had completely closed and only trabecular bone was seen at the presumed old NCJ site. As expected, no NCJ image was seen on the DESS or the TSE sequence at this phase of development and the NCJ site displayed just the signal characteristics of routine trabecular bone as seen elsewhere in the image of the vertebra.

DISCUSSION

This study represents the first characterization of NCJ development using a combination and correlation of gross examination, sectioning, histologic visualization and MRI (Table 4-1). Presumably, the results and conclusions can be extended beyond the NCJ to include other epiphysial junctions. The results clearly show that gross examination of the lateral surfaces of the vertebral body was not an effective technique

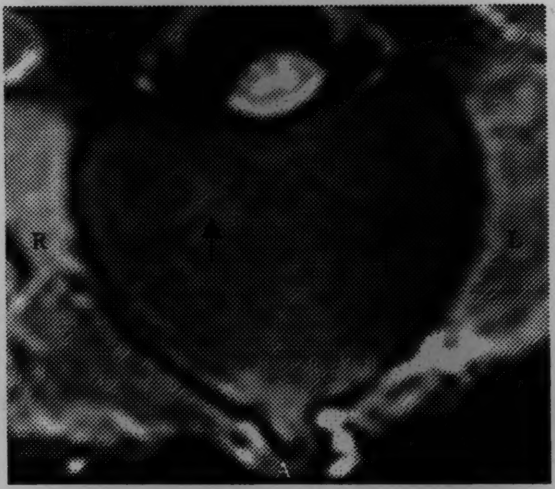

Figure 4-4a. T2 TSE image of L1 from a 13-month-old pig. Note that the NCJ appeared as a continuous black line (indicated by arrows).

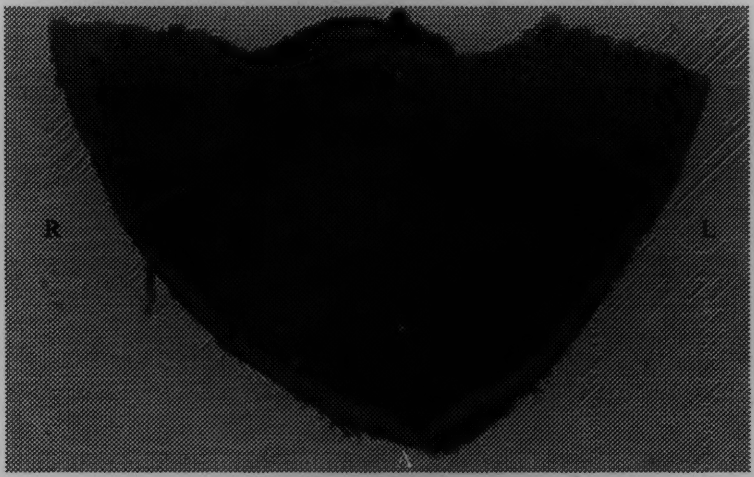

Figure 4-4b. Gross section taken at the same position as the MRI in Figure 4-4a. On histologic examination, the medial portion of the NCJ showed disorganized growth columns and discontinuous areas of cartilage. The arrows indicated the point at which the NCJ began to show signs of closure. The segment of the NCJ that was closing was represented by a continuous line on the MR image.

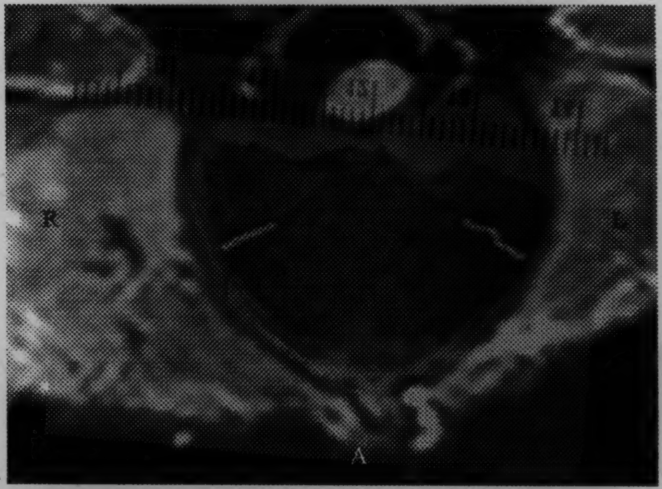

Figure 4-4c. Correlation of the MR image from Figure 4-4a with the gross section from Figure 4-4b. The areas in which the NCJ appeared open on histologic examination are indicated by the white lines drawn on the lateral aspect of the NCJ. In contrast, the MR image of the NCJ was continuous and extended well beyond the region where the NCJ was actually open.

for visualizing the NCJ site, since the NCJ does not extend through the periosteum (Table 4-2). Even in cases where the periosteum was removed, the NCJ site could not be consistently visualized or even detected using a very fine needle as a probe. These difficulties were apparent in the youngest specimen in this study and would be expected to increase as the specimens neared the age of NCJ closure where the width of the NCJ cartilage decreased significantly. These findings advocate the use of extreme caution in interpreting ages of NCJ closure as determined simply by gross anatomic examination. In contrast, examination of unstained anatomic sections provided superior visualization of the NCJ since this site was clearly seen in all cases where resorption had not yet occurred. However, histologic examination of these sections was required to determine unambiguously whether the NCJ cartilage was open or closed. Upon histologic visualization, it was clear that the NCJ growth columns were in fact bipolar, as found previously by Tondury et al (1990) (Figure 4-3a). It was also evident that histologic examination could potentially be used to determine the extent of NCJ closure by assessing the thickness of the NCJ cartilage and the organization of the growth columns.

Potential error

Before the MR correlation results of this study could be accepted it was necessary to determine whether the correlation procedure was valid. There are several limitations inherent in using this procedure. Firstly, the MR images were only two-dimensional constructions of three dimensional volumes since each MR voxel represented an average of all signal intensities within a 1.0 mm^3 volume. This averaging procedure on MRI limited precise correlation to a particular surface although the effects of averaging were minimized by decreasing slice thickness to 1.0 mm. A further limitation of the procedure was the difficulty inherent in ensuring that sections were taken at the precise location that MR images were acquired. This was addressed by using the inbuilt three-dimensional coordinate system of the MR magnet to determine the precise position that MR slices were taken and then by identifying the same site on the actual vertebra very precisely. The sections used in this study displayed excellent correlation with the appropriate MR image as seen by the similarity in the size, shape and contour of the vertebrae and the NCJ (where present) in two dimensions. In contrast, sections that were out-of-position by 1 mm to 3 mm displayed a significant decrease in the degree of correlation as seen by the noticeable differences in size, shape and contour of the vertebrae and the NCJ (where present).

The correlation results showed that the NCJ image seen on both the TSE and DESS sequences included the NCJ cartilage although these results considerably overestimated the extent of this cartilage. In all three specimens, the NCJ image was two to three times wider in the anterior-posterior dimension than the actual width of the NCJ cartilage. Since the NCJ image on the DESS sequence showed superior resolution, a detailed explanation of this phenomenon was sought using this sequence. After correlation it was apparent that the white line seen on the DESS sequence encompassed a region of cartilage, woven bone and trabecular bone. This was surprising since it was anticipated that the signal from woven bone and trabecular bone would be hypointense (black) based on the T2 sequence parameters. The increased thickness of the line on MRI likely arose because the MR pixels used (dimensions = 0.3 mm x 0.4 mm) were unable to differentiate distances in the order of microns. The region spanned by the cartilage and adjoining woven bone was approximately 800 μm in the six-month-old specimen and was therefore represented by only two pixels (Figure 4-3a). Within these picture elements, the T2 hyperintense (white) cartilage signal overwhelmed the T2 hypointense bone signal, resulting in a line thicker than the true thickness of the NCJ cartilage. Since the pixel dimensions used in this study were those routinely used for the clinical MRI of scoliosis patients, similar findings would be anticipated in other MRI investigations of the NCJ. In living samples, decreasing the pixel dimensions to allow increased resolution of the NCJ would not be feasible as the increased scan acquisition time would likely lead to artifacts caused by patient motion including heartbeat and breathing.

In the NCJs from the older specimens, MRI was shown to overestimate the extent of cartilage along the NCJ and underestimate the extent of closure. NCJs in which the medial portion showed signs of closure appeared as a continuous line on MRI, which led to the erroneous conclusion that these NCJs were earlier in the course of development than histologically indicated. Again, this probably occurred because of the large size of the MR pixels which allowed the presence of any cartilage within a pixel to overwhelm the surrounding T2 hypointense elements. Furthermore, MRI did not discriminate between the presence of cartilage with organized growth columns (commonly seen in earlier NCJ development) and the presence of cartilage that was highly disorganized (seen in later NCJ development). When the NCJ was undergoing closure and small discontinuous areas of cartilage were present between larger areas of woven bone, MR consistently underestimated the extent of closure in the medial-lateral direction. Once these areas of cartilage disappeared and the woven bone was remodeled completely into trabecular bone, the NCJ image disappeared. In this study, there was no case where woven bone existed on its own without some degree of intervening cartilage. This would account for the fact that no images of the NCJ were seen where the NCJ line was only partially complete in the transverse plane. This phase may occur in the pig, but likely exists for only a very short period of time, making it almost impossible to collect appropriate images.

Conclusion

Although MRI overestimated the extent of NCJ cartilage in the anterior-posterior and the medial-lateral dimensions, MRI was sensitive at detecting the presence or absence of cartilage. The presence of an NCJ image correlated with the presence of cartilage at the NCJ site and an open NCJ, whereas the absence of such an image correlated with the absence of cartilage at the site and a closed NCJ.

Although this study is based on a porcine model, the results can likely be extrapolated to human NCJ development. The porcine model was chosen since the pig vertebrae are similar to the human vertebrae in size and structure and have been used as a model for human vertebrae in past studies (Ottander, 1963; Beguiristain et al., 1980; Coillard et al., 1999). Furthermore the NCJs appear to be quite similar, to the extent that previous authors have attempted to evaluate the asymmetric growth hypothesis by causing growth arrest at a single porcine NCJ and have found a resulting scoliosis (Ottander, 1963; Beguiristain et al., 1980; Coillard et al., 1999).

Based on the results of this study, the MR determination of the ages of NCJ closure appears to be correct which would suggest that the human NCJ is likely open in the adolescent period as suggested by Yamazaki et al (1998). The overestimation of the extent of NCJ cartilage is most pronounced during the period of its closure. Since this period encompasses approximately two years in the human (Rajwani et al., 2002), this effect does not appear to alter significantly the age of closure data generated from MR studies of the NCJ. Even if MRI slightly overestimates the extent of closure, NCJ closure does not occur at less than the age of 10 years as suggested by anatomic studies.

The debate over the asymmetric growth hypothesis has lasted over a century, with much controversy centered on the age of NCJ closure. This study shows that the age of closure data generated by gross anatomic visualization does not appear to be as reliable or accurate as the data generated by MRI studies. Although MRI may underestimate the extent of closure, it is an accurate tool for determining whether the NCJ is open or closed in an absolute sense of presence and absence of cartilage. For this reason, it is likely that the NCJ remains open well into the adolescent time period as initially suggested by Yamazaki (1998), which would allow the theory that asymmetrical NCJ growth may be cause of AIS to be resurrected. If asymmetric NCJ growth was proven to be a cause of AIS, MRI characterization of this asymmetric NCJ growth might offer a new way to diagnose early cases of AIS, with surgical epiphyseodesis of the more open NCJ as a potential treatment.

REFERENCES

Beguiristain JL, De Salis J, Oriaifo A, Canadell J. Experimental scoliosis by epiphysiodesis in pigs. Int Ortho 1980;3:317-21.

Coillard C, Rhalmi S, Rivard CH. Experimental scoliosis in the minipig: study of vertebral deformations. Ann Chir 1999;53:773-80.

Haines RW. The histology of epiphyseal union in mammals. J Anat 1975;120:1-25.

Knutsson F. Vertebral genesis of idiopathic scoliosis in children. Acta Radiol 1966;4:395-402.

Maat GJ, Matricali B, Van Meerten EL. Postnatal development and structure of the neurocentral junction. Spine 1996;25:661-66.

Ottander HG. Experimental progressive scoliosis in a pig. Acta Orthop Scand 1963;33:91-7.

Roaf R. The basic anatomy of scoliosis. J Bone Joint Surg (Br) 1966;48-B:786-92.

Schmorl G, Junghanns H, Besemann EF (ed.). The human spine in health and disease. Grune and Stratton. New York and London, 1971.

Taylor JR. Scoliosis and growth : patterns of asymmetry in normal vertebral growth. Acta Orthop Scand 1983;54:596-602.

Töndury G, Theiler K. Entwicklungsgeschichte und fehlbildungen der wirbelsäule, 2nd ed. Hippokrates Verlag. Stuttgart, 1990.

Vital JM, Beguiristain JL, Algara C, Villas C, Lavignolle B, Grenier N, Sénégas J. The neurocentral vertebral cartilage: anatomy, physiology and physiopathology. Surg Radiol Anat 1989;11:323-28.

Williams PL (ed.), Warwick, Dyson et al. Gray's Anatomy, 37th ed. Churchill Livingstone. Edinburgh and New York, 1989.

Yamazaki A, Mason DE, Caro PA. Age of closure of the neurocentral cartilage in the thoracic spine. J Ped Ortho 1998;18:168-72.

CHAPTER 5

ASYMMETRIC NEUROCENTRAL JUNCTION DEVELOPMENT IN ADOLESCENT IDIOPATHIC SCOLIOSIS PATIENTS

INTRODUCTION

The neurocentral junctions are bilateral cartilaginous growth plates situated between the neural arch and the centrum of a vertebra. These bipolar growth plates are thought to contribute to the growth of both the vertebral body and the neural arch in the transverse plane (Vital et al., 1989; Töndury and Theiler, 1990; Maat et al., 1996; Yamazaki et al., 1998) as well as having the potential to contribute to vertebral height although this extent is unknown (Vital et al., 1989). In discussing the development of the neurocentral junction, the terms 'open' and 'closed' refer to the presence and absence, respectively, of cartilage at this site.

Most knowledge about the NCJ has been acquired in the context of assessing its potential role in AIS. In the early 1900s, Nicoladoni (1909) examined histologic sections of vertebrae from children with infantile scoliosis and concluded that the NCJ in the region of the apex on the concave side of the primary curve was open (less developed) to a much greater degree than that on the convex side. He suggested that being open implied an eventual increase in relative growth of the NCJ on the concave side resulting in an increased length of the pedicle. In this way, a torsional force causing vertebral rotation could be created with an eventual scoliosis concave to the side of greater pedicle length. Although Nicoladoni (1909) and several other authors (Knutsson, 1963; Taylor, 1983; Vital et al., 1989) have found that the more open NCJ was consistently on the concave side in the apical region which supports this hypothesis, one author has produced the opposite findings (Maat et al., 1996). Furthermore, there is considerable debate as to which side of the curve the longer pedicle is to be found in scoliosis and whether or not this is even a consistent finding (Nicoladoni, 1909; Roaf, 1960; Knutsson, 1963; Taylor, 1983; Vital et al., 1989; Liljenqvist et al., 2002). Nonetheless, the original asymmetric growth hypothesis was considered sufficiently feasible to be applied experimentally in animal models and the results have been both consistent and supportive (Ottander, 1963; Beguiristain et al., 1980; Coillard et al., 1999). For example, Beguiristain et al. (1980)

found that the unilateral fusion of four or five NCJs in the mid-thoracic region of the pig consistently produced a structural scoliosis as predicted, convex on the side of the operation where NCJ growth was restricted.

Over the course of the last century, the major challenge to the asymmetric growth hypothesis for scoliosis has been the idea that the NCJ closes well before adolescence, between the ages of six and 10 years when growth at this site ceases (Knutsson, 1963; Ottander, 1963; Roaf, 1966; Schmorl et al., 1971; Taylor, 1983; Vital et al., 1989; Maat et al., 1996). If this were the case, then asymmetric growth of the NCJ could not be a cause of idiopathic scoliosis in adolescents. However, the age of closure was determined primarily from the results of several anatomic studies (Knutsson, 1963; Ottander, 1963; Roaf, 1966; Schmorl et al., 1971; Taylor, 1983), whereas recent MRI studies have suggested that this growth plate actually remains open well into the adolescent period (Yamazaki et al., 1998; Rajwani et al., 2002). These MRI results have recently been verified by histologic correlation using porcine specimens (Chapter 4) and it has now been extrapolated that the NCJ stays open until adolescence, at least in the thoracolumbar vertebrae. Consequently, the theory that asymmetric growth of the NCJ can result in scoliosis has been resurrected (Yamazaki et al., 1998; Rajwani et al., 2002). Using the MRI technique, the stages and variation in normal NCJ development have been developed in a previous study (Rajwani et al., 2002) with the purpose of examining possible asymmetric development in cases of AIS. Accordingly, in this study, vertebrae from AIS patients were assessed for evidence of asymmetric NCJ development using MRI. Asymmetrical development at any vertebral level was noted and related to the position of the vertebrae in the primary or secondary scoliotic curve.

MATERIALS AND METHODS

Three hundred and six thoracolumbar NCJs from 11 patients (four males, seven females) with AIS were examined with the informed consent of the patients involved and the full permission of the institutional review board. The age range of these patients was 10-16 years, with a mean age of 13.6 years.

Stringent criteria were established to select AIS patients for the study population.

Patients that were not considered to have idiopathic scoliosis or those that had any clinical history of conditions that may have affected vertebral growth or NCJ development were excluded (e.g. neoplastic growths, vertebral abnormalities, muscular abnormalities, neurological conditions, vertebral surgeries). Although 41 potential scoliosis patients were sent for MRI from the scoliosis clinic between March 2000-July 2002, only 11 patients were deemed suitable for inclusion in the study population. Two of the patients (A,B) were both ten years old and had significant primary curves, which suggested that the scoliotic curves in these patients likely developed before the adolescent time period. Since juvenile idiopathic scoliosis (JIS) after the age of six years presents with similar curve directions, gender distributions and progression characteristics as AIS (Lovell and Winter, 2001), these patients were included in this study. Although two of the other patients (J, K) were found to have primary curves of less than 10 degrees at the time of MRI examination, they had notable back asymmetry, clear cosmetic deformity and later went on to develop scoliosis. For this reason, these two patients were included since they represented an early stage of scoliosis development.

Anterior-posterior (10 mAs, 81 kV) and lateral radiographs (25 mAs, 90 kV) of each patient were examined to characterize the scoliotic curve. The Cobb angles for the primary and secondary curvatures were determined by two orthopedic surgeons (M.M., J.M.). MR imaging was performed using a 1.5 T imager (Siemens, Erlanger, Germany) and T_2 Turbo Spin Echo transverse (Figure 5-1a) and sagittal views (Figure 5-1b) were acquired using a routine clinical protocol (TR = 3100, TE = 120, matrix = 230 X 512, slice thickness = 3.0 mm). Sagittal images were acquired through the entire thoracolumbar spine with an initial coronal image taken prior to sagittal imaging to ensure that the sagittal images were not acquired obliquely. Transverse images were generally acquired through the apical vertebra and the two adjacent vertebrae of the scoliotic curves. These transverse images were acquired after adjusting for the inclination of each scoliotic vertebra as seen on the coronal and sagittal images and were therefore acquired parallel to the superior endplate of each vertebra (R.B.).

MR images from each patient were examined randomly with all identifying information removed (T.R., K.M.). The appearance of the NCJ was recorded as a digital

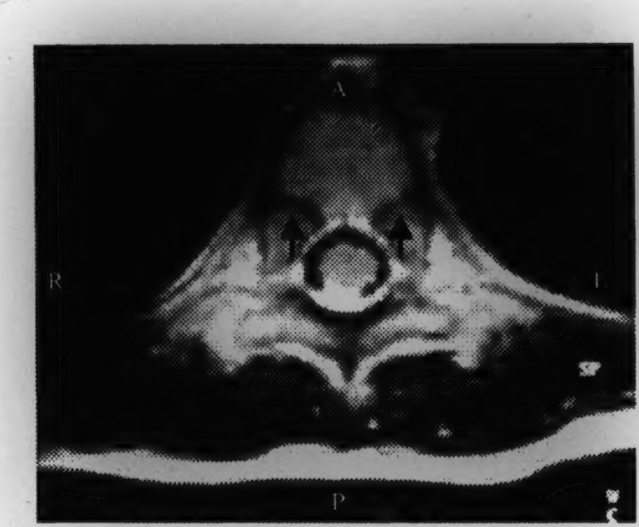

Figure 5-1a. MR image of a T10 vertebra from a 10-year-old demonstrates that the neurocentral junction (black arrows) is a concave shaped cartilage, with the concave portion facing posteriorly.

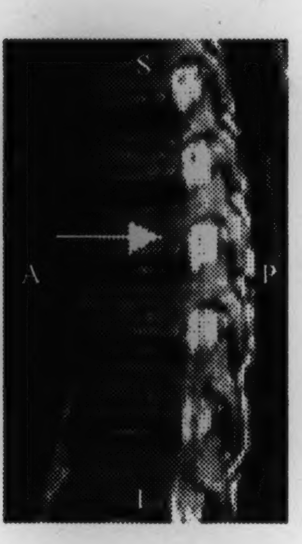

Figure 5-1b. MR image of the thoracolumbar vertebrae from a 12-year-old demonstrates that the neurocentral junction (white arrow) presents as a vertical line in the sagittal plane.

photograph and as a schematic drawing. In cases where the NCJ was present, each complete NCJ appeared on sagittal view as a composite of two or three sagittal images, which were categorized using an established staging system (Table 5-1) (Rajwani et al., 2002). Based on in-house testing with novice and experienced observers, this staging system was previously found to produce reliable results when performed by the same observer or different observers. Using this staging system, asymmetric development was identified in the sagittal plane as a difference of at least two stages between the NCJ on the right and the left sides within a particular vertebra or a difference of one stage between the NCJ on the right and the left side at two or more consecutive vertebral levels. These criteria were based on a previous study (Rajwani et al., 2002) which had established that this extent of difference between NCJ stages at the same vertebral level represented a significant difference from normal variation. In the few cases where the sagittal images did not include the complete right and left NCJs at a particular level, transverse images were used to supplement the detection of asymmetric development. In these few cases, the degree of asymmetric development was identified qualitatively on the basis of a significant visual difference in the right and left NCJ at a particular vertebral level. Once asymmetric NCJ development was identified, it was assessed in relation to the position of the given vertebra in the patient's scoliotic curve (Table 5-2).

RESULTS

On the MRI views, the NCJ was easily identified as a low-intensity black line between the neural arch and the centrum (Figure 5-1, Figure 5-2). The NCJ image appeared as a concave line posteriorly directed in the transverse plane (Figure 5-1a) and as a vertical line in the sagittal plane (Figure 5-1b). The line was more difficult to visualize in older patients, since it was thinner and was no longer contiguous between consecutive vertebrae across large sections of the vertebral column (Rajwani et al., 2002). On the basis of a past MRI-histologic correlation (Chapter 4), the presence or absence of the NCJ image on MRI visualization was established to represent the presence or absence, respectively, of cartilage at the site of the NCJ. Therefore, when referring to the MR images, the term 'open' could be used to refer to cases in which any part of a NCJ image was visible and the term 'closed' was used to denote the complete absence of a

Table 5-1. Staging system for NCJ development

Stage of NCJ Development	Pictorial Representation (medial view on left)
1	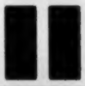
2	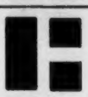
3a	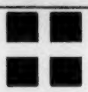
3b	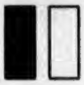
4	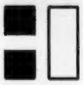
5	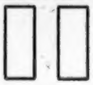

Table 5-1. The five stages of neurocentral junction development are arranged in developmental sequence, with each neurocentral junction passing through either of stage 3a or stage 3b. In the pictorial representation the black areas correspond to the presence of the neurocentral junction as a low intensity line on MRI, whereas the areas of no black correspond to the absence of the neurocentral junction on MRI. Therefore, stages 1-3 represent stages where the low intensity line is greater than 50% present, whereas stages 4 and 5 represent stages where the low intensity line is greater than 50% absent.

Table 5-2. Comparison of right and left NCJ development in AIS patients

Patient (Gender)	Age at Time of MRI	Primary Curve (Apex), Direction, Cobb Angle	Secondary Curve (Apex),Direction, Cobb Angle	Region Visualized	Location of Open NCJs	Comparison of Right and Left Sided NCJ Development
A (F)	10	T6-T12 (T9), Convex right, 30°	L1-L4 (L2/L3), Convex left, 17°	T1-L5	T1-L5	No disparate NCJ growth noted.
B (M)	10	T6-T12 (T9), Convex right, 30°	T12-L4 (L2), Convex left, 22°	T1-L5	T1-L5	Disparate NCJ growth in primary curve with NCJs on the concave side showing advanced closure (best seen at T9, T10).
C (F)	12	T10-L2 (T12), Convex left, 26°	T5-T10 (T7/T8), Convex right, 22°	T1-L3	T1-T11 (T12-L3 were unclear)	No disparate NCJ growth noted.
D (F)	13	T12-L3 (L1/L2), Convex right, 29°	T8-T12 (T10), Convex left, 23°	T2-L2	T3-L1	Disparate NCJ growth noted in the compensatory curve at T8, with NCJ on the concave side showing advanced closure.
E (F)	13	T8 – L1 (T10/T11), Convex right, 22°	N/A	T2-L2	T2-L2	Disparate NCJ growth in primary curve and two vertebrae above the curve (T5,T7), with NCJs on the concave side showing advanced closure (best seen at T7,T9).
F (M)	14	T6-T11 (T8/T9), Convex right, 42°	T12-L3 (L1/L2), Convex left, 32°	T9-L1	T9-L1	Disparate NCJ growth in primary curve with NCJs on the concave side showing advanced closure (best seen at T10, T11).
G (F)	15	T11-L3 (L1), Convex left, 40°	T6-T10 (T8), Convex right, 29°	T2-L1	T7-T9, L1	Disparate NCJ growth seen in compensatory curve with NCJs on the concave side showing advanced closure (best seen at T8).
H (M)	15	T12-L4 (L2), Convex right, 22°	T8-T11 (T9/T10), Convex left, 15°	T1-L5	T1-T11 (T12-L5 were unclear)	No disparate NCJ growth noted.
I (F)	16	T6-T12 (T9), Convex right, 46°	T12-L4 (L2), Convex left, 15°	T1-L5	None	Disparate NCJ growth could not be assessed since all NCJs were closed.
J (F)	16	T3-T11 (T7), Convex left, 9°	T11-L4, Convex right, 10°	T1-L3	T8, T10	No disparate NCJ growth noted.
K (M)	16	T5-T12 (T8/T9), Convex left, 4°	T12-L5 (L2/L3), 8°	T1-L1	T3, T6-T11	No disparate NCJ growth noted.

Table 5-2. In the last column, disparate NCJ growth was noted for individual vertebrae in which the right-sided and the left-sided neurocentral junctions showed a difference of at least two stages in the sagittal staging system or consecutive vertebrae in which the right-sided and left-sided neurocentral junctions showed a difference of at least one stage. Note that five patients showed evidence of asymmetric neurocentral junction growth, with advanced closure of the neurocentral junction on the concave side of the primary curve (three of five cases) or secondary curve (two of five cases).

Figure 5-2a. Transverse image of the T10 vertebra from a 10-year-old shows that the image of the neurocentral junction in the transverse plane first disappears on the lateral aspect (indicated by black arrow).

Figure 5-2b. Sagittal image of the T7-T9 vertebrae from a 13-year-old shows that the image of the neurocentral junction in the sagittal plane first disappears in the middle of the vertebra (indicated by black arrow).

NCJ image in any view. Among the 306 NCJs examined, 196 open NCJs and 90 closed NCJs were noted (Table 5-2). The open or closed status of 20 NCJs could not be conclusively determined due to poor image quality.

In the sagittal plane there were usually two or three images of the NCJ on either side of the midline, which allowed for accurate staging of the NCJ according to apreviously developed staging system (Rajwani et al., 2002). One difficulty encountered with the sagittal images was that sometimes portions of some of the vertebrae extended beyond the region that was being imaged in the sagittal plane due to the degree of lateral curvature. Time constraints in the clinic prevented the entire sagittal diameter from being imaged and the technique employed allowed for only eleven slices (thickness = 3.0 mm) to be acquired throughout the entire sagittal diameter. In a few vertebrae (<10%), this prevented complete staging of the NCJ on either the left or right sides and the transverse images were used for comparison of NCJ development.

The transverse sections through the vertebrae were particularly useful for comparing NCJ development at any particular level since both the right and the left sides were present in a single image. As a result, asymmetric development could be qualitatively assessed using the transverse images without the need for a grading system although a staging system would have allowed quantification of the difference in development.

The transverse images clearly showed that the image of the NCJ became absent from the lateral to the medial aspect (Figure 5-2a). The sagittal images showed that the image of the NCJ became absent from the center of an individual vertebra and progressed towards the superior and the inferior borders (Figure 5-2b). The NCJ was completely absent in some vertebrae and comparison of images between patients illustrated that this absence occurred in a progressive sequence with only slight variation. The image of the NCJ first started to disappear at the upper thoracic and lumbar levels at approximately age 13. By 15 or 16 years of age, the NCJ was also no longer visible in the T2-T6 region. Ultimately, the mid-thoracic NCJs (T7-T10) were the last to disappear and were still visible in some cases at 16 years of age (Figure 3-3).

In the five patients that showed significant asymmetric NCJ development, one to three of the NCJs on the concave side of the primary or secondary curve were more developed (nearer to the closed stage) (Table 5-2, Figure 5-3, Figure 5-4). In all cases, the NCJs on the convex side of either the primary or secondary curve were less developed. In cases where more than one NCJ showed asymmetric development, it was noted that these particular NCJs were usually adjacent or in closely related vertebrae (Table 5-2).

Asymmetric development was not limited to either the primary curve or the secondary curve. Three patients exhibited advanced NCJ closure on the concave side of the primary curve (Figure 5-4) and two patients exhibited advanced NCJ closure on the concave side of the secondary curve (Figure 5-3). Interestingly, no single patient showed asymmetric development in both the primary and the secondary curve. Similarly, asymmetric development did not appear to be limited only to the apex, with two patients exhibiting asymmetric development at the apex of the primary curve, two patients towards the end of the primary curve and one patient towards the end of the secondary curve.

Five of the eleven patients showed no asymmetric development. In one sixteen-year-old patient (I), the NCJs were sufficiently advanced to be closed throughout the entire thoracolumbar region. The results from this patient were included to validate the endpoint of the staging system.

DISCUSSION

To date, most cases of adolescent scoliosis are of unknown cause and are called idiopathic. Originally, all cases of scoliosis were idiopathic but over time various causes were determined (neurofibromatosis, Friedrich's ataxia, etc.). These cases were removed from the idiopathic pool but a large group of patients (80%) remained in the pool with many authors believing that several different causes remained to be identified (Lonstein, 1994). Using this paradigm, this study examined one particular theory, asymmetric NCJ growth, as a possible cause of a subset of cases of AIS.

The NCJ was effectively visualized in both the transverse and sagittal planes using MRI. The image of the NCJ became absent from the lateral to the medial aspect in the transverse plane (Figure 5-2a) and from the center of the vertebra towards the superior and inferior endplates in the sagittal plane (Figure 5-2b). The image also

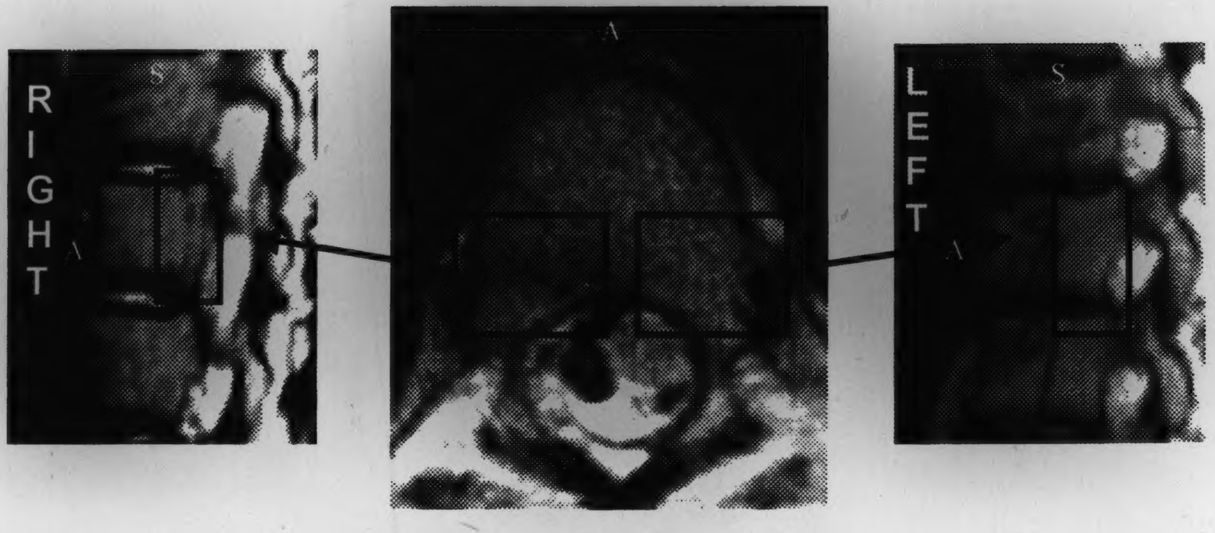

Figure 5-3. In the center, an example of asymmetric neurocentral junction growth is seen in a transverse image through the T8 vertebra of a 15-year-old female. Advanced neurocentral junction closure is seen on the left side, which is the concave aspect of the secondary curve. This finding is verified by the images in the sagittal plane.

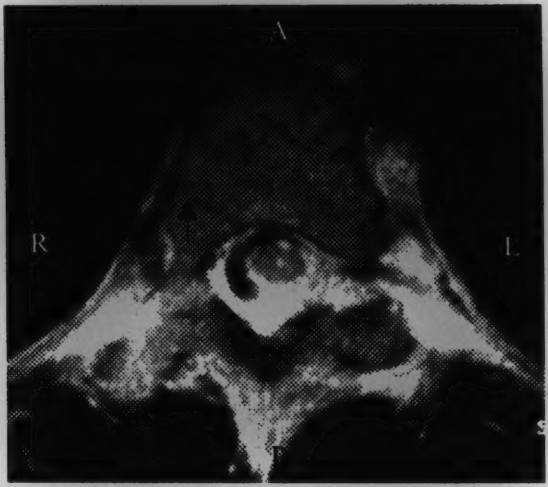

Figure 5-4a. Transverse image of T10 from a 14-year-old male shows asymmetric neurocentral junction growth with delayed neurocentral junction closure (indicated by black arrow) on the convex aspect of the primary curve.

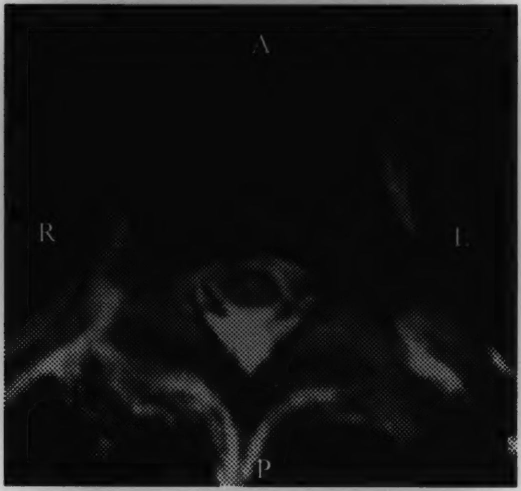

Figure 5-4b. Transverse image of T11 from the same 14-year-old male shows asymmetric neurocentral junction growth with delayed neurocentral junction closure (indicated by black arrow) also on the convex aspect of the primary curve.

displayed a regional pattern of disappearance with the NCJs in the midthoracic region being the last to become absent. All of these findings were in agreement with previous work concerning the developmental characteristics of the image of the NCJ in normal subjects (Rajwani et al., 2002) and suggested that the NCJ closed by the development of bony bridges across the cartilage junction in the pattern described.

This study represents the first characterization of the extent of asymmetric NCJ development among AIS patients in a clinical setting. In the past, there have been concerns about the validity and the use of MRI in assessing NCJ growth and development (Yamazaki et al., 1998). These concerns were based on the discrepancy in the age of NCJ closure determined by MRI and anatomic studies, the lack of histologic verification of MRI results and inadequate resolution of the NCJ image. However, recent work has verified that MRI is an effective and sensitive technique for visualizing the NCJ. Using a porcine model, it has been shown that absence of an NCJ image correlates with the absence of NCJ cartilage and complete closure of the growth plate (Chapter 4). In dealing with the limitations of specific MRI parameters, Yamazaki et al. (1998) suggested that the spatial resolution of the MRI views used in their study (T1 and T2 spin echo sequences, slice thickness = 4.0 mm) was not sufficient for the detection of asymmetry in the thickness of the NCJ. In the current study, the resolution of MR images was improved by the use of thinner MR slices to reduce pixel averaging (slice thickness = 3.0 mm) and the use of the superior T2 turbo-spin echo sequence. With this increased resolution, the thickness of the right and left NCJs at a particular vertebral level could be better compared. Furthermore, the use of a staging system for the sagittal images that had been developed and verified previously (Rajwani et al., 2002) provided a method to quantify the degree of asymmetric development using MRI.

The most important finding of this study was that significant asymmetric NCJ development was clearly noted in five of 10 patients (I being excluded because all NCJs were closed) with advanced development being found on the concave side of the curve in both primary (three patients) and secondary (two patients) curves. Based on previous work (Rajwani et al., 2002), the extent of NCJ asymmetry noted represented a significant difference from normal variation in the stages of NCJ development at the same vertebral level. However, this asymmetric development was not consistent with the findings of

Nicoladoni (1909) who found that the NCJ on the convex side of the curve was always more developed. The latter findings are difficult to reconcile with the findings of the current study. However, it remains to be seen whether advanced development of the NCJ translates into a longer or shorter pedicle and whether this is a consistent finding in patients with AIS. Unfortunately, pedicle lengths could not be assessed for many of the patients in this study as transverse images were only acquired at the apical and adjacent levels of the scoliotic curves and were not acquired at many of the levels at which NCJ asymmetry was noted.

The model created by Nicoladoni (1909) would suggest that the greatest extent of asymmetrical NCJ development would consistently occur in the apical vertebra of the primary curve. However, in this study, the greatest extent of asymmetric development was found to occur at different sites along the curve, either at the apex (two patients) or at the extremities of the primary (two patients) and secondary curves (one patient). Interestingly, any asymmetric NCJ development was always found between the T5 to T11 levels, although the NCJ was often also visualized in numerous other thoracolumbar vertebrae (Table 5-2). This latter finding is significant since the mid-thoracic NCJs are open for the longest period of time and therefore would presumably have the greatest time for the effects of any asymmetrical growth to become manifest. On the basis of these results, the site of asymmetric NCJ development appears to be related to the position of the vertebrae in the vertebral column rather than the position of the vertebrae relative to the apex of the scoliotic curve, as suggested by the model. This may simply be a biomechanical effect of curve development related to the spine as a whole especially when the sequence of NCJ closure is taken into account.

The discrepancy between the pattern of NCJ asymmetry found in this study and the pattern predicted by the model of Nicoladoni (1909) and supported by several animal studies (Ottander, 1963; Beguiristain et al., 1980; Coillard et al., 1999) reinforces the need to reconsider the heterogeneity within any given pool of AIS patients. In any random sample of AIS patients, asymmetric NCJ development could be either a cause or an effect of the scoliosis. Furthermore, if the asymmetrical vertebrae were the cause, then the asymmetry might be amplified as a consequence or an effect of the curve development itself. In this study, it was expected that the number of selected AIS patients with asymmetric NCJ development as the presumed underlying cause would be small and that perhaps we would be fortunate to find even a single patient where this might be the case. It is entirely possible that none of the cases selected for study had asymmetrical vertebral growth as the underlying cause. If so, the results might simply reflect the effects of scoliosis development (for whatever reason) on the development of the NCJ rather than being the underlying cause. This would agree with Roaf's idea (1960) that in all cases of scoliosis, advanced NCJ closure should occur on the side of the concavity due to the increased compressive force on this side of the curve produced by the curve itself. It is possible that the asymmetric development found in this study was perhaps an effect of the scoliosis rather than a cause. We intend to continue to examine MR images of young patients with AIS to determine whether our findings are a consistent feature or if there are indeed some cases in which NCJ development is reduced on the convex side as would be predicted by the model and which is supported by the animal studies (Ottander, 1963; Beguiristain et al., 1980; Coillard et al., 1999). The fact that a pattern of asymmetric development was not seen in five of the other patients who exhibited no detectable NCJ asymmetry emphasizes the complexity of this model and warrants further investigation.

REFERENCES

Beguiristain JL, De Salis J, Oriaifo A, Canadell J. Experimental scoliosis by epiphysiodesis in pigs. Int Ortho 1980;3:317-21.

Coillard C, Rhalmi S, Rivard CH. Experimental scoliosis in the minipig: study of vertebral deformations. Ann Chir 1999;53:773-80.

Knutsson F. A contribution to the discussion of the biological cause of idiopathic scoliosis. Acta Orthop Scand 1963;33:98-104.

Lonstein JE. Adolescent idiopathic scoliosis. Lancet 1994;344:1407-12.

Lovell, Winter B. Pediatric orthopaedics. Lippincott, Williams and Wilkins. Philadelphia, 2001.

Maat GJ, Matricali B, Van Meerten EL. Postnatal development and structure of the neurocentral junction. Spine 1996;21:661-66.

Nicoladoni C. Anatomie und mechanismus der skoliose. Urban and Schwarzernburg. Munchen, 1909.

Ottander HG. Experimental progressive scoliosis in a pig. Acta Orthop Scand 1963;33:91-7.

Rajwani T, Bhargava R, Moreau M, Mahood J, Raso VJ, Jiang H, Bagnall KM. MRI characteristics of the neurocentral synchondrosis. Ped Rad 2002;32:811-16.

Roaf R. Vertebral growth and its mechanical control. J Bone Joint Surg (Br) 1960;42-B:40-59.

Roaf R. The basic anatomy of scoliosis. J Bone Joint Surg (Br) 1966;48-B:786-92.

Rönning O, Kylämarkula S. Reactions of transplanted neurocentral synchondroses to different conditions of mechanical stress. J Anat 1979;128:789-801.

Schmorl G, Junghanns H, Besemann EF (ed.). The human spine in health and disease. Grune and Stratton. New York and London, 1971.

Stokes IAF, Spence H, Aronsson DD, Kilmer N. Mechanical modulation of vertebral body growth. Spine 1996;21:1162-67.

Taylor JR. Scoliosis and growth: patterns of asymmetry in normal vertebral growth. Acta Orthop Scand 1983;54:596-602.

Töndury G, Theiler K. Entwicklungsgeschichte und Fehlbildungen der Wirbelsäule, 2nd ed. Hippokrates Verlag. Stuttgart, 1990.

Vital JM, Beguiristain JL, Algara C, Villas C, Lavignolle B, Grenier N, Sénégas J. The neurocentral vertebral cartilage: anatomy, physiology and physiopathology. Surg Radiol Anat 1989;11:323-28.

Yamazaki A, Mason DE, Caro PA. Age of closure of the neurocentral cartilage in the thoracic spine. J Ped Ortho 1998;18:168-72.

CHAPTER 6

PEDICLE ASYMMETRY IN NORMAL SUBJECTS AND ADOLESCENT IDIOPATHIC SCOLIOSIS PATIENTS[*]

INTRODUCTION

Adolescent idiopathic scoliosis (AIS) is characterized by global changes in the vertebral column as well as local changes in the individual vertebrae (Parent et al., 2002). To date, the changes in the individual vertebrae remain poorly described (Parent et al., 2002) especially pedicle morphology. For example, although Liljenqvist et al. (2000) found no differences in pedicle length in the apical region, several authors have found that the longer pedicle is consistently located on the concavity in the apical and adjacent vertebrae (Nicoladoni, 1909; Taylor, 1983; Vital et al., 1989) whereas Roaf (1960) has found that the longer pedicle is on the convexity. Even artistic representations of vertebrae from scoliosis patients are unclear and in one case, the same artist has depicted exactly opposite representations (Keim, 1972, 1979). Clearly, better characterization of pedicle morphology is needed to improve the understanding of the etiology of AIS, especially as AIS has often been attributed to the asymmetric growth of the neurocentral junction (NCJ) and the associated pedicle (Nicoladoni, 1909; Roaf, 1960; Michelsson, 1965; Knutsson, 1966; Vital et al., 1989; Yamazaki, 1998). The relationship between asymmetric NCJ growth, pedicle length and the direction of rotation of the vertebral body remains to be conclusively determined.

Unfortunately, most studies of pedicle asymmetry have been conducted on patients in the late stages of adolescent scoliosis (Xiong et al., 1995; Liljenqvist, 2002) or even outside the adolescent age group (Smith et al., 1991; Wever et al., 1999; Parent et al., 2002), instead of including patients in the early stages of AIS when asymmetries are developing in conjunction with spinal curves. It has been strongly suggested that this could affect the description of vertebral morphology noted (Vital et al., 1989). Furthermore, in those cases in which measurements have been acquired from unknown cadavers whose scoliosis has long been established, the idiopathic nature of the scoliosis cannot be verified. Regardless of the patient population examined, the definitions used for vertebral morphology measurement are inconsistent and in most cases cannot be applied to both normal and deformed vertebrae or to images acquired by different imaging modalities. In fact, the study of pedicle morphology has also been hindered by the lack of suitable in vivo imaging techniques. Vertebral morphology has been difficult to assess using conventional plain radiographs (O'Brien et al., 2000) due to the overlapping of landmarks (Parent et al., 2002). Although computed tomography (CT) has been used (Vital et al., 1989; Smith et al., 1991; Xiong et al., 1995; Wever et al., 1999; Liljenqvist et al., 2000; O'Brien et al., 2000), the gantry cannot be angled to compensate for curves in the sagittal plane. As a result, some vertebrae are always transected obliquely which has been found to impair measurement accuracy (Xiong et al., 1995). Currently magnetic resonance imaging (MRI) is being promoted as the most accurate means of characterizing pedicle morphology since the plane of acquisition can be altered in all three dimensions and imaging parallel to vertebral endplates can be consistently achieved. MRI also has the additional benefit of being radiation-free, which facilitates routine clinical use in the visualization of patients in the early stages of AIS (Liljenqvist et al., 2002).

---

[*] *A version of this chapter has been published.*
Rajwani T, Bagnall KM, Lambert R, Videman T, Kautz J, Moreau M, Mahood J, Raso VJ, Bhargava R. Using MRI to characterize pedicle asymmetry in both normal patients and patients with adolescent idiopathic scoliosis. Spine 2004;29:E145-152.

Accordingly, the aim of this study was to use MRI to characterize and to compare the pedicle asymmetry in the transverse plane of vertebrae from normal patients and AIS patients in the early stages of scoliosis development.

MATERIALS AND METHODS

Patient Population

MR images from seventy-six pedicles (38 vertebrae) from eight normal patients and 80 pedicles (40 vertebrae) from 10 AIS patients were examined with the permission of the institutional review board (Table 6-1). The age range for the normal patients was one year to eighteen years (mean age: nine years, seven months) and for the AIS patients was 10 years to sixteen years (mean age: thirteen years, two months).

Table 6-1. Normal and AIS patient information.

Population	Patient	Vertebrae Included	Age	Gender	Direction of Curve (Cobb Angle)
Normal	a	T9,T11-L2	1.3	Female	N/a
Normal	b	L3-L5	3.3	Male	N/a
Normal	c	T7-T9,T12-L2	4.5	Male	N/a
Normal	d	T1,T5-T9	8.2	Female	N/a
Normal	e	L2-L5	11.9	Female	N/a
Normal	f	T5-T7,T12-L2	14.7	Male	N/a
Normal	g	L3-L4	15	Male	N/a
Normal	h	T5-T10	18	Female	N/a
AIS	A	L3-L5	10	Female	Right
AIS	B	T9-T11,L3-L5	10	Male	Right
AIS	C	T8-L1	12	Female	Left
AIS	D	T9-T11	13	Female	Right
AIS	E	T8-T10	13	Female	Right
AIS	F	T8-T9, T11-L1	14	Male	Right
AIS	G	T7-T9	15	Female	Left
AIS	H	T10-T11,L3-L5	15	Male	Right
AIS	J	T7, L1-L2	16	Female	Right
AIS	K	Tll, L1-L2	16	Male	Left

Table 6-1. The normal patients are identified with lowercase letters and the AIS patients are identified with uppercase letters. The same AIS patients were also used in a previous study (Chapter 5) and the letters assigned to specific AIS patients were consistent between studies. The age of each patient indicates the age at the time of MR imaging. The direction of the curve indicates the direction of the primary curve. The average Cobb angle for the primary curve in the AIS patients was 29° (range 8°-46°). All of these primary curves were located in the thoracic region, with secondary curves developing either above the primary curve in the thoracic region or below the primary curve in the lumbar region. One patient (E) did not exhibit a secondary curve. One AIS patient (K) had a primary curve of less than 10 degrees at the time of MRI examination, but had notable back asymmetry and later went on to develop scoliosis. This patient (K) was included in the AIS group to represent an early stage of scoliosis development.

Stringent criteria were established to select all patients. Each normal patient had clinical indications for MRI, but did not exhibit any abnormal findings on MRI as assessed by a pediatric radiologist. Patients with any clinical history of conditions that may have affected vertebral growth (e.g. history of cancer, vertebral abnormalities, muscular abnormalities, neurological conditions) were excluded. From an initial pool of 98 potential normal patients, only eight met all inclusion criteria. All AIS patients were carefully screened to ensure that their scoliosis was idiopathic and patients with proven or suspected congenital, muscular, neurologic or hormonal causes of scoliosis were excluded. As a result, only 10 of the 41 scoliosis patients sent for MRI from the scoliosis clinic were included.

MR Imaging and Measurement

T2 Turbo Spin Echo sagittal and transverse MR images (TR = 3100, TE = 120, slice thickness = 3.0 mm) were acquired for each patient using a 1.5 T imager (Siemens, Erlanger, Germany). For all patients, transverse images were acquired through two to six thoracolumbar vertebrae depending on clinical indications. For the AIS patients, the vertebrae included were from the apical and adjacent vertebrae of either the primary, secondary, or primary and secondary curves. Three to four MR images were acquired per vertebra in the transverse plane and the image closest to the mid-pedicle level used for measurement purposes.

Each MRI was measured using the software program Image J 1.28 (Sun Microsystems, Palo Alto, California). The measurements recorded for each patient included posterior body length (PBL), pedicle length (PL), lamina length (LL), pedicle width at three positions (PW1, PW2, PW3), pedicle area (PA), pedicle perimeter (PP) and NCJ angle (NCJ°) (Figure 6-1, Figure 6-2).

A single investigator was responsible for recording measurements to avoid interobserver error. To determine the intraobserver error, all measured parameters from the same image were recorded 10 times and the percent error for each parameter was expressed as the standard deviation of measured values divided by the mean and multiplied by one hundred. To determine the potential interobserver reliability and therefore to determine if the description of these measurements was sufficiently reliable

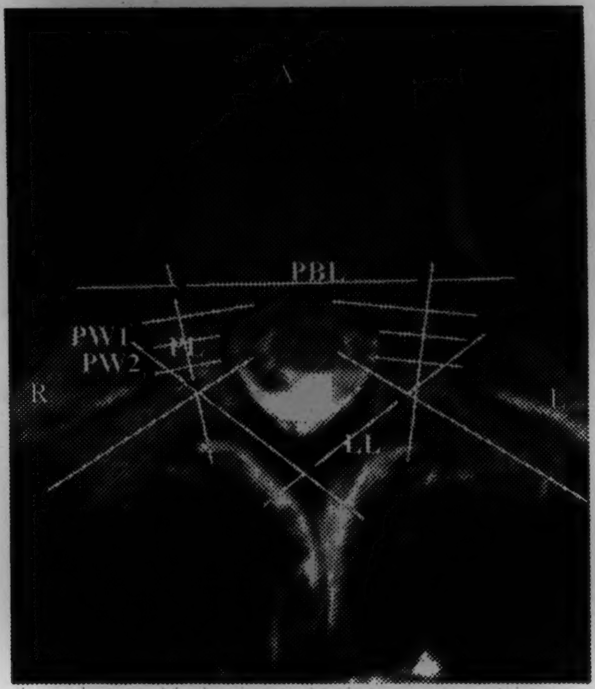

Figure 6-1. The PBL (posterior body length), right PL (pedicle length), right LL (lamina length), left PL (pedicle length) and left LL (lamina length) formed a pentagon that enclosed the vertebral canal and described all segments of the neural arch. The PBL was determined by drawing a straight line perpendicular to the axis of the vertebra that passed through the anterior tip of the vertebral canal. The distance between the outer aspect of the compact bone on both borders of the vertebra was defined as the PBL. Lines were then drawn through the long axis of each pedicle and lamina equidistant from the lateral and medial borders to form a pentagon. The PL on each side was defined as the distance along the line through the axis of the pedicle from its intersection with the PBL to its intersection with the line through the axis of the lamina. The LL on each side was defined as the distance along the line through the axis of the lamina from its intersection with the line through the axis of the pedicle to its intersection with the line through the axis of the lamina on the other side. The total length (TL) for a particular side was defined as the sum of the PL and LL on that side. All pedicle widths (PW1, PW2, PW3) were taken perpendicular to the line through the axis of the pedicle. PW1, PW2 and PW3 were taken at distances of one-fourth, one-half and three-fourth, respectively, of the PL along the line through the axis of the pedicle. To define the regions for the pedicle area and pedicle perimeter, an additional line was drawn through the axis of the transverse process equidistant from the medial and lateral borders of the process. Using the line through the transverse process, the border of the vertebral canal, the PBL, the lateral border of the vertebra and the line through the axis of the lamina, the region of the pedicle could be traced out using Image J and the pedicle area and pedicle perimeter could be determined. All measurements were recorded bilaterally except for PBL.

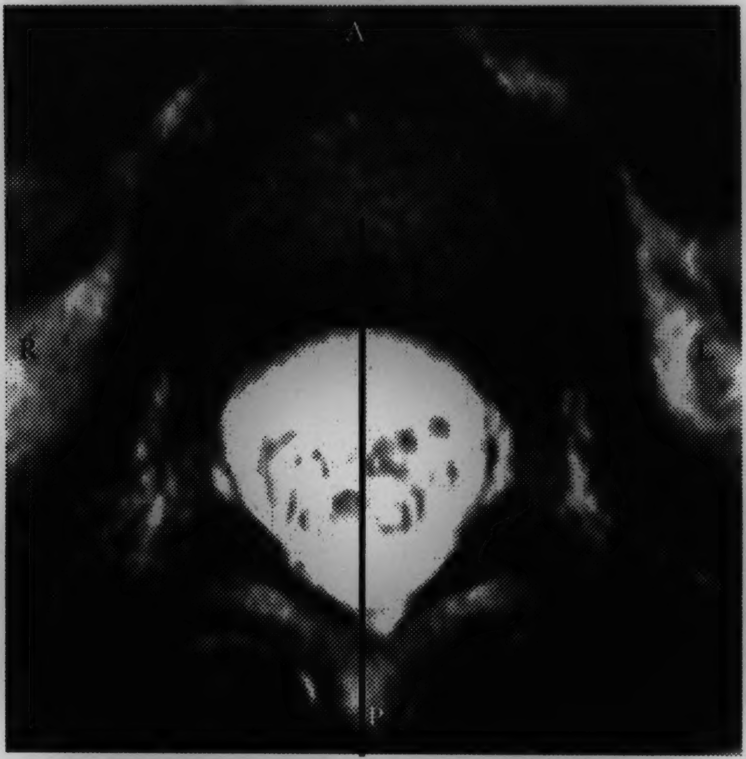

Figure 6-2. The NCJ° (labeled with θ) was determined by drawing a line that connected the medial and lateral border of the NCJ and by measuring the angle (θ) between this line and the PBL (posterior body length).

to be used in other studies, a second observer also measured the parameters from the same image 10 times.

It was recognized that the different ages of the patients and different vertebrae imaged would negate any comparison of absolute values of length. Therefore, several directional indices were calculated for each patient so that ratios of values could be compared as opposed to absolute values. These included the pedicle length index (PLI), the lamina length index (LLI), the total length index (TLI), the pedicle area index (PAI), the pedicle perimeter index (PPI) and the pedicle width indexes at each of the pedicle widths (PWI1, PWI2, PWI3). Each index was a measurement of asymmetry between the two sides of the vertebra and identified the direction of any asymmetry. These indices were calculated by dividing the measurement on the right by the measurement on the left (normal population) or by dividing the measurement on the convexity by the measurement on the concavity (AIS population). With such indices, a symmetrical vertebra would have values close to 1.0. Therefore, indices with a value of less than 0.95 or greater than 1.05 identified the vertebrae with potentially significant asymmetry, as suggested by Taylor (1983). In addition to these directional indices, absolute indices (for PLI, LLI, TLI, PAI, PPI, PWI1, PWI2 and PWI3) were also determined by dividing the greater measurement by the lesser measurement. These absolute indices measured the extent of vertebral asymmetry without indicating the direction.

Statistical Analysis

Statistical analysis was performed using Statview 5.0 (SAS Institute, Cary, North Carolina). Findings were considered significant when $p \leq 0.05$ for the Students-t tests and when the Pearson correlation coefficient was greater than 0.5. The specific statistical analysis performed for each patient population is outlined in Table 6-2.

In analyzing the average absolute and directional indices, these indices were compared between groups and also to the expected value of 1.0. If the average absolute index was significantly different from 1.0, this implied that a significant extent of asymmetry was present. If the average directional index was significantly less than 1.0, this implied that the measurements on the left (normal population) or the convexity (AIS) were greater. Alternatively, if the average directional index was significantly greater than

1.0, this meant that the measurements on the right (normal population) or the concavity (AIS population) were greater.

The extent of pedicle and lamina asymmetry in the AIS patients from this study were also related to a recent study (Chapter 5) done on disparate NCJ growth in the same population of AIS patients to determine if a more open NCJ resulted in a specific pattern of pedicle or lamina asymmetry (Table 6-3).

RESULTS

All the measurements defined in this study could be applied easily and consistently to both the normal and deformed vertebrae. Intraobserver error was considered satisfactory as it was less than five percent for all measurements except for pedicle width, which was slightly higher (six percent). The statistical analysis was extensive and is separated into several categories with only the significant and important findings being reported (Table 6-2).

Normal Patient Population

Analysis of the average absolute indices (for length, width, area and perimeter) showed that the average vertebra from the normal patients displayed pedicle and lamina asymmetry of more than five percent between the right and the left sides. The TLI (combined lamina and pedicle length) for the normal vertebra (mean=0.99, SD=0.05) showed that on average the sum of the left pedicle and lamina lengths was significantly greater than the sum of the right pedicle and lamina lengths. Examining individual patients, this point was emphasized further by finding that the total length on the left side was significantly greater (a difference of more than five percent) in eight of the 38 vertebrae from five patients (Figure 6-3, left). Conversely, the total length on the right side was significantly greater in only one vertebra. Analysis of the average PWI1 (pedicle width at the one-fourth position) (mean=0.93, SD=0.20) and the average PWI2 (mean=0.93, SD=0.21) showed that the pedicle widths on the left side were greater than the widths on the right side. In examining individual vertebrae, the average PWI1 showed a significantly greater width (a difference of more than five percent) on the left

Table 6-2. Summary of statistical analysis

Patient Group	Measurement Analysis	Rationale	Statistically Significant Findings
Normal	Each measured average index (directional and absolute) was compared to 1.0. The right and the left NCJ° were compared. Correlation coefficients were calculated to assess the relationship between PLI and LLI (directional and absolute), left PL and left LL, right PL and right LL, PL on either side and patient age, LL on either side and patient age, NCJ° and PL on either side, and average NCJ° and patient age.	To assess the extent and direction of asymmetry in the normal population. To determine if pedicle and lamina lengths were independent and to determine if these lengths could be used to predict patient age, regardless of vertebral level. To determine if NCJ° could be used as a measure of growth and development.	All average absolute indices (for length, width, area and perimeter) showed absolute asymmetry that was greater than five percent. The directional TLI for the normal vertebrae showed that the total left length (lamina and pedicle) was greater than the total right length (p=0.04). The directional PWI1 and PWI2 showed that the pedicle widths on the left side were greater than the same widths on the right side (p<0.01). The directional PPI showed that the left pedicle had a greater perimeter (p<0.01).
Normal patient subsets a) patients greater than the age of seven years and those younger than the age of seven years	Each measured average index (directional and absolute) was compared to 1.0. All measured indices (directional and absolute) for both groups were compared.	To assess the extent and direction of asymmetry in the normal population subsets. To test Taylor's (1983) finding that patterns of pedicle asymmetry were different within these two groups.	No significant findings were noted and this aspect of the study does not agree with Taylor's work (1983). Taylor found that the right pedicle was longer than the left in patients under the age of seven, whereas the left pedicle was longer than the right in patients older than the age of seven. In this study, the left pedicle was consistently longer in all normal pediatric patients.
AIS	Each measured average index (directional and absolute) was compared to 1.0. The right and the left NCJ° were compared. Correlation coefficients were calculated to assess the relationship between PLI and LLI (directional and absolute), left PL and left LL, right PL and right LL, PL on either side and patient age, LL on either side and patient age, PLI and Cobb angle, NCJ° and PL on either side, and average NCJ° and patient age.	To assess the extent and direction of asymmetry in the AIS population. To determine if pedicle and lamina lengths were independent, to determine if these lengths could be used to predict patient age and to determine if there was a link between pedicle asymmetry and the degree of curvature. To determine if NCJ° could be used a measure of growth and development.	All absolute indices (for length, width, area and perimeter) showed that absolute asymmetry was greater than five percent although the longer pedicle and laminae were not consistently on the concave or convex side of the curve.
AIS patient	Each measured average index (directional and	To assess the extent and	a) No significant findings

subsets: a) left and right curves b) primary and secondary curves c) primary and secondary curves without left curves d) apical and adjacent vertebrae	absolute) was compared to 1.0. All measured indices (directional and absolute) for both groups were compared.	direction of asymmetry in the AIS population subsets. To determine if the extent or the direction of asymmetry differed in different types or regions of the scoliotic curve.	b) Directional LLI was significantly different between the primary and the secondary curves ($p=0.04$), with the average LLI being greater for the primary curve ($p=0.04$). c) Significant difference between the directional PLI for the primary and secondary curves ($p=0.03$), with the primary curve having a greater PLI. Significant difference between the directional LLI ($p<0.01$) with the secondary curve having a greater LLI. The average LLI for both the primary and the secondary curves differed from 1.0 ($p=0.01$, $p=0.01$). d) No significant findings
Normal and AIS Patients	All measured indices (directional and absolute) and NCJ° measurements for both groups were compared.	To determine if the extent or direction of asymmetry differed between the normal and the AIS populations.	The directional PWI1 was significantly greater in the AIS patients ($p=0.04$).

Table 6-2. Findings were considered significant for $p \leq 0.05$ and for Pearson correlation coefficients>0.5. PLI refers to pedicle length index, PPI refers to pedicle perimeter index, PWI refers to pedicle width index, LLI refers to lamina length index and TLI refers to total length index.

Table 6-3. Indices for vertebrae from AIS patients exhibiting disparate NCJ development

Vertebra	Location	Patient (Gender)	Primary Curve (Apex), Direction, Cobb Angle	Secondary Curve (Apex), Direction, Cobb Angle	Pedicle Length Index (PLI)	Lamina Length Index (LLI)	Total Length Index (TLI)
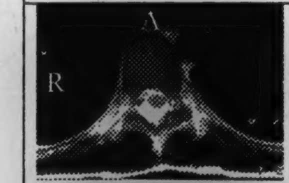	T9	SB(M)	T6-T12 (T9), Right, 30°	T12-L4 (L2), Left, 22°	1.11	0.89	1.00
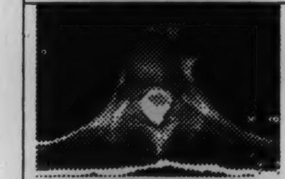	T10	SB(M)	T6-T12 (T9), Right, 30°	T12-L4 (L2), Left, 22°	1.07	0.96	1.02
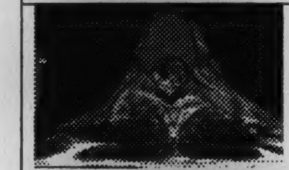	T9	SW(F)	T8 – L1 (T10/T11), Right, 22°	N/A	1.06	0.87	0.95
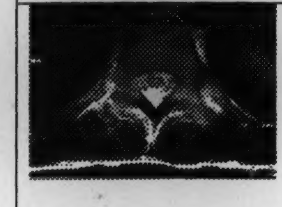	T11	SM(M)	T6-T11 (T8/T9), Right, 42°	T12-L3 (L1/L2), Left, 32°	1.10	0.93	0.99

Vertebra	Location	Patient (Gender)	Primary Curve (Apex), Direction, Cobb Angle	Secondary Curve (Apex), Direction, Cobb Angle	Pedicle Length Index (PLI)	Lamina Length Index (LLI)	Total Length Index (TLI)
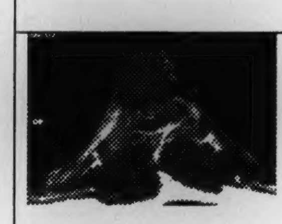	T8	BG(F)	T11-L3 (L1), Left, 40°	T6-T10 (T8), Right, 29°	1.05	0.92	0.99

Table 6-3. The five vertebrae shown in this table exhibited disparate NCJ development and were identified as part of a previous study (Chapter 5) on asymmetrical NCJ development in AIS patients. Note that the PLI are consistently above 1.05 (with one exception) suggesting that the convex pedicle is longer, the LLI are consistently below 0.95 (with one exception) suggesting that the convex lamina is shorter and the TLI are between 0.95-1.05 suggesting that there is no significant asymmetry on the right or left side when the total lengths of the lamina and pedicle are considered.

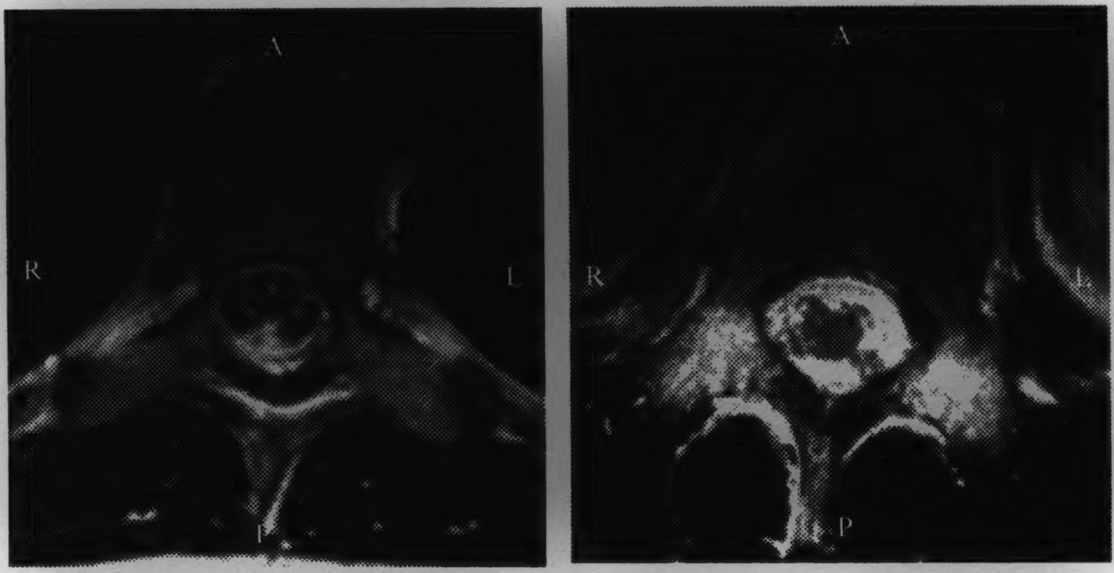

Figure 6-3. Left: T7 vertebra from a normal 18-year-old female shows asymmetry of the pedicles and laminae. The TLI for this patient was 0.91, which indicated that the pedicle and laminae on the left side (right side of diagram) were significantly greater in length than the pedicle and laminae on the right side (left side of diagram). **Right**: L1 vertebra from a 16-year-old male with AIS shows clear asymmetry of the pedicle and laminae. The vertebrae from this patient exhibited the greatest degree of asymmetry in the AIS patient population and this asymmetry was seen visually to be greater than the degree of asymmetry in the normal patient population. The TLI for this vertebra is 1.11, which indicates the convex pedicle and lamina are greater in length than the concave pedicle and lamina. Simple observation of this vertebra confirms that the right and left sides of the neural arch are asymmetric as determined by the actual measurements.

side in 21/38 vertebrae and the average PWI2 indicated a greater width on the left side in 23/38 vertebrae.

AIS Patient Population

Using the absolute indices, it was apparent that the average vertebra from the AIS population displayed pedicle and lamina asymmetry of more than five percent between the two sides (Figure 6-3, right). In contrast, analysis of the directional indices showed no significant findings and therefore no consistent pattern of asymmetry was exhibited in the vertebrae from the AIS patients. Although a significant asymmetry of more than five percent was found in 13/40 vertebrae, the longer side was not consistently situated on the convexity or the concavity of the curve for the patients as a whole. However in considering multiple vertebrae within the same patient, the side of the vertebra with the longer total length remained consistent. For example, the TLI (combined lamina and pedicle lengths) for three of 10 patients indicated that the total length on the convex side was significantly greater than the total length on the concave side in at least two of the vertebrae included from each patient. Although the other vertebrae from these patients displayed no significant difference in total length between the two sides, none of the vertebrae showed a significantly longer total length on the concave side. Conversely, four patients displayed the opposite findings with all of the vertebrae from these patients either showing a greater total length on the concave side or no significant difference in total length between the two sides.

Subsets of the AIS Patient Population

When the AIS vertebrae were separated into groups of apical and neighboring vertebrae, no statistically significant differences were noted. These data suggest that the apical vertebrae did not display a different morphology to the adjacent vertebrae within this population, although the difference between these vertebrae may become more pronounced with progression of the scoliotic curve.

The AIS patient population was then separated into patients with left sided curves (three patients, 12 vertebrae) and right sided curves (10 patients, 28 vertebrae). No significant differences were found between any of the compared indices within each group, which indicates no difference in vertebral morphology based on curve direction.

The AIS patient vertebrae were also separated into vertebrae from primary curves (17 vertebrae) and vertebrae from secondary curves (23 vertebrae). There was a significant difference in the average directional LLI (lamina length index) between the primary and the secondary curves, with the average LLI of the primary curve (mean=0.97, SD=0.11) being less than the average LLI of the secondary curve (mean=1.03, SD=0.10). This concept was further explored by separating the AIS patient population into vertebrae from primary curves (13 vertebrae) and vertebrae from secondary curves (15 vertebrae) with the exclusion of vertebrae from patients with a left curve (12 vertebrae were excluded), who are not thought to represent the traditional pattern of AIS (Robin, 1990). A significant difference was noted in the average directional PLI (pedicle length index) of the two groups, with the average PLI of the primary curve (mean=1.04, SD=0.09) being greater than the PLI of the secondary curve (mean=0.96, SD=0.07). The average directional LLI of the primary curve (mean=0.93, SD=0.07) was significantly less than the LLI of the secondary curve (mean=1.06, SD=0.09). In addition, the average LLI for both the primary and secondary curve differed significantly from 1.0, although the same finding was not noted for the average PLI. These findings show that the distribution of the pedicle and lamina asymmetry between the primary and secondary curves was completely opposite with the lamina on the concavity being significantly longer in the primary curve while the lamina on the convexity was significantly longer in the secondary curve.

Comparing AIS and Normal Populations

No statistical differences were noted among the average absolute indices between the two groups. Although the average absolute PLI (pedicle length index) and the average absolute LLI (lamina length index) were both greater for the AIS population, this difference did not reach significant levels (p=0.07, p=0.10 respectively). However, it is entirely possible that this difference would increase with further development of the scoliotic curve.

No statistical differences in average directional indices were noted between the AIS population and the normal patient population, except for the PWI1. The convex/concave pedicle width index in the AIS patients (mean=1.04, SD=0.23) was significantly greater than the right/left pedicle width index at the same position in normal patients (mean=0.93, SD=0.20).

NCJ Angle

There were no significant differences between the right and the left NCJ angles within the normal patient group, within the AIS patient group or between the two groups. There was no correlation between NCJ° and age or NCJ° and PL for either the normal or the AIS patient group, suggesting that the NCJ° may not be useful as a measure of growth and development.

PLI, LLI, TLI, PWI1, PWI2, PWI3 in Vertebrae with Disparate NCJ Development

In a previous study on the extent of disparate NCJ development seen in the same population of AIS patients, NCJs from several patients showed disparate NCJ development using both sagittal and/or transverse MR images (Chapter 5). In all cases, the NCJ on the convex side was less developed (i.e. open to a greater extent) (Table 6-2). In four out of five vertebrae, the directional PLI (pedicle length index) showed that the pedicle on the convex side of the curve was significantly greater in length, which strongly suggested that a more open NCJ is accompanied by a longer pedicle. In contrast to the pedicle findings, the directional LLI (lamina length index) showed that the lamina on the convex side was significantly shorter. As a result of the inverse relationship between pedicle and lamina lengths, the TLI did not show any significant asymmetry and therefore the overall length of the neural arch appeared to remain constant (Table 6-1).

DISCUSSION

In previous research, a variety of definitions have been used to measure pedicle morphology, which has led to differences in conclusions between studies. Unfortunately, many of these definitions have been based on landmarks from normal vertebrae and do not apply to the measurement of deformed vertebrae from AIS patients. Furthermore, some definitions have depended on the technique used for imaging. In this study, MRI based definitions were used since MRI allowed for improved acquisition of true transverse vertebral images and allowed visualization of scoliotic curves during development. Definitions were created specifically to apply to both normal and deformed vertebrae. The intraobserver error of all measurements was judged to be well within reliable limits as it was under five percent for all quantities, except for pedicle width (6%), which was still considered acceptable. The increased error for pedicle width was probably due to the fact that the transition between compact bone and surrounding connective tissue was hard to establish on MRI. The definitions used were also considered to be reliable between observers since a second observer generated values that were all within five percent of the values generated by the first observer. This suggests that these definitions could reliably be applied in other investigations and could be consistently applied as a method of measuring vertebral morphology. In evaluating asymmetry this study used Taylor's criterion that a difference of more than five percent in a measured vertebral parameter between the right and the left side was significant (1983). The strict definitions of vertebral morphology measurements as well as the high extent of measurement reliability in this study, in relation to the other studies that have used Taylor's criterion (Taylor, 1983; Sevastik et al., 1995) would strongly suggest that this criterion could be applied.

Although the number of patients (n=18) examined in this study was limited by the strict inclusion criteria, these criteria were necessary to ensure that vertebral growth was not affected in normal patients and that all AIS patients exhibited scoliosis that could be considered idiopathic. Even with the strict criteria, this study included significantly more patients than several other comparable studies on vertebral morphology in AIS (Smith et al., 1991; Wever et al., 1999).

Perhaps the most significant and surprising finding in this study was that average normal patients displayed significant asymmetry in neural arch length, with the left pedicle and lamina length being significantly greater. This was clearly seen in eight of the nine vertebrae (from five patients) that exhibited significant asymmetry, whereas only one vertebra had a total right pedicle and lamina length that was significantly greater. In addition, it was also established that the left pedicles were thicker in width at the one-fourth (21/38 vertebrae) and the one-half position (23/38 vertebrae). This is the first time that these findings have been established in vivo in a pediatric population. These findings support the work of Taylor (1983) who measured anatomic specimens and concluded that the left pedicle was longer than the right pedicle in children between the ages of seven and 13. The findings also support the work of Sevastik et al. (1995) who examined pedicle length in the adult population. The explanation for this asymmetry in the normal pediatric population is unclear, although it has been suggested that it may be due to asymmetry in NCJ fusion (Taylor, 1983), the influence of aortic pressure (Dale-Stewart, 1952) or handedness (Burwell, 1977; Taylor and Slinger, 1980; Haderspeck and Schultz, 1981). This asymmetry may also reflect the fact that a vertebra is a composite of several bones, each of which has possibly retained individual identity in relation to growth and development. Taylor (1983) and Sevastik et al. (1995) both suggested that a longer left pedicle may be responsible for the slight right thoracic scoliosis usually found in the normal population. Regardless of the cause or implications of neural arch asymmetry in normal patients, this finding shows that the baseline currently used to evaluate asymmetry in vertebrae from AIS patients must be reconsidered. Vertebral asymmetry in AIS patients has usually been assessed with the assumption that normal vertebrae are symmetrical. Instead, it should be assessed in relation to the extent of asymmetry found in normal vertebrae, since this would have more value in diagnosis and assessment of etiology.

In the AIS patient population, all absolute indices indicated that on average the neural arches were significantly asymmetric. In comparing the extent of asymmetry to the normal population, the AIS patients showed greater asymmetry in the average absolute PLI (pedicle length index) (p=0.07) and the average absolute LLI (lamina length index) (p=0.10). However this asymmetry did not reach significant levels. It is entirely possible that the difference in absolute asymmetry could become significant as the scoliotic curves further developed. Visual examination of individual vertebrae from normal patients and AIS patients suggested strongly that the vertebrae from AIS patients exhibited greater asymmetry in length (Figure 6-3). Surprisingly, there was no consistent distribution of this asymmetry between the convex and the concave sides of the curve. However, in considering that AIS is thought to be due to multiple different causes, a likely explanation is that individual causes might display specific patterns of asymmetry but these patterns are not evident when the data from different causes are pooled together.

In dividing the AIS patients into subsets, several interesting findings were noted when left sided curves, which are not thought to represent traditional AIS (Robin, 1990) were removed from the data. In the primary curve, the pedicle on the convex side and the lamina on the concave side were significantly longer on average than their counterparts whereas in secondary curves, the pedicle on the concave side and the lamina on the convex side were significantly longer. The fact that the longer pedicle and lamina were on one side of the primary curve and the opposite side of the secondary curve was expected since the primary and secondary curves were oriented in opposite directions. However, the inverse relationship between pedicle and lamina length is surprising (Roaf, 1960) and suggests that an increase in the amount of bone deposition and growth in one area (such as the pedicle) may result in a decrease in the amount of bone deposition and growth in an adjacent area (such as the lamina) so that the overall length of the neural arch surrounding the spinal cord remains constant.

The measurement of NCJ° has been performed in the past by Taylor (1983) and Vital et al. (1989). Vital et al. (1989) suggested that the NCJ° (NCJ angle) decreases with age, so that the NCJ becomes more transversely oriented over the course of development. Taylor (1983) has suggested that a greater NCJ° is accompanied by a longer pedicle. In this study, the findings of these two authors were not supported since the NCJ° did not correlate with patient age or pedicle lengths. In addition, the NCJ° did not show any significant difference between normal and AIS patients. The failure of the NCJ° to correlate with pedicle growth could be due to the fact that the definition for pedicle length did not include the region immediately posterior to the NCJ. As a result, any contribution of the NCJ to pedicle length would only be evident over a substantial period of time and after a significant period of bone remodeling. Interestingly, the use of the NCJ° as a sign of development has recently been challenged by the work of Ganey and Ogden (2001). Ganey and Ogden (2001) have suggested that there is a large extent of normal regional variation in the NCJ°, with the NCJs being sagittally oriented and almost parallel in the cervical region and then becoming more transversely oriented in the thoracic and the lumbar regions. Ganey and Ogden's findings (2001) strongly suggest that NCJ angle measurements cannot be evaluated without a consideration of vertebral level.

In relating this study to previous work done on disparate NCJ development in the same AIS population (Chapter 5) it is important to note that the more open NCJ (less developed) was located on the side of the longer pedicle (Table 6-2). This is a significant finding since the relationship between NCJ development and pedicle length has not been explicitly determined. In the past, it has remained unclear whether an open NCJ should be accompanied by a longer pedicle since an open growth plate would permit a greater period of growth or whether an open NCJ should be accompanied by a shorter pedicle on the basis that the contribution of the NCJ to pedicle growth has not yet manifested. This finding that a more open NCJ is accompanied by a longer pedicle is currently being investigated using fluorochrome markers which show bone deposition at the NCJ site. Nonetheless, the preliminary implications of this finding form an important element of the disparate NCJ growth model for AIS.

The methods employed in this study have been shown to be valuable since they allow analysis of vertebral malformations as the scoliotic curve develops. The majority of morphologic studies completed to date have employed older specimens with a greater extent of scoliotic deformity (Smith et al., 1991; Wever et al., 1999; Parent et al., 2002) and these older populations provide little information about pedicle and vertebral asymmetry as AIS is developing. The fact that the left pedicle and lamina were greater in length than the right pedicle and lamina in normal patients is significant and strongly suggests that the baseline used to characterize AIS vertebral morphology should be reevaluated. The AIS patient population also displayed significant asymmetry. However the direction of this asymmetry was not consistent. In fact, a distinct group of patients with a longer neural arch on the convex side and another group of patients with a longer neural arch on the concave side could be identified. This would suggest that the patterns of vertebral morphology in AIS may depend on the specific cause. Further elucidation of the relationship between vertebral morphology and specific causes of AIS would provide insight into AIS diagnosis, treatment and etiology.

REFERENCES

Burwell RG, Dangerfield PH. Anthropometry and scoliosis. In: Zorab PA (ed.). Scoliosis and Growth 5th Symposium. Academic Press. London, 1977:123-64.

Dale-Stewart T. Flattening of centra in Pueblo and Eskimo adult vertebral bodies. Amer J Phys Anthrop 1952;10:17.

Haderspeck K, Schultz AB. Progression of idiopathic scoliosis: an analysis of muscle actions and body weight influences. Spine 1981;6:447-55.

Keim HA. Scoliosis. Clin Symp 1972;24:3-32.

Keim HA. Scoliosis. Clin Symp 1979;31:2-34.

Knutsson F. Vertebral genesis of idiopathic scoliosis in children. Acta Radiol 1966;4:395-402.

Liljenqvist UR, Link TM, Halm HF. Morphometric analysis of thoracic and lumbar vertebrae in idiopathic scoliosis. Spine 2000;25:1247-1253.

Liljenqvist UR, Allkemper T, Hackenberg L, Link TM, Steinbeck J, Halm HFH. Analysis of vertebral morphology in idiopathic scoliosis with use of magnetic resonance imaging and multiplanar reconstruction. J Bone Joint Surg (Am) 2002;84-A:359-368.

Michelsson JE. The development of spinal deformity in experimental scoliosis. Acta Orthop Scand 1965;36(Suppl 81):9-91.

Nicoladoni C. Anatomie und mechanismus der skoliose. Urban and Schwarzernburg. Munchen, 1909.

O'Brien MF, Lenke LG, Mardjetko S, Lowe TG, Kong Y, Eck K, Smith D. Pedicle morphology in thoracic adolescent idiopathic scoliosis. Spine 2000;25:2285-93.

Parent S, Labelle H, Skalli W, Latimer B, de Guise J. Morphometric analysis of anatomic scoliotic specimens. Spine 2002;27:2305-11.

Roaf R. Vertebral growth and its mechanical control. J Bone Joint Surg (Br) 1960;42-B:40-59.

Robin GC. The aetiology of idiopathic scoliosis. Freund Publishing House. Boca Raton, 1990.

Sevastik B, Xiong B, Sevastik J. Vertebral rotation and pedicle length asymmetry in the normal adult spine. Eur Spine J 1995;4:95-97.

Smith RM, Pool RD, Butt WP, Dickson RA. The transverse plane deformity of structural scoliosis. Spine 1991;16:1126-9.

Taylor JR. Scoliosis and growth : patterns of asymmetry in normal vertebral growth. Acta Orthop Scand 1983;54:596-602.

Taylor JR, Slinger BS. Scoliosis screening and growth in Western Australian students. Med J Aust 1980;1:450-78.

Vital JM, Beguiristain JL, Algara C, Villas C, Lavignolle B, Grenier N, Sénégas J. The neurocentral vertebral cartilage: anatomy, physiology and physiopathology. Surg Radiol Anat 1989;11:323-28.

Wever DJ, Veldhuizen AG, Klein JB, Webb PJ, Nijenbanning G, Cool JC, v Horn JR. A biomechanical analysis of the vertebral and rib deformities in structural scoliosis. Eur Spine J 1999;8:252-60.

Xiong B, Sevastik B, Sevastik J. Horizontal plane morphometry of normal and scoliotic vertebrae : A methodological study. Eur Spine J 1995;4:6-10.

Yamazaki A, Mason DE, Caro PA. Age of closure of the neurocentral cartilage in the thoracic spine. J Ped Ortho 1998;18:168-72.

CHAPTER 7

VERTEBRAL CANAL GROWTH IN A RAT MODEL

INTRODUCTION

The process of vertebral canal growth remains largely a mystery especially with regards to the contribution made by the different growth plates and the mechanism of growth after closure of these plates. This lack of knowledge is unfortunate because it is an essential prerequisite for understanding normal vertebral growth. It is difficult to explain how a vertebra that was initially almost small enough to fit inside the vertebral canal of an adult vertebra can attain adult size (Figure 7-1) particularly when growth plates are thought to close relatively early in development. Further characterization of the growth plates thought to be responsible for canal growth would also permit assessment of the consequences of abnormal development at these sites. For example, asymmetric NCJ development has long been considered to be a potential cause of adolescent idiopathic scoliosis (AIS) by numerous authors (Michelsson, 1965; Roaf, 1966; Knutsson, 1966; Vital et al., 1989; Yamazaki et al., 1998). This asymmetry at the site of the NCJ is thought to create pedicle asymmetry, subsequently causing rotation of the vertebral body and an eventual scoliosis. Knowledge of the growth contribution of the NCJ to the pedicle and the vertebral canal is needed to evaluate further this hypothesis.

Currently, the progressive expansion of the vertebral canal is thought to depend almost entirely on the presence of three cartilaginous junctions within each vertebra – the two NCJs and the posterior synchondrosis (PS), although some modeling also occurs by the process of periosteal deposition and resorption both before and after growth plate closure (Figure 7-1) (Ganey and Ogden, 2001). The age of closure of these growth plates in the human is a controversial topic and appears to depend on both the technique of visualization as well as the region of the vertebral column examined. For example, the PS has been reported to close as early as three months (Lord et al., 1995) and as late as six years of age (Moore et al., 1999). Similarly, the NCJ has been reported to close well

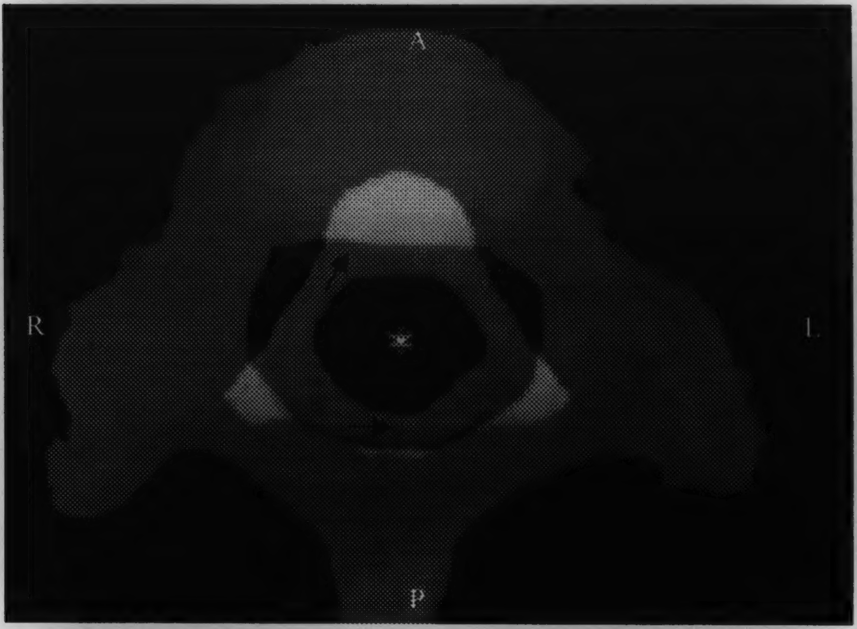

Figure 7-1. The image of the T8 vertebra from a one-week-old Sprague Dawley rat superimposed on the image of the T8 vertebra from a ten-week-old rat showing the tremendous extent of growth and remodeling that occurs during vertebral development. The figures have been superimposed so that the centers of the vertebral canal overlap (at the site of the star). Note that the cartilaginous NCJs and the cartilaginous PS (indicated by arrows) can be visualized on the one-week-old vertebra from gross anatomic examination of the superficial surface of the vertebra but are clearly absent in the adult vertebra.

before 10 years of age based on gross examination of anatomic specimens (Knutsson, 1966; Ottander, 1963; Roaf, 1966; Taylor, 1983; Williams et al., 1989) or as late as 16 years of age using MRI techniques (Yamazaki et al., 1998; Rajwani et al., 2002). Despite the large range of closure ages suggested, current models of vertebral canal growth suggest that once the NCJ and the PS have closed, the vertebral canal should have attained its adult diameter (Ganey and Ogden, 2001). This is supported by radiologic visualization where most authors have concluded that the attainment of adult canal diameters occurs between six and 10 years of age (Knutsson, 1961; Hinck et al., 1966; Hinck et al., 1966; Yousefzadeh et al., 1982; Ganey and Ogden, 2001) which coincides with the ages of growth plate closure based on gross examination. In contrast, the recent MRI studies suggest that these growth plates remain open much longer and might well have more influence on canal growth than previously thought. Ganey and Ogden (2001) have suggested that slight changes in vertebral canal contours are still possible after growth plate closure by the process of periosteal deposition and resorption but these changes have been considered minimal and insignificant. Interestingly, the pattern of periosteal deposition has not been found to be uniform around the vertebral canal. The position of the anterior surface of the vertebral canal has been thought to be fixed relatively early in the course of development with the absence of any subsequent periosteal bone deposition at this site (Knutsson, 1958; Erdheim in Knutsson, 1958; Lord et al., 1995). Consequently, most growth is thought to occur around the remaining periphery of the vertebral canal.

Studies of *in vivo* vertebral development in the human have been limited to measurement of vertebral parameters using radiologic techniques and examination of anatomic specimens. Unfortunately, radiologic methods of growth assessment based on serial examination of patients require the use of assumptions and inferences to explain growth between temporally separated images. Examination of anatomic specimens is even further complicated since these specimens usually come from individuals of different size, gender, race and bone age. In contrast, the use of the fluorochrome method in an animal model permits a method of directly monitoring the sites and amounts of bone deposition in conjunction with anatomical measurements. Fluorochromes, such as tetracycline and alizarin, are chemicals that bind to newly deposited bone (Hilton, 1962;

Wallman and Hilton, 1962; Urist and Ibsen, 1963) and can be identified because they fluoresce differently on exposure to a variety of wavelengths of light. The use of several fluorochromes with different emission and excitation characteristics provides a means of identifying newly formed bone and determining the pattern of bone deposition. In this study, the Sprague-Dawley rat was chosen as the animal model since the rat has commonly been used as a model for the assessment of bone growth using the fluorochrome technique (Baron et al., 1984). The vertebrae of the rat are similar to those of the human, except that rats exhibit little or no haversian remodeling in compact bone (Frost, 1976; Baron et al., 1984; Frost and Jee, 1992). Although it is commonly thought that a rat skeleton continues to grow in length throughout life this is apparently incorrect as in older rats it has been shown that longitudinal bone growth becomes undetectable or stops (Frost and Jee, 1992).

The purpose of this study was to characterize vertebral canal growth and to create a model of canal growth that could explain the role of growth plates and periosteal mechanisms (periosteal deposition and resorption) in canal development. Although maximal vertebral canal diameters were previously thought to be closely related to the age of growth plate closure, the recent MRI studies, which suggest a later age of closure for these growth plates, have shown that the mechanisms of canal growth are not well understood. In this study, vertebral canal growth was directly assessed in rats of different ages using injection of two different fluorochromes, which allowed the pattern and sequence of bone deposition to be determined. Fluorochrome-based visualization of bone deposition was complemented by direct measurement of vertebral canal, growth plate and neural arch parameters.

MATERIALS AND METHODS

Fluorochrome Protocol

Sixty-nine male Sprague-Dawley rats of varying ages (Table 7-1) were housed at 20°C in a 12-hr light/12-hr dark cycle with free access to water and a commercial rat diet (LabDiet 500I, Bimeda-MTC Animal Health Inc., Brentwood, Missouri, United States). Only male rats were included in the experiment to prevent any variations in bone deposition between rats due to gender. Rats were of varying ages on arrival, as shown in Table 7-1, with six rats in each group except for Group 1 which had nine rats. The rats in

Table 7-1. Age of rats on arrival, fluorochrome injection and euthanization for each group

Group Number	Number of Rats in Group	Age of Rats on Arrival (days)	Age of Tetracycline Injection (days)	Age of Alizarin Injection (days)	Age at Euthanization (days)
1	9	1	3	5	7
2	6	3	4	8	12
3	6	12	13	17	21
4	6	21	22	26	30
5	6	28	29	33	37
6	6	35	36	40	44
7	6	42	43	47	51
8	6	49	50	54	58
9	6	56	57	61	65
10	6	63	64	68	72
11	6	70	71	75	79

Table 7-1. For all groups except group 1, rats were injected with tetracycline one day after arrival, injected with alizarin four days later and euthanized four days after alizarin administration. The group 1 rats were injected with tetracycline two days after arrival, injected with alizarin two days later and euthanized two days after alizarin administration. As seen from the table above, the group numbers used in this study correspond approximately to the age in weeks at the time of euthanization.

Groups 1, 2 and 3 were housed in three separate, single cages because they were too young to be separated from their mothers. All other rats had been weaned and were housed in pairs of the same age in different cages. One day after arrival (two days for Group 1), each rat was injected intraperitoneally with a solution of tetracycline hydrochloride (Sigma Chemical Co., St. Louis, Missouri, United States) in 2.1% $NaHCO_3$ saline at a dose of 50mg/kg. After four days had elapsed (two days for Group 1), each rat was given a second intraperitoneal injection of the fluorochrome alizarin red S (Sigma Chemical Co.) in 2.1% $NaHCO_3$ saline at a dose of 30mg/kg. The solutions were saturated and so were spun using a centrifuge prior to injection. The solution injected was drawn from the supernatant so that a consistent concentration was administered. After another four days had elapsed (two days for Group 1), each rat was euthanized with an overdose (0.5 mg/kg) of sodium pentobarbital (Euthanyl, Bimeda-MTC Animal Health Inc., Cambridge, Ontario, Canada) according to established animal care protocols. The age of the rats at the time of euthanization is summarized in Table 7-1. All experimental protocols were performed with the full permission of the institutional review board.

The seventh, eighth and ninth thoracic vertebrae were harvested from each rat with individual vertebrae being placed in OCT compound (Tissue-Tek, Sakura Finetek U.S.A. Inc., Torrance, California, United States) and frozen immediately at -70°C to form solid blocks. These vertebrae were sectioned transversely using a cryostat (Minotome, International Equipment Company, Needham Heights, Massachusetts, United States) to produce sections of approximately 30 μm thickness which were mounted on slides and covered, being held in place by a non-quenching mounting medium (Cytoseal 60, Richard Allen Scientific, Kalamazoo, Michigan, United States) designed to protect the fluorescence.

For each vertebra, the most complete section acquired at the mid-pedicle level was visualized at 200X using a fluorescence microscope (Axioskop 2, Carl Zeiss Inc.). A pilot study had shown that both fluorochromes could be visualized simultaneously using a Fluorescein filter block (excitation 450-490 nm, beam splitter 510 nm, emission 515 nm). In some cases, a Hoescht filter block (excitation 365 nm, beam splitter 395 nm, emission 397 nm) which could only visualize tetracycline hydrochloride was used to differentiate between the two fluorochromes and eliminate any confusion particularly when fluorescent areas overlapped. The pattern of fluorochrome deposition was recorded for each vertebra as a schematic drawing and digital photographs were taken where appropriate so that montages could be created to visualize larger areas.

The selection of specific fluorochromes, dosages, dosing intervals and sectioning protocol was based on past studies (Landry et al., 1964; Baylink et al., 1970; Hammer et al., 1973; Hammond and Storey, 1974; Deeb and Herrmann, 1974; Baron et al., 1984; Sontag et al., 1986; Sun et al., 1992; Ito et al., 1993; Lepola et al., 1996; Kidder et al., 1997; Mente et al., 1999) and a series of pilot experiments used to develop an optimum protocol for visualization of bone deposition. Tetracycline hydrochloride and alizarin red S were chosen for use instead of other fluorochromes such as calcein blue and xylenol orange since the pilot studies had shown that tetracycline and alizarin allowed superior visualization of bone deposition under the fluorescence microscope filter sets available. For each fluorochrome, dosages of 20mg/kg, 30mg/kg, 40mg/kg and 50mg/kg were compared. Dosages of 50mg/kg were not exceeded since Harris et al. (1968) had found that administration of tetracycline at dosages greater than 60 mg/kg results in mineralization defects. After selection of fluorochromes, dosing intervals between one to six days were compared and a four-day interval was chosen for clear visualization and optimum separation of fluorochromes. Rats were not euthanized until four days after administration of the second label as this allowed additional unlabelled bone to be deposited after the second fluorochrome had been incorporated. The deposition of this unlabelled bone allowed unambiguous separation between the second fluorochrome and the background fluorescence of bone, which tended to be most pronounced at the edges of bone sections.

Several different sectioning protocols were considered including plastic embedding and subsequent sectioning with a 300 μm diamond wafering blade (Buehler, Lake Bluff, Illinois) with and without grinding with sandpaper, and simple cryostat sectioning. Sectioning with a diamond wafering blade did not allow bone sections thinner than 100 μm to be acquired and any form of grinding even with the finest of sandpaper resulted in deterioration of bone surfaces, especially vertebral trabecular bone.

For this reason, the cryostat sectioning technique was preferred since it enabled sections to be acquired at 30 μm thickness and preserved vertebral trabecular bone.

Measurement of NCJ Parameters

Digital photomicrographs were acquired of each microscope field that included a section of the vertebral canal or the NCJ. These photomicrographs were exported to Adobe Photoshop 6.0 (Adobe Systems Inc., Kennesaw, Georgia, United States) and assembled to form a complete montage image of each NCJ and vertebral canal. For each vertebra, the presence or absence of the cartilaginous NCJ and the PS was noted.

Having created a montage depicting the complete NCJ, the area, the perimeter, the width, the length of the NCJ at five points and the area of bone deposited anterior and posterior to this growth plate were measured using the software program Image J 1.28 (Sun Microsystems, Palo Alto, California, United States). Measurement definitions are shown in Figure 7-2. On first glance, the direction measured for NCJ length may seem counterintuitive, but the NCJ length was defined to be in the same axis as pedicle length. A single investigator recorded all measurements to avoid variation caused by interobserver error. To determine the intraobserver error, all measured parameters from the same image were recorded 10 times and the percent error for each parameter was expressed as the standard deviation of measured values divided by the mean and multiplied by one hundred. To determine if these measurement definitions were sufficiently reliable to be used in other studies, a second observer also measured the parameters from the same image 10 times and the observer errors were compared.

Measurement of Vertebral Canal Parameters

For each complete montage image of the vertebral canal, the area, perimeter, AP diameter and transverse diameter were measured using Image J 1.28. Measurement definitions are shown in Figure 7-3. The same method used for the NCJ parameters was used to determine intraobserver and interobserver error. In a pilot study, the same vertebral parameters were also recorded from images of 10 complete T8 vertebrae dissected from Sprague-Dawley rats of ages one week to 10 weeks to determine if the rat vertebrae continued to grow in size after week seven.

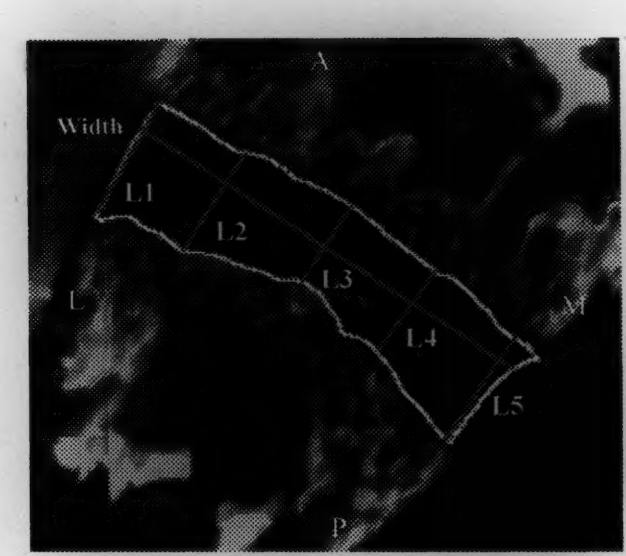

Figure 7-2. Using Image J 1.28, the borders of the cartilaginous NCJ were traced to form a polygon and the area and the perimeter of the NCJ measured by calculating the area and perimeter of this polygon. The center was calculated and a line passing through the center perpendicular to the perimeter and limited by the anterior and posterior NCJ borders was used to calculate the central length (L3). A line passing through the center perpendicular to L3 and with its endpoints on the lateral and medial aspects of the NCJ was used to calculate the width of the NCJ. The L2 and L4 were calculated by drawing lines parallel to the L2 with endpoints on the anterior and posterior NCJ borders at 2/5 and 4/5 the width (measuring from the lateral aspect), respectively, of the NCJ. The L1 and the L5 were the most lateral and medial lines, respectively, that could be drawn parallel to the L3 and within the borders of the NCJ. The area of bone deposited anterior and posterior to the NCJ were determined by tracing out the region of fluorochrome deposition anterior and posterior to the NCJ and then calculating the area of this polygon.

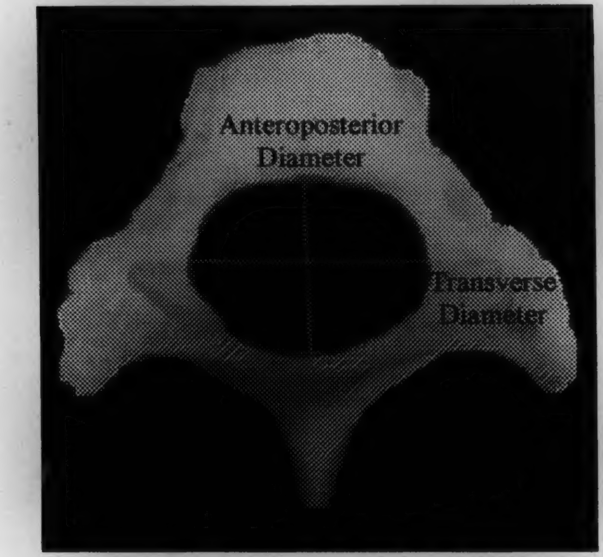
Anteroposterior
Diameter
Transverse
Diameter

Figure 7-3. Using Image J 1.28, the borders of the vertebral canal were traced out and the area and perimeter of the canal was determined. A computer-generated ellipse was fit to the vertebral canal and the major and minor axes of the ellipse determined (seen in gray). The major axis corresponded to the transverse diameter of the canal and the minor axis corresponded to the anteroposterior diameter.

Measurement of Neural Arch Parameters

In addition to the measurement of NCJ and canal parameters, the pedicle lengths, lamina lengths, posterior body lengths and pedicle widths (at three positions) were also measured for each rat using 40X digital photomicrographs of the entire vertebra as seen using a conventional light microscope (Carl Zeiss Inc.). Measurement definitions were based on previous work (Chapter 6) and are shown in Figure 7-4. Absolute pedicle length indices (PLI), lamina length indices (LLI), total length indices (sum of pedicle and lamina length on the same side) (TLI) and pedicle width indexes at the one-fourth (PWI1), one-half (PWI2) and three-fourth positions (PWI3) were calculated to determine the extent of asymmetry between the two sides of the vertebra. These indices were calculated by dividing the greater measurement by the lesser measurement and therefore indicated the extent of asymmetry but did not provide information about the direction of this asymmetry. Index values greater than 1.05 were considered to represent a significant extent of asymmetry in normal vertebrae as suggested by Taylor (1983).

Statistical Analysis

Statistical analysis was performed using Statview 5.0 (SAS Institute, Cary, North Carolina). All comparisons were performed using the Students-t test and findings were considered significant when $p \leq 0.05$. Correlation analysis was performed by calculation of the Pearson correlation coefficient, with values greater than 0.5 being considered significant. The specific statistical analyses performed in this study are outlined in Table 7-2.

RESULTS

The fluorochromes used in this study, tetracycline hydrochloride and alizarin red S, could be visualized easily under the fluorescence microscope since they fluoresced different colors, with the tetracycline appearing yellow-green and the alizarin appearing orange (Figure 7-5). The fluorochromes could be easily differentiated from the background autofluorescence of bone since they were clearly a different color and were also spatially separated from the edges of the vertebral sections where the background

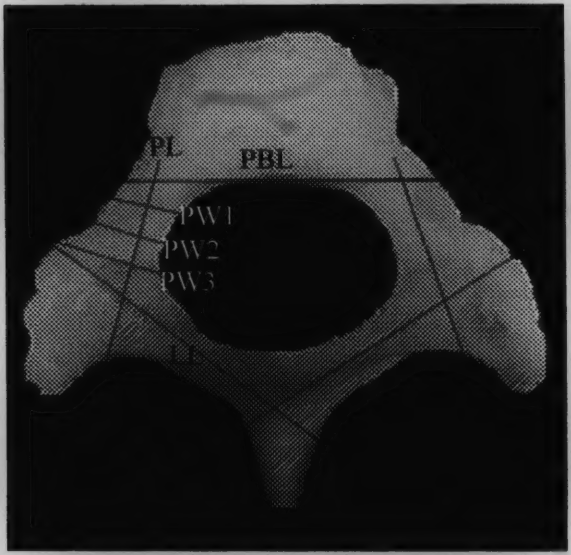

Figure 7-4. The PBL (posterior body length), right PL (pedicle length), right LL (lamina length), left PL (pedicle length) and left LL (lamina length) formed a pentagon that enclosed the vertebral canal and described all segments of the neural arch. The PBL was determined by drawing a straight line perpendicular to the axis of the vertebra that passed through the anterior tip of the vertebral canal. The distance between the outer aspect of the compact bone on both borders of the vertebra was defined as the PBL. Lines were then drawn through the long axis of each pedicle and lamina equidistant from the lateral and medial borders to form a pentagon. The PL on each side was defined as the distance along the line through the axis of the pedicle from its intersection with the PBL to its intersection with the line through the axis of the lamina. The LL on each side was defined as the distance along the line through the axis of the lamina from its intersection with the line through the axis of the pedicle to its intersection with the line through the axis of the lamina on the other side. The total length (TL) for a particular side was defined as the sum of the PL and LL on that side. All pedicle widths (PW1, PW2, PW3) were taken perpendicular to the line through the axis of the pedicle. PW1, PW2 and PW3 were taken at distances of one-fourth, one-half and three-fourth, respectively, of the PL along the line through the axis of the pedicle.

Table 7-2. Statistical analysis for NCJ, vertebral canal and neural arch parameters

Parameters	Measurement Analysis	Rationale	Statistically Significant Findings
NCJ	Within the Group 1 rats (age 3-7 days), Group 2 rats (age 4-12 days) and Group 3 rats (age 13-21 days), all NCJ measurements were compared between the two sides of the vertebra. For each group and for all of the rats as a whole, the bone deposited at the anterior surface and the posterior surface of the NCJ was compared. The length measurements acquired at five different positions for the NCJs in each group and for all of the NCJs as a whole were compared.	To assess the extent of asymmetry in each NCJ parameter. To determine if the NCJ made a greater growth contribution in the anterior or the posterior direction. To determine if the length of the NCJ changes from the medial to the lateral aspect and to characterize NCJ shape.	The area of bone deposited on the anterior NCJ surface was greater than the area of bone deposited on the posterior NCJ surface ($p=0.012$) for the Group 2 rats. For all of the Groups, the L2 was greater than L1($p=0.003$), L5 was greater than L2 ($p=0.001$) and L5 was greater than L4 ($p=0.004$) which showed that the NCJ is a concave structure with the lateral edge thicker than the medial edge.
	All measured values were also compared between the Group 1, Group 2 and Group 3 rats.	To determine if NCJ parameters change with increasing NCJ development.	In comparing Group 1 and Group 2, the NCJ width ($p=0.010$) was decreased as was the area of bone deposited on the anterior ($p=0.004$) and posterior $p=0.003$) surface. In comparing Group 2 and Group 3, the NCJ area and L1,L2,L4 and L5 were significantly decreased in Group 3 ($p<0.001$) as was the NCJ width ($p<0.001$) and the area of bone deposited on the anterior surface of the NCJ($p=0.042$).
	A correlation matrix was calculated to determine how NCJ parameters correlated with bone deposition at the anterior and posterior NCJ surfaces.	To determine which parameters best predict the activity (bone deposition) at the NCJ site.	The extent of bone deposited at the anterior and posterior NCJ surface correlated with average NCJ length (0.664,0.565).
Vertebral Canal	Average values for vertebral canal area, perimeter, AP diameter and lateral diameter for each age group are shown in Table 2.	To determine if these canal parameters continued to increase after growth plate closure.	Between Group 3 and the successive groups in which both the NCJ and the PS had closed, there were significant differences in all parameters. For example, canal area increased significantly from Group 3 to Group 5 ($p=0.028$), canal perimeter increased from Group 3 to Group 5 ($p=0.013$), AP diameter increased from Group 3 to Group 7 ($p=0.05$) and transverse diameter increased from Group 3 to Group 5 ($p=0.029$).
	A correlation matrix was created for all measured NCJ parameters and vertebral canal parameters. For the purpose of this correlation, the NCJ measurements used were the average of the right and the left NCJ measurements.	To determine the presence and direction of a correlation (positive or negative) between NCJ development and vertebral canal development.	The area of bone deposited on the posterior aspect of the NCJ correlated negatively with canal area (-0.503), canal perimeter (-0.599), canal AP diameter (0.652) and canal transverse diameter (-0.599).
Neural Arch	Absolute pedicle length indices, lamina length indices, total length indices (pedicle length and lamina length on the same side) and pedicle width indices were calculated.	To determine if the normal vertebra shows a significant extent of asymmetry.	The pedicle length index was 1.096, the lamina length index was 1.106, the total length index was 1.123 and the pedicle width indices were all greater than 1.2.
	A correlation matrix was attempted for all NCJ parameters and neural arch parameters.	To determine the presence and direction of a correlation (positive or negative) between NCJ development and neural arch development.	This correlation matrix could not be calculated since many of the neural arch parameters in the Group 1,2 and 3 rats could not be measured due to fracture of the borders of the vertebra on sectioning.

autofluorescence was the most apparent. Upon examining the pattern of fluorochrome deposition in the compact bone on the outside of the vertebral canal and the vertebral body, it was evident that the fluorochromes were deposited as fairly continuous lines with only a small degree of fragmentation. Two different patterns of fragmentation were noted as seen in Figure 7-5. In some areas neither fluorochrome was present and these areas were thought to represent unequal patterns of bone deposition during the approximately 24 hour to 48 hour time period that the particular fluorochrome was available for deposition. In other areas, only alizarin was visible and it was inferred that tetracycline had been resorbed at these sites.

A consistent model of bone deposition was observed for the vertebral canal and the vertebral body. From the inner layer of compact bone surrounding the vertebral canal and moving towards the outer layer of the compact bone surrounding the canal, an unlabelled layer of bone could be seen, followed by a layer of tetracycline, another layer of unlabelled bone and finally a layer of alizarin (Figure 7-5). Although another area of unlabelled bone was likely present beyond the layer of alizarin, this layer could not discerned since it would have been continuous with the trabecular bone of the vertebral body. Usually, there was a clear distinction between the two fluorochrome layers but at a few sites around the vertebral canal, there was only one layer of a fluorochrome or the layers of tetracycline and alizarin were located so closely together that there was little unlabelled bone between them and the two separate layers could not be distinguished. Surprisingly, there was fluorochrome deposition on the anterior portions of the vertebral canal in rats of all ages, which suggested that bone was being deposited in a posterior direction in relation to the vertebral body, contrary to the findings of past studies (Knutsson, 1958; Erdheim in Knutsson, 1958; Lord et al., 1995).

In comparison to the compact bone around the vertebral canal, the layer of compact bone surrounding the anterior surface of the vertebral body also showed the same pattern of bone deposition with a layer of unlabelled bone on the inner layer of compact bone, followed by a layer of tetracycline, a layer of alizarin on the outer layer of the compact bone of the body and finally another layer of unlabelled bone (Figure 7-5b). However, at these sites in the vertebral body, there were fewer cases in which only one

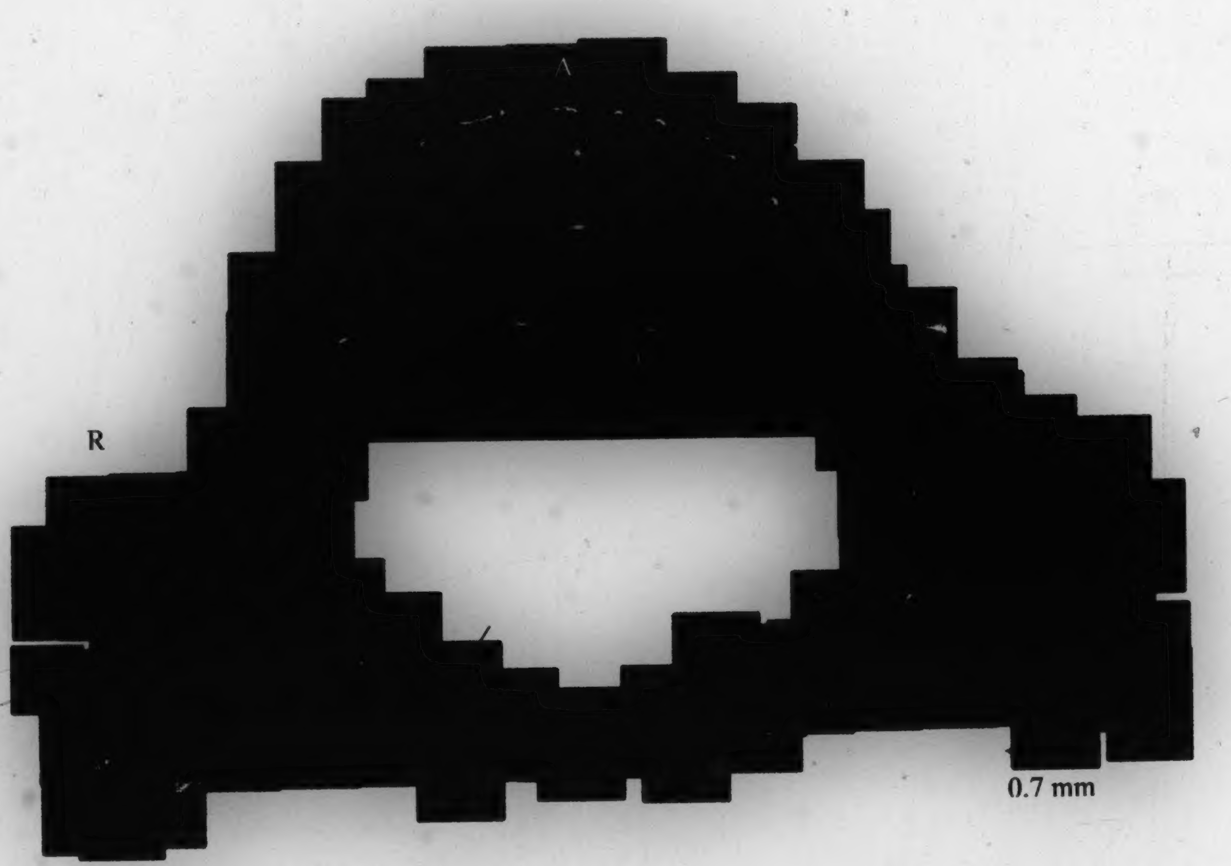

Figure 7-5a. Complete montage image of the T8 vertebra from a Group 8 rat. The tetracycline (yellow) and alizarin (orange) lines can clearly be observed. At some sites (gray arrow), only alizarin is visible. At other sites (red arrow), the fluorochrome lines are discontinuous and neither alizarin nor tetracycline is visible. The area enclosed by the square is shown in magnified view in Figure 7-5b.

Figure 7-5b. Visualization of the cortical bone from the T8 vertebral body from a Group 8 rat shows the pattern of tetracycline and alizarin deposition. A layer of unlabelled bone is seen on the inner layer of the compact bone (1), followed by a layer of tetracycline (2), another area of unlabelled bone between the fluorochromes (3), a layer of alizarin (4) and finally another layer of unlabelled bone (5). The same pattern of deposition was noted for the vertebral canal, except that the layer of unlabelled bone beyond the layer of alizarin could not be discerned as it was continuous with the trabecular bone of the vertebral body.

layer of fluorochrome was visualized or the two layers of fluorochrome could not be distinguished (Figure 7-5). Furthermore, the layers corresponding to the regions of fluorochrome deposition appeared thicker visually, with a greater area of unlabelled bone in between the two fluorescent layers. This suggested that more bone was being deposited than in the comparable regions of the vertebral canal. In the trabeculae of the vertebral body, fluorochrome deposition could be noted on the endosteum yet the two fluorochromes could not be distinguished and appeared to be located so closely together that resolution of individual fluorochromes was not possible (Figure 7-6). The same general patterns of fluorochrome deposition in the vertebral canal and the vertebral body were noted for rats of all age groups. Since fluorochromes were not deposited equally at all points of the vertebral canal or vertebral body in any particular rat, the model created to describe bone deposition and resorption was a composite from all members of each group.

In examining the hyaline cartilage plates, the PS was clearly visible in some of the Group1 (day 3-7) and Group 2 rats (day 4-12) but was not visible in any of the Group 3 rats (day 13-21) (Figure 7-7), suggesting that the PS closed sometime between days 12 and 21. In contrast, the NCJ was clearly visible in all of the rats in Group 1,2 and 3 but could not be seen in any of the Group 4 rats (day 22-30) suggesting that the NCJ closed a little later between days 21-30. Interestingly, the NCJ and the PS showed apparently equal amounts of fluorochrome deposition on both extreme surfaces. Whereas it was difficult to separate the fluorochromes that were deposited at the PS (Figure 7-7), different layers could sometimes be distinguished on both sides of the NCJ. In some cases, it was noted that a layer of alizarin was located closer to the cartilaginous plate and a layer of tetracycline was located further from the growth plate (Figure 7-8). Differences in bone deposition from the lateral to medial aspect of the NCJ did not appear to show any consistent pattern.

The difference in the appearance of the NCJ between the Group 1, 2 and 3 rats was also assessed by measurements and statistical comparisons (all p-values and correlation coefficients are shown in Table 7-2). For all statistical parameters, the intraobserver error was less than 5% and no significant differences were noted between

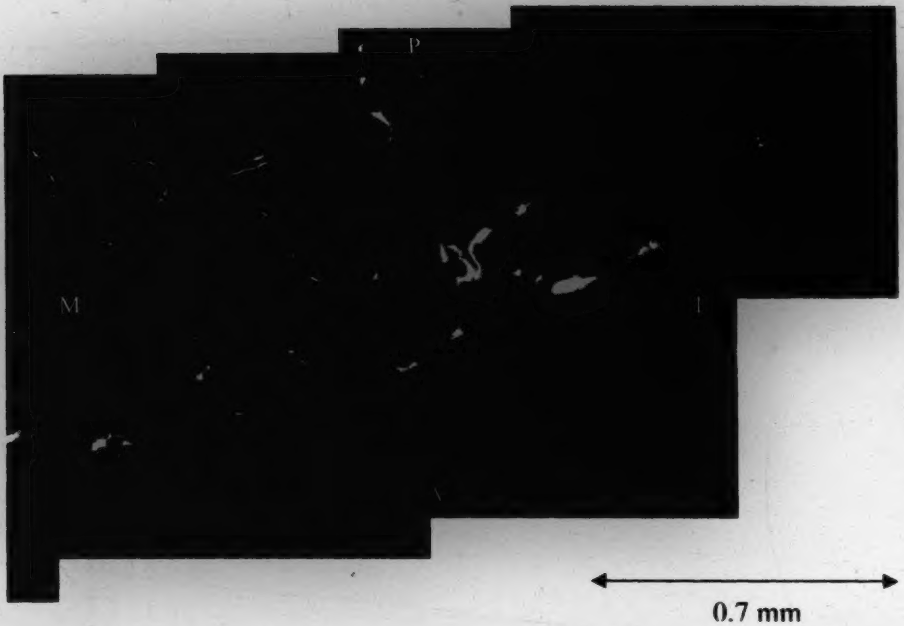

Figure 7-6. In the vertebral trabeculae of a Group 3 rat (day 21-29), fluorochrome deposition was clearly seen on the endosteum. However, the two fluorochromes could not be distinguished and appeared to be grouped so closely together that resolution of individual fluorochromes was not possible.

Figure 7-7. The PS (seen inside the black rectangle) can be clearly visualized in a Group 1 rat (day 3-11) and bone deposition was clearly occurring on both surfaces of the growth plate. The entire field of view represents 0.7 mm.

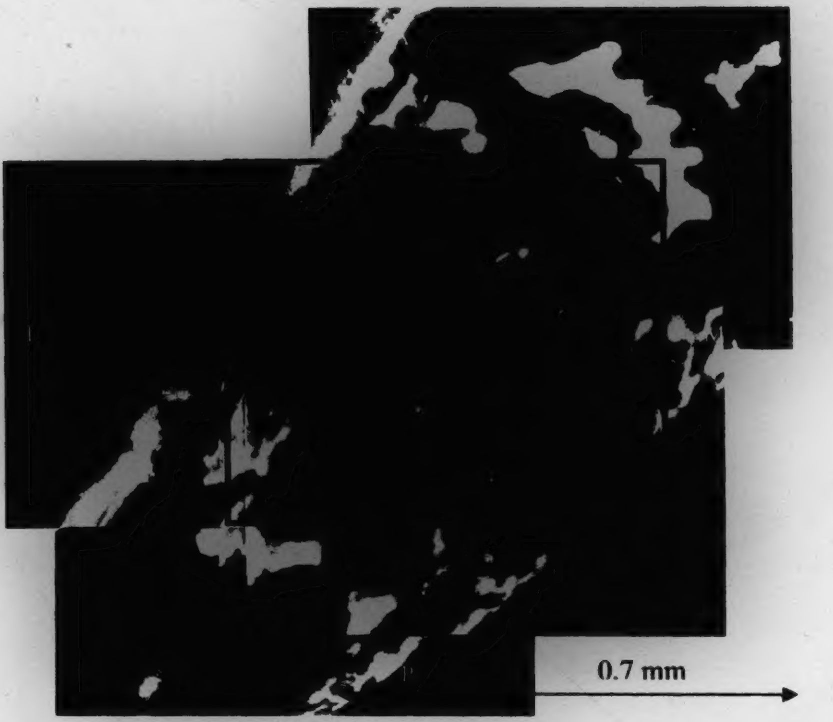

Figure 7-8a. Typical NCJ (inside the black rectangle) from a Group 2 rat (day 4-12).

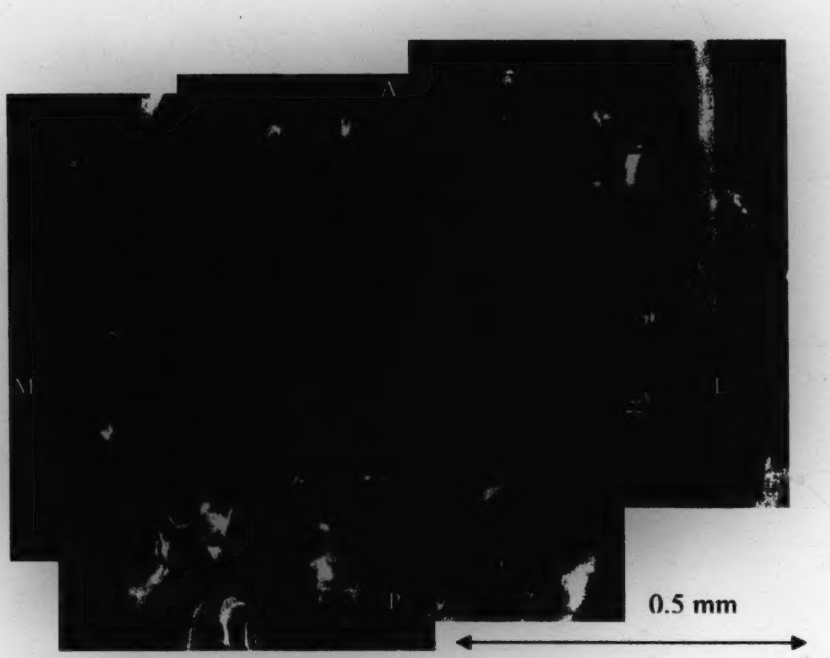

Figure 7-8b. Typical NCJ (black rectangle) from a Group 3 rat (day 13-21). Note the decreased NCJ length as compared to the NCJ from a Group 2 rat in Figure 7-8a.

observers. The area of bone deposited on the anterior and posterior surface of the NCJ did not show a significant difference for the Group 1 and Group 3 rats, however the amount of bone deposited on the anterior NCJ surface was significantly greater than the amount of bone deposited on the posterior NCJ surface for the Group 2 rats. For Groups 1-3, it was found that the medial border of the NCJ was generally thicker than the lateral border. Furthermore, a decreased length (L3) was found in the middle of the NCJ which was a reflection of the fact that the NCJ was a concave-shaped growth cartilage (Figure 7-8). In comparing Group 1 and Group 2, the area of bone deposited on the anterior and the posterior surface of the NCJ decreased suggesting that the activity of the NCJ was decreasing. Similarly, in comparing Group 2 and Group 3, the area of bone deposited on the anterior surface of the NCJ decreased. The NCJ area, the L1, L2, L4 and L5 were also significantly decreased suggesting that the NCJ cartilage was starting to become absent. Analyzing the groups as a whole, correlation analysis illustrated that the activity of the NCJ, as measured by the area of bone deposited on the anterior and posterior surfaces of the growth plate correlated significantly with NCJ area and average NCJ length. The two parameters of NCJ area and average NCJ length may therefore be useful in assessing the extent of growth remaining at the NCJ site.

The average values for vertebral canal area, perimeter, AP diameter and lateral diameter for each age group are shown in Table 7-3. Even after the NCJ and the PS closed (Group 4 onwards), the vertebral canal continued to enlarge its area, perimeter, anteroposterior and transverse diameters (Table 7-3, Figure 7-9). For example, from Group 3 to Group 5, there was a significant increase in canal area, canal perimeter and transverse diameter. An increase in AP diameter was significant in comparing Group 3 to Group 7. Interestingly, the greatest canal diameters and area were noted in Group 7. This may be due to the fact that the Group 1-7 rats and the Group 8-11 rats were acquired from different sources, since it was necessary to switch suppliers after an outbreak of parvovirus at the original supplier. In correlating NCJ parameters with vertebral canal dimensions, the only significant correlations were found between the area of bone deposited posterior to the NCJ and the canal area, perimeter, AP diameter and lateral

Table 7-3. Average area, perimeter, AP diameter and lateral diameter of the vertebral canal at different ages

Group	Average Area(mm^2) / Standard Deviation	Average Perimeter (mm) / Standard Deviation	Average AP Diameter (mm) / Standard Deviation	Average Lateral Diameter (mm) / Standard Deviation
1 (Day 3-7)	2.418 0.23	5.873 0.37	1.523 0.12	2.014 0.09
2 (Day 4-12)	4.071 0.91	7.414 0.90	1.999 0.17	2.450 0.38
3 (Day 13-21)	4.389 0.79	7.832 0.68	2.083 0.39	2.703 0.12
4 (Day 22-30)	5.154 0.37	8.459 0.28	2.266 0.12	2.863 0.18
5 (Day 29-37)	5.653 0.70	9.212 0.70	2.322 0.37	2.971 0.19
6 (Day 36-44)	5.833 0.38	9.314 0.26	2.339 0.27	3.196 0.19
7 (Day 43-51)	6.444 0.47	9.445 0.31	2.525 0.17	3.203 0.23
8 (Day 50-54)	5.912 0.59	9.233 0.41	2.196 0.16	3.428 0.05
9 (Day 57-65)	5.924 0.59	9.407 0.35	2.125 0.15	3.506 0.20
10 (Day 64-72)	6.215 0.31	9.508 0.39	2.252 0.14	3.477 0.17
11 (Day 71-79)	6.476 1.18	9.744 0.78	2.360 0.25	3.558 0.32

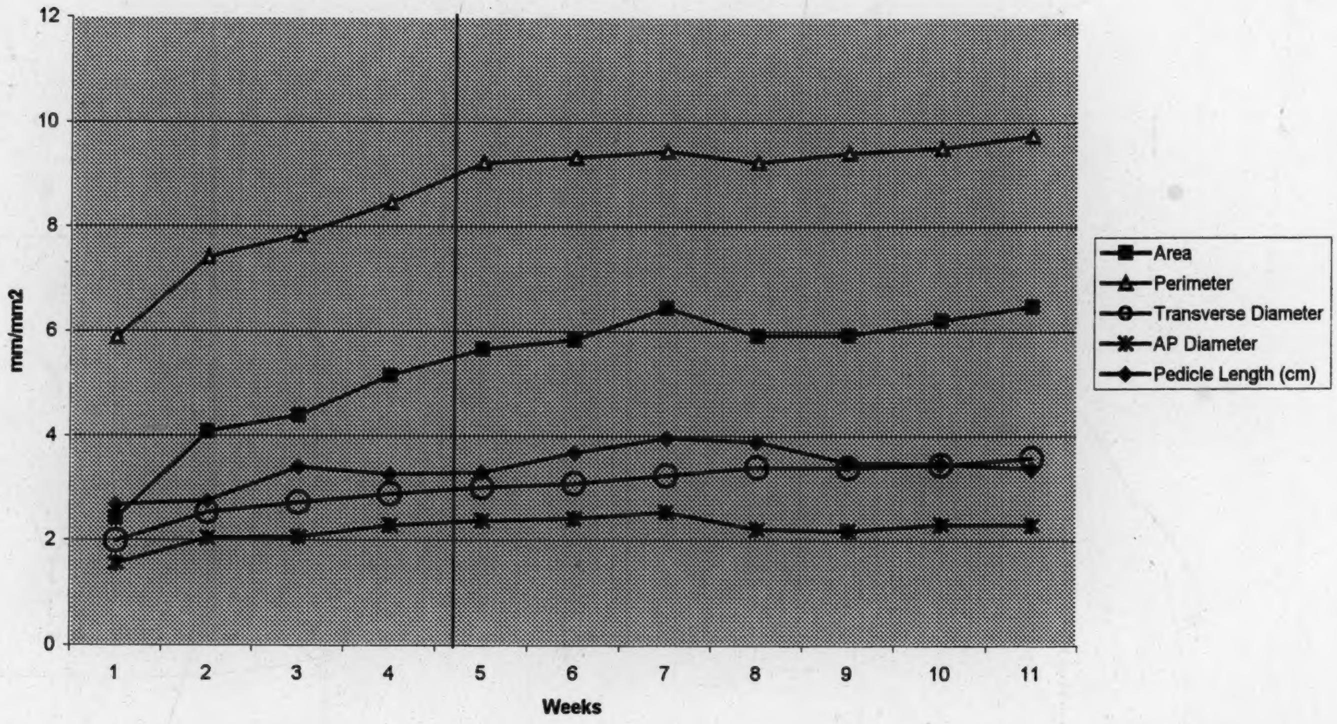

Figure 7-9. Area, perimeter and diameters of the vertebral canal in rats of ages one to eleven weeks. The vertical black line represents the approximate age of NCJ closure, with the area of the graph to the left of the line signifying the time period when the NCJ was open. Note the significant increase in canal parameters after the NCJ has closed, suggesting the importance of periosteal mechanisms in vertebral growth.

diameters. All four of these correlations were significantly negative which suggests that more bone may be deposited posterior to the NCJ site in younger animals, further confirming that NCJ activity likely decreases with age.

The measurement of neural arch parameters was more difficult than the measurement of NCJ or canal dimensions, since the outer borders of the vertebrae were sometimes more difficult to visualize because of the processing technique. Consequently, a correlation matrix could not be calculated for NCJ parameters and neural arch parameters. However, from the available measurements the average pedicle length index (1.096), the average lamina length index (1.106), the average total length index (1.123) and the average pedicle width indices at three different positions (all three indices greater than 1.2) were determined. All of these measurements were notably larger than the index value of 1.05, which has been conventionally used to represent significant asymmetry in normal vertebral parameters (Taylor, 1983). This suggests that the normal pedicles and the lamina on both sides of the neural arch may show significant asymmetry, in contrast to the immediate assumption that the right and left halves of the neural arch would have the same length.

DISCUSSION

The major finding of this study was that the dimensions of the vertebral canal and the neural arch continued to grow long after the closure of both the NCJ and the PS. This challenges the conventional model of canal growth which suggests that canal diameters are fully attained by the time that these growth plates have closed and also the basic concept that growth in length ceases with closure of the cartilaginous growth plates (Ganey and Ogden, 2001). In this study, the PS closed between days 12-21 and the NCJ closed between days 21-30, which agreed with the work of Canadell et al. (1978). During the period that these growth plates were open, both made a bipolar contribution to growth as evidenced by fluorochrome deposition on both surfaces of the growth plates. From the pattern of fluorochrome deposition and the orientation of the growth plates relative to the canal, it could be seen that the NCJ contributed to growth of both the anteroposterior and transverse canal diameters whereas the PS contributed almost exclusively to growth of the transverse diameter. Surprisingly even if the NCJ closed as late as day 30, the vertebral canal had only reached 69% of the area, 86% of the AP diameter and 83% of the lateral diameter attained by seven weeks (Table 7-3, Figure 7-9). However, the percentage of the true adult canal area and diameter attained by day 30 would likely be lower. In this study, the rat vertebrae measured at seven weeks had the greatest area and diameter yet this is likely because the Group 1-7 rats and the Group 8-11 rats were acquired from different suppliers although they were supposed to be exactly the same. In fact, an earlier pilot study conducted on Sprague-Dawley rats (ages one to 10 weeks) acquired from the same supplier clearly showed that the vertebral canal areas and diameters continued to enlarge between seven and 10 weeks of age.

Although conventional bone growth models suggest that periosteal mechanisms of bone modeling are responsible for changes in bone shape rather than bone size, it would seem that in this rat model periosteal mechanisms also account for changes in vertebral size both after and during growth plate activity. The role of periosteal mechanisms in increasing neural arch and canal size after growth plate closure was directly observed from measurements of canal parameters and patterns of fluorochrome deposition. During growth plate activity, the contribution of periosteal mechanisms to changes in vertebral size could be seen from patterns of fluorochrome deposition, although this mechanism was obviously complemented by endochondral ossification at the site of the NCJ and the PS. The relative importance of periosteal mechanisms and growth plates in vertebral canal growth could be inferred by examining the change in vertebral canal area, diameters and perimeter over time (Figure 7-9). To the extent that growth of the vertebral canal was due to growth at the sites of the NCJ and the PS, an accelerated rate of change in canal areas and diameter might be expected while the NCJ and the PS remained open and contributed to growth. Following closure of the cartilage plates, a reduced growth rate might be expected when only periosteal mechanisms were contributing to growth (Knutsson, 1961; Ganey and Ogden, 2001). Interestingly, the rate of change in canal area and canal diameter appeared to stay almost the same before and after growth plate closure at day 30 with no change in the rate of increase in either parameter. Since it does not seem likely that periosteal mechanisms of growth would accelerate to compensate for decreased growth at the site of the growth plates and this is not supported by the existing model of canal growth (Ganey and Ogden, 2001), it seems likely that periosteal mechanisms have a greater role at all stages than previously thought in vertebral canal growth.

In addition to allowing an assessment of the relative importance of growth plates and periosteal mechanisms in vertebral canal growth, the fluorochrome technique revealed the specific manner in which the NCJ, PS and periosteal mechanisms contributed to vertebral growth. This knowledge is essential in evaluating the potential role of these mechanisms in abnormal vertebral growth. For example, asymmetrical NCJ growth has long been considered a potential cause of AIS with the asymmetry in NCJ growth thought to produce pedicle asymmetry, a subsequent torsional force resulting in vertebral rotation and an eventual scoliosis. However, a lack of knowledge concerning the contributions of the NCJ to vertebral growth and the age of closure of this growth plate has prevented further assessment of this idea.

Patterns of fluorochrome deposition clearly showed that the PS and the NCJ made a bipolar contribution to growth, as suggested by other authors (Töndury and Theiler, 1990; Ganey and Ogden, 2001). This differs from the traditional ideas regarding growth of the epiphyseal plates of long bones, which are thought to basically grow in a unipolar fashion, with growth on the epiphyseal side being more poorly defined. Interestingly, the anterior and the posterior growth contributions of the NCJ were not always equal, with the area of bone deposited anteriorly being significantly greater than the area of bone in the Group 2 (Day 4-12). This differential bone deposition may account for the apparent posterior recession in the position of the NCJ over time (Taylor, 1983; Vital et al., 1989).

In the past, study of the asymmetric NCJ growth hypothesis of AIS has often assumed that the presence of the NCJ corresponds to growth at the site of the NCJ. However, the results of this study clearly indicate that the activity of the NCJ is not equal at all phases of growth plate development and that the activity of the NCJ decreases with time especially towards the time of actual closure. In comparing groups 1, 2 and 3, it was found that the area of bone deposited on the anterior surface of the NCJ decreased significantly from Group 1 to Group 2 and from Group 2 to Group 3. In a similar fashion, the area of bone deposited on the posterior surface of the NCJ decreased significantly from Group 1 to Group 2. A more quantitative estimate of the decrease in NCJ activity with time can be developed if it is assumed that the bone deposited on the posterior aspect of the NCJ contributes to an increased pedicle area and that none of the bone deposited posterior to the NCJ was resorbed during the time period of the study. The first assumption seems quite reasonable considering the position and orientation of the NCJ. The second assumption can also be defended because at most vertebral sites the first injected fluorochrome, tetracycline, was still readily visible with approximately the same thickness as the alizarin injected four days later. Between the Group 1 (Day 3-7) and Group 2 (Day 4-12) rats, the average area of the pedicle increased by 0.111 mm^2 while the average NCJ area increased by 0.010 mm^2. The average bone deposited posterior to the NCJ during this time period was 0.064 mm^2. If the above assumptions are made, then the change in NCJ area and the bone deposition posterior to the NCJ accounted for approximately 67% of the increase in pedicle area during this time period. Between the Group 2 (Day 4-12) and Group 3 (Day 12-20) rats, the average area of the pedicle increased by 0.329 mm^2, while average NCJ area decreased by 0.046 mm^2 and on average, 0.052 mm^2 of bone was deposited posterior to the NCJ. At this point, the change in NCJ area and the bone deposition posterior to the NCJ only accounted for 2% of the change in pedicle area. In this analysis, area measurements were used instead of length measurements primarily because the length measurements that would have been required, such as the length of the NCJ and the length of the bone deposited at certain points along the NCJ, were highly variable and depended on position. It was thought that the use of area measurements would reduce variability and provide more accurate values for analysis.

This approach demonstrates that the contribution of the NCJ to pedicle area likely declines sharply with time. Applying this idea to the asymmetric growth hypothesis of AIS it is possible that although the NCJ is present during adolescence in the human, its growth contribution is sharply decreased or negligible. This would mean that even if NCJ asymmetry developed during adolescence, the extent of vertebral deformity created would be negligible and likely insufficient to produce a scoliosis. Of course, this would not limit the possibility of asymmetric NCJ growth causing infantile or juvenile idiopathic scoliosis.

In other parts of the vertebrae, there was a consistent pattern to the sequence in which fluorochrome lines appeared in the regions of compact bone, both before and after growth plate closure. From the inner layer of the compact bone surrounding the vertebral canal and advancing towards the outer layer of compact bone surrounding the canal, a layer of unlabelled bone could be seen, followed by a layer of tetracycline, another layer of unlabelled bone and then a layer of alizarin (Figure 7-5). The same sequence of lines was noted moving from the inner layer of the compact bone surrounding the anterior surface of the vertebral body towards the outer layer of compact bone surrounding the anterior surface of the body (Figure 7-5b). This pattern of deposition agreed, in general, with past studies of fluorochrome deposition in rat vertebrae (Hammond and Storey, 1974; Smith et al. 1991). The results showed that the compact bone of the vertebra grew by expanding outwards in all directions, with successive layers of compact bone being formed further outwards from the center of the vertebral canal.

In this study, periosteal deposition was noted at all ages on the anterior aspect of the vertebral canal, which conflicted with human studies that have suggested that the anterior surface of the vertebral canal is established early in development and consequently does not have the potential to encroach on the spinal cord during development (Knutsson, 1958; Erdheim in Knutsson, 1958; Lord et al., 1995). The relative growth rate of the compact bone of the vertebral canal and the vertebral body also appeared to be quite different. Simple visual inspection revealed that tetracycline and alizarin lines were thicker in the compact bone of the vertebral body, with a greater distance between these lines, both of which would imply that the compact bone of the vertebral body was growing at a faster rate. Subjectively, there also appeared to be differences in the rate of bone deposition between different regions of the compact bone around the vertebral canal, and similarly between different regions of the vertebral body as shown by examining the distance between the fluorochrome lines.

The pattern of fluorochrome deposition noted was surprising in relation to past studies, which have generally implied that fluorochromes were deposited in continuous lines across large areas of compact bone. In one particular study examining vertebral growth in Wistar rats (Hammond and Storey, 1974), photomicrographs showed tetracycline deposited in continuous rings around the entire circumference of the compact bone surrounding the vertebral canal. In contrast, in this study, fluorochrome deposition around the vertebral canal and the vertebral body occurred as a series of discontinuous lines (Figure 7-5). These discontinuous lines were not artifacts caused by fractures during the sectioning procedure, since a continuous layer of unlabelled bone could be visualized around the inner circumference of the vertebral canal and the vertebral body. This discontinuity implied that bone was not being deposited uniformly around the vertebral canal or the vertebral body, but was being deposited instead in a series of localized areas. This would suggest that equal amounts of resorption were not noted around the entire circumference of the vertebral canal or the vertebral body, but this cannot be proved using this approach. In some areas of compact bone around the vertebral canal, only a layer of alizarin was noted with no tetracycline layer located closer to the center of the vertebral canal whereas in most cases, a layer of tetracycline and a layer of alizarin could be noted on the outside of the vertebral body. In cases where no tetracycline layer was present, this would imply that the tetracycline in the compact bone had already been resorbed over the seven days since it was injected or that no bone had been deposited at this site during the time that tetracycline was present in the circulation. The fact that bone did not appear to be deposited around the circumference of the vertebral canal and body would seem to imply that different areas of the canal and body grow at different rates and different times, with a certain degree of independence. This would have implications for changes in vertebral shape, which would depend on relative differences in vertebral growth and might also play a role in the development of vertebral abnormalities, although further studies are required to investigate these ideas.

Measurement of the pedicle length index (1.096), the lamina length index (1.106), the total length index (1.123) and the pedicle width indices (all greater than 1.2) suggested that the normal neural arch shows a significant extent of asymmetry in the rat according to Taylor's criteria (1983). Taylor's value of 1.05 (1983) has been commonly used as an index to represent significant asymmetry in normal vertebral parameters (Sevastik et al., 1995). Both Taylor (1983) and Sevastik et al. (1995) have used this asymmetry to explain the predominance of a slight right thoracic scoliosis in the normal adolescent population. Unfortunately, the direction of this asymmetry could not be confirmed in this study since the right/left orientation of vertebrae was not preserved in the sectioning process.

Prior studies have established that the rat is a good model for human bone growth (Frost and Jee, 1992) and on the basis of this study, the existing model for vertebral canal growth in the human may need reconsideration. Although vertebral canal growth has traditionally been thought to depend almost exclusively on the contributions of the NCJ and the PS, a significant percentage of growth at all times may be due to periosteal mechanisms. This would account for the tremendous growth and modeling of the vertebra from early development to adulthood, especially after the closure of growth plates. In fact, one repercussion of these findings might be that abnormalities of periosteal growth could play a larger role in the creation of vertebral growth abnormalities than previously thought. For example, if significant growth of the pedicle is possible after NCJ closure, then asymmetrical growth of the vertebra could occur during adolescence without asymmetric growth contributions from the NCJ. Furthermore, these findings suggest that the traditional long bone model based on epiphyseal growth may not apply to vertebrae and that a vertebra, which represents a composite of several bones each with different growth patterns, likely requires a different model of growth.

REFERENCES

Baron R, Tross R, Vignery A. Evidence of sequential remodeling in rat trabecular bone : morphology, dynamic histomorphometry, and changes during skeletal maturation. Anat Rec 1984;208:137-145.

Baylink D, Stauffer M, Wergedal J, Rich C. Formation, mineralization and resorption of bone in Vitamin D-deficient rats. J Clin Invest 1970;49:1122-1134.

Burwell RG, Dangerfield PH. Anthropometry and scoliosis. In: Zorab PA (ed.). Scoliosis and Growth 5th Symposium. Academic Press. London, 1977:123-64.

Canadell J, Beguiristain JL, Gonzalez Iturri J, Reparaz B, Gili JR. Some aspects of experimental scoliosis. Arch Orth Traum Surg 1978;93:75-85.

Deeb S, Herrmann H. Tetracycline-labeling as a method for detecting the bone demineralization of parathormone-treated rats. Acta Histochem 1974;50:35-42.

Frost HM, Jee WSS. On the rat model of human osteopenias and osteoporoses. Bone Miner 18:227-236;1992.

Frost HM. Some concepts crucial to the effective study of bone turnover and bone balance in human skeletal disease and in experimental models of skeletal physiology and pathophysiology. In : ZFG Jaworski (ed.). Bone Morphometry. Ottawa University Press. Ottawa, 1976: 219-223.

Ganey TM, Ogden JA. Development and maturation of the axial skeleton. In : Weinstein SL (ed.). The pediatric spine : principles and practice, 2nd ed. Lippincott Williams and Wilkins. Philadelphia, 2001: 3-54.

Hammer WS, Soni NN, Fraleigh CM. Quantitative study of bone activity in the diabetic rat mandible: triple fluorochrome study. Oral Surg 1973;35:718-729.

Hammond RH, Storey E. Measurement of growth and resorption of bone in the seventh caudal vertebra of the rat. Calc Tiss Res 1974;15:11-20.

Harris WH, Lavorgna J, Hamblen DL, Haywood EA. The inhibition of ossification *in vivo*. Clin Orthop Rel Res 1968;61:52-60.

Hilton HE. Skeletal pigmentation due to tetracycline. J Clin Path 1962;15:112-115.

Hinck VC, Hopkins CE, Clark WM. Sagittal diameter of the lumbar spinal canal in children and adults. Rad 1966;85:929-937.

Ito H, Ke HZ, Jee WSS, Sakou T. Anabolic responses of an adult cancellous bone site to prostaglandin E_2 in the rat. Bone Min 1993;21:219-236.

Kidder LS, Schmidt IU, Evans GL, Turner RT. Effects of growth hormone and low dose estrogen on bone growth and turnover in long bones of hypophysectomized rats. Calc Tiss Int 1997;61:327-335.

Knutsson F. Growth and differentiation of the post natal vertebra. Acta Radiol 1961;55:401-408.

Knutsson F. Vertebral genesis of idiopathic scoliosis in children. Acta Radiol 1966;4: 395-402.

Landry LM, Fleisch DH. The influence of immobilization on bone formation as evaluated by osseous incorporation of tetracyclines. J Bone Joint Surg (Br) 1964;46-B:764-771.

Lepola VT, Hannuniemi R, Kippo K, Laurén L, Jalovaara P, Väänänen HK. Long-term effects of clodronate on growing rat bone. Bone 1996;18:191-196.

Lord MJ, Ogden JA, Ganey TM. Postnatal development of the thoracic spine. Spine 1995;20:1692-1698.

Mente PL, Aronsson DD, Stokes IAF, Iatridis JC. Mechanical modulation of growth for the correction of vertebral wedge deformities. J Ped Ortho 1999;17:518-24.

Michelsson JE. The development of spinal deformity in experimental scoliosis. Acta Orthop Scand 1965;36(Suppl 81):9-91.

Moore KL, Dalley AF. Clinically oriented anatomy, 4th ed. Lippincott Williams and Wilkins. Baltimore, 1999.

Ottander HG. Experimental progressive scoliosis in a pig. Acta Orthop Scand 1963;33:91-7.

Rajwani T, Bhargava R, Moreau M, Mahood J, Raso VJ, Jiang H, Bagnall KM. MRI characteristics of the neurocentral synchondrosis. Ped Rad 2002;32:811-16.

Roaf R. The basic anatomy of scoliosis. J Bone Joint Surg (Br) 1966;48-B:786-92.

Sevastik B, Xiong B, Sevastik J, Hedlund R, Suliman I. Vertebral rotation and pedicle length asymmetry in the normal adult spine. Eur Spine J 1995;4:95-97.

Smith RM, Pool RD, Butt WP, Dickson RA. The transverse plane deformity of structural scoliosis. Spine 1991;16:1126-1129.

Sontag W. Quantitative measurement of periosteal and cortical-endosteal bone formation and resorption in the midshaft of female rat femur. Bone 1986;7:55-62.

Sontag W. Age-dependent morphometric change in the lumbar vertebrae of male and female rats : comparison with the femur. Bone 1994;15:593-601.

Sun TC, Mori S, Roper J, Brown C, Hooser T, Burr DB. Do different fluorochrome labels give equivalent histomorphometric information? Bone 1992;13:443-446.

Taylor JR. Scoliosis and growth : patterns of asymmetry in normal vertebral growth. Acta Orthop Scand 1983;54:596-602.

Töndury G, Theiler K. Entwicklungsgeschichte und Fehlbildungen der Wirbelsäule, 2nd ed. Hippokrates Verlag. Stuttgart, 1990.

Urist MR, Ibsen KH. Chemical reactivity of mineralized tissue with oxytetracycline. Arch Path 1963;76:484-496.

Vital JM, Beguiristain JL, Algara C, Villas C, Lavignolle B, Grenier N, Sénégas J. The neurocentral vertebral cartilage: anatomy, physiology and physiopathology. Surg Radiol Anat 1989;11:323-28.

Wallman IS, Hilton HB. Teeth pigmented by tetracycline. Lancet 1962;1:827-828.

Williams PL (ed.), Warwick, Dyson et al. Gray's Anatomy, 37th ed. Churchill Livingstone. Edinburgh and New York, 1989.

Yamazaki A, Mason DE, Caro PA. Age of closure of the neurocentral cartilage in the thoracic spine. J Ped Ortho 1998;8:168-172.

Yousefzadeh DK, El-Khoury GY, Smith WL. Normal sagittal diameter and variation in the pediatric cervical spine. Rad 1982;144:319-325.

CHAPTER 8

ASYMMETRIC NEUROCENTRAL JUNCTION GROWTH AS A POTENTIAL CAUSE OF SCOLIOSIS IN A PORCINE MODEL

INTRODUCTION

The neurocentral junctions (NCJs) are cartilaginous growth plates located between the neural arch and the centrum on either side of the vertebra. The contribution of the NCJ to vertebral growth has been compared to the way that an epiphyseal plate contributes to growth in length of the long bones such as the tibia, with growth in length of the bone stopping when the growth plate ceases to exist. The manner in which an epiphyseal plate contributes to growth in dimensions other than length has never really been explained but in the case of a vertebra, the NCJ is thought to make a significant contribution to the growth in height, length and width of both the vertebral body and the pedicle (Vital et al., 1989; Yamazaki et al., 1998; Ganey and Ogden, 2001). Although the extent of this contribution has not been experimentally assessed, asymmetric growth at the site of the neurocentral junction (NCJ) has been implicated as a potential cause of adolescent idiopathic scoliosis (AIS) by numerous authors (Nicoladoni, 1909; Michelsson, 1962; Knutsson, 1966; Roaf, 1966; Yamazaki et al., 1998). The asymmetric NCJ growth hypothesis was first suggested by Nicoladoni (1909) after he conducted autopsy studies on children with scoliosis and found asymmetric NCJ development and pedicle asymmetry at the apex of the primary curve. Based on these findings, Nicoladoni proposed that asymmetric growth of the NCJ resulted in pedicle asymmetry, which caused vertebral rotation and the subsequent development of a scoliotic curvature (Figure 8-1). Although this hypothesis was not fully developed to explain how vertebral rotation resulted in a lateral curvature of the vertebral column and whether this asymmetry was a cause or an effect of the scoliosis, Nicoladoni's clinical findings were sufficient for other authors to evaluate the asymmetric NCJ growth hypothesis. Over the next 90 years, this hypothesis was discredited by a series of anatomic studies that found that the NCJ closed well before adolescence between six and 10 years of age (Knutsson, 1963; Ottander, 1963; Roaf, 1966; Schmorl et al., 1971; Taylor, 1983; Vital et al., 1989; Maat et al., 1996). It was argued that if this were the case, then asymmetric growth of the NCJ could

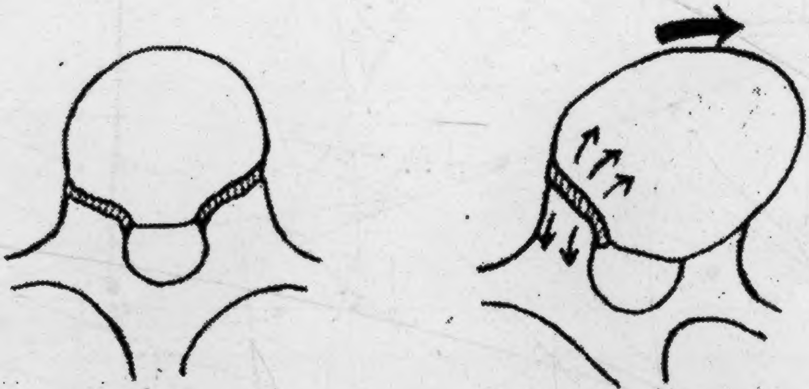

Normal

Unilateral closure

Figure 8-1 (adapted from Yamazaki et al., 1998). Nicoladoni (1909) proposed that asymmetric growth of the NCJ on one side would result in a longer pedicle. The longer pedicle would eventually be on the concave side of any lateral curve as the spinous process would rotate into the concavity. The actual mechanism by which vertebral rotation would result in lateral curvature was not described. Furthermore, why rotation of the complete vertebra would occur and not simple adaptation of the developing vertebra to the abnormal forces was also not explained.

not be a cause of idiopathic scoliosis in adolescents. More recently, the asymmetric NCJ growth hypothesis was resurrected by a series of MRI investigations (Yamazaki et al., 1998; Rajwani et al., 2002) and MRI-histologic correlations (Chapter 4) which showed that the NCJ was clearly recognizable as a prominent image on MRI indicating that it was actually present during adolescence.

In investigating the asymmetric NCJ growth hypothesis, examination of pedicle asymmetry in AIS patients has limited value for several reasons. Primarily, since most AIS patients present to the scoliosis clinic after their vertebral deformities are well-established, it is impossible to separate cause from effect and determine if a given vertebral change is a primary cause of the scoliosis or simply an effect of the altered biomechanics of the scoliotic spine. Secondly, it is quite possible that AIS has multiple different causes (Robin, 1990; Coillard and Rivard, 1996). Consequently, observation of a group of AIS patients who have varied underlying causes will contain a mixture of data from which it would be impossible to identify those patients whose problem lies in asymmetric NCJ development. Another confounding issue is the simple measurement of pedicle length. There are no clear boundaries and even if consistent and precise definitions could be created, considerable doubt surrounds their application to the multitude of deformities found in vertebrae from scoliotic spines. Considering these factors, it is not surprising to find that studies of pedicle asymmetry have generated widely conflicting results. For example, some authors have found no differences in pedicle length in the apical region (Liljenqvist et al., 2002) where it is generally accepted that the degree of deformity is greatest. In contrast, other authors have found that the longer pedicle is consistently located in the apical and adjacent vertebrae on the concave side of the scoliotic curve (Nicoladoni; 1909; Knutsson, 1963; Taylor, 1983; Vital et al., 1989) or alternatively on the convex side (Roaf, 1960).

Faced with these limitations, it seems that evaluation of the asymmetric NCJ growth hypothesis will not benefit from clinical investigations and animal models will have to be employed. These animal models would allow evaluation of the early stages of curve development and separation of the cause, the experimental intervention itself, from the effects of this intervention. Furthermore, if an animal model of asymmetric NCJ growth successfully produced scoliosis, the experimental population created would have the same potential cause for their scoliosis which would better facilitate measurements of vertebral morphology. Ultimately, a successful animal model would also allow the evaluation of surgical epiphyseodesis of the NCJ as a means of treating curve development due to asymmetric NCJ growth or other causes of AIS.

To date, three authors have used porcine models to investigate the asymmetric NCJ growth theory of AIS. However, the results have been inconsistent (Ottander, 1963; Beguiristain et al., 1980; Coillard et al., 1999). After using a dental drill to destroy the right NCJ at just L2, Ottander created a slight scoliosis. However, the extent of lateral curvature noted radiographically was negligible and the Cobb angle was far less than the 10 degree value generally used to define scoliosis. Ottander's model (1963) was extended by Beguiristain et al. (1980) with more successful results. In two-month old pigs, selective epiphyseodesis of the NCJ was performed by inserting partially threaded cancellous screws through five successive mid-thoracic vertebrae. After four to 12 months post-operatively, scoliosis with Cobb angles between 10° and 80° was noted. In addition to the significant extent of lateral curvature, the operated vertebrae appeared to show vertebral rotation with the bodies rotating towards the convexity, a shorter pedicle on the convex side and wedging with reduced vertebral height on the concave side. Unfortunately, these changes were inferred from visualization of anatomic specimens, since objective measurement criteria were not applied in this study. Nonetheless, it is interesting to note that these findings are representative of the changes typically noted in AIS (Nicoladoni, 1909; Arkin et al., 1950; Knutsson, 1966; Taylor, 1983; Vital et al., 1989) and conform to the predictions of the NCJ model proposed. On the whole, Beguiristain's (1980) results were promising although the lack of any control or sham groups made it difficult to infer if the scoliosis created was a result of the actual NCJ perturbation or inadvertent circulatory, muscular, ligamentous or periosteal interference during the surgical approach. Unfortunately, attempts to replicate Beguiristain's work by Coillard et al. (1999) were unsuccessful. After duplicating the experimental approach used by Beguiristain et al. (1980), none of the mini-pigs used in the Coillard et al. study (1999) displayed a Cobb angle of greater than 10 degrees at six or even 12 months of age. Direct comparisons with Beguiristain's work (1980) were made difficult since Coillard et al. (1999) used mini-pigs instead of 'grower' pigs. The implications of this difference are unclear although mini-pigs grow at a much slower growth velocity than 'grower' pigs and do not display the periods of rapid growth that appear to be necessary for scoliosis to develop (Coillard et al., 1999).

On the basis of the conflicting results from these animal studies, the potential role of the NCJ in AIS remains unclear and further animal work is clearly required to replicate and extend prior studies. The purpose of this study was to investigate in a pilot project if disturbance of the NCJ by the unilateral placement of partially threaded cancellous screws would result in pedicle asymmetry and the creation of scoliosis. To improve upon the work completed to date, this study incorporated the use of serial radiographs with the hope that these might aid in elucidating the potential mechanism by which intervention with the NCJ resulted in changes in vertebral morphology. Furthermore, criteria were created for the precise measurement of parameters such as pedicle and lamina length so that changes in vertebral morphology could be objectively assessed.

MATERIALS AND METHODS

Surgical Model

Four two-month-old male 'grower' pigs (weights 21-27 kg) were obtained from the University of Alberta Swine Unit and housed at the University of Alberta Farm Metabolic Unit. The choice of animal model was based on previous porcine surgical models of asymmetric NCJ growth (Ottander et al., 1963; Beguiristain et al., 1980) as well as prior work which had shown that the thoracolumbar NCJs in 'grower' pigs were open until at least one year of age (Chapter 4). The surgical approach was based on the work of Beguiristain et al. (1980) and was optimized by examination of several porcine vertebral columns from pigs of the same age. Using these anatomic specimens, the optimal point of entry for screw placement was determined to be just below the edge of the upper facet, approximately 5 mm lateral to the center of the facet near the base of the transverse process. The required screw lengths were measured to be between 28 to 35 mm and the angle of screw insertion was estimated at approximately 20 to 30 degrees relative to the midline (Figure 8-2).

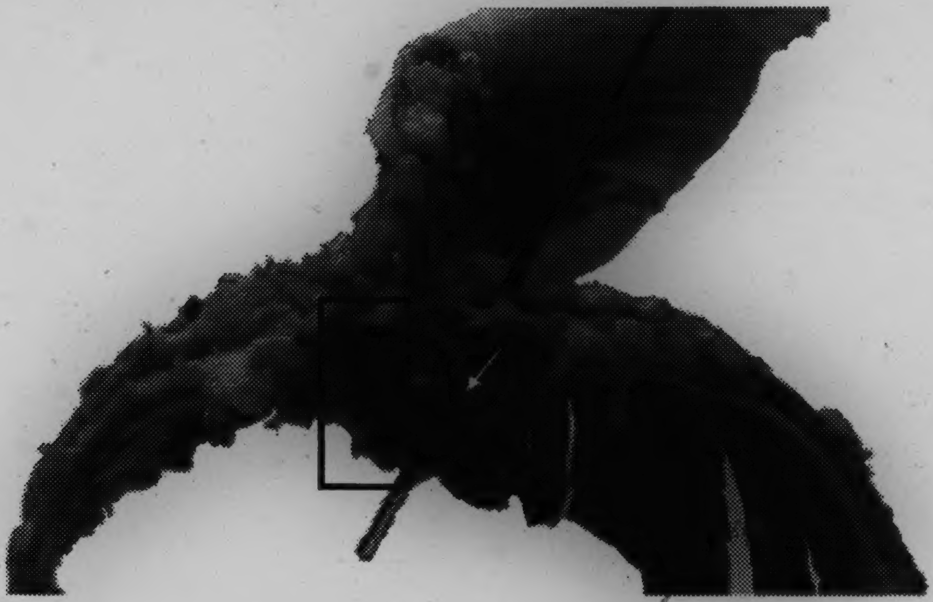

Figure 8-2. Using an anatomic specimen from a two-month-old pig, the angle of screw insertion (indicated with the surgical probe) was estimated at approximately 20-30 degrees relative to the midline. The position of the NCJ is shown with the white arrow. On the side without the probe, the path of a test screw inserted by the surgeon can be seen (black rectangle).

Surgical Technique

On the day of the surgery, approximately three days after the pigs had arrived at the Metabolic Unit, the animals were not fed from 12 hours before the surgery to the time of surgery. Each animal was weighed and tranquilized with xylozene/Rompun (2 mg/kg) and ketamine hydrochloride (20 mg/kg) injected into the muscle behind the ear. During the surgery, anesthesia was maintained with a mixture of medical oxygen (1.5 L/min), nitrous oxide (0.75 L/min) and 2.0% halothane administered by respiratory mask. All surgeries were performed by a team of orthopedic surgeons and residents from the University of Alberta Department of Orthopedic Surgery (Drs. M. Moreau, A. Woo, M. Clark, C. Secretan).

The four animals were divided into two groups, with one group of two animals (Pig 1 and Pig 2) undergoing screw placement on the left side and another group of two animals (Pig 3 and Pig 4) undergoing screw placement on the right side to ensure that any resulting curves were not a reflection of normal physiologic curves in the lateral direction. All steps of the surgery were performed with fluoroscopic guidance. Under sterile conditions, a surgical incision was made into the superior dorsal aspect of the vertebral column. After dissection of the vertebral muscles on the left side (Pig 1 and Pig 2) or the right side (Pig 3 and Pig 4) of T6-T10, the screw site was uncovered below the edge of the facet joint and periosteum stripped at this site. A canal was created for the screw using a drill with an oscillating attachment and a pedicle feeler was used to verify the quality of bone within the canal. The first screw was then inserted at T6, with subsequent screws inserted at T7, T8, T9 and T10. All screws were partially threaded cancellous screws (diameter 3.5 mm, length 28-35 mm) made of stainless steel. The head of the screw was left outside the posterior vertebral cortex while the screw threads were placed just beyond the NCJ to ensure sufficient compression across the growth plate. Considerable care was taken to ensure that the screw tips did not penetrate the anterior vertebral cortex as this would have risked damaging the aorta. Upon placement of each screw, the screw position was carefully verified by intraoperative fluoroscopy (25 kV), which was also used throughout the surgical procedure as a guide.

Shortly after surgery, all pigs received injections of the antibiotics buprenorphine hydrochloride (2 mL) and ceftiofur hydrochloride (1.5 mL) and post-operative care was administered by the animal care staff at the Metabolic Unit. Post-operatively, the pigs remained housed at the Metabolic Unit and were fed and watered *ad libitum*. No abnormal post-operative complications were noted in any of the animals, all of which quickly recovered and appeared to behave quite normally.

Radiographic Visualization

At weekly intervals after surgery, the weight and the length of the pigs were recorded (Table 8-1). The lengths were measured from the mastoid process behind the ear to the base of the tail. Repeated measurements by the same observer showed an intraobserver variation of 0.5 cm for length (95% confidence interval) and 0.5 kg for weight (95% confidence interval).

At biweekly intervals after surgery, each pig was tranquilized and AP radiographs of the thoracolumbar spine were acquired using a portable fluoroscope (60-85 kV, 80 mAs). Unfortunately, equipment problems with the fluoroscope prevented the acquisition of immediate post-operative radiographs but they were recorded therefore at biweekly intervals. To ensure that the placement of pigs did not significantly affect the radiographs generated, a consistent procedure was applied to position pigs on the wooden table used for imaging. Both of the shoulders, forelimbs and hindlimbs were aligned and the cranial and caudal aspects of each pig were also aligned with respect to the X-ray film. Three successive repetitions of the alignment procedure with a single porcine specimen (at one month post-operatively) showed that radiographic differences due to the placement of pigs appeared to be negligible.

Using the portable fluoroscope to acquire radiographs, one of the limitations was that only three to five vertebrae could fit on each field of view and therefore four to five separate radiographs were required to encompass the entire thoracolumbar region. These overlapping radiographs were arranged into a single composite radiograph using the variable opacity function of Adobe Photoshop 6.0 software (Adobe Systems Inc., Kennesaw, Georgia, United States). To ensure that image magnification could be determined from each composite radiograph, a circular marker of diameter 2.4 cm was included in at least one of the images used to make each composite radiograph.

Table 8-1. Average weight and length for the porcine specimens from the time of surgery to 18 weeks post-operatively

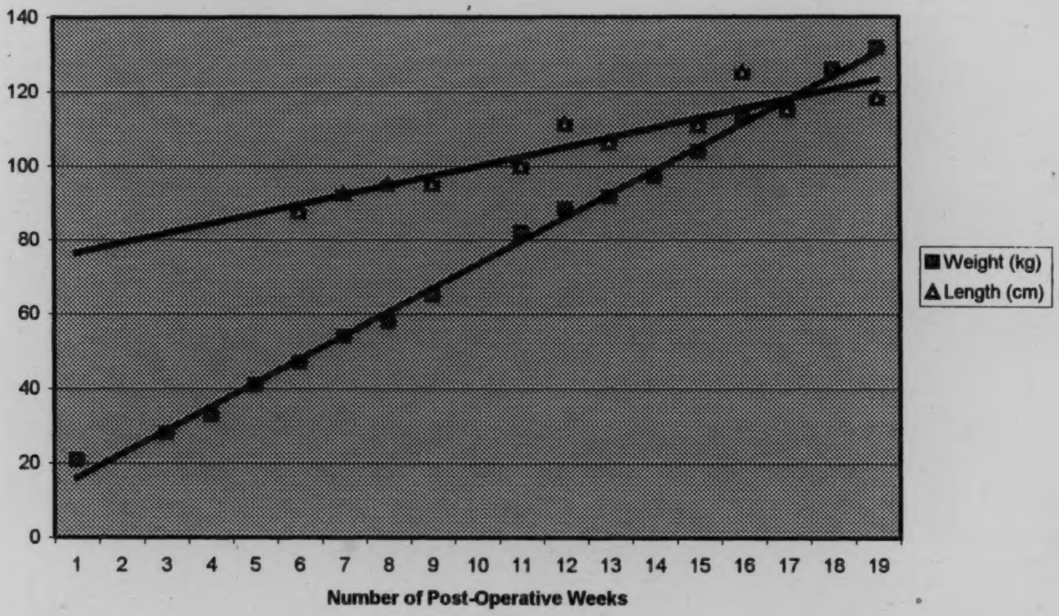

Table 8-1. Weekly measurements of weight and length showed that both quantities were increasing rapidly during the post-operative period. The measurements were taken by technical staff and the variation in 'shift times' meant that different technicians made the measurements at different times with consequent small variations that can be seen.

Upon creation of the composite radiographs, vertebral rotation was measured from the radiographs acquired at 9, 11 and 13 weeks post-operatively using the Stokes method (Russell et al., 1990). Depending on the results generated, it was thought that measurements could later be performed for all radiographs if necessary. Among the commonly used methods to measure vertebral rotation, the Stokes method was chosen since it did not require marking of the spinous processes, which were difficult to accurately discern, or the use of any morphometric coefficients that were specific to human vertebrae. Using this method, from the radiographs, eight points were marked on each vertebra: the center of the two pedicles, the four corners of the vertebra and the vertebral body waists (the most medial portion of the vertebral body as seen on an AP or PA radiograph) (Figure 8-3). These points were subsequently digitized and rotation calculated using a computer program created by the Northern Alberta Scoliosis Research Center. From previous work, the mean error of calculating vertebral rotation using this method was 6°, with a standard deviation of 2° (Russell et al., 1990).

Euthanization and Computed Tomography Imaging

The four porcine specimens were euthanized 4.5 months post-operatively with an intravenous injection of euthanyl (240 mg/mL). Immediately after, the vertebral column was removed and cleared of all soft tissue. The ribs in the thoracic region were cut approximately 10 cm from their articulation with the vertebral body. Each vertebral column was then wrapped in paper towels soaked in formalin and stored in an opaque bag. Within 48 hours, the vertebral columns were imaged using CT (slice thickness = 1.25 mm, overlap between slices = 0.625 mm). Since the vertebrae had been freed of muscular and ligamentous attachments, the aim of CT imaging and subsequent image reformatting was only to assess the vertebral morphology of individual vertebrae and not to measure the Cobb angle of the vertebral column or not to judge the presence or absence of a scoliotic curve.

Measurement of Computed Tomographic Images

In the interests of acquisition time, the original CT images were acquired through the entire vertebral column without ensuring that each image was truly transverse to the

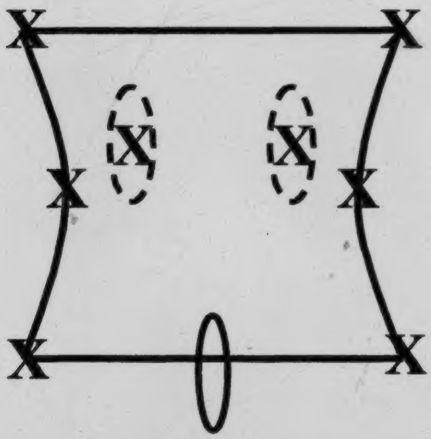

Figure 8-3. On this schematic diagram of a vertebra as seen on a conventional AP or PA radiograph, the pedicles are represented with ovals composed of dotted lines and the spinous process is represented with an oval composed of a solid line. The eight points that must be marked to measure vertebral rotation using Stokes method (Russell et al., 1990) are each shown with an X.

endplates of each vertebra. For this reason, the original CT images were sent to the Advanced Workstation Volume Analysis 3.1 software (General Electric Medical Systems) for reformatting. Using the reformatting option, true transverse images that were parallel to the superior and inferior vertebral endplates (no significant vertebral wedging was present among these specimens) could be acquired for each vertebra. These true transverse images were acquired by starting with the sagittally reformatted images and altering the slicing plane to generate coronally reformatted images that were parallel to the anterior and posterior aspects of the vertebral body. From these true coronal images, a slicing plane parallel to the superior and inferior endplates of the vertebra was used to generate true transverse images.

Using this method of reformatting and maintaining the same 1.25 mm slice thickness of the original CT images, approximately 30 transverse images were generated for each vertebra. Five transverse images (the 5th, 10th, 15th, 20th and 25th image from the superior endplate) from the T5-T11 vertebra of each porcine specimen were used for measurement purposes. Using these five images, the posterior body length, pedicle lengths, pedicle thicknesses, lamina lengths and lamina thicknesses were measured using definitions adapted from previous work (Chapter 6) on the measurement of pedicle asymmetry in normal and scoliotic patients (Figure 8-4). All measurements were performed with the Advanced Workstation Volume Analysis 3.1 software and subsequent statistical analysis of measurements was completed using the Statview 5.0 software (SAS Institute, Cary, North Carolina, United States). Findings were considered significant when $p \leq 0.05$ for the Students-t tests.

RESULTS

The surgical technique used for this pilot study was judged to be acceptable. Intra-operative fluoroscopic visualization confirmed that pedicle screws were placed along the axis of the pedicle with no infringement on the vertebral canal. The screw head was placed outside the posterior cortex of the vertebra, while the tip of the screw was placed within the cancellous bone of the vertebral body and did not penetrate the anterior cortex as this may have caused vascular damage. Since the threads of the screw anchored the body of the vertebra (anterior to the NCJ) and the head of the screw anchored the

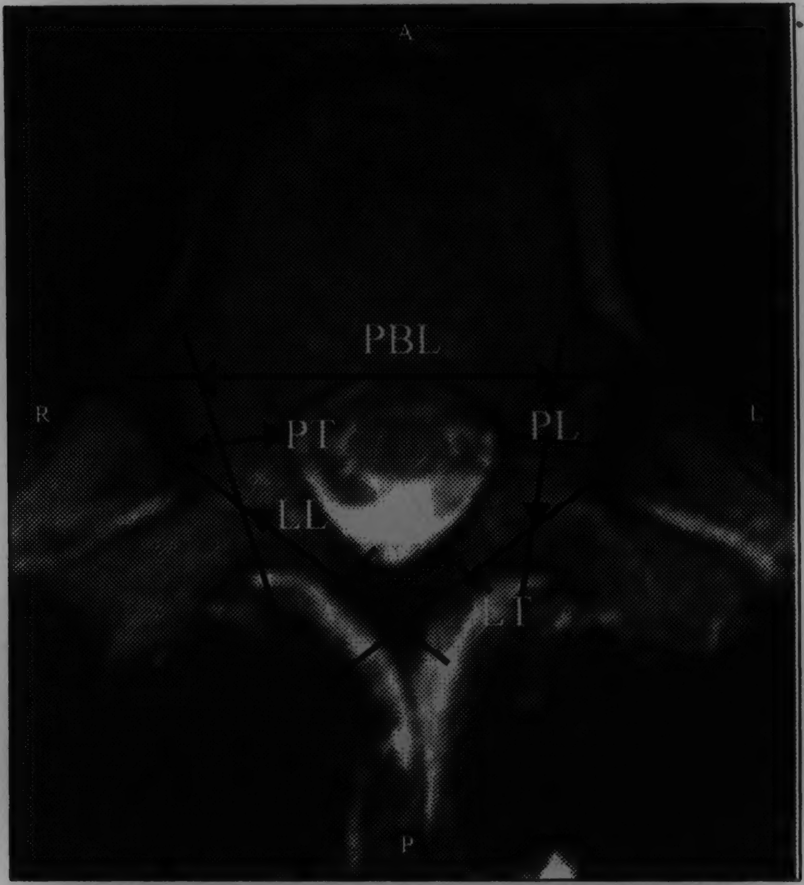

Figure 8-4. The definitions used to measure the posterior body length (PBL), pedicle lengths (PL), pedicle thicknesses (PT), lamina lengths (LL) and lamina thicknesses (LT) were adapted from previous work (Chapter 6) and applied to the CT images acquired from the porcine specimens. The posterior body length, right and left pedicle length and right and left lamina length formed a pentagon that enclosed the vertebral canal and described all segments of the neural arch. The posterior body length was determined by drawing a straight line perpendicular to the axis of the vertebra that passed through the anterior tip of the vertebral canal. The distance between the outer aspect of the compact bone on both borders of the vertebra was defined as the posterior body length. Lines were then drawn through the long axis of each pedicle and lamina equidistant from the lateral and medial borders to form a pentagon. The pedicle length on each side was defined as the distance along the line through the axis of the pedicle from its intersection with the posterior body length to its intersection with the line through the axis of the lamina. The lamina length on each side was defined as the distance along the line through the axis of the lamina from its intersection with the line through the axis of the pedicle to its intersection with the line through the axis of the lamina on the other side. The pedicle thickness was measured at a distance of one-half of the pedicle length along the line through the axis of the pedicle. Similarly, the lamina thickness was measured at a distance of one-half of the lamina length along the line through the axis of the lamina. All measurements were recorded bilaterally except for posterior body length.

vertebral arch (posterior to the NCJ), it was assumed that a compressive force would be exerted across the NCJ in a manner similar to that commonly used for epiphyseodesis of growth plates. This compressive force was expected to prevent growth at the site of the NCJ and result in a shortened pedicle (Tencer and Johnson, 1994).

The size of the porcine specimens used was appropriate for the placement of pedicle screws and for the surgical approach chosen. Weekly measurements of weight and length showed a substantial increase in both quantities post-operatively (Table 8-1) and confirmed that the pigs were growing quite rapidly during the course of this study. On average, weights increased from 24 kg (pre-operative) to 123.6 kg (18 weeks post-operatively) and lengths increased from 87.5 cm (first length measurement was taken at five weeks post-operatively) to 117.3 cm (18 weeks post-operatively). As seen in Table 8-1, the rate of increase in weight was greater than the rate of increase in length which would have been expected since length was a linear quantity and weight was a reflection of volume, which was a cubic quantity. Measurements of length appeared to show fairly significant interobserver variation which was not originally considered since it was assumed that length measurements would be performed by the same individual. However, these variations did not affect experimental results since only an indication of growth was needed.

Examination of the radiographic images acquired at biweekly intervals generally showed no evidence of lateral curvature (Figure 8-5, Figure 8-6, Figure 8-7, Figure 8-8, Figure 8-9). The only evidence of any curvature appeared in Pig 1 at 15 weeks post-operatively. However, the extent of curvature noted was not sufficiently large to be considered a scoliosis as defined by a Cobb angle of greater than 10 degrees. In examining the serial images from each pig, there did not appear to be a progressive deformity that developed over time. Interestingly, some of the pedicle screws in Pig 1 and Pig 2 appeared to show rotation between successive images (Figure 8-5, Figure 8-6, Figure 8-10) with the heads of the screws rotating towards the side of screw placement. The radiographic images were collected until 18 weeks post-operatively, as it was expected that any scoliosis would manifest by 16 weeks, at which point Beguiristain et al. (1980) had noted a Cobb angle of 20 degrees.

2 weeks 7 weeks 11 weeks 15 weeks

Figure 8-5. AP radiographs obtained from Pig 1 (screws placed on left side of T6-T10) at 2,7,11 and 15 weeks post-operatively. The screws at T6, T7 and T8 appear to have rotated between the composite radiograph acquired at 2 weeks and the composite radiograph acquired at 15 weeks.

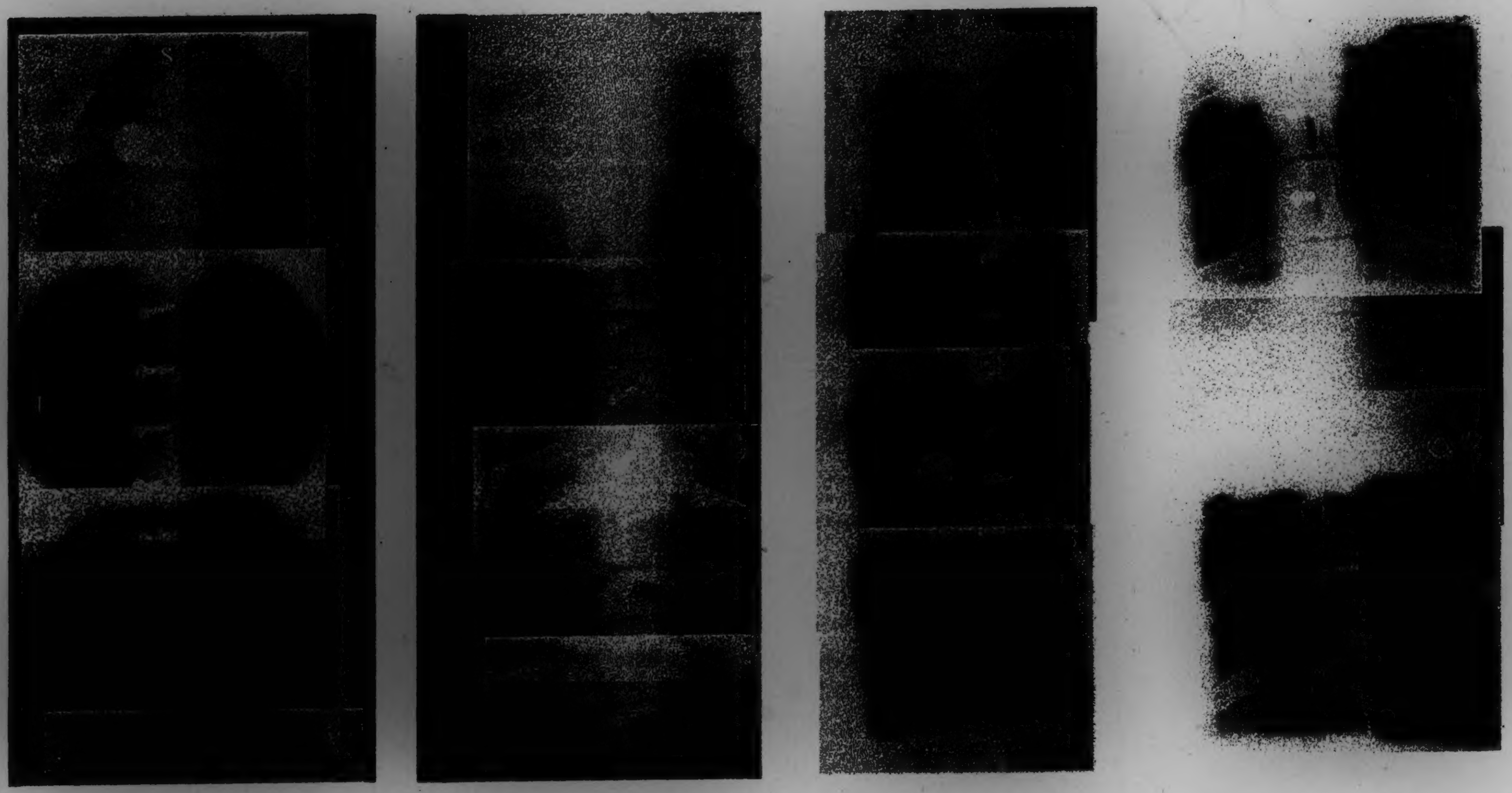

2 weeks 7 weeks 11 weeks 15 weeks

Figure 8-6. AP radiographs obtained from Pig 2 (screws placed on left side of T6-T10) at 2,7,11 and 15 weeks post-operatively. The T6, T7 and T8 screws appear to have rotated between the composite radiograph acquired at 2 weeks and the composite radiograph acquired at 15 weeks.

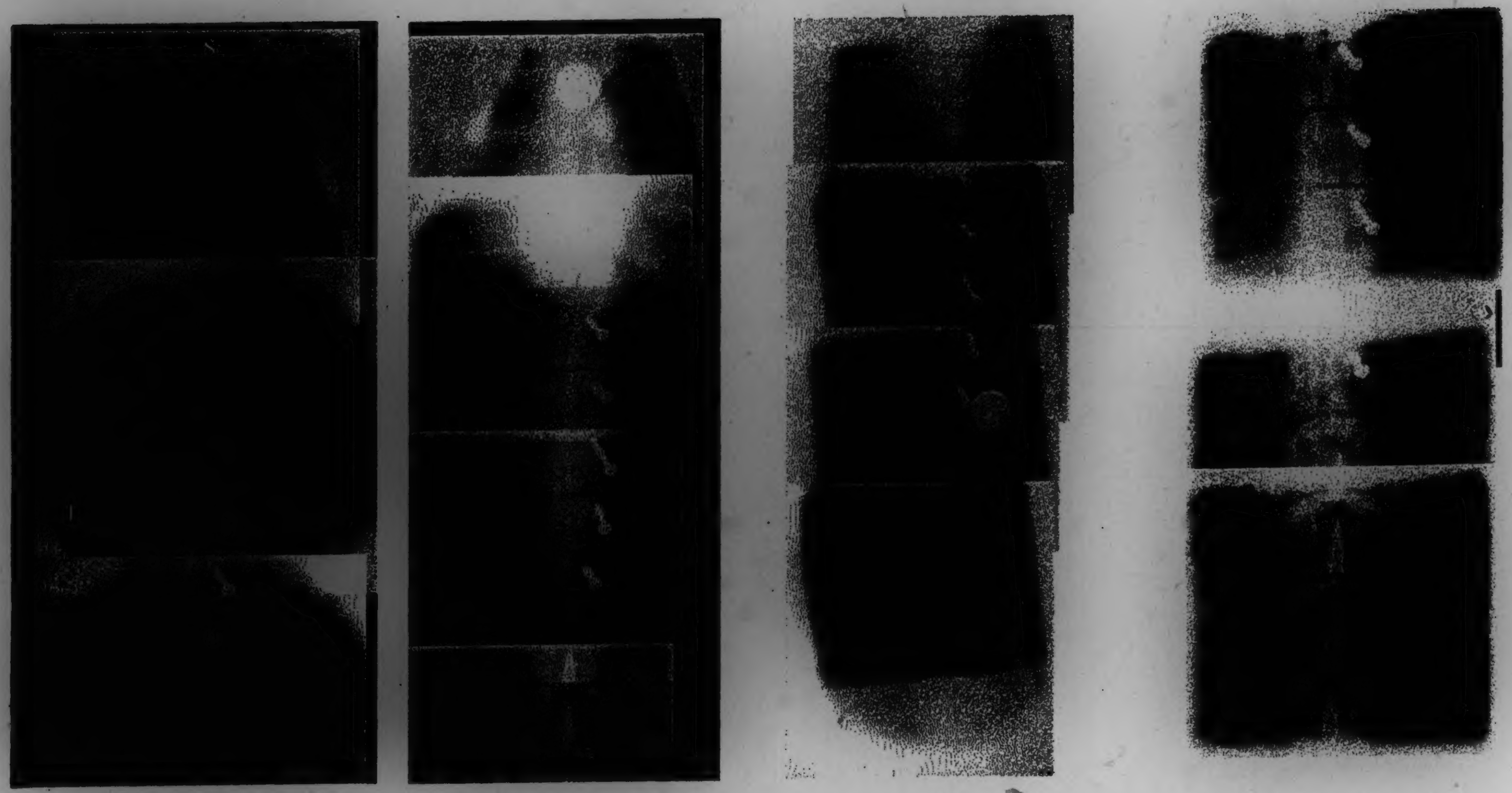

2 weeks 7 weeks 11 weeks 15 weeks

Figure 8-7. AP radiographs obtained from Pig 3 (screws placed on right side of T6-T10) at 2,7,11 and 15 weeks post-operatively.

2 weeks 7 weeks 11 weeks 15 weeks

Figure 8-8. AP radiographs obtained from Pig 4 (screws placed on right side of T6-T10) at 2,7,11 and 15 weeks post-operatively.

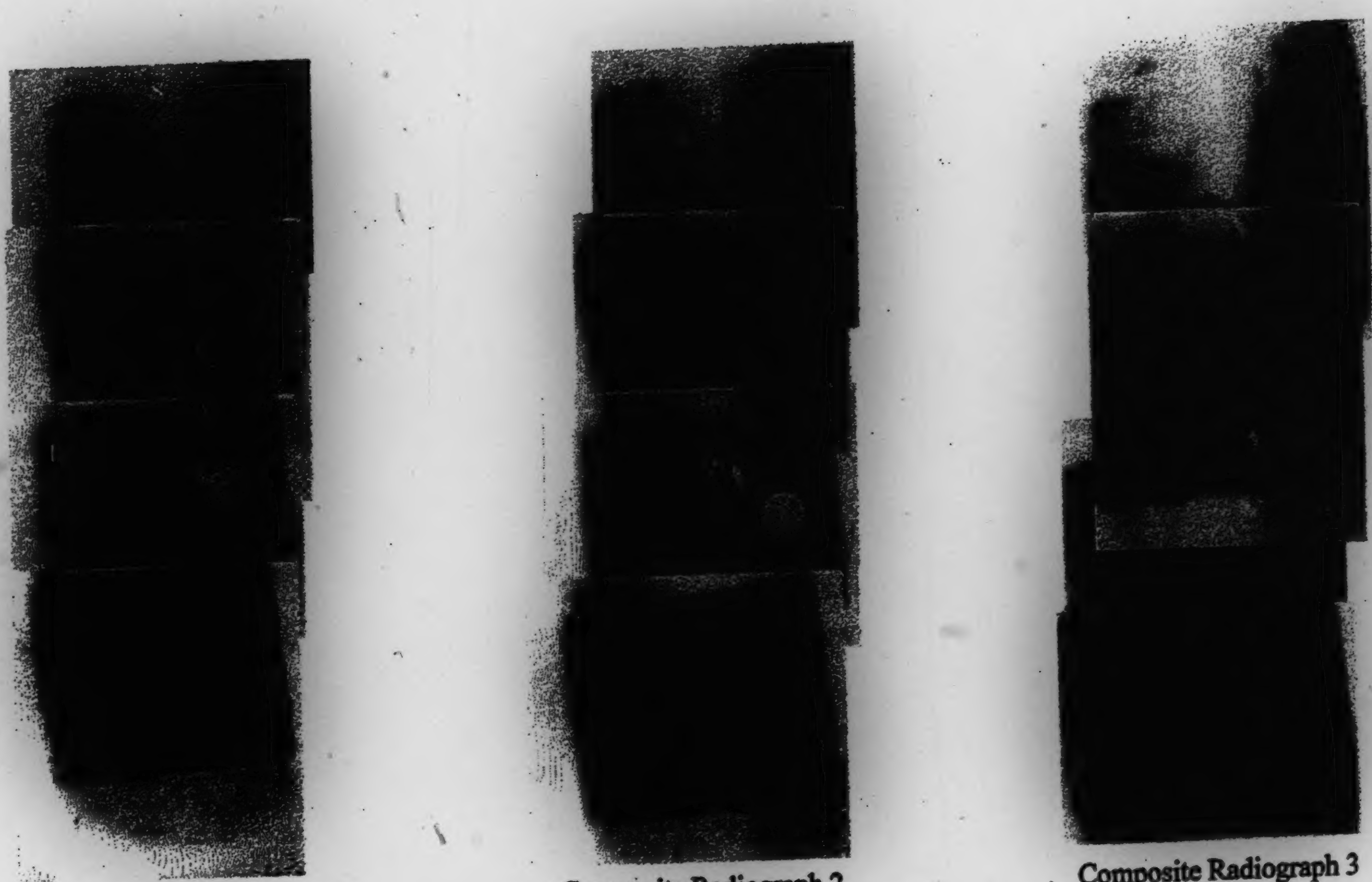

Composite Radiograph 1 Composite Radiograph 2 Composite Radiograph 3

Figure 8-9. The three sets of composite radiographs acquired for Pig 3 at 11 weeks post-operatively showed negligible differences.

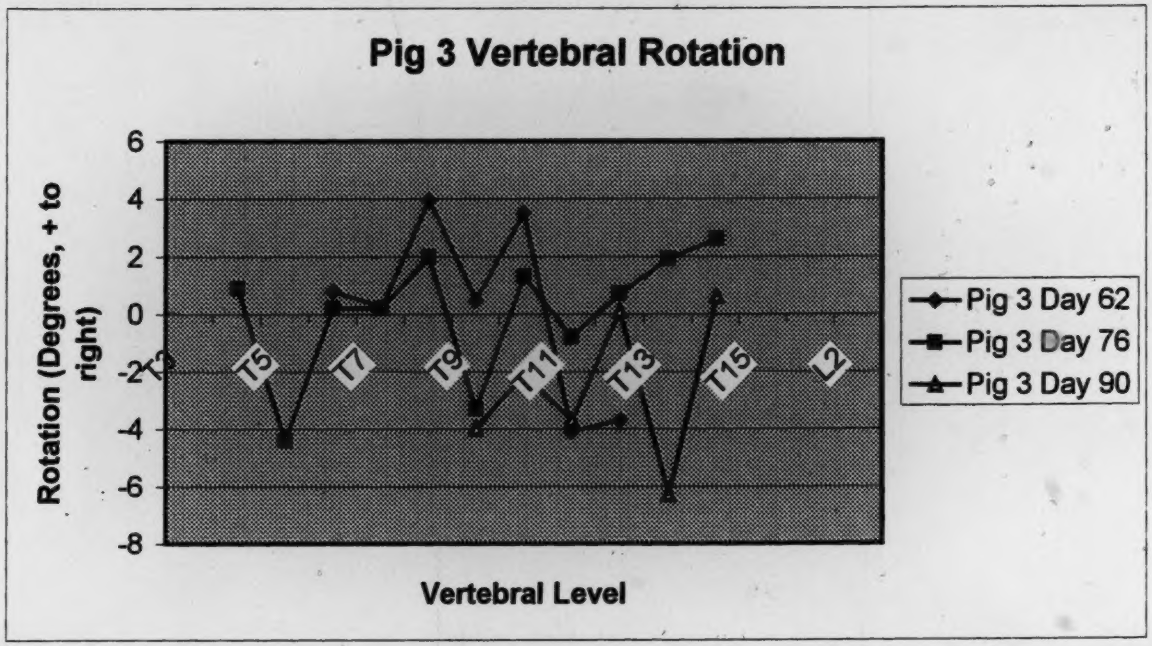

Figure 8-10. Rotation of thoracolumbar vertebrae for Pig 3 calculated using composite radiographs from 9, 11 and 13 weeks post-operatively. Although individual vertebrae showed significant rotation (>5°) at a specific post-operative time, no trends were seen when comparing vertebral rotation between successive radiographs. Missing values on the above graph at particular post-operative times indicate that one of the eight points required to measure rotation using the Stokes method (Russell et al., 1990) was not clearly discernable. Rotation results are only shown for Pig 3 although all other pigs displayed similar results.

The method of acquiring and piecing together individual radiographs to form a composite radiograph appeared to produce acceptable results. To test this process, Pig 3 was radiographed three times at 11 weeks and three sets of composite radiographs were created. These composite radiographs showed negligible differences (Figure 8-9).

The extent of vertebral rotation was measured at 9, 11 and 13 weeks post-operatively using the Stokes method. Unfortunately, although vertebral rotation beyond the normal limit of five degrees (Russell et al., 1990) was noted for single vertebrae at a specific post-operative time (Figure 8-10), the same vertebrae did not show significant rotation in successive radiographs. For this reason, the extent of vertebral rotation was not judged to be significant using the Stokes method of measurement.

Changes in vertebral morphology were best assessed by examination of the transverse CT images since numerous vertebral landmarks overlapped on the conventional radiographs. Simple observation of the operated vertebrae (T6-T10) clearly showed that the thickness of the lamina and the thickness of the pedicle on the side of the vertebra with the screw were much greater than the thickness of the lamina ($p<0.001$) and pedicle ($p=0.002$) on the side without the screw (Figure 8-11, Figure 8-12). Although a shorter pedicle was expected on the side of the operated vertebrae with the screw, measurement of pedicle length showed that the pedicle was actually longer on the side with the screw ($p<0.001$). The side without the screw exhibited a longer lamina ($p<0.001$). Testing for differences in total length (the sum of pedicle length and lamina length) between the side of the vertebra with the screws and the side of the vertebra without the screws showed no significant differences. Comparing the operated (T6-T10) and the non-operated (T5, T11) vertebrae, only the lamina thickness was significantly different between the two groups and was greater for the operated side ($p=0.0093$). This showed that the lamina thickness for the operated vertebrae was greater than the normal lamina thickness. Similar conclusions could not be made for any of the other quantities as there were no statistical differences in posterior body length, pedicle length, pedicle thickness or lamina length.

The position of the pedicle screws as visualized on the CT images at 18 weeks post-operatively was surprising (Figure 8-11). The heads of the screws, which were

T8 T9 T10

Figure 8-11. CT images acquired at the mid-pedicle level of T8, T9 and T10 from Pig 2 show that the lamina and the pedicle appear thicker on the screwed side. Visualization of the screw shows that the head of the screw is buried in bone and that the screw has clearly medialized (see vertebra T10).

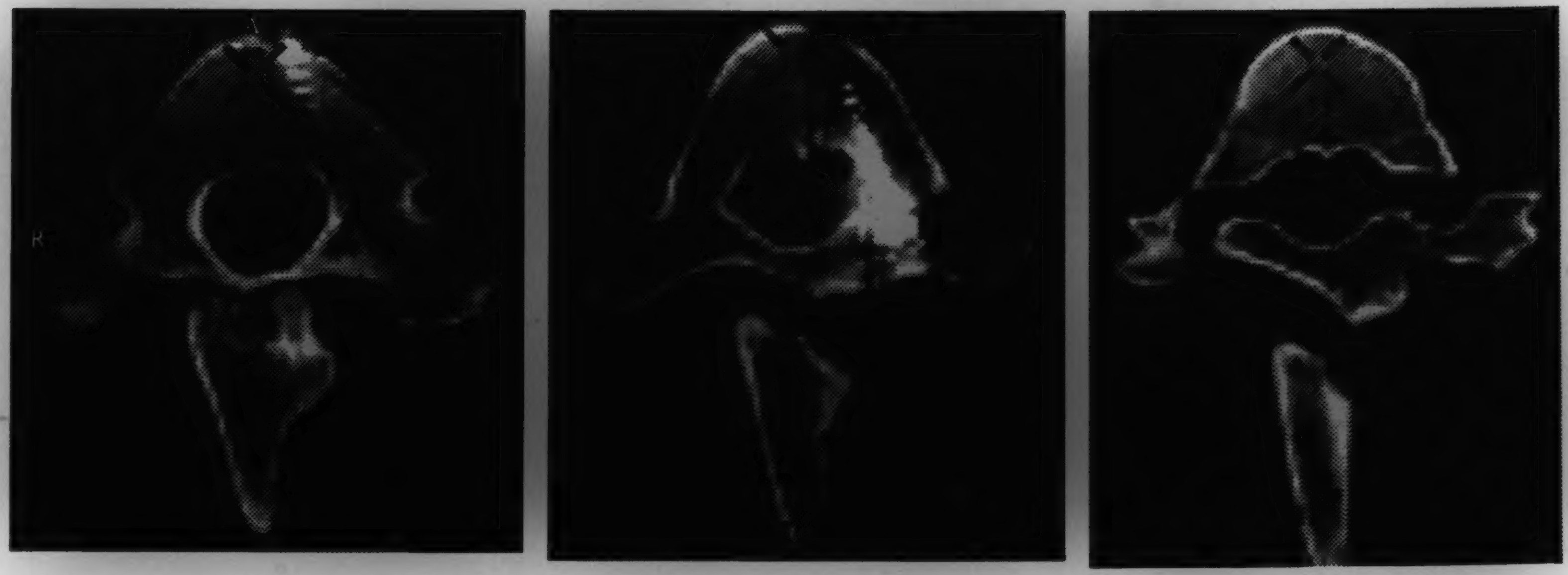

5 mm above the site of the screw

At the site of the screw

5 mm below the site of the screw

Figure 8-12. CT images acquired 5 mm above the site of the pedicle screw, at the site of the pedicle screw and 5 mm below the site of the pedicle screw in T9 from Pig 2 show that the NCJ appears to be open above and below the site of screw placement.

originally situated outside the posterior cortex of the vertebral body, were all covered by a significant amount of bone. The tips of the screws had stayed in the same position relative to the anterior cortex of the vertebra and were still located in the cancellous bone a few mm away from the anterior cortex. Although the screws were still oriented parallel to the axis of the pedicle, the screws had medialized in position. Despite taking greater care to ensure screw positioning during surgery, this medialization was quite apparent with some of the screws penetrating the medial border of the canal although no neurologic symptoms were noted in any of the porcine specimens. Examination of all screws showed that the screws were oriented in approximately the same superior-inferior position (i.e. vertebral height) and were consistently placed at the mid-pedicular level. Interestingly, CT visualization of the NCJ above and below the screw position showed that the NCJ appeared to be open at these sites (Figure 8-12), suggesting that screw placement may not have resulted in the formation of a bony bridge across the NCJ.

DISCUSSION

The major finding of this study was that scoliosis was not created after the unilateral placement of partially threaded cancellous screws across the NCJ in a porcine model. In addition to the lack of any significant lateral curvature or progressive deformity on examination of the serial radiographs, a significant pattern of vertebral rotation was not measured using the Stokes method (Russell et al., 1990).

In this study, it was most surprising that the pedicle on the side with the screw was not shortened in relation to the contralateral pedicle and was actually longer based on the measurement definitions (discussed later). This was unexpected since the NCJ is assumed to make a significant contribution to the growth in length of the pedicle (Vital et al., 1989; Yamazaki et al., 1998) and therefore compression across this growth plate would be assumed to result in a shorter pedicle. In this study, all evidence suggests that compression was achieved across the site of the NCJ since fluoroscopic visualization showed that the screw was correctly positioned. Furthermore, the threads of the pedicle screw maintained a consistent distance from the anterior aspect of the NCJ which is difficult to explain if compression was not achieved and maintained. If no compressive force was exerted, one would expect that the anterior growth contribution of the NCJ would decrease the distance between the NCJ and the screw threads. Assuming that compression was achieved across the NCJ, this study showed that the NCJ was not making a significant contribution to the growth of the pedicle at this phase of development.

If the NCJ was not responsible for the increase in pedicle length, another mechanism would be required to explain this increase. The increase in pedicle length is hard to dispute since the anterior portion of the pedicle screws stayed in the same relative location while the heads of the screws were located outside the posterior cortex at the time of surgery and in the mid-pedicle region after 4.5 months post-operatively. Considering the shape and position of the pedicle, it is entirely possible that the pedicle, unlike a long bone, does not require a growth plate for growth in length (Figure 8-13). Since the pedicle is a curved structure, periosteal deposition on the lateral aspect of the pedicle and resorption on the medial aspect would increase pedicle length. In this study, the extent of resorption on the medial aspect of the pedicle was shown to be quite extensive since pedicle screws that were originally placed in the middle of the pedicle ended up nearly inside or even inside the vertebral canal (Figure 8-11).

Among the morphologic changes noted in the vertebra there was a significant change in lamina thickness on the side of the vertebra with the screw, based on both visual evidence and measured values. This increase in laminar thickness seemed to be a result of reactive bone formation in response to the screw rather than a result of altered vertebral growth since the additional bone did not take on the normal shape of the vertebra (Figure 8-11). Although some bone formation over the head of the screw was expected due to interference with the vertebral periosteum, the orthopedic surgeons involved in this study confirmed that the amount of reactive bone formed in this study was surprising based on previous experiences with the negligible amount of reactive bone formed in procedures such as epiphyseodeses in children. The second morphologic change detected on both gross visualization and measurement was an increased pedicle thickness on the side of the vertebra with the screws. This was surprising since reactive bone formation is typically expected in relation to periosteal disturbance and no periosteum appeared to be damaged at this site. It is possible that periosteum on the medial aspect of the pedicle was disturbed as resorption on this surface resulted in the

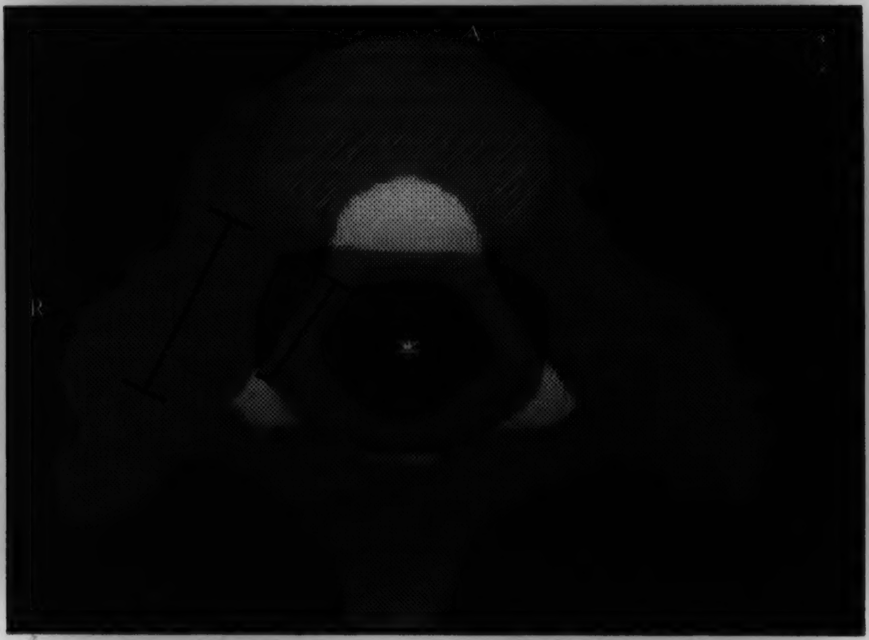

Figure 8-13. The image of the T8 vertebra from a one-week-old Sprague-Dawley rat has been superimposed on the image of the T8 vertebra from a ten-week-old rat. The black bars indicate the approximate pedicle lengths at the two ages. Examining the pedicle, it is possible to see how resorption of the pedicle on the medial aspect combined with deposition on the lateral aspect would actually result in an increase in pedicle length over time.

screw medializing, yet if this were the case, then the medial aspect of the screw would be encased in bone, which was not seen. Although the mechanism of the increase in pedicle thickness requires further explanation, it is interesting to note that other authors have also noted an increase in pedicle thickness after screw placement (Schulze et al., 1998). In the current study, the changes noted in lamina and pedicle thickness appeared to represent morphologic changes caused by reactive bone formation, but these findings have implications for other animal models where screws have been placed across the NCJ (Ottander, 1963; Beguiristain et al., 1980; Coillard et al., 1999). In some of these studies, the increased laminar and pedicle thickness (Ottander et al., 1963; Beguiristain et al., 1980) have been suggested to represent the changes noted in scoliotic vertebrae (Roaf, 1960; Smith et al., 1991; Wever et al., 1999; Liljenqvist et al., 2000; 2002; Parent et al., 2002), but it was impossible to determine if these changes represented reactive bone growth or were secondary to the intervention at the NCJ and the scoliosis created.

The longer pedicle length and the shorter lamina length noted on the side of the vertebra with the screw are difficult to explain. Unlike the changes in pedicle and lamina thickness, these changes were not apparent on visualization of the CT images. Furthermore, it is difficult to explain how compression of the NCJ could result in an increased contribution to pedicle length. A more likely explanation is that these findings are a result of the measurement definitions used (Figure 8-14). On the side of the vertebra with the screw, the lamina thickness was grossly affected in relation to all other measured values. This resulted in a posterior displacement of the axis of the lamina, with the end result that the measured lamina length was shorter and the measured pedicle length was longer. Although the measured values for the individual lengths of the pedicle and lamina were altered, it is interesting to note that the total length of the neural arch (pedicle and lamina) between the two sides of the vertebra did not show a significant difference. This supports the idea that the changes noted were a result of the definitions used. Since measurement definitions for pedicle length and lamina length were not independent, changes in one parameter resulted in compensatory changes in neighboring parameters. This aspect of the study highlights the difficulty involved in creating valid

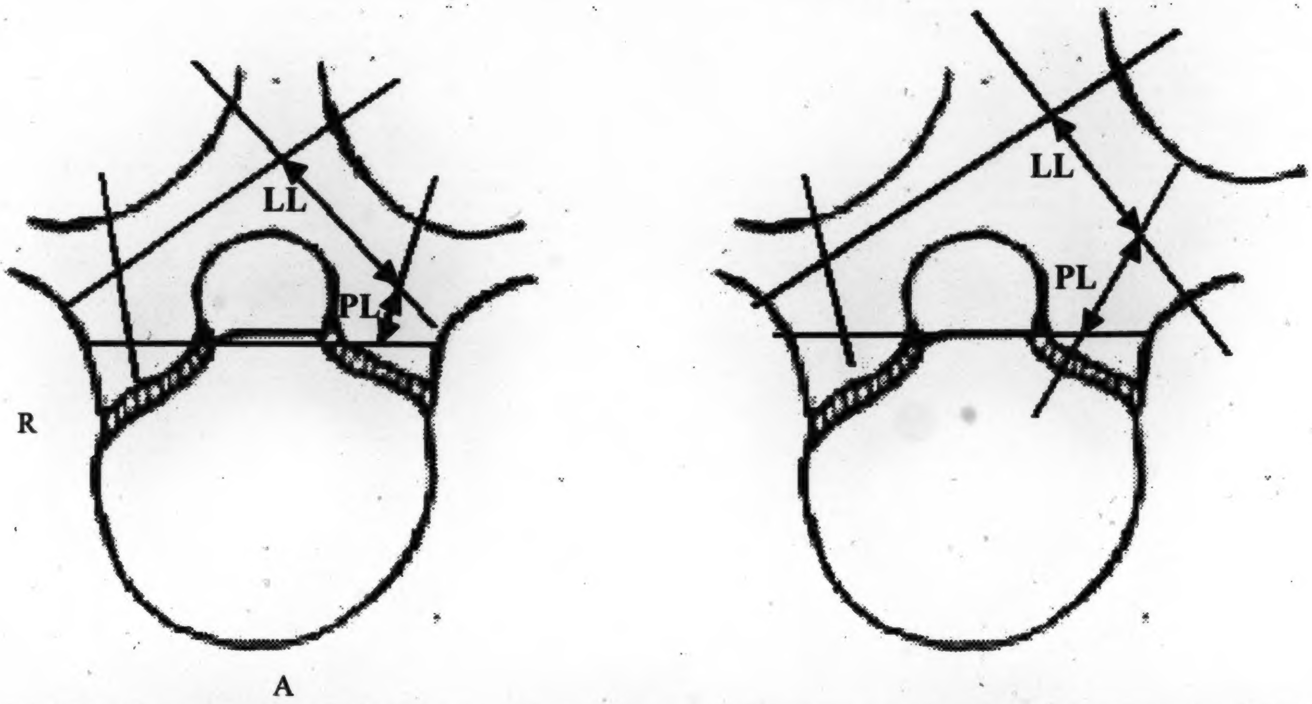

Figure 8-14. The diagram on the left depicts a normal vertebra and the lines drawn are based on the measurement definitions for posterior body length, pedicle lengths (PL) and lamina lengths (LL) used in this study. The application of these definitions would produce measured values for the pedicle length and lamina length that were approximately equal between the two sides of the vertebra, allowing for the limits of normal anatomic variation. The diagram on the right depicts a vertebra with an increased lamina thickness, as seen on the screwed side of the operated vertebrae in this study. The increased lamina thickness results in the axis of the lamina being displaced further posteriorly, with the end result that the lamina length measurement is decreased on the side with the screw. As a result of the axis of the lamina being displaced, the apparent length of the pedicle also increases.

measurement criteria for vertebral morphologic parameters such as pedicle and lamina length and may explain why studies of these parameters in AIS have produced conflicting results (Nicoladoni; 1909; Roaf, 1960; Knutsson, 1963; Taylor, 1983; Vital et al., 1989; Liljenqvist et al., 2002). These definitions were originally developed for the measurement of normal vertebrae and vertebrae from AIS patients (Chapter 6), but were not valid for measurement of the deformed vertebrae from these porcine specimens. This would suggest that definitions of vertebral morphology have specific applications and require extensive testing before application outside their originally intended populations. Furthermore, the validity of measurement definitions should always be evaluated to ensure that the results generated are indicative of true changes in vertebral morphology.

The results of this study directly conflict with the work of Beguiristain et al. (1980) who noted a significant scoliosis of 20 degrees by four months after the same surgical procedure, with the scoliosis progressing to 80 degrees by twelve months post-operatively. This study is not the first (see Coillard et al., 1999) to produce results that conflict with those of Beguiristain et al. (1980). It has been suggested that one of the potential problems with Beguiristain's study was the failure to include control or sham groups which made it difficult to determine if the scoliosis created was a result of NCJ perturbation or inadvertent circulatory, muscular, ligamentous or periosteal interference during the surgical approach. However, further work will clearly be required to understand the differing results between this study and that of Beguiristain et al. (1980).

If this pilot study is extended, in may be useful to operate on younger pigs to ensure that the growth contribution of the NCJ is maximal. The surgical procedure and selection of screw types would likely stay the same, although a larger diameter screw could be used to interfere with a greater extent of the NCJ. Most importantly, it would be useful to include control animals to differentiate the potential scoliosis that resulted from the surgical procedure from the indirect effects of drilling into the vertebra or interfering with muscles, ligaments and vasculature. If a scoliosis was created by interfering with five successive NCJs, the creation of scoliosis by interfering with non-successive NCJs (e.g. operating on the NCJ of T5, T7 and T9) would be quite interesting. The vertebrae between the operated NCJs (i.e. T6, T8) could be used to assess the secondary effects of scoliosis on vertebral morphology.

From the standpoint of evaluating normal and scoliotic morphology, this study demonstrates the difficulty of creating and applying measurement definitions for vertebral morphology. In addition, this study shows that results from any animal model of scoliosis must be reproduced and that control specimens should be included to decrease the ambiguity of experimental findings. Most importantly, this pilot study challenges the traditional ideas about the contribution of the NCJ to the growth of the pedicle and conflicts with past animal models of asymmetric NCJ growth (Beguiristain et al., 1980). In this study, the growth contribution of the NCJ to the pedicle appeared to be minimal. This would strongly suggest that the presence of the NCJ cannot be considered to represent growth activity at this site and that the presence of the NCJ in an adolescent child does not show that the NCJ is contributing to growth. In this study, a potential mechanism for an increase in pedicle length, independent of the NCJ contribution, was identified. These conclusions suggest that although asymmetric NCJ growth may not be a cause of AIS, asymmetric pedicle growth could be a result of other mechanisms.

REFERENCES

Arkin AM, Pack GT, Ranshohoff NS, Simon N. Radiation scoliosis: an experimental study. J Bone Joint Surg (Amer) 1950;32A:396-404.

Beguiristain JL, De Salis J, Oriaifo A, Canadell J. Experimental scoliosis by epiphysiodesis in pigs. Int Ortho 1980;3:317-21.

Coillard C, Rivard CH. Vertebral deformities and scoliosis. Eur Spine J 1996;5:91-100.

Coillard C, Rhalmi S, Rivard CH. Experimental scoliosis in the minipig: study of vertebral deformations. Ann Chir 1999;53:773-80.

Ganey TM, Ogden JA. Development and maturation of the axial skeleton. In : Weinstein SL (ed.). The pediatric spine : principles and practice, 2nd ed. Lippincott Williams and Wilkins. Philadelphia, 2001: 3-54.

Keim HA. Scoliosis. Clin Symp 1979;31:2-34.

Knutsson F. A contribution to the discussion of the biological cause of idiopathic scoliosis. Acta Orthop Scand 1963;33:98-104.

Knutsson F. Vertebral genesis of idiopathic scoliosis in children. Acta Radiol 1966;4: 395-402.

Liljenqvist UR, Link TM, Halm HF. Morphometric analysis of thoracic and lumbar vertebrae in idiopathic scoliosis. Spine 2000;25:1247-1253.

Liljenqvist UR, Allkemper T, Hackenberg L, Link TM, Steinbeck J, Halm HFH. Analysis of vertebral morphology in idiopathic scoliosis with use of magnetic resonance imaging and multiplanar reconstruction. J Bone Joint Surg (Am) 2002;84-A:359-368.

Maat GJ, Matricali B, Van Meerten EL. Postnatal development and structure of the neurocentral junction. Spine 1996;21:661-66.

Michelsson JE. The pathogenesis of experimental progressive scoliosis. Acta Orthop Scand 1962;Supp 59.

Miller NH. Adolescent idiopathic scoliosis: etiology. In : Weinstein SL (ed.). The pediatric spine : principles and practice, 2nd ed. Lippincott Williams and Wilkins. Philadelphia, 2001: 347-354.

Nicoladoni C. Anatomie und mechanismus der skoliose. Urban and Schwarzernburg. Munchen, 1909.

Ottander HG. Experimental progressive scoliosis in a pig. Acta Orthop Scand 1963;33:91-7.

Parent S, Labelle H, Skalli W, Latimer B, de Guise J. Morphometric analysis of anatomic scoliotic specimens. Spine 2002;27:2305-11.

Rajwani T, Bhargava R, Moreau M, Mahood J, Raso VJ, Jiang H, Bagnall KM. MRI characteristics of the neurocentral synchondrosis. Ped Rad 2002;32:811-16.

Roaf R. Vertebral growth and its mechanical control. J Bone Joint Surg (Br) 1960;42-B:40-59.

Roaf R. The basic anatomy of scoliosis. J Bone Joint Surg (Br) 1966;48-B:786-92.

Robin GC. The aetiology of idiopathic scoliosis. Freund Publishing House. Boca Raton, 1990.

Russell GG, Raso VJ, Hill D, McIvor J. A comparison of four computerized methods for measuring vertebral rotation. Spine 1990;15:24-27.

Schmorl G, Junghanns H, Besemann EF (ed.). The human spine in health and disease. Grune and Stratton. New York and London, 1971.

Schulze CJ, Munzinger E, Weber U. Clinical relevance of accuracy of pedicle screw placement. Spine 1998;23:2215-20.

Smith RM, Pool RD, Butt WP, Dickson RA. The transverse plane deformity of structural scoliosis. Spine 1991;16:1126-9.

Taylor JR. Scoliosis and growth : patterns of asymmetry in normal vertebral growth. Acta Orthop Scand 1983;54:596-602.

Robin GC. The aetiology of idiopathic scoliosis. Freund Publishing House. Boca Raton, 1990.

Tencer AF, Johnson KD. Biomechanics in orthopedic trauma. JB Lippincott Company. Nashville, 1994.

Vital JM, Beguiristain JL, Algara C, Villas C, Lavignolle B, Grenier N, Sénégas J. The neurocentral vertebral cartilage: anatomy, physiology and physiopathology. Surg Radiol Anat 1989;11:323-28.

Wever DJ, Veldhuizen AG, Klein JB, Webb PJ, Nijenbanning G, Cool JC, v Horn JR. A biomechanical analysis of the vertebral and rib deformities in structural scoliosis. Eur Spine J 1999;8:252-60.

Yamazaki A, Mason DE, Caro PA. Age of closure of the neurocentral cartilage in the thoracic spine. J Ped Ortho 1998;8:168-172.

CHAPTER 9

COMPUTERISED BIOMECHANICAL SIMULATION OF PEDICLE ASYMMETRY AS A POTENTIAL CAUSE OF ADOLESCENT IDIOPATHIC SCOLIOSIS

INTRODUCTION

In recent years, the advent of computerized biomechanical modeling of the spine using the finite element (FE) method has provided a new technique to improve the understanding of scoliosis biomechanics, an area in which there is limited knowledge. FE models of the spine have been used to simulate the effects of brace treatment (Andriacchi et al., 1976; De Georgi et al., 1990; Wynarsky and Schultz, 1991; Aubin et al., 1993; Gignac et al., 1998), to predict the outcome of scoliosis surgery (Stokes and Laible, 1990; Aubin et al., 1995; Poulin et al., 1998), to understand the process of curve progression (Villemure et al., 2002) and most recently, to evaluate different hypotheses for the pathogenesis of adolescent idiopathic scoliosis (AIS) (Villemure et al., 2004). These biomechanical models of the spine have several advantages over clinical studies of AIS patients since there is the potential to alter or measure an unlimited number of variables, to study the early phases of curve development and to determine cause and effect relationships that are often obscured by the late presentation of patients to the scoliosis clinic. With continued refinement and verification, these models may be able to predict accurately the three-dimensional shape of the spine in relation to growth or the application of different treatments. Realizing the potential value of the FE modeling approach, this approach was used in this study to explore one potential cause of AIS.

Since 1909, numerous authors have implicated asymmetric growth at the site of the neurocentral junction (NCJ) as a potential cause of AIS (Nicoladoni, 1909; Michelsson, 1965; Knutsson, 1966; Roaf, 1966; Yamazaki et al., 1998). Asymmetric growth of the NCJ has been thought to cause pedicle asymmetry, which then produces vertebral rotation and the subsequent development of a scoliotic curvature (Figure 9-1) although the precise mechanism by which this occurs still needs to be clarified. Yet, even after numerous clinical studies (Nicoladoni, 1909; Knutsson, 1963; Roaf, 1966;

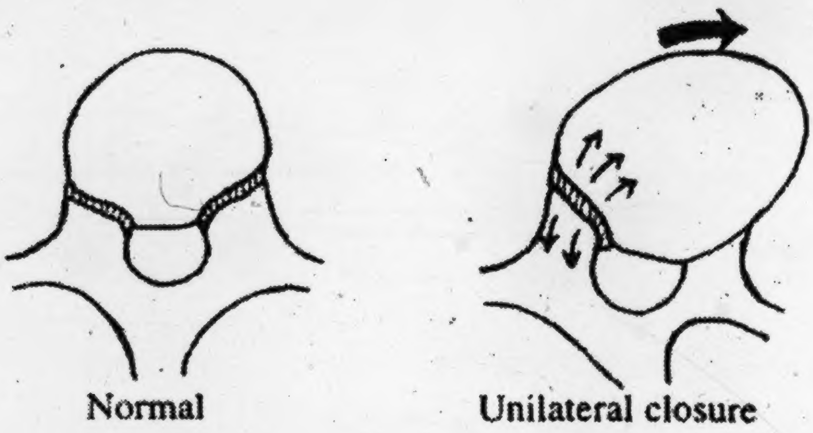

Figure 9-1 (adapted from Yamazaki et al., 1998). Nicoladoni (1909) originally proposed that increased growth of the pedicle on the concave side would exert a torsional force on the vertebral body. This was thought to result in rotation of the vertebral body towards the convexity and an eventual scoliosis, although the link between vertebral rotation and the creation of lateral curvature was not explained.

Taylor, 1983; Vital et al., 1989; Yamazaki et al., 1998; Rajwani et al., 2002) and animal experiments (Ottander et al., 1963; Beguiristain et al., 1980; Coillard et al., 1999), this hypothesis remains to be conclusively proven or disproven. The link between pedicle asymmetry and rotation requires further development to explain why pedicle asymmetry results in rotation rather than the developing vertebra simply adapting to the abnormal forces induced by a longer pedicle. After all, the vertebra is a developing structure (rather than a single unit) that responds to pressure at sites. It is also not understood why the creation of a longer pedicle causes the vertebral body to rotate towards the convexity of the scoliotic curve, as seen empirically in animal models (Beguiristain et al., 1980) instead of causing the posterior elements to displace towards the convexity of the curve. Furthermore, the link between rotation and subsequent lateral curvature requires further explanation. The mechanism by which rotation results in lateral curvature is unclear, although if the vertebral column acts as a fixed rod, then rotation of a portion of this rod might only be accommodated by producing a lateral curvature. Alternatively, it has also been suggested that vertebral rotation results in increased pressure and inhibited growth on the concave side of the superior and inferior physeal growth plates. This would result in the creation of wedged vertebrae and the development of scoliosis (Beguiristain et al., 1980). Once this scoliosis was present, it would likely further accent asymmetric spinal loading and result in a self-perpetuating cycle of curve progression (Stokes, 1996; Villemure et al., 2002). Finally, past models of pedicle asymmetry as a potential cause of AIS have concentrated on pedicle asymmetry being a sole cause of AIS, but have failed to integrate this cause with other potential causes. In fact, it is entirely possible that pedicle asymmetry acts in conjunction with other mechanisms or deformations to result in AIS. For example, pedicle asymmetry might simply be the catalyst that provides the initial curve upon which other factors work to create a more extensive scoliosis.

The objective of this study was to incorporate pedicle growth into an original biomechanical model developed by Villemure et al. (2004) and to investigate whether pedicle asymmetry, either alone or in conjunction with other deformations, would result in scoliosis. To investigate this hypothesis, the FE model that was used (Villemure et al., 2004) incorporated vertebral growth in the longitudinal direction, growth of the pedicle in length and growth modulation. Growth modulation was based on the Heuter-Volkman principle which states that increased pressure on growth plates retards growth (Heuter) and reduced pressure on the growth plates accelerates growth (Volkmann) (Arkin and Katz, 1956). In addition to evaluating the final spinal configuration, vertebral and spinal parameters such as Cobb angle, vertebral rotation and vertebral wedging were evaluated serially to characterize any scoliosis that developed.

MATERIALS AND METHODS

Finite Element Model of the Thoracic and Lumbar Spine

The reference spinal configuration for the FE model used in this study was obtained from a non-pathologic female subject (approximated mass = 45 kg) without scoliosis. The measured lateral curvature in this subject was minimal (Figure 9-2), with a Cobb angle of 0.3° between T6-T9. In the sagittal plane (Figure 9-2), the thoracic kyphosis (34° between T4-T11) appeared normal (typically 30-35°) with no evidence of the hypokyphosis often noted in AIS patients after diagnosis (Lovell and Winter, 2001). Individual vertebrae did not show any features of AIS vertebral morphology, with minimal wedging (T8 = 1.6°) and vertebral rotation values below 5° for the thoracolumbar vertebrae.

Applying a multiview radiographic technique (Dansereau et al., 1990; Villemure et al., 2002) to the reference subject, calibrated PA (acquired at 0° and 20° to the plane of the patient) and lateral radiographs were obtained. A personalized geometric model (Figure 9-3) was acquired from three-dimensional reconstruction of the vertebrae and the application of a direct linear transformation algorithm (Dansereau et al., 1990). Starting with this geometric model, an atlas of meshed geometric vertebrae acquired from previous work (Aubin et al., 1995) was deformed to fit the reconstructed points from the reference subject to create a surface model. Using this surface model, an FE model was generated by computer.

The detailed aspects of the FE model used are outlined in Villemure et al. (2004) although the major aspects of the model have been included in this paper (Figure 9-4). In this FE model, each vertebral body (26 elements total) was represented by 10 three-dimensional beam elements oriented longitudinally, which were connected by a rigid

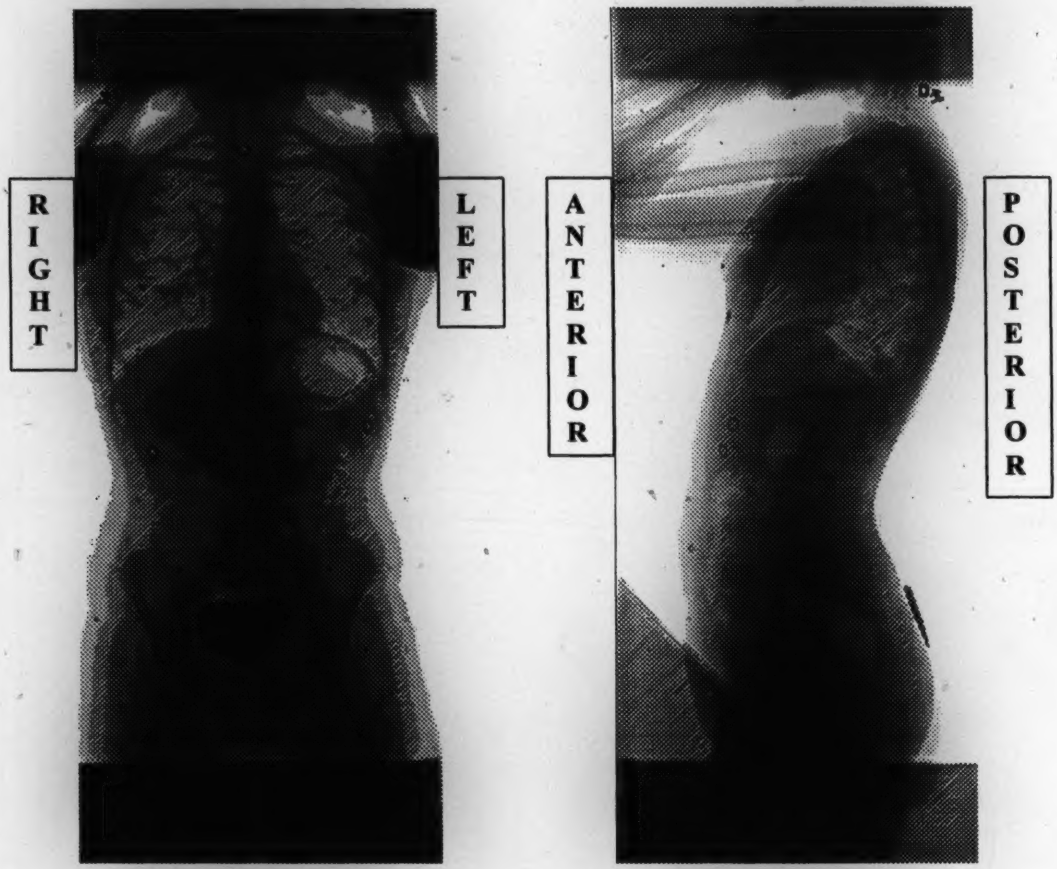

Figure 9-2. Left: PA radiograph obtained from the female subject used for the reference spinal configuration clearly shows the lack of a scoliosis (Cobb angle = 0.3° between T6-T9). **Right**: Lateral radiograph shows normal physiologic curves in the sagittal plane, with a normal thoracic kyphosis and a normal lumbar lordosis.

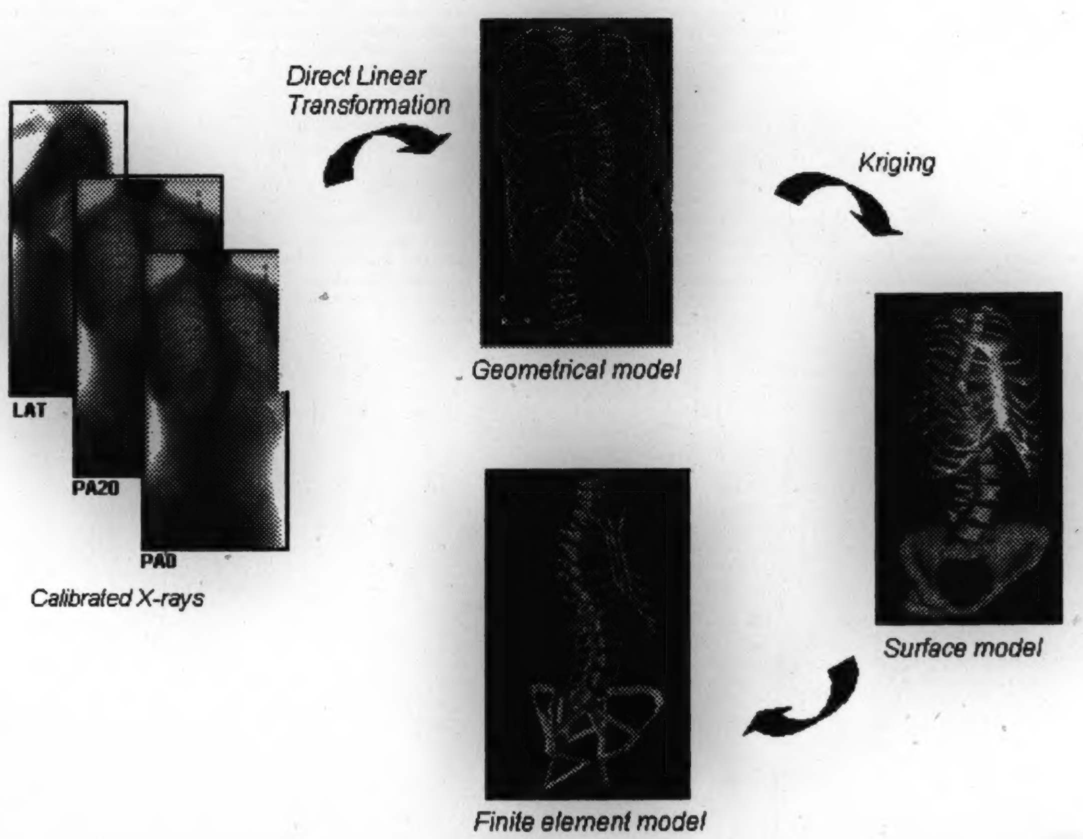
LAT
PA20
PA0
Calibrated X-rays
Direct Linear Transformation
Geometrical model
Kriging
Surface model
Finite element model

Figure 9-3. Starting with the three calibrated X-ray views of the reference subject, a geometrical model was acquired by three-dimensional reconstruction of the vertebrae and the application of a direct linear transformation algorithm (Dansereau et al., 1990). Using kriging analysis, an atlas of meshed geometric vertebrae acquired from previous work (Aubin et al., 1995) was fit to the reconstructed points of the geometric model to create a surface model. Using the surface model, an FE model was generated by computer.

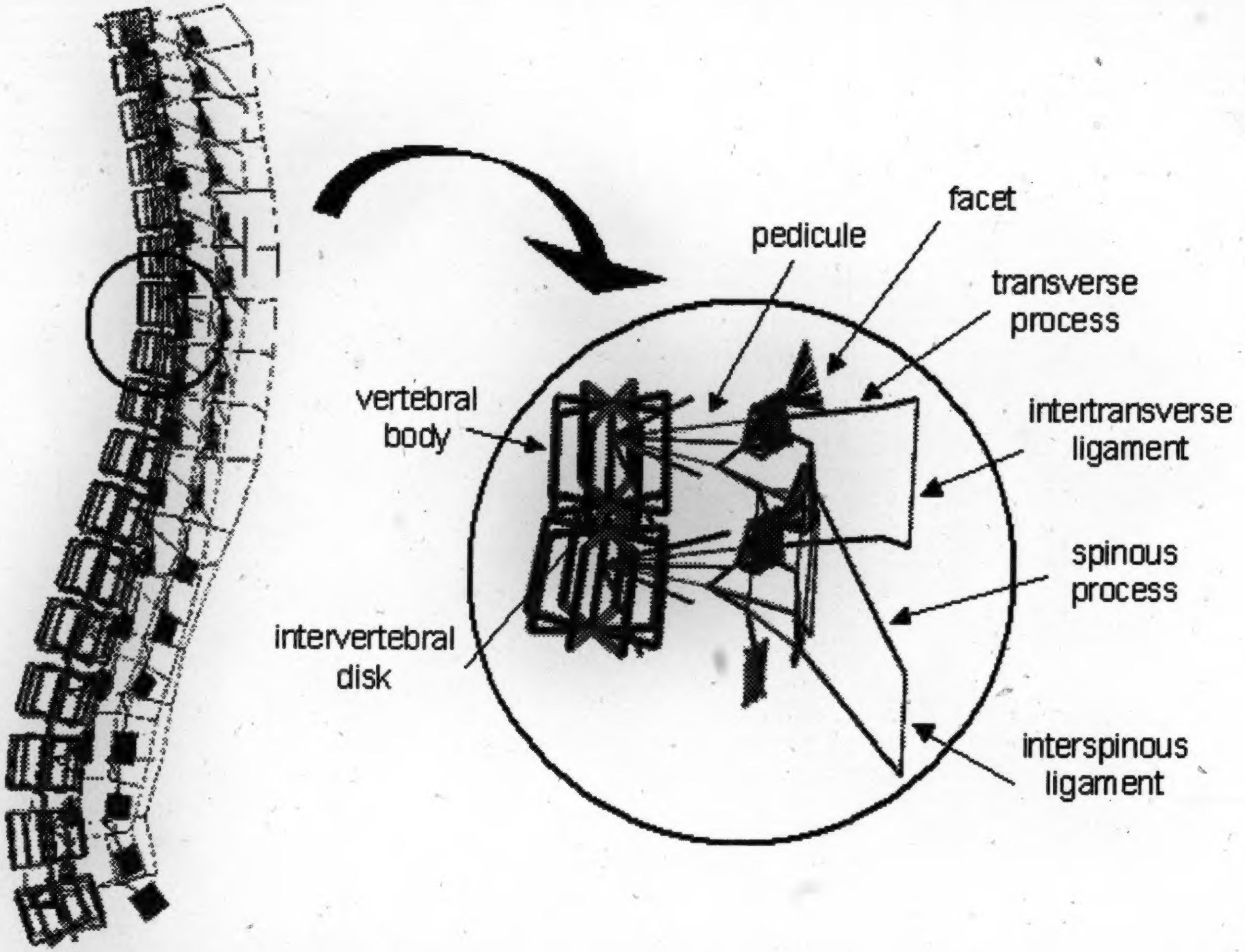
facet
pedicule
transverse process
vertebral body
intertransverse ligament
spinous process
intervertebral disk
interspinous ligament

Figure 9-4 (adapted from Villemure et al., 2004). A schematic representation of the FE model used in this study. The representation of the intervertebral disc has not been shown for the sake of clarity.

crossbar system of 16 beam elements. Since many of the beam elements were concentrated at the edges of the vertebra, this allowed a representative distribution of the internal forces within the vertebral body as well as a means to represent vertebral wedging. The pedicles on each side of the vertebra were represented by single beam elements and were connected to one of the outer beams in the vertebral body. Finally, the posterior arches and the transverse processes were also modeled with the use of beam elements, with the facets being modeled in more detail with point-to-surface contact, shell and spring elements. The intervertebral disc was represented by a beam element and the intervertebral ligaments were represented by three-dimensional spring elements. Muscles were not included in the model due to the difficulty of modeling and because it was not thought, based on previous studies, that the inclusion of muscles would impact experimental results (Villemure et al., 2002; 2004). To ensure that the different anatomic structures of the vertebra were characterized with the appropriate mechanical properties, such as Young's modulus of stiffness and Poisson's ratio, these properties were based on past experimental studies with cadaveric specimens (Aubin et al., 1995; Descrimes et al., 1995). The entire FE model was built and later manipulated using the ANSYS 7.0 finite element package (ANSYS Inc., Canonsburg, Pennsylvania, U.S.A.). Throughout this study, a consistent global axis system was used and defined by three perpendicular axes that corresponded to the anterior (X), left (Y) and upward (Z) directions. This was different from the local axes for each vertebra. The local x-axis was defined as the direction perpendicular to the superior and inferior physeal growth plates while the y and the z axes were defined as the directions parallel to the growth plates.

Biomechanical Modeling of Bone Growth Modulation

Since the principles of the biomechanical model used in this study have been presented in detail in previous work (Villemure et al., 2002), only a summary has been presented in this paper. In this model, the calculated displacement in a particular plane depended on both bone growth and growth modulation, as shown below:

Displacement = Baseline growth + Growth modulation

$$\delta\varepsilon = \delta G + \delta G\beta\sigma$$

As seen by the equation (Stokes and Laible, 1990), growth modulation incorporated a functional biomechanical stimulus which represented the internal stresses σ and a parameter β which represented the sensitivity of the bone tissue to the stimulus. In this study, longitudinal baseline growth was included for the vertebral body and growth in length was included for the pedicle. From in-house testing, it was determined that there was no difference in the vertebral parameters noted regardless of whether pedicle growth was modeled at the anterior aspect of the beam or the posterior aspect of the beam. Since the Villemure et al. (2004) model applied constraints to displacement of the anterior surface of the vertebral body, the additional growth of the pedicle was modeled from the posterior surface of the beam representing the pedicle.

Growth modulation was included in the same directions as growth. Growth and growth modulation were not considered for the posterior parts of the vertebra since these parts are thought to stop growing before the end of the first decade (Vital et al., 1989; Yamazaki et al., 1998) whereas the vertebral body has been shown to continue growing throughout adolescence (Weinstein et al., 1994). Although growth modulation of the disc was incorporated, intervertebral disc growth was not included since prior studies (Villemure et al., 2002; 2004) had shown that mean growth of the disc was considered negligible compared to vertebral body growth. Growth of the ligaments was implicitly included since the insertion sites changed during spinal growth.

For each simulation, vertebral growth and growth modulation were considered separately in a stepwise iterative procedure. Each iteration of the simulation typically represented a one month time period, with each simulation running for 24 months. Growth was considered first at each iteration and after application of the baseline growth increment, the geometry of the vertebrae was updated with relocation of the model nodes. The monthly values for the growth in height of the vertebral body were adapted from the experimentally determined values of 0.8 mm/year for the thoracic vertebrae and 1.1 mm/year for the lumbar vertebrae (Taylor, 1975; Dimeglio and Bonnel, 1990). The monthly growth rate for the length of the pedicle was adapted from the experimentally derived value of 0.1 mm/year (Dimeglio and Bonnel, 1990). Next, growth modulation forces were applied and the geometry was updated based on these forces. The cycle was repeated 24 times to represent the number of monthly growth increments used in this study.

The loading forces on the spine were based on the assumption that any geometrical shift from the initial profile changed the relative distribution of loads among vertebral components, which in turn produced growth modulation. The gravity loads associated with each vertebral level were based on measurements taken by Schultz et al. (1982) and remained constant for all iterations of each simulation. These loads were applied to the center of the superior vertebral endplate along the global Z-axis, with the points of application moving laterally depending on the position of the superior vertebral endplates. These loads produced internal stress states σ and σ' when applied to the reference configuration and on the altered scoliotic profile. Growth modulation was generated using the differential stress state $\Delta\sigma=\sigma'-\sigma$ with respect to the initial reference configuration (Villemure et al., 2004).

For each simulation, all degrees of freedom were fixed at L5 to model the tethering effects of the pelvis. Only lateral flexion, forward flexion and vertical translation were permitted at T1.

The representations of growth modulation were thought to accurately represent the effects of the Heuter-Volkmann principle along the bone x-axis (local coordinate system) with forces resulting in reduced and accelerated growth in regions of increased and decreased pressure (Villemure et al., 2002; Villemure et al., 2004). Based on in-house simulations, the effects of growth modulation exerted in parallel directions to the endplate were found to be negligible (Villemure et al., 2004).

SIMULATIONS

In a previous study conducted by Villemure et al. (2004), different pathogenesis hypotheses were evaluated including the following:

a) 3 mm linear shifts (anteriorly) in the frontal plane
b) 3 mm linear shifts (to the right) in the sagittal plane (equivalent to a Cobb angle of 2°)
c) 2° rotational shift in the transverse plane

Villemure et al. (2004) performed all of these simulations at a single vertebral level (T8), which was assumed to be the apical vertebra of the future scoliotic curve. In this study, the only modification made to the Villemure et al. (2004) model was the addition of pedicle growth. After modification of the original model (Villemure et al., 2004), simulations of pedicle growth asymmetry alone and pedicle growth asymmetry in combination with the above scenarios were performed. Other than the addition of pedicle asymmetry, the original scenarios used by Villemure et al. (2004) were not modified except for the extent of the rotation used in the rotational shift scenario. This was changed to a five degree rotational shift since five degrees of vertebral rotation is generally assumed to represent a significant deviation from normal (Russell et al., 1990).

In general, two different types of pedicle asymmetry were modeled. Asymmetry of the pedicle growth rates (i.e. one pedicle growing at the normal growth rate while the other failed to grow) was modeled to assess any effects that occurred while asymmetry developed. In addition, asymmetry of pedicle geometry (i.e. one pedicle having a 0.5 cm, 1.0 cm or 1.5 cm greater length) was also modeled to investigate the effects of pedicle asymmetry after asymmetry had already manifested. The 1.5 cm difference in length between the two pedicles was estimated to represent the maximal potential degree of pedicle asymmetry since this represented approximately 10 times the asymmetry noted by Parent et al. (2004) in their morphometric analysis of vertebrae from AIS patients. In modeling asymmetry of pedicle geometry, both constant asymmetry (T6-T10 presenting with a 1.5 cm pedicle length asymmetry) and graded asymmetry (T6 and T10 presenting with a 0.5 cm pedicle length asymmetry, T7 and T9 presenting with a 1.0 cm pedicle length asymmetry and T8 presenting with 1.5 cm pedicle length asymmetry) were modeled. The graded asymmetry scenario was modeled to determine if the extent of pedicle length asymmetry corresponded to the location of the apical vertebra in any subsequent scoliosis created. A summary of all simulations performed is included in Tables 9-1, 9-2 and 9-3.

For each simulation, the Cobb angle in the frontal plane was assessed at each iteration to characterize the extent of spinal curvature created. To eliminate intraobserver and interobserver variation, Cobb angle was assessed with the use of a computer program that calculated the position of the vertebrae, automated the selection of the superior and

Table 9-1. Results from simulations involving asymmetry of pedicle geometry

1.5 cm longer pedicle at T8	**Month**	**Longer pedicle on the left**	**Longer pedicle on the right**
	1	**Cobb: -5.2° (T4-T9)** Rotation T8: -0.9°, Wedging T8: 1.6°	**Cobb: 4.2° (T5-T9)** Rotation T8: -0.9°, Wedging T8: 1.6°
	12	**Cobb: -5.0° (T4-T9)** Rotation T8: -0.9°, Wedging T8: 1.6°	**Cobb: 4.1° (T5-T9)** Rotation T8: -0.9°, Wedging T8: 1.6°
	24	**Cobb: -4.8° (T4-T9)** Rotation T8: -0.9°, Wedging T8: 1.6°	**Cobb: 3.9° (T5-T9)** Rotation T8: -0.9°, Wedging T8: 1.6°
1.5 cm longer pedicle from T6-T10 (constant asymmetry from T6-T10)	**Month**	**Longer pedicle on the left**	**Longer pedicle on the right**
	1	**Cobb: -14.7° (T4-T9)** Secondary: 14.0° (T1-T4), 5.5° (T9-L1) Rotation T8: -0.9°, Wedging T8: 1.6°	**Cobb: 13.8 (T4-T9)** Secondary: -21.1° (T1-T4), -9.7° (T9-L1) Rotation T8: -0.9°, Wedging T8: 1.6°
	12	**Cobb: -14.2° (T4-T9)** Secondary: 13.2° (T1-T4), 5.3° (T9-L1) Rotation T8: -0.9°, Wedging T8: 1.6°	**Cobb: 13.3° (T4-T9)** Secondary: -20.7° (T1-T4), -9.4° (T9-L1) Rotation T8: -0.9°, Wedging T8: 1.6°
	24	**Cobb: -13.8° (T4-T9)** Secondary: 12.5° (T1-T4), 5.2° (T9-L1) Rotation T8: -0.9°, Wedging T8: 1.6°	**Cobb: 12.8° (T4-T9)** Secondary: -20.2° (T1-T4), -9.1° (T9-L1) Rotation T8: -0.9°, Wedging T8: 1.6°
1.5 cm longer pedicle at T8, 1.0 cm longer pedicles at T7 and T9, 0.5 cm longer pedicles at T6 and T10 (graded asymmetry from T6-T10)	**Month**	**Longer pedicle on the left**	**Longer pedicle on the right**
	1	**Cobb: -10.8° (T4-T9)** Secondary: 14.0° (T1-T4), 5.5° (T9-L1) Rotation T8: -0.9°, Wedging T8: 1.6°	**Cobb: 9.6 (T4-T9)** Secondary: -17.3° (T1-T4), -7.8° (T9-L1) Rotation T8: -0.9°, Wedging T8: 1.6°
	12	**Cobb: -10.4° (T4-T9)** Secondary: 13.2° (T1-T4), 5.3° (T9-L1) Rotation T8: -0.9°, Wedging T8: 1.6°	**Cobb: 9.2 (T4-T9)** Secondary: -16.9° (T1-T4), -7.6° (T9-L1) Rotation T8: -0.9°, Wedging T8: 1.6°
	24	**Cobb: -10.0° (T4-T9)** Secondary: 12.5° (T1-T4), 5.2° (T9-L1) Rotation T8: -0.9°, Wedging T8: 1.6°	**Cobb: 8.9 (T4-T9)** Secondary: -16.0° (T1-T5), -7.4° (T9-L1) Rotation T8: -0.9°, Wedging T8: 1.6°

Table 9-2. Results from simulations involving asymmetry of pedicle geometry in combination with scenarios tested by Villemure et al. (2004)

3 mm anterior displacement of T8 with symmetric and asymmetric pedicle geometry	Month	Symmetric pedicle growth	Longer pedicle on the left	Longer pedicle on the right
	1	**Cobb: 0.3° (T6-T8)** Rotation T8: -0.9°, Wedging T8: 1.6°	**Cobb: -5.2° (T4-T9)** Secondary: 4.5° (T1-T4), 1.0° (T9-T12) Rotation T8: -0.9°, Wedging T8: 1.6°	**Cobb: 4.2° (T5-T9)** Secondary: -10.1° (T1-T5), -5.1° (T9-L2) Rotation T8: -0.9°, Wedging T8: 1.6°
	12	**Cobb: -3.4° (T7-L4)** Rotation T8: -0.8°, Wedging T8: 1.8°	**Cobb: -5.6° (T4-T9)** Secondary: 4.0° (T1-T4), 0.7° (T9-T12) Rotation T8: -0.7°, Wedging T8: 1.8°	**Cobb: 3.6° (T5-T9)** Secondary: -10.1° (T1-T5), -5.2° (T9-L2) Rotation T8: -0.7°, Wedging T8: 1.8°
	24	**Cobb: -10.3° (T1-L2)** Rotation T8: -0.4°, Wedging T8: 2.7°	**Cobb: -10.3° (T3-L3)** Secondary: 3.7° (T1-T3) Rotation T8: 0°, Wedging T8: 2.8°	**Cobb: 1.3° (T5-T8)** Secondary: -10.0° (T1-T5), -6.3° (T8-L1) Rotation T8: 0.1°, Wedging T8: 2.7°
3 mm displacement of T8 to the right with symmetric and asymmetric pedicle geometry	Month	Symmetric pedicle growth	Longer pedicle on the left	Longer pedicle on the right
	1	**Cobb: 2.6° (T5-T10)** Rotation T8: -0.9°, Wedging T8: 1.5°	**Cobb: -2.8° (T4-T8)** Secondary: 5.6° (T1-T4), 1.8° (T8-T11) Rotation T8: -0.9°, Wedging T8: 1.5°	**Cobb: 6.8° (T5-T10)** Secondary: -8.8° (T1-T5), -6.5° (T10-L2) Rotation T8: -0.9°, Wedging T8: 1.5°
	12	**Cobb: 9.0° (T3-T10)** Rotation T8: -1.7°, Wedging T8: 0.3°	**Cobb: 5.9° (T5-T11)** Secondary: 5.9° (T1-T5), -6.3° (T11-L3) Rotation T8: -1.9°, Wedging T8: 0.4°	**Cobb: 12.5° (T4-T10)** Secondary: -7.5° (T1-T4), -7.4° (T10-L3) Rotation T8: -2.0°, Wedging T8: 0.4°
	24	**Cobb: 35.4° (T2-T11)** Rotation T8: -5.4°, Wedging T8: 7.7°	**Cobb: 40.3° (T1-T12)** Secondary: -14.6° (T12-L4) Rotation T8: -7.7°, Wedging T8: 7.6°	**Cobb: 37.7° (T3-T11)** Secondary: -4.5° (T1-T3), -14.3° (T11-L4) Rotation T8: -7.5°, Wedging T8: 7.6°
Rotation of T8 by 5° towards the right with symmetric and asymmetric pedicle geometry	Month	Symmetric pedicle growth	Longer pedicle on the left	Longer pedicle on the right
	1	**Cobb: -7.8° (T1-L4)** Rotation T8: -5.9°, Wedging T8: 1.6°	**Cobb: -8.4° (T4-T9)** Secondary: 5.2° (T1-T4), 2.0° (T9-L1) Rotation T8: -5.9°, Wedging T8: 1.6°	**Cobb: 1.6° (T5-T9)** Secondary: -10.0° (T1-T5), -3.5° (T9-L1) Rotation T8: -5.9°, Wedging T8: 1.6°
	12	**Cobb: -10.7° (T1-T12)** Rotation T8: -5.7°, Wedging T8: 2.6°	**Cobb: -11.2° (T3-T10)** Secondary: 4.9° (T1-T3), 1.5° (T10-L1) Rotation T8: -5.1°, Wedging T8: 2.5°	**Cobb: -4.4° (T7-L1)** Secondary: -10.5° (T1-T6), 1.5° (L2-L4) Rotation T8: -5.1°, Wedging T8: 2.5°
	24	**Cobb: -33.2° (T1-T12)** Rotation T8: -3.5°, Wedging T8: 7.3°	**Cobb: -28.8° (T3-T11)** Secondary: 3.9° (T1-T3), 5.6° (T11-L5) Rotation T8: -2.3°, Wedging T8: 6.7°	**Cobb: -33.7° (T1-T12)** Secondary: 7.0° (T12-L4) Rotation T8: -2.0°, Wedging T8: 6.8°

Table 9-3. Results from simulations involving asymmetry of pedicle growth rates in combination with scenarios tested by Villemure et al. (2004)

3 mm anterior displacement of T8 with symmetric and asymmetric pedicle growth rates	**Month**	**Symmetric pedicle growth**	**Left pedicle growth only**	**Right pedicle growth only**
	1	**Cobb: 0.3° (T6-T8)** Secondary: -3.6° (T1-T6), -3.0° (T8-L4) Rotation T8: -0.9°, Wedging T8: 1.6°	**Cobb: 0.2° (T6-T8)** Secondary: -3.6° (T1-T6), -3.0° (T8-L4) Rotation T8: -0.9°, Wedging T8: 1.6°	**Cobb: 0.3° (T6-T8)** Secondary: -3.6° (T1-T6), -3.1° (T8-L4) Rotation T8: -0.9°, Wedging T8: 1.6°
	12	**Cobb: -3.4° (T7-L4)** Secondary: -4.0° (T1-T7) Rotation T8: -0.8°, Wedging T8: 1.8°	**Cobb: -7.5° (T1-L2)** Rotation T8: -0.8°, Wedging T8: 1.8°	**Cobb: 0.0° (T6-T8)** Secondary: -4.0° (T1-T6), -3.4° (T8-L4) Rotation T8: -0.8°, Wedging T8: 1.8°
	24	**Cobb: -10.3° (T1-L2)** Rotation T8: -0.4°, Wedging T8: 2.7°	**Cobb: -11.4° (T1-L1)** Rotation T8: -0.2°, Wedging T8: 3.0°	**Cobb: -10° (T1-L2)** Rotation T8: -0.3°, Wedging T8: 2.7°
3 mm displacement of T8 to the right with symmetric and asymmetric pedicle growth rates	**Month**	**Symmetric pedicle growth**	**Left pedicle growth only**	**Right pedicle growth only**
	1	**Cobb: 2.6° (T5-T10)** Secondary: -2.1° (T1-T5), -4.5° (T10-L3) Rotation T8: -0.9°, Wedging T8: 1.5°	**Cobb: 2.6° (T5-T10)** Secondary: -2.0° (T1-T5), -4.5° (T10-L3) Rotation T8: -0.9°, Wedging T8: 1.5°	**Cobb: 2.6° (T5-T10)** Secondary: -2.0° (T1-T5), -4.5° (T10-L3) Rotation T8: -0.9°, Wedging T8: 1.5°
	12	**Cobb: 9.0° (T3-T10)** Secondary: -1.4° (T1-T3), -6.4° (T10-L3) Rotation T8: -1.7°, Wedging T8: 0.3°	**Cobb: 9.1° (T3-T10)** Secondary: -1.1° (T1-T3), -6.4° (T10-L3) Rotation T8: -1.7°, Wedging T8: 0.4°	**Cobb: 8.9° (T3-T10)** Secondary: -1.2° (T1-T3), -6.4° (T10-L3) Rotation T8: -1.7°, Wedging T8: 0.4°
	24	**Cobb: 35.4° (T2-T11)** Secondary: -1.1 (T1-T2), -14.7° (T11-L5) Rotation T8: -5.4°, Wedging T8: 7.7°	**Cobb: 37.6° (T1-T11)** Secondary: -14.8° (T11-L5) Rotation T8: -5.4°, Wedging T8: 7.5°	**Cobb: 35.2° (T1-T11)** Secondary: -14.4° (T11-L5) Rotation T8: -5.7°, Wedging T8: 7.3°
Rotation of T8 by 5° towards the right with symmetric and asymmetric pedicle growth rates	**Month**	**Symmetric pedicle growth**	**Left pedicle growth only**	**Right pedicle growth only**
	1	**Cobb: -7.8° (T1-L4)** Rotation T8: -5.9°, Wedging T8: 1.6°	**Cobb: -7.8° (T1-L4)** Rotation T8: -5.9°, Wedging T8: 1.6°	**Cobb: -7.8° (T1-L4)** Rotation T8: -5.9°, Wedging T8: 1.6°
	12	**Cobb: -10.7° (T1-T12)** Secondary: 0.4° (T12-L2) Rotation T8: -5.7°, Wedging T8: 2.6°	**Cobb: -10.1° (T1-T12)** Secondary: 0.3° (T12-L2) Rotation T8: -5.6°, Wedging T8: 2.6°	**Cobb: -10.3° (T1-T12)** Secondary: 0.3° (T12-L2) Rotation T8: -5.6°, Wedging T8: 2.6°
	24	**Cobb: -33.2° (T1-T12)** Secondary: 6.7° (T12-L4) Rotation T8: -3.5°, Wedging T8: 7.3°	**Cobb: -28.5° (T1-T11)** Secondary: 5.1° (T11-L5) Rotation T8: -3.8°, Wedging T8: 7.3°	**Cobb: -31.2° (T1-T11)** Secondary: 5.6° Rotation T8: -3.6°, Wedging T8: 7.3°

inferior vertebrae in the curve and measured the Cobb angle automatically. Based on standard conventions (Lovell and Winter, 2001), values greater than 10 degrees Cobb were considered to represent lateral curvature that could be characterized as scoliosis. Curvatures that arose outside of the T6-T10 region were termed secondary, since they arose secondary to the asymmetry or deformation in the T6-T10 region. Local descriptors (axial vertebral rotation, maximum three-dimensional wedging angle) were assessed at the 8th thoracic vertebra, which was typically the most deformed vertebra (Villemure et al., 2004). Vertebral rotation (θ_z) was calculated by computer (Stokes et al., 1986; Villemure et al., 2004) with a positive value representing counterclockwise rotation as seen from above and a negative value signifying clockwise rotation.

RESULTS

For each tested scenario, the Cobb angle, vertebral rotation (θ_z) and wedging angle (ω) are shown after 1, 12 and 24 months of the simulation in Tables 9-1, 9-2 and 9-3. In some cases, when Cobb angles were measured by computer, there were slight variations in the vertebrae identified as the superior and inferior extents of the curve just as there would be if Cobb angles were measured clinically. For this reason, the superior and inferior vertebrae of the curve are indicated in brackets. Unfortunately, the computer program used to measure Cobb angles was not valid for all of the vertebral deformities modeled. In measuring the Cobb angles from the simulations of geometric pedicle asymmetry, the vertebrae with geometric pedicle length asymmetry exhibited a far greater extent of deformity than normal vertebrae. Cobb angle values were greatly exaggerated since the automated measurement procedure used the vertebral centroid to calculate the position of the vertebra. This meant that the extreme changes in vertebral morphology (Table 9-4) were represented as a shift in position away from the midline of the vertebral column.

The simulation of the same extent and type of deformity on the right side of the vertebra in one simulation and on the left side of the vertebra in another simulation produced results that were not identical. This was expected, since the FE model used a reference configuration from a real patient and this real patient, although normal, was expected to have slight variations in vertebral symmetry at the different vertebral levels.

Asymmetry of Pedicle Geometry (Table 9-1, Table 9-4)

For the scenarios involving asymmetric pedicle growth without the addition of other deformations, only asymmetries of pedicle geometry were tested. From preliminary trials, asymmetries of pedicle growth rates without the addition of other deformations did not generate significant growth modulation forces. In addition, the asymmetries of pedicle geometry were of a far greater magnitude (1.5 cm) than any asymmetry created by a discrepancy in pedicle growth rates (maximum asymmetry of 0.2 mm after two years). For this reason, it was assumed that the potential changes in vertebral and spinal morphology due to asymmetries of pedicle geometry would also be of a far greater magnitude.

Among the three types of scenarios tested (longer pedicle at T8, longer pedicles from T6-T10 and graded differences in pedicle length from T6-T10), the scenarios involving constant pedicle asymmetry from T6-T10 and graded pedicle asymmetry from T6-T10 produced measured Cobb angles greater than 10 degrees (Table 9-1). However, this was not a reflection of a scoliotic lateral curvature (Table 9-4) and instead reflected the fact that the measurement program used to assess Cobb angle interpreted the grossly altered vertebral morphologies to represent a deviation of the vertebral position from the midline. The rotation and wedging created at the levels where pedicle geometry had been altered were not changed from the initial rotation (-0.9°) and initial wedging (1.6°). This showed that pedicle asymmetry did not produce any rotation or wedging in the thoracolumbar vertebrae.

Pedicle Geometry Asymmetry and Growth Asymmetry in Combination With Other Deformities (Table 9-2, Table 9-3, Table 9-5)

The addition of pedicle geometry asymmetry and pedicle growth asymmetry to the scenarios that involved anterior, lateral and rotational displacement of T8 did not appear to create significant additional vertebral or spinal deformities beyond those created by the given displacements (Table 9-2, Table 9-3).

Among the displacements tested, anterior, lateral and rotational displacements all created lateral curvatures of greater than 10 degrees. However, the lateral curvatures

Table 9-4. Configurations from simulations involving constant and graded pedicle asymmetry from T6-T10 at 1, 12 and 24 months of simulation

Graded pedicle asymmetry from T6-T10 (1 month) 	Graded pedicle asymmetry from T6-T10 (12 months) 	Graded pedicle asymmetry from T6-T10 (24 months)
Constant pedicle asymmetry from T6-T10 (1 month) 	Constant pedicle asymmetry from T6-T10 (12 months) 	Constant pedicle asymmetry from T6-T10 (24 months)

Table 9-4. In all cases, the vertebral columns are viewed from the posterior aspect as this best visualizes the pedicle asymmetry being modeled. In the graded pedicle asymmetry scenario, the T6 and T10 vertebrae are 0.5 cm longer on the left, the T7 and T9 vertebrae are 1.0 cm longer on the left and the T8 vertebra is 1.5 cm longer on the left. In the constant pedicle asymmetry scenario, the T6-T10 vertebrae are all 1.5 cm longer on the left. Examination of the above images shows no lateral curvature, although the gross degree of deformity present in the T6-T10 vertebra prevented the accurate computerized determination of Cobb angle.

Table 9-5. Configurations from simulations involving 3 mm displacement of T8 anteriorly, 3 mm displacement of T8 to the right and rotation of T8 by 5° all with symmetric pedicle growth

3 mm anterior displacement of T8 (1 month) 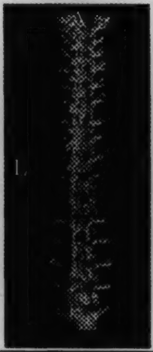	3 mm anterior displacement of T8 (12 months) 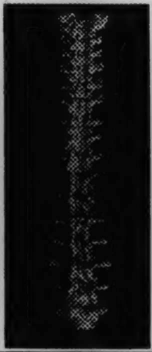	3 mm anterior displacement of T8 (24 months) 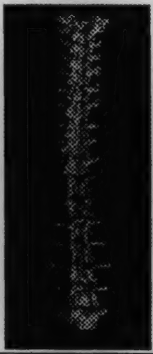
3 mm displacement of T8 to the right (1 month) 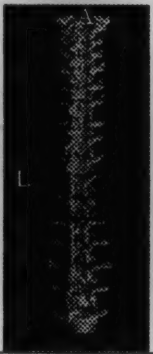	3 mm displacement of T8 to the right (12 months) 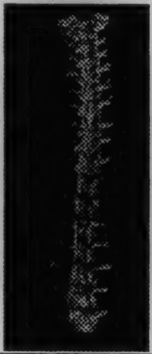	3 mm displacement of T8 to the right (24 months) 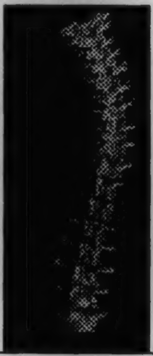
5° rotation of T8 to the right (1 month) 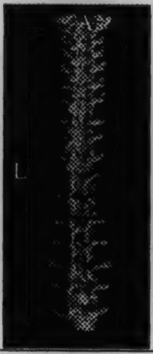	5° rotation of T8 to the right (12 months) 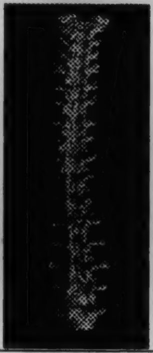	5° rotation of T8 to the right (24 months) 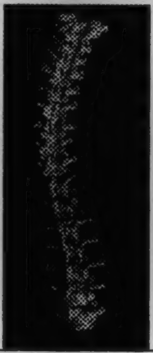

Table 9-5. Vertebral columns are shown from the posterior aspect. The lateral curvatures created by lateral displacement to the right and rotational displacement appeared to be the most significant and were accompanied by significant vertebral rotation and vertebral wedging.

created by lateral displacement to the right and rotational displacement were the most significant and were accompanied by significant (greater than five degree) rotation and wedging at T8. The progression of the Cobb angle, wedging and rotation occurred in a non-linear manner, with the change in all three parameters being much greater from 12-24 months than from 0-12 months. Although it was entirely expected that displacement to the right would create a scoliosis to the right (positive Cobb angle), it was unexpected that rotation towards the right would create a scoliosis to the left (negative Cobb angle). Typically, rotation of the vertebral body occurs towards the convexity of the scoliosis in AIS (Keim, 1979), whereas in this simulation the opposite was observed. The scenario involving lateral displacement to the right produced the pattern of curvature most typically seen in AIS since a primary thoracic curve and a secondary left lumbar curve were created.

DISCUSSION

The main finding in this study was that differences in pedicle length, modeled as either a graded asymmetry or a constant geometric asymmetry, were not sufficient for the creation of scoliosis (Table 9-1, 9-4). Although Cobb angles greater than 10 degrees were measured for several simulations involving asymmetric pedicle geometry (Table 9-1), these measured values were not valid since the computerized method used to measure Cobb angle misinterpreted the large extent of vertebral deformity as a shift in position of the vertebrae. In fact, the failure to produce scoliosis was clearly seen on visualization of the final vertebral configurations (Table 9-4) and was also evident in the lack of significant vertebral rotation or vertebral wedging. This would suggest that the computerized method of Cobb angle assessment used in this study was not valid for gross levels of vertebral deformation. Based on these results, it appeared that the forces created by geometric pedicle asymmetry did not exert enough torque on the vertebral body to cause any degree of rotation. This was surprising, since the extent of pedicle asymmetry modeled far exceeded the normal amount of pedicle asymmetry noted in AIS patients (Parent et al., 2004). The failure of pedicle asymmetry to produce rotation in this model conflicts with the suggestion by numerous authors, based on findings from animal models (Beguiristain et al., 1980) as well as anatomic studies of normal (Taylor, 1983; Sevastik et al., 1995) and scoliotic vertebrae (Nicoladoni, 1909; Knutsson, 1963; Taylor, 1983; Vital et al., 1989) that a longer pedicle typically causes vertebral body rotation towards the side of the shorter pedicle. The discrepancy between the simulation results and the results of the porcine model (Beguiristain et al., 1980) requires further investigation. However, it is difficult to speculate on the significance of the difference between the simulation results and the findings from anatomic studies, since all of these anatomic studies were based on cross-sectional measurement of morphologic parameters from normal vertebrae or vertebrae with well-established scoliosis. In these anatomic studies, despite the finding that pedicle asymmetry and rotation presented together in a characteristic manner, it could not actually be inferred whether pedicle asymmetry was the cause or the result of the vertebral rotation. Nonetheless, on the basis of this study, pedicle asymmetry did not appear to be a sole initiating factor for scoliosis.

It would be entirely plausible that although pedicle asymmetry was not an independent cause of scoliosis, it could result in the induction of complex three-dimensional deformities which would then be amplified in combination with other processes. For this reason, the effects of pedicle asymmetry were also assessed in combination with other deformations (Table 9-2, Table 9-3, Table 9-5). However, geometric or growth asymmetry of the pedicle was not found to increase the degree of scoliosis, rotation or wedging created by anterior, lateral or rotational displacement of T8. This suggested that pedicle asymmetry did not act in conjunction with other deformations to cause scoliosis.

In the past, the link between vertebral rotation and lateral curvature of the vertebral column has been questioned. In this study, the rotation of the T8 vertebra by 5° towards the right (with symmetric pedicle growth) resulted in a scoliosis of greater than 30 degrees (Table 9-3, Table 9-5) with significant vertebral rotation and wedging. The apex of this scoliosis was close to T8, agreeing with the general finding that the apical vertebra of a scoliotic curve is maximally rotated (Lovell and Winter, 2001). Interestingly, vertebral rotation, wedging and lateral curvature increased in a non-linear manner over the course of the simulation cycles. This would agree with other work that has suggested that once scoliosis is present, it causes further asymmetric spinal loading and results in a self-perpetuating cycle of curve progression (Stokes, 1996; Villemure et al., 2002). Based on the findings in this study, rotation was a sufficient initiating factor for the production of scoliosis. This is a significant finding, since numerous studies in the past have disputed whether rotation is a cause or an effect of lateral curvature. The results of this model would suggest that rotation might precede lateral curvature, at least in some cases. In this model, the relationship between rotation and the direction of the lateral curvature was unexpected. A rotational displacement of the vertebral body to the right created a left scoliosis, instead of the expected right scoliosis. This expectation was based on the well-established finding that rotation of the vertebral body in AIS usually occurs towards the convexity of the curve (Keim, 1979). Yet, the failure of this model to correctly predict the direction of lateral curvature caused by a given direction of vertebral rotation is not surprising, as the facet joints in this study were not characterized in enough detail to reflect the complexity of human facet articulations, which restrict motion in certain planes. At this stage, further data on the characterization of facet properties may be required to increase the predictive value of FE models of the spine.

The results of this model, in conjunction with other experimental evidence (Chapter 8) do not support the idea that asymmetric NCJ growth is a potential cause of AIS or at the very least, suggest that aspects of the asymmetric NCJ theory remain to be proved. The current asymmetric NCJ growth theory of AIS is based on three successive steps: NCJ asymmetry is thought to produce pedicle asymmetry, pedicle asymmetry is thought to produce vertebral rotation and vertebral rotation is thought to result in lateral curvature. In addressing the first of the three steps, recent experimental studies involving fluorochrome-based assessment of the NCJ contribution to the pedicle (Chapter 7) and the placement of pedicle screws unilaterally across the NCJ in pigs (Chapter 8) have shown that the contribution of the NCJ to the growth of the pedicle is far less than traditionally thought. In fact, NCJ activity has been shown to decrease over the course of development. This could suggest that the contribution of the NCJ to pedicle length may be minimal in the late stages of NCJ development during adolescence. In evaluating the second step in the theory, this study suggested that pedicle asymmetry was not sufficient to produce vertebral rotation, even when the extent of asymmetry modeled was far beyond the normal pedicle asymmetry seen in a scoliotic patient population. In addressing the last step of the theory, this study supported the idea that vertebral rotation was sufficient to produce lateral curvature. Of course, the cause of this vertebral rotation could be any one of a number of different factors, including pedicle asymmetry, asymmetric muscular action, asymmetric ligamentous forces or abnormal biomechanical forces. Therefore, this finding cannot be inferred to support the asymmetric NCJ growth theory or any other etiologic theory. Based on an overall assessment of the current evidence, it is difficult to support a theory for asymmetric NCJ development as a cause of AIS. However, before the asymmetric NCJ growth theory can be disproven, it will be necessary to account for all of the findings which have been interpreted as supporting evidence, most significantly Beguiristain's (1980) porcine model in which it was found that unilateral placement of pedicle screws across the T6-T10 vertebrae resulted in the production of scoliosis.

In this study, in addition to the production of scoliosis by rotational displacement of the T8 vertebra, the displacement of the T8 vertebra 3 mm to the right also resulted in the production of scoliosis as found by Villemure et al. (2004). The scoliosis produced had numerous characteristics which could be considered representative of AIS: a primary thoracic curvature of greater than 30 degrees, a secondary lumbar curvature, significant vertebral rotation and significant vertebral wedging. These results would appear to show, as suggested by other authors (White, 1971) that the coronal balance of the spine is quite unstable and that when this balance is upset, a self-sustaining progression of deformities is activated (Villemure et al., 2004). Of course, this coronal balance instability could represent another entirely different mechanism of scoliosis production in addition to the mechanism in which scoliosis is produced by vertebral rotation, although correlation with other clinical and animal findings is likely required to develop this theory.

The biomechanical model used in this particular study has been used previously to model the progression of vertebral and scoliotic deformities (Villemure et al., 2002) and to test different pathogenesis hypotheses of scoliosis (Villemure et al., 2004). Yet, like all FE models, this model is continually being refined to improve predictive value and works towards the eventual goal of patient specific prediction and validation. In testing hypotheses of vertebral growth as a cause of scoliosis, this model could be further refined by the inclusion of the rib cage, costovertebral joints and the vertebral muscles, all of which might alter the stiffness of the spinal segments. In further testing of hypotheses related to the NCJ, it would be beneficial to include the NCJ in the model since growth at the site of the NCJ might exert a greater torque on the adjacent vertebral body than growth at the site of the pedicle. Of course, the inclusion of the NCJ would require that the growth contribution be precisely quantified during the adolescent time period. Further experimental work might also be required to develop the mechanobiological concept of growth plates so the growth modulation is more accurately modeled. Current models have assumed that the relationship between loading and altered vertebral growth is linear, however numerous authors have suggested that growth plates have a threshold effect before growth modulation occurs (Frost, 1990; Shefelbine and Carter, 2000). In general, the further refinement of this type of model will depend heavily on characterizing mechanical properties and experimental validation. Ultimately, the value of the model created will be a reflection of the data used to create it, provided that the model is used within its scope of validity (Aubin in Burwell et al., 2000).

This study represented the first time that a biomechanical model of the thoracolumbar spine was used to test the hypothesis that pedicle asymmetry might lead to the production of scoliosis. Results showed that pedicle asymmetry did not appear to cause scoliosis independently and furthermore, did not amplify the scoliotic deformity caused by other deformations. With the continuous acquisition of further experimental data to refine the model used and the use of FE modeling in conjunction with clinical and animal studies, this approach has great potential for improving understanding of the complex mechanisms involved in scoliotic curve development.

REFERENCES

Andriacchi TP, Schultz AB, Belytschko RB, DeWald RL. Milwaukee brace correction of idiopathic scoliosis: a biomechanical and a retrospective study. J Bone Joint Surg (Am) 1976;58-A:806-815.

Arkin AM, Katz JF. The effects of pressure on epiphyseal growth. J Bone Joint Surg (Am) 1956;38-A:1056-76.

Aubin CE, Dansereau J, Labelle H. Biomechanical simulation of the Boston brace effect on a model of the scoliotic spine and thorax. Ann Chir 1993;47:881-887.

Aubin CE, Descrimes JL, Dansereau J, Skalli W, Lavaste F, Labelle H. Geometrical modeling of the spine and the thorax for the biomechanical analysis of scoliotic deformities using the finite element method. Ann Chir 1995;49:749-761.

Aubin CD, Dansereau J, Petit Y, Parent F, De Guise JA, Labelle H. Three-dimensional measurement of wedged scoliotic vertebrae and intervertebral discs. Eur Spine J 1998;7:59-65.

Aubin CE. Finite element analysis for the biomechanical study of scoliosis. In : Burwell et al. (eds.). Etiology of adolescent idiopathic scoliosis. Hanley and Belfus. Philadelphia, 2000: 489-504.

Beguiristain JL, De Salis J, Oriaifo A, Canadell J. Experimental scoliosis by epiphyseodesis in pigs. Int Ortho 1980;3:317-21.

Coillard C, Rhalmi S, Rivard CH. Experimental scoliosis in the minipig: study of vertebral deformations. Ann Chir 1999;53:773-80.

Dansereau J, Beauchamp A, De Guise JA, Labelle H. Three-dimensional reconstruction of the spine and rib cage from stereoradiographic and imaging techniques. Proceedings of the Canadian Society of Mechanical Engineering 1990;2:61-64.

De Giorgi G, Gentile A, Mantriota G, Gafario G. Analisi, con programma agli elementi finiti, delle spine correttive sviluppate dai corsetti nella scoliosis lombare. Riv Int Technica Orthopedica Internacional. 1990.

Descrimes JL, Aubin CE, Skalli W, Zeller R, Dansereau J, Lavaste F. Modeling of facet joints in a finite element model of the scoliotic spine and thorax: mechanical aspects. Rachis 1995;7:301-14.

Dimeglio A, Bonnel F. Le rachis en croissance. Springer. Paris, 1990.

Frost HM. Skeletal structural adaptations to mechanical usage: the hyaline cartilage modeling problem. Anat Rec 1990;226:423-432.

Gignac D, Aubin CE, Dansereau J. Biomechanical study of new orthotic approaches for 3D orthotic correction of scoliosis. Ann Chir 1998;52:795-800.

Keim HA. Scoliosis. Clin Symp 1979;31:2-34.

Knutsson F. A contribution to the discussion of the biological cause of idiopathic scoliosis. Acta Orthop Scand 1963;33:98-104.

Knutsson F. Vertebral genesis of idiopathic scoliosis in children. Acta Radiol 1966;4: 395-402.

Lovell, Winter B. Pediatric orthopaedics. Lippincott, Williams and Wilkins. Philadelphia, 2001.

Michelsson JE. The development of spinal deformity in experimental scoliosis. Acta Orthop Scand 1965;36(Suppl 81):9-91.

Nicoladoni C. Anatomie und mechanismus der skoliose. Urban and Schwarzernburg. Munchen, 1909.

Ottander HG. Experimental progressive scoliosis in a pig. Acta Orthop Scand 1963;33:91-7.

Parent S, Labelle H, Skalli W,de Guise J. Thoracic pedicle morphometry in vertebrae from scoliotic spines. Spine 2004;29:239-248.

Poulin F, Aubin CE, Stokes IAF. Biomechanical modeling of scoliotic spine instrumentation using flexible mechanisms: feasibility study. Ann Chir 1998;52:761-767.

Rajwani T, Bhargava R, Moreau M, Mahood J, Raso VJ, Jiang H, Bagnall KM. MRI characteristics of the neurocentral synchondrosis. Ped Rad 2002;32:811-16.

Roaf R. The basic anatomy of scoliosis. J Bone Joint Surg (Br) 1966;48-B:786-92.

Russell GG, Raso VJ, Hill D, McIvor J. A comparison of four computerized methods for measuring vertebral rotation. Spine 1990;15:24-27.

Schultz A, Andersson G, Ortengren R, Haderspeck K, Nachemson A. Loads on the lumbar spine – validation of a biomechanical analysis by measurements of intradiscal pressures and myoelectric signals. J Bone Joint Surg Am 1982;64:713-720.

Sevastik B, Xiong B, Sevastik J, Hedlund R, Suliman I. Vertebral rotation and pedicle length asymmetry in the normal adult spine. Eur Spine J 1995;4:95-97.

Shefelbine SJ, Carter DR. Mechanical regulation of growth in the physis. Eighth Annual Symposium: Computational methods in orthopaedic biomechanics. Florida, 2000.

Stokes IAF, Bigalow LC, Moreland MS. Measurement of axial rotation of vertebrae in scoliosis. Spine 1986;11:213-218.

Stokes IAF, Laible JP. Three-dimensional osseo-ligamentous model of the thorax representing initiation of scoliosis by asymmetric growth. J Biomech 1990;23:589-595.

Stokes IAF, Spence H, Aronsson DD, Kilmer N. Mechanical modulation of vertebral body growth. Spine 1996;21:1162-67.

Taylor JR. Growth of human intervertebral discs and vertebral bodies. J Anat 1975;120:49-68.

Taylor JR. Scoliosis and growth : patterns of asymmetry in normal vertebral growth. Acta Orthop Scand 1983;54:596-602.

Villemure I, Aubin CE, Dansereau J, Labelle H. Simulation of progressive deformities in adolescent idiopathic scoliosis using a biomechanical model integrating vertebral growth modulation. J Biomech Eng 2002;124:784-790.

Villemure I, Aubin CE, Dansereau J, Labelle H. Biomechanical simulations of the spine deformation process in adolescent idiopathic scoliosis from different pathogenesis hypotheses. Eur Spine J 2004;13:83-90.

Vital JM, Beguiristain JL, Algara C, Villas C, Lavignolle B, Grenier N, Sénégas J. The neurocentral vertebral cartilage: anatomy, physiology and physiopathology. Surg Radiol Anat 1989;11:323-28.

Weinstein SL. The pediatric spine: principles and practice, 1st ed. Lippincott Williams and Wilkins. Philadelphia, 1994.

White AA. Kinematics of the normal spine as related to scoliosis. J Biomech 1971;4:405-11.

Wynarsky GT, Schultz AB. Optimization of skeletal configuration: studies of scoliosis correction biomechanics. J Biomech 1991;24:721-732.

Yamazaki A, Mason DE, Caro PA. Age of closure of the neurocentral cartilage in the thoracic spine. J Ped Ortho 1998;18:168-72.

CHAPTER 10

GENERAL CONCLUSIONS AND DISCUSSION

GENERAL CONCLUSIONS

The major results of the experiments contained within this thesis were:

1) Gross anatomic visualization of the vertebra was not an effective technique for judging the presence or absence of NCJ cartilage

-Nicoladoni's original asymmetric NCJ growth hypothesis (1909) was dismissed on the basis of anatomic studies which found that the NCJ closed well before adolescence between six and 10 years of age (Knutsson, 1963; Ottander, 1963; Roaf, 1966; Schmorl et al., 1971; Taylor, 1983; Vital et al., 1989; Maat et al., 1996). However, correlation of gross anatomic visualization with histologic examination showed that gross anatomic visualization of the superficial surfaces of the vertebral body was not an effective technique for visualizing the NCJ site or determining the extent of NCJ closure, since the NCJ did not extend through the periosteum. Even if the periosteum was removed, the NCJ site remained difficult to detect using a fine needle as a probe due to the thin anteroposterior diameter of this growth plate. The most reliable means of assessing NCJ closure was by microscopic examination of transverse sections taken through the NCJ, however this technique has not been applied in most previous studies.

-In addition to the factors mentioned, since the NCJ closed from lateral to medial over a period of approximately two years, visualization of the NCJ from the lateral aspect could easily underestimate the age of closure by up to two years.

-Based on MRI visualization, the NCJ was found to display a regional pattern of development with closure occurring earlier in some regions than others. Unfortunately, gross anatomic studies in the past have implicitly assumed that the NCJ closed at the same age along the entire vertebral column. This resulted in conclusions being derived from examination of single vertebrae in specific regions and the results being extrapolated to the entire vertebral column, rather than conclusions being developed from systematic analysis of vertebrae from the entire vertebral column. This may further account for the underestimation of the age of NCJ closure, particularly in the mid-thoracic region and emphasizes the danger of making conclusions about the whole vertebral column from examination of single vertebrae.

2) MRI was a sensitive technique for detecting the presence or absence of NCJ cartilage and using this technique the thoracolumbar NCJs were found to be open during adolescence

-MRI-histologic correlation using porcine specimens showed that MRI was a sensitive technique for detecting the presence of very small amounts of cartilage *in vivo* and therefore could be used to determine the age of NCJ closure (i.e. when no cartilage remains)

-Based on MRI, the NCJ showed a regional pattern of development with closure first occurring in the cervical region (age 6), then in the lumbar region (age 12) and finally in the mid-thoracic region (age 15). The late closure of the NCJ in the mid-thoracic region was potentially significant as this implied that the mid-thoracic NCJs might have the longest time and the greatest probability for asymmetric growth to develop.

-In the past, evaluation of the asymmetric growth hypothesis was fixated on determining the age of NCJ closure, with other aspects of this hypothesis being ignored. These findings resurrected the asymmetric NCJ growth hypothesis and it was hoped that they would lead to critical evaluation of other aspects of the hypothesis.

3) MRI was an effective tool for staging NCJ development

-Past studies simply classified the NCJ as either open or closed (Yamazaki et al., 1998). With the realization that NCJ closure occurred in a continuous fashion and determination of the extent of normal variation in NCJ asymmetry, a staging system for NCJ development was created. This staging system enabled the assessment of the degree of asymmetric NCJ development in AIS patients, which was not previously possible.

4) NCJ asymmetry was clearly visible in AIS patients

-Application of the staging system showed that five of eleven AIS patients had asymmetric NCJ development in one to three vertebrae located at or near the apex (two patients) or at the extremities of the primary (two patients) and secondary curves (one patient). Asymmetry was defined as a difference of two or more stages between the NCJs at a particular vertebral level, since normal vertebrae only showed up to one stage of variation within a single vertebra. In all cases, the NCJ on the convex side of the curve was less developed which was the opposite side of the curve than predicted by Nicoladoni (1909) or previous animal models (Beguiristain, 1980).

-The location of the asymmetric NCJ development appeared unrelated to the location of the apex of the scoliotic curve as suggested by the model.

-Since the subjects represented a random group of AIS patients, the number with asymmetric NCJ development as the underlying cause of their scoliosis was expected to be small because it was thought that AIS had multiple different causes. The large number of patients displaying asymmetric NCJ development, as well as the failure of the pattern of asymmetry to agree with the asymmetric growth model suggested that the NCJ asymmetry observed possibly reflected the effects of scoliosis on NCJ development rather than being an underlying cause.

-This study highlighted the difficulty of separating cause from effect in patients with AIS.

5) Pedicle asymmetry was clearly noted in normal and AIS patients

-Measurements of pedicle length have traditionally been used as surrogate markers of NCJ development since it has been assumed that pedicle length is determined almost entirely by growth at the site of the NCJ (Ganey and Ogden, 2001).

-Interestingly, normal patients showed significant neural arch asymmetry, with the left pedicle and lamina being significantly greater in length. This asymmetry could be associated with the small right thoracic scoliosis seen in the normal population and strongly suggested that the baseline currently used to assess pedicle asymmetry in AIS must be reconsidered.

-A random pool of AIS patients displayed significant neural arch asymmetry, although the longer pedicle was not consistently located on the convexity or the concavity of the scoliotic curve. The lack of a consistent pattern of pedicle asymmetry may reflect that these patients presented with scoliosis due to different causes. It is possible that the pattern of pedicle length noted depends on the particular cause of scoliosis, with no consistent pattern evident when patients with different causes are mixed.

6) The NCJ made a bipolar growth contribution

-Histologic analysis and fluorochrome-based visualization of bone deposition confirmed that the NCJ was a bipolar growth plate that made a contribution to the growth of the vertebral body anteriorly and the pedicle posteriorly in the transverse plane.

-This is in contrast to the primarily unipolar growth plates associated with long bones where growth appears to be mainly on the diaphyseal side.

7) In contrast to traditional concepts of vertebral growth, periosteal mechanisms appeared to play a major role in accounting for the increased length of the pedicle

-Traditionally, the growth of the pedicle and changes in the dimensions of the canal are thought to depend almost exclusively on growth at the site of the NCJ and the PS (Ganey and Ogden, 2001). However, this is too simplistic since careful observation of the vertebra clearly shows that the pedicle gets larger (in both length and width) after NCJ closure as the vertebra increases in size.

-Using fluorochromes to assess vertebral canal growth in the rat, it was found that the pedicle and the vertebral canal continued to increase significantly in length and width by periosteal mechanisms well after the closure of the NCJ and PS. Since the pedicle is a curved structure, lateral deposition and medial resorption will result in increased pedicle length without growth along the axis of the pedicle.

-These findings challenge traditional concepts of the pedicle as a long bone and suggest that asymmetric pedicle growth could potentially be a result of periosteal mechanisms, similar to the growth of a short bone.

8) The growth activity of the NCJ decreased with time

-Using fluorochrome-based measurements of bone deposition in the rat, it was shown that the bone deposited by the NCJ declined sharply (approximately thirtyfold) between the first and second week. The NCJ contribution to the pedicle was almost negligible during the second week.

-The presence of the NCJ could not necessarily be correlated with growth at the site of the NCJ. Extending these results to the adolescent human, it is possible that the NCJ may be present, but its contribution to pedicle length may not be significant.

9) The placement of pedicle screws across the NCJ in porcine specimens did not result in the creation of scoliosis or a shorter pedicle on the operated side

-Past studies involving the placement of pedicle screws across the NCJ in porcine specimens have yielded conflicting results (Ottander, 1963; Beguiristain et al., 1980; Coillard et al., 1999) and findings have not been successfully replicated.

-After placing pedicle screws unilaterally across the NCJs from T6-T10 in porcine specimens, neither scoliosis nor a significant pattern of vertebral rotation was achieved. Interestingly, the pedicle on the operated side was not shorter. Since the screws were correctly placed and screw positions were verified fluoroscopically, these findings suggested strongly that the contributions of the NCJ to increased pedicle length were minimal.

-The creation of valid definitions for the assessment of morphologic parameters such as pedicle length and lamina length was extremely difficult. Since these structures are not clearly separated, the creation of boundaries between them is subjective. Even if consistent and precise definitions could be created, considerable doubt surrounds their application to the multitude of deformities found in vertebrae from scoliotic spines.

10) Computerized biomechanical simulations suggested that pedicle asymmetry was not sufficient for the creation of vertebral rotation and scoliosis

-After incorporating pedicle asymmetry into a previously created computerized model of the scoliotic spine (Villemure et al., 2004), the simulation of pedicle asymmetry from T6-T10 for a period of 24 months did not create either vertebral rotation nor vertebral wedging. Although a small extent of scoliosis was initially noted, this appeared to be a result of the measurement techniques used rather than the creation of a true lateral curvature.

-Other scenarios not involving pedicle asymmetry such as the displacement of the T8 vertebra by 3 mm to the right and the rotation of the T8 vertebra by 5° produced scoliosis with Cobb angles of greater than 30 degrees, with significant vertebral rotation and vertebral wedging.

-Although vertebral rotation appeared to potentially result in scoliosis, pedicle asymmetry did not appear to be sufficient on its own to cause vertebral rotation.

The development of an explicit and consistent model is a prerequisite to evaluating the potential role of the NCJ in AIS. Based on experimental findings from this thesis and other studies, what would be the most plausible model for asymmetric NCJ development as a cause of AIS?

a) Asymmetric NCJ growth – The first step in the model would be the unilateral and relative advanced growth of the NCJs in several adjacent vertebrae in the mid-thoracic region. The suggestion that NCJ asymmetry manifests with one NCJ showing advanced growth and the other showing normal growth, instead of one NCJ showing delayed growth and the other showing normal growth is based on the work of Parent et al. (2004). In a morphometric analysis of scoliotic vertebral specimens, it was found that the pedicle lengths in scoliosis patients were greater on average than the pedicle lengths in normal patients. This finding would suggest that it is more likely that the contribution of the NCJ to pedicle growth in scoliosis is increased and not decreased. The mid-thoracic region would be the most likely site for asymmetric NCJ development since these NCJs are the last to close and thus have the greatest time for asymmetric growth to manifest. This would also correlate well with the high incidence of apical vertebrae in this region in AIS. Although some authors have suggested that asymmetric NCJ growth at one level is sufficient for scoliosis production (Nicoladoni, 1909), animal models (Ottander, 1963; Beguiristain et al., 1980) appear to suggest that several consecutive NCJs must exhibit asymmetric growth for a sufficient scoliosis to develop. It would be suspected that these consecutive NCJs do not exhibit the same extent of asymmetric growth, since the apical vertebra of the scoliotic curve is usually the most rotated with rotation decreasing towards the neutral vertebrae (Lovell and Winter, 2001).

b) **Rotation of the vertebral body** – Nicoladoni's observations (1909) as well as the results of animal epiphyseodesis experiments (Beguiristain et al., 1980) have suggested that accelerated NCJ development on the future concave side of the curve results in rotation of the vertebral body towards the future convex side. This idea has been further supported by several anatomic studies which have found increased pedicle length on the concave side at the apex of the scoliotic curve (Nicoladoni, 1909; Knutsson, 1963;

Taylor, 1983; Vital et al., 1989). However, the direction of vertebral body rotation is still controversial with the finite element models used in this thesis as well as some anatomic studies finding that the longer pedicle is on the opposite side of the curve (Roaf, 1960). Further work is also required to determine if the vertebral changes associated with unilateral accelerated NCJ development should actually be classified as torsion, rotation or both torsion and rotation. With asymmetric NCJ development, it is poorly understood whether the vertebra is actually growing into a deformed shape (torsion), whether abnormal pedicle growth is causing rotation of a fairly normally shaped vertebral body (rotation) or whether both mechanisms are operating together.

c) **Lateral curvature of the vertebral column** – The link between vertebral rotation and lateral curvature is somewhat unclear. One suggestion is that the vertebral column behaves similar to a fixed rod in which vertebral rotation can only be accommodated by lateral curvature, which would appear to agree with the results of the biomechanical models used in this thesis. Another plausible idea is that vertebral rotation results in an increased pressure on the concave side of the vertebrae, which results in growth inhibition on this side of the superior and inferior physeal growth plates and the creation of wedged vertebrae. Vertebral body wedging does not appear to be related to any potential contribution of the NCJ to height (Vital et al., 1989) since this would manifest with decreased height on the convex side of the curve, which conflicts with the findings of NCJ epiphyseodesis experiments (Beguiristain et al., 1980).

d) **Secondary changes in the NCJ** – Regardless of whether asymmetric NCJ growth is the underlying cause of scoliosis or even in cases where scoliosis is due to other causes, it is entirely possible that upon creation of a lateral curvature, compensatory changes begin to occur in some of the NCJs as a result of the altered biomechanics of the spine. These compensatory changes would likely depend on factors such as the degree of alteration of normal biomechanical forces, the duration of time that scoliosis is allowed to progress and the presence of open or at least partially open NCJs, that are capable of growth, in the compensatory region. The presence of compensatory changes in the NCJ might account for the pattern of asymmetric NCJ development noted in this thesis, which was opposite to the pattern predicted on the basis of the asymmetric NCJ growth model.

Is asymmetric NCJ development a cause of AIS?

For years, the asymmetric NCJ growth hypothesis of AIS was discredited entirely on the basis of anatomic studies (Knutsson, 1963; Ottander, 1963; Roaf, 1966; Schmorl et al., 1971; Taylor, 1983; Vital et al., 1989; Maat et al., 1996) which found that the NCJ closed between the ages of six and 10 years. If the NCJ closed prior to the adolescent time period then asymmetric NCJ growth could not be a cause of AIS. On the basis of MRI visualization of the NCJ and correlation of the MR images with histology, it was shown that the NCJ remains open during the adolescent time period, which resurrected the asymmetric NCJ growth hypothesis for consideration.

In times past, the fixation on the age of NCJ closure has distracted from other potential considerations regarding the asymmetric NCJ growth hypothesis, such as the growth contributions of the NCJ. Although the results from this study and other work (Vital et al., 1989, Töndury and Theiler, 1990; Maat et al., 1996; Yamazaki et al., 1998) have confirmed that the NCJ makes a growth contribution to the growth of the vertebral body and the pedicle, the growth contribution of the NCJ has not been quantified. Furthermore, the time period during which the NCJ contributes to growth has not been explored. In the past, it has typically been assumed that simply the presence of the NCJ could be correlated with activity at this site. From the results of this thesis, this did not appear to be the case since fluorochrome work showed that NCJ activity decreased with time. The failure of the porcine surgery to produce scoliosis also suggested that the growth contribution of the NCJ may not be sufficient for the production of pedicle asymmetry. Although further human work is required to quantify the NCJ contribution, the finding that adult canal diameters are attained by the age of 10 based on cross-sectional radiographic studies (Knutsson, 1966) further suggests that NCJ activity may not be sufficient to create pedicle asymmetry during adolescence, regardless of whether this pedicle asymmetry is sufficient to cause scoliosis.

From a clinical perspective, evidence gathered regarding the potential role of the NCJ in scoliosis is ambiguous since it is impossible to separate primary and secondary changes in the NCJ, particularly when patients are acquired late in the course of their scoliosis. Further, measurements of NCJ or pedicle asymmetry are made more difficult since a random pool of AIS patients represents multiple different causes, making it difficult to draw conclusions about any one single cause.

To date, animal experiments of asymmetric NCJ growth have generated interesting results and have overcome some of the limitations inherent in clinical studies, with Beguiristain et al. (1980) noting the most significant scoliosis. Unfortunately, the failure to include control groups in Beguiristain's study as well as the failure for the results to be replicated by Coillard et al. (1999) or in this thesis suggests that further experimentation is clearly required.

Weighing the evidence, it seems likely that asymmetric NCJ growth may not be a cause of scoliosis in adolescents due to the minimal contribution of the NCJ to pedicle growth during this time period. Of course, this does not rule out the possibility that asymmetric NCJ growth might be a cause of scoliosis in the juvenile on infantile age groups. In the future, exploration of the asymmetric NCJ growth hypothesis will likely benefit more from animal models than clinical studies. Unless patients with asymmetric NCJ development can be separated from other AIS patients and the secondary effects of scoliosis on the NCJ can be separated from primary NCJ changes, clinical studies will likely continue to produce ambiguous findings. Animal models have great potential for the exploration of asymmetric NCJ development, although the use of appropriate control groups is absolutely essential.

IMPLICATIONS FOR SCOLIOSIS RESEARCH

In addition to exploring the potential role of the NCJ in AIS, the aim of this thesis was also to evaluate critically the manner in which scoliosis has been studied in the past and to offer insight into the manner that scoliosis research should be conducted in the future. Without a fundamental shift in approach, a cure for AIS does not appear likely within the next fifty or even one hundred years. Some of the points that should be considered in the study of AIS etiology are the following:

1) Experimental studies must reflect the fact that AIS has multiple different causes – A growing body of research and circumstantial evidence strongly suggests that AIS has multiple different causes (Robin, 1990). Although this has major repercussions for experimental design, most current studies have failed to consider this underlying principle. If AIS has more than a single cause, then etiologic studies in which random AIS patients are assigned to a single group are fundamentally unsound in design. The average measured values could potentially obscure any measured values pertaining to the cause of interest. Ideally, much more progress would be made if attention were focused on a particular cause of AIS and a complete model for this cause was developed. If the clinical presentation of patients with this particular cause could be determined and distinguished from other potential causes of AIS, then measured values could be obtained and progress made in the investigation of a particular cause of AIS. Of course, this approach presumes a certain amount of knowledge considering a particular cause of AIS. In the interim, while this knowledge is being acquired, it may be necessary to conduct preliminary studies with random groups of AIS patients provided that the limitations of these studies are acknowledged and that analysis of the results is based on more than acquisition of average measured values. As more knowledge concerning a particular cause is acquired, the goal would be for successive studies to incorporate an increasing number of patients with the particular cause being investigated among all of the patients in the study population.

2) Experimental studies must acknowledge that it is difficult to infer cause and effect relationships in patients with well-established scoliosis and that the initial cause of the scoliosis may no longer be present or detectable in these patients – There is a very narrow window of time between the initial presentation of patients to the scoliosis clinic and the development of biomechanical changes in the vertebrae as a secondary result of scoliosis. As a result, it is impossible to infer if given changes such as alterations in vertebral morphology are a cause or an effect of the scoliosis created. To add to the complexity of separating cause and effect, current research also suggests that a scoliotic curve might continue to progress due to mechanical disturbance of the vertebral column, even if the initial factors responsible for curve development were no longer present or identifiable (Roaf, 1966; Stokes and Gardner-Morse, 1991; Lonstein, 1994). This would mean that obtaining measurements from patients with well-established scoliosis might not reflect the initial cause of the deformity and these patients might appear completely 'normal'.

Although these difficulties cannot be overcome, they can be minimized by focusing on patients that are in the earlier stages of curve development. This may require the enlisting of patients into clinical studies at the time that these patients are first diagnosed by their family doctor, rather than at the time of presentation to a scoliosis clinic.

3) Potential etiologic factors for AIS cannot be viewed in complete isolation – It has been suggested and seems plausible that each potential cause of AIS may require or interact with other factors (Lonstein, 1994). Although the ability to consider additional factors assumes a certain background knowledge of the potential cause being investigated, it is important that etiologic factors not be viewed in complete isolation from one another. As an example, although individual hormones such as melatonin could be implicated in the etiology of AIS, there is also considerable value in considering the potential interactions of melatonin with other hormones such as calmodulin and growth hormone instead of focusing solely on melatonin. As a general trend, scoliosis research in the past has been "vertical" and has focused on separate, individual topics that are seemingly unrelated. A more "horizontal" approach in which different etiologic factors are integrated into comprehensive theories of AIS may contribute to the development of a more logical progression of thought in etiologic research.

4) Clinical studies of AIS etiology require supplementation with animal models – In the study of AIS etiology, animal models are absolutely essential since they overcome many of the limitations inherent in clinical investigations of AIS patients. For example, animal models allow the early identification of a population that is likely to get scoliosis (due to the experimental intervention) and therefore permit evaluation of the early stages of curve development. At the same time, these models also allow the creation of populations that potentially represent the same cause or pathomechanism of scoliosis development, so that measured values are not obscured by values that represent a different cause of scoliosis. From an ethical perspective, animal models are considered to have potential value in testing different treatment methods for scoliosis whereas it is considered unethical to test these novel therapeutic interventions on human patients. Given the advantages of animal models, the potential value of these models is enormous, particularly if the limitations of these modeling procedures are recognized and addressed.

One of the major problems with animal models of AIS (Robin, 1990) is that scoliosis has been almost too easy to produce with the use of numerous interventions. In many cases, interventions have been attempted which are obviously not the same means by which AIS manifests in humans, such as rib resection. A more fundamental problem is that in many cases, any degree of lateral curvature has been assumed to represent scoliosis, without consideration of the degree to which this scoliosis represents AIS. To facilitate the critical evaluation of animal models, it would be useful to implement a grading system (Table 10-1) to evaluate the degree to which scoliosis represents the human condition and to allow comparison between animal models. While recognizing that no animal model has the same vertebrae or vertebral column biomechanics found in the human, the continued development and exploration of bipedal models such as the pinealectomized chicken and the bipedal rat still seems to have great potential value.

5) Clinical studies can benefit from supplementation with biomechanical finite element models – Although the finite element modeling approach to AIS is still in its infancy, biomechanical models offer many of the same advantages as animal models as well as the additional potential of being able to alter or measure an unlimited number of variables. The potential benefits of the modeling process may be enormous, since with continued refinement and verification, these models may be able to predict accurately the three-dimensional shape of the spine in relation to growth or the application of treatment procedures. Of course, the primary limitation of these models is the difficulty of validation. Further progress will depend on the careful acquisition of the parameters required for validation and the use of FEM models within their scope of validity.

Table 10-1. Preliminary Grading Considerations for the Evaluation of Animal Models of AIS

GRADING CONSIDERATION	Explanation
Section 1: Choice of animal model	
Small phylogenetic gulf between the animal and the human	In general, the smaller the phlyogenetic gulf between the animal species and the human, the greater the degree to which the animal species is representative of the human.
Bipedal stance	The influence of the force of gravity along the longitudinal plane of the spine has important effects on the structure of the vertebrae, the alignment of the vertebral column, the response to instability and the progression of the scoliotic curve.
Growth spurt in the animal that mimics the adolescent growth spurt	Numerous authors have suggested that there is an intrinsic link between AIS and the growth spurt of adolescence (Asher in Burwell et al., 2000). One of the characteristics that animals with a scoliotic predisposition share is a growth-velocity curve interrupted by periods of rapid growth.
Spontaneous appearance of scoliosis	The spontaneous appearance of scoliosis in a given species suggests a certain basic level of vertebral column instability, which can manifest with superimposed factors.
Section 2 : Vertebral morphology observed	
Vertebral morphology representative of AIS	Although there is still contention over the vertebral morphology observed in AIS, the following vertebral changes are currently considered to be representative of AIS: vertebral rotation towards the convexity of the curve (Keim, 1979), pedicle length asymmetry with shorter pedicles on the convex side of the curve (Nicoladoni, 1909; Knutsson, 1966; Taylor, 1983; Vital et al., 1989), base of the spinous process projecting into the concavity (Smith et al., 1991), wedging with decreased vertebral height on the concavity (Xiong et al., 1995, Parent et al., 2002), posterior bulge of the ribs on the convexity of the curve ("rib hump) (Keim, 1979).
Presence of a compensatory curve	The presence of a compensatory curve strengthens an animal model by showing that vertebral changes are not limited to the operated segment and is indicative of AIS.
Variation in the site of the apical vertebrae and types of scoliotic curves created	This would strengthen the case that a given etiology might be responsible for a greater percentage of AIS cases. This variation assumes that a single etiology of AIS might present with variation in the site and types of curvature, which appears to be the case from analysis of the pinealectomized chicken model of scoliosis (see Wang et al., 1997).
Progression of the curve over time, in at least some cases	The variable progression of a scoliotic curve is an inherent aspect of AIS (Asher in Burwell et al., 2000).
Section 3 : Experimental Methodology	
Feasibility of the intervention	An intervention is more likely to represent a true etiology of AIS if the intervention represents a situation that could naturally occur in a human population.
Presence of control groups	Animal experiments require control groups/sham groups to verify that a given intervention is the cause of scoliosis and that the scoliosis is not a byproduct of the surgical approach, experimental technique or other confounding factors.
Collateral experimentation	If an animal model suggests that a given etiology presents with certain characteristics, then the presence of these characteristics in a scoliotic patient population strengthens the case for a particular etiology to be a true cause of AIS.
Reproducibility of experimentation	Reproducibility decreases the probability that findings are due to chance, improper technique or confounding factors.

6) Studies of AIS etiology will require the careful integration of clinical work, animal studies and computer models – There is much to be gained from integrating these approaches since they can be used in a complementary fashion. For example, the development of a theory with the use of a numerical model may allow the determination of the precise surgical intervention that could potentially cause scoliosis in an animal model. Eventually, if this intervention was successful, measurement and observation of the clinical presentation in the animal population might allow the determination of the clinical presentation of AIS patients with a particular cause for their scoliosis. With this knowledge, a subset of AIS patients could be gathered and used for the investigation of a specific theory.

7) Measurement of vertebral morphology requires the creation of valid and reliable measurement definitions that apply to both normal and abnormal vertebrae – Numerous theories of AIS have focused on the role of abnormal growth as a potential cause of AIS, which has created a need for the evaluation and measurement of vertebral morphology. Yet since the boundaries of anatomic regions like the pedicle are subjective and can move with vertebral deformities, it is no surprise that different studies of vertebral morphology have generated different definitions as well as different results. The creation of a consistent set of valid and reliable definitions that are appropriate for the measurement of normal and deformed vertebrae would be extremely valuable. The creation of such definitions might enable comparison between different studies and address whether the variety of morphologic presentations noted are a result of variation in the way scoliosis presents or variation in the measurement definitions themselves.

The measurement definitions created in this thesis were objective, reliable and appeared to be valid for normal patients and AIS patients with vertebral deformities. However, these measurement definitions were applied to porcine vertebrae without confirmation of the validity and reliability of the definitions for this particular application. Unfortunately, these definitions were not valid for the grossly deformed porcine vertebrae, which suggested that these definitions should not be used for new populations without further verification of validity and reliability.

8) Vertebral growth does not conform to the traditional long bone model – Traditionally, the vertebra has been viewed using the long bone model. In the coronal plane, the vertebral body was regarded as the diaphysis, with the annular rings thought to behave like epiphyses. In the transverse plane, the neural arch was viewed as a long bone with epiphyseal plates on either side: the NCJ and the PS. Unfortunately, this conception of the vertebra does not appear entirely accurate. In the coronal plane, the ring apophyses make no growth contribution and although the human physes are similar to epiphyses, cell column formation in the physeal growth plates is not as organized as in a long bone physis (Lord et al., 1995). Unlike long bone formation, the growth of the vertebral body shows elements of round bone growth such as the absence of a primary bone collar. In the transverse plane, unlike a long bone, each neural arch only arises from a single ossification center. As found in this thesis, the growth of the neural arch resembles a short bone such as the talus in the way that it is heavily dependent on periosteal mechanisms, with periosteal deposition and resorption likely playing a greater role in increasing the length of the neural arch than the growth plates. Based on these considerations, it is evident that the vertebra does not fit a simple long bone or short bone model. From an embryologic standpoint, this would not be unexpected since the vertebra is a composite of several bones, each of which has possibly retained its own identity in relation to growth and development but also has the potential to affect neighboring elements (Roaf, 1960). Recognizing these differences and the fact that the vertebra is a composite structure, it may be useful to consider vertebral growth outside the limiting paradigms of short bone and long bone growth.

9) Scoliosis must be measured and described in a different manner - Although scoliosis is clearly a three-dimensional deformity, many current measurements and descriptions of scoliosis are still two-dimensional. This often leads to a poor understanding and conception of the scoliotic deformity. For example, visualization of the Cobb angle with a single radiograph in the coronal plane could misrepresent a scoliotic curve as being of a low magnitude, when in fact the curve is much more significant as seen along the plane of maximum deformity. This could result in treatment strategies being less aggressive than required. Yet despite this limitation many scoliosis clinics continue to measure Cobb angle from a single set of PA films. Ultimately, as new imaging technologies are developed it may eventually be possible to develop methods of visualizing scoliosis that are three-dimensional, non-invasive and do not involve ionizing radiation, such as three-dimensional MRI visualization.

An additional problem is that since scoliosis is a continuous process, any approach that relies on static radiographs can only provide a limited understanding. The technique of 'morphing' (which involves using a computer to visualize changes between serial radiographs as a continuous process) is a potentially valuable method of assessing curve development, which would likely offer insight into mechanisms of curve progression.

10) Further etiologic research requires greater collaboration between researchers, surgeons and interventional radiologists - The end goal of many etiologic studies is to ultimately suggest potential interventions for the treatment of AIS. For example, it has been suggested by numerous authors that if asymmetric NCJ growth was a cause of AIS, then surgical fusion of the more open NCJs might help to treat the scoliosis due to asymmetric NCJ growth or even other causes. However, surgeons and researchers have not yet collaborated in determining what degree of evidence would be required before a hypothetical treatment approach, based on etiology, could even be attempted on a human subject. Without addressing this issue, the practical impact of clinical investigations and animal experiments of AIS etiology may never be applied to human patients.

Upon development of potential surgical techniques, these techniques could be further refined to make them less invasive and to enable real time three-dimensional visualization of hardware placement inside the vertebrae. The refinement of such procedures would benefit from collaboration between surgeons and interventional radiologists.

FUTURE EXPERIMENTS

Experiment 1: Faced with the conflicting results of the porcine study in this thesis and that of Beguiristain et al. (1980), the porcine surgeries performed in this thesis could be repeated with larger screws on a group of younger pigs, which would ensure that the contribution of the NCJ to growth was maximized and that more of the NCJ was destroyed. To decrease the ambiguity of potential experimental results, control and appropriate sham groups (surgical incision only, incision through the muscles, creation of the tunnel for pedicle screw placement without actual screw placement) could be included. If possible, the NCJs from T6-T10 could be unilaterally destroyed in one porcine specimen by boring across the majority of the NCJ with a drill under fluoroscopic guidance. The results of this specimen could be compared to the specimens with pedicle screws placed across the NCJ to verify that effective screw compression was achieved. In another porcine specimen, a few days after the placement of pedicle screws, fluorochromes could be serially injected to directly monitor the pattern of bone formation at the site of the NCJ. After approximately two to three weeks, this animal could be euthanized and dissected. This would allow direct observation of the effect of pedicle screws on growth at the site of the NCJ, as well as direct assessment of reactive bone formation. As alternatives to the above methods which entail surgical intervention with the NCJ, approaches such as laser ablation or gamma knife surgery could also be considered.

Experiment 2: Regardless of the potential primary role of the NCJ in the causation of scoliosis, understanding the secondary effects of scoliosis on the NCJ would potentially explain the morphologic changes noted in scoliosis patients. Furthermore, if the NCJ was found to have a primary role in scoliosis, this would enable categorization of a given change in the NCJ as primary or secondary. One potential way to assess the secondary changes in the NCJ would be to create scoliosis in an animal model using another method, such as the removal of the pineal gland in chickens, and to then monitor NCJ changes and growth contributions using fluorochromes.

Experiment 3: Although growing evidence suggests that AIS is the result of numerous different causes, it is still not understood if different causes of scoliosis present in a different manner or even if a similar cause of scoliosis presents in a consistent manner. Without understanding which factors, if any, vary in presentation between cases of scoliosis due to different causes, it is impossible to assemble a group of patients with one potential cause for their scoliosis. This significantly limits the value of any measurements obtained from a group of AIS patients. Furthermore, without being able to separate patients on the basis of clinical presentation, diagnosis and treatment of scoliosis is severely handicapped. To explore these ideas, it would be useful to characterize morphologic, curve and cosmetic parameters in animal models presenting with scoliosis due to different causes. The extent of variation in these parameters due to a single potential cause could be assessed and an understanding of which parameters varied between cases of scoliosis due to different causes could be developed. Potential animal models that could be used in this type of study are populations of pinealectomized chickens with scoliosis, or rabbits with scoliosis as a result of rib resection since both of these animal models are fairly well-established.

Experiment 4: One of the central problems in AIS research has been the difficulty of obtaining scoliosis patients before vertebral deformities are well-established. This has severely limited etiologic research as well as the investigation of mechanisms of curve development. For example, it is still poorly understood if vertebral rotation is a cause of lateral curvature or lateral curvature is a cause of vertebral rotation, which makes the significance of vertebral rotation entirely unknown. To obtain AIS patients in the early stages of scoliosis, it would be useful to follow the siblings of patients with scoliosis or populations of twins in which one twin already presented with scoliosis. These populations have a greater than average chance of being affected by scoliosis, ranging from 11% for siblings of scoliosis patients to 73% for the unaffected twin in a set of monozygotic twins (Lovell and Winter, 2001). Once this type of population was acquired, individuals could be followed with serial radiographs or MRIs and a group of patients in the early stages of scoliosis could be acquired. This group of AIS patients in the early stages of curve development could be used for a number of different etiologic and morphologic studies.

REFERENCES

Andriacchi TP, Schultz AB, Belytschko RB, DeWald RL. Milwaukee brace correction of idiopathic scoliosis: a biomechanical and a retrospective study. J Bone Joint Surg (Am) 1976;58-A:806-815.

Asher MA. Foreword. In : Burwell et al. (eds.). Etiology of adolescent idiopathic scoliosis. Hanley and Belfus. Philadelphia, 2000: Xiv-xv.

Aubin CE, Dansereau J, Labelle H. Biomechanical simulation of the Boston brace effect on a model of the scoliotic spine and thorax. Ann Chir 1993;47:881-887.

Beguiristain JL, De Salis J, Oriaifo A, Canadell J. Experimental scoliosis by epiphyseodesis in pigs. Int Ortho 1980;3:317-21.

Coillard C, Rhalmi S, Rivard CH. Experimental scoliosis in the minipig: study of vertebral deformations. Ann Chir 1999;53:773-80.

De Giorgi G, Gentile A, Mantriota G, Gafario G. Analisi, con programma agli elementi finiti, delle spine correttive sviluppate dai corsetti nella scoliosis lombare. Riv Int Technica Orthopedica Internacional. 1990.

Ganey TM, Ogden JA. Development and maturation of the axial skeleton. In : Weinstein SL (ed.). The pediatric spine : principles and practice, 2nd ed. Lippincott Williams and Wilkins. Philadelphia, 2001: 3-54.

Gignac D, Aubin CE, Dansereau J. Biomechanical study of new orthotic approaches for 3D orthotic correction of scoliosis. Ann Chir 1998;52:795-800.

Keim HA. Scoliosis. Clin Symp 1979;31:2-34.

Knutsson F. A contribution to the discussion of the biological cause of idiopathic scoliosis. Acta Orthop Scand 1963;33:98-104.

Knutsson F. Vertebral genesis of idiopathic scoliosis in children. Acta Radiol 1966;4: 395-402.

Lonstein JE. Adolescent idiopathic scoliosis. Lancet 1994;344:1407-1412.

Lovell, Winter B. Pediatric orthopaedics. Lippincott, Williams and Wilkins. Philadelphia, 2001.

Lord MJ, Ogden JA, Ganey TM. Postnatal development of the thoracic spine. Spine 1995;20:1692-1699.

Maat GJ, Matricali B, Van Meerten EL. Postnatal development and structure of the neurocentral junction. Spine 1996;21:661-66.

Nicoladoni C. Anatomie und mechanismus der skoliose. Urban and Schwarzernburg. Munchen, 1909.

Ottander HG. Experimental progressive scoliosis in a pig. Acta Orthop Scand 1963;33:91-7.

Parent S, Labelle H, Skalli W, Latimer B, de Guise J. Morphometric analysis of anatomic scoliotic specimens. Spine 2002;27:2305-11.

Parent S, Labelle H, Skalli W, de Guise J. Thoracic pedicle morphometry in vertebrae from scoliotic spines. Spine 2004;29:239-248.

Roaf R. Vertebral growth and its mechanical control. J Bone Joint Surg (Br) 1960;42-B:40-59.

Roaf R. The basic anatomy of scoliosis. J Bone Joint Surg (Br) 1966;48-B:786-92.

Robin GC. The aetiology of idiopathic scoliosis. Freund Publishing House. Boca Raton, 1990.

Schmorl G, Junghanns H, Besemann EF (ed.). The human spine in health and disease. Grune and Stratton. New York and London, 1971.

Smith RM, Pool RD, Butt WP, Dickson RA. The transverse plane deformity of structural scoliosis. Spine 1991;16:1126-1129.

Stokes IA, Gardner-Morse M. Analysis of the interaction between vertebral lateral deviation and axial rotation in scoliosis. J Biomech 1991;24:753-759.

Taylor JR. Scoliosis and growth : patterns of asymmetry in normal vertebral growth. Acta Orthop Scand 1983;54:596-602.

Töndury G, Theiler K. Entwicklungsgeschichte und fehlbildungen der wirbelsäule, 2nd edn. Hippokrates Verlag. Stuttgart, 1990.

Villemure I, Aubin CE, Dansereau J, Labelle H. Biomechanical simulations of the spine deformation process in adolescent idiopathic scoliosis from different pathogenesis hypotheses. Eur Spine J 2004;13:83-90.

Vital JM, Beguiristain JL, Algara C, Villas C, Lavignolle B, Grenier N, Sénégas J. The neurocentral vertebral cartilage: anatomy, physiology and physiopathology. Surg Radiol Anat 1989;11:323-28.

Wang X, Jiang H, Raso J, Bagnall KM. Characterization of the scoliosis that develops after pinealectomy in the chicken and comparison with adolescent idiopathic scoliosis in humans. Spine 1997;22:2626-2635.

Wynarsky GT, Schultz AB. Optimization of skeletal configuration: studies of scoliosis correction biomechanics. J Biomech 1991;24:721-732.

Xiong B, Sevastik B, Sevastik J. Horizontal plane morphometry of normal and scoliotic vertebrae : A methodological study. Eur Spine J 1995;4:6-10.

Yamazaki A, Mason DE, Caro PA. Age of closure of the neurocentral cartilage in the thoracic spine. J Ped Ortho 1998;18:168-72.